ADVANCES IN

QUANTUM CHEMISTRY

QUANTUM SYSTEMS IN CHEMISTRY AND PHYSICS, PART I

EDITOR-IN-CHIEF

PER-OLOV LÖWDIN

PROFESSOR EMERITUS

DEPARTMENT OF QUANTUM CHEMISTRY   AND   QUANTUM THEORY PROJECT
UPPSALA UNIVERSITY   UNIVERSITY OF FLORIDA
UPPSALA, SWEDEN   GAINESVILLE, FLORIDA

EDITORS

JOHN R. SABIN
MICHAEL C. ZERNER

ERKKI BRÄNDAS

QUANTUM THEORY PROJECT
UNIVERSITY OF FLORIDA
GAINESVILLE, FLORIDA

DEPARTMENT OF QUANTUM CHEMISTRY
UPPSALA UNIVERSITY
UPPSALA, SWEDEN

GUEST EDITORS

S. WILSON

RUTHERFORD APPLETON
LABORATORY
CHILTON, OXFORDSHIRE
UNITED KINGDOM

J. MARUANI

LABORATOIRE DE CHIMIE
PHYSIQUE
CNRS AND UPMC
PARIS, FRANCE

Y. G. SMEYERS

INSTITUTO DE ESTRUCTURA DE
LA MATERIA, CSIC
MADRID, SPAIN

P. J. GROUT

PHYSICAL AND THEORETICAL CHEMISTRY
LABORATORY
UNIVERSITY OF OXFORD
OXFORD, UNITED KINGDOM

R. McWEENY

DIPARTIMENTO DI CHIMICA E CHIMICA
INDUSTRIALE
UNIVERSITA DI PISA
PISA, ITALY

VOLUME 31

ACADEMIC PRESS

San Diego   London   Boston   New York   Sydney   Tokyo   Toronto

Contributors Volume 31

Numbers in parentheses indicate the pages on which the authors' contributions begin.

J. Avery (201), Department of Chemistry, Copenhagen University, DK-2100 Copenhagen, Denmark

Ya. I. Delchev (53), Institute of Nuclear Research and Nuclear Energy, Bulgarian Academy of Sciences, 1784 Sofia, Bulgaria

T. H. Dunning, Jr. (105), Environmental Molecular Sciences Laboratory, Pacific Northwest Laboratory, Richland, Washington 99352

E. Eliav (313), School of Chemistry, Tel Aviv University, 69978 Tel Aviv, Israel

A. Famulari (251), Dipartimento di Chimica Fisica ed Elettrochimica, Università di Milano, 20133 Milan, Italy

E. Gianinetti (251), Dipartimento di Chimica Fisica ed Elettrochimica, Università di Milano, 20133 Milan, Italy

I. Hubač (75), Department of Chemical Physics, Faculty of Mathematics and Physics, Comenius University, 842 15 Bratislava, Slovakia

U. Kaldor (313), School of Chemistry, Tel Aviv University, 69978 Tel Aviv, Israel

I. G. Kaplan (137), Instituto de Física, Universidad Nacional Autónoma de México, 01000 México, D.F., Mexico

C. Kozmutza (231), Department of Theoretical Physics, Institute of Physics, Technical University of Budapest, Budapest, Hungary

A. I. Kuleff (53), Institute of Nuclear Research and Nuclear Energy, Bulgarian Academy of Sciences, 1784 Sofia, Bulgaria

M. P. de Lara-Castells (37), Instituto de Matemáticas y Física Fundamental, Conséjo Superior de Investigacious Científicas, 28006 Madrid, Spain

J. Maruani (53), Laboratoire de Chimie Physique, Université Pierre et Marie Curie, 75231 Paris Cedex 05, France

J. Mášik (75), Department of Chemical Physics, Faculty of Mathematics and Physics, Comenius University, 842 15 Bratislava, Slovakia

R. McWeeny (15), Dipartimento di Chimica e Chimica Industriale, Università di Pisa, 56100 Pisa, Italy

D. Moncrieff (157), Supercomputer Computations Research Institute, Florida State University, Tallahassee, Florida 32306

T. van Mourik (105), Environmental Molecular Sciences Laboratory, Pacific Northwest Laboratory, Richland, Washington 99352

R. L. Pavlov (53), Institute of Nuclear Research and Nuclear Energy, Bulgarian Academy of Sciences, 1784 Sofia, Bulgaria

E. Pérez-Romero (37), Instituto de Matemáticas y Física Fundamental, Conséjo Superior de Investigacious Científicas, 28006 Madrid, Spain

K. A. Peterson (105), Environmental Molecular Sciences Laboratory, Pacific Northwest Laboratory, Richland, Washington 99352

M. Raimondi (251), Dipartimento di Chimica Fisica ed Elettrochimica, Università di Milano, 20133 Milan, Italy

S. Rettrup (267), Department of Chemistry, Chemistry Laboratory IV, Copenhagen University, DK-2100 Copenhagen, Denmark

J. Rychlewski (173), Department of Chemistry, A. Mickiewicz University, 60-780 Poznan, Poland

A. S. Shalabi (283), Department of Chemistry, Benha University, Benha, Egypt

B. T. Sutcliffe (1), Department of Chemistry, University of York, Heslington, York YO1 5DD, United Kingdom

L. M. Tel (37), Departamento de Química Física, Universidad de Salamanca, Salamanca 37008, Spain

E. Tfirst (231), Central Research Institute of Chemistry of the Hungarian Academy of Sciences, Budapest, Hungary

T. Thorsteinsson (267), Department of Chemistry, Chemistry Laboratory IV, Copenhagen University, DK-2100 Copenhagen, Denmark

C. Valdemoro (37), Instituto de Matemáticas y Física Fundamental, Conséjo Superior de Investigacious Científicas, 28006 Madrid, Spain

I. Vandoni (251), Dipartimento di Chimica Fisica ed Elettrochimica, Università di Milano, 20133 Milan, Italy

A. K. Wilson (105), Environmental Molecular Sciences Laboratory, Pacific Northwest Laboratory, Richland, Washington 99352

S. Wilson (157,283), Rutherford Appleton Laboratory, Chilton, Oxfordshire OX11 0QX, United Kingdom

D. E. Woon (105), Environmental Molecular Sciences Laboratory, Pacific Northwest Laboratory, Richland, Washington 99352

Contributors Volume 32

Numbers in parentheses indicate the pages on which the authors' contributions begin.

C. Amovilli (227), Dipartimento di Chimica e Chimica Industriale, Università di Pisa, 56100 Pisa, Italy

V. Barone (227), Dipartimento di Chimica e Chimica Industriale, Università di Pisa, 56100 Pisa, Italy

M. Bylicki (207), Instytut Fizyki, Uniwersytet Mikolaja Kopernicka, 87-100 Torun, Poland

R. Cammi (227), Dipartimento di Chimica e Chimica Industriale, Università di Pisa, 56100 Pisa, Italy

E. Cancès (227), Dipartimento di Chimica e Chimica Industriale, Università di Pisa, 56100 Pisa, Italy

D. L. Cooper (51), Department of Chemistry, University of Liverpool, Liverpool L69 7ZD, United Kingdom

M. Cossi (227), Dipartimento di Chimica e Chimica Industriale, Università di Pisa, 56100 Pisa, Italy

G. Day (93), Physical and Theoretical Chemistry Laboratory, University of Oxford, Oxford OX1 3QZ, United Kingdom

G. H. F. Diercksen (181), Max Planck Institut für Astrophysik, D-85740 Garching bei München, Germany

A. Famulari (263), Dipartimento di Chimica Fisica ed Elettrochimica, Università di Milano, 20133 Milan, Italy

J. Gerratt (51), School of Chemistry, University of Bristol, Cantocks Close, Bristol BS8 1TS, United Kingdom

E. Gianinetti (263), Dipartimento di Chimica Fisica ed Elettrochimica, Università di Milano, 20133 Milan, Italy

I. P. Grant (1), Mathematical Institute, University of Oxford, Oxford OX1 3LB, United Kingdom

P. J. Grout (93,285), Physical and Theoretical Chemistry Laboratory, University of Oxford, Oxford OX1 3QZ, United Kingdom

M. Hoffmann (109), Department of Chemistry, A. Mickiewicz University, 60-780 Poznan, Poland

A. Kalemos (69), Department of Chemistry, Laboratory of Physical Chemistry, National and Kapodistrian University of Athens, 157 10 Zografou, Athens, Greece

J. Karwowski (181), Instytut Fizyki, Uniwersytet Mikolaja Kopernicka, 87-100 Torun, Poland

G. J. A. Keith (285), Physical and Theoretical Chemistry Laboratory, University of Oxford, Oxford OX1 3QZ, United Kingdom

C. Lavín (181), Departamento de Química Física, Facultad de Ciencias, 47005 Valladolid, Spain

J. Linderberg (315), Department of Chemistry, Aarhus University, DK-8000 Aarhus C, Denmark

A. Maquet (197), Laboratoire de Chimie Physique-Matière et Rayonnement, Université Pierre et Marie Curie, 75231 Paris Cedex 05, France

I. Martin (181), Departamento de Química Física, Facultad de Ciencias, 47005 Valladolid, Spain

A. Mavridis (69), Department of Chemistry, Laboratory of Physical Chemistry, National and Kapodistrian University of Athens, 157 10 Zografou, Athens, Greece

B. Mennucci (227), Dipartimento di Chimica e Chimica Industriale, Università di Pisa, 56100 Pisa, Italy

E. Pérez-Delgado (181), Departamento de Química Física, Facultad de Ciencias, 47005 Valladolid, Spain

C. Petrongolo (127), Dipartimento di Chimica, Università di Siena, I-53100 Siena, Italy

C. S. Pomelli (227), Dipartimento di Chimica e Chimica Industriale, Università di Pisa, 56100 Pisa, Italy

H. M. Quiney (1), Clarendon Laboratory, Department of Physics, University of Oxford, Oxford OX1 3PU, United Kingdom

M. Raimondi (263), Dipartimento di Chimica Fisica ed Elettrochimica, Università di Milano, 20133 Milan, Italy

J. Rychlewski (109), Department of Chemistry, A. Mickiewicz University, 60-780 Poznan, Poland

M. L. Senent (145), Instituto de Estructura de la Materia, CSIC, E-28006 Madrid, Spain

M. Sironi (263), Dipartimento di Chimica Fisica ed Elettrochimica, Università di Milano, 20133 Milan, Italy

H. Skaane (1), Mathematical Institute, University of Oxford, Oxford OX1 3LB, United Kingdom

Y. G. Smeyers (145), Instituto de Estructura de la Materia, CSIC, E-28006 Madrid, Spain

R. Specchio (263), Dipartimento di Chimica Fisica ed Elettrochimica, Università di Milano, 20133 Milan, Italy

A. Szarecka (93,109), Department of Chemistry, A. Mickiewicz University, 60-780 Poznan, Poland

R. Taïeb (197), Laboratoire de Chimie Physique-Matière et Rayonnement, Université Pierre et Marie Curie, 75231 Paris Cedex 05, France

T. Thorsteinsson (51), Department of Chemistry, Chemistry Laboratory IV, Copenhagen University, DK-2100 Copenhagen, Denmark

J. Tomasi (227), Dipartimento di Chimica e Chimica Industriale, Università di Pisa, 56100 Pisa, Italy

I. Vandoni (263), Dipartimento di Chimica Fisica ed Elettrochimica, Universitè di Milano, 20133 Milan, Italy

V. Véniard (197), Laboratoire de Chimie Physique-Matière et Rayonnement, Université Pierre et Marie Curie, 75231 Paris Cedex 05, France

M. Villa (145), Departamento de Química, UAM, Iztapalapa, CP 09340 Mexico, D.F., Mexico

S. Wilson (93,285), Rutherford Appleton Laboratory, Chilton, Oxfordshire OX11 0QX, United Kingdom

R. G. Woolley (167), Department of Chemistry and Physics, Nottingham Trent University, Nottingham NG11 8NS, United Kingdom

Preface

The description of quantum systems is fundamental to an understanding of many problems in chemistry and physics. It is a vibrant field of research in which the countries of Europe have an established tradition of excellence. This volume records a representative selection of the papers delivered at the Second European Workshop on Quantum Systems in Chemistry and Physics. The Workshop was held at Jesus College, Oxford, April 6–9, 1997. The meeting was sponsored by the European Union, as a part of the COST chemistry initiative for stimulating cooperation in science and technology within the states of the European Union and those of Central and Eastern Europe. Workshop participants came from Bulgaria, Denmark, England, Finland, France, Greece, Hungary, Israel, Italy, Mexico, Norway, Poland, Slovakia, Spain, Wales, and the United States.

Like the first Workshop, which was held in San Miniato, near Pisa, Italy, a year earlier, the purpose of the Workshop recorded here was to bring together chemists and physicists with a common interest—the quantum mechanical many-body problem—and to encourage collaboration and exchange of ideas in the fundamentals by promoting innovative theory and conceptual development rather than improvements in computational techniques and routine applications.

The Workshop was opened with a personal view of the status of the quantum mechanical description of systems in chemistry and physics by a leading British authority. Professor Brian T. Sutcliffe, of the University of York, gave a stimulating and often provocative lecture in which he highlighted the formidable problems which stand in the way of further progress in many of the areas addressed during the Workshop. Not all agreed with Sutcliffe's perspective. Indeed, he succeeded in provoking some lively debate. In the article reproduced here, "No alteration has been made from that which was said at the time," since "it seemed honest, if unflattering, to leave things as they were." I am deeply grateful to Professor Sutcliffe for sharing his perspective on the field.

The Workshop was organized into eight sessions, each addressing a different aspect of the quantum mechanical many-body problem. Together with a poster session, the sessions were arranged as follows:

Density matrices and density functionals *(Chair: R. Pauncz)*
Electron correlation effects—Many-body methods and configuration interaction
   (Chairs: U. Kaldor and I. P. Grant)
Relativistic formulations *(Chair: B. T. Sutcliffe)*
Valence theory: Chemical bonds and bond breaking *(Chair: I. G. Kaplan)*

Nuclear motion, vibronic effects, and flexible molecules *(Chair: J. Maruani)*
Response theory—Properties and spectra: Atoms and molecules in strong electric and magnetic fields *(Chair: J. Gerratt)*
Condensed matter: Crystals and clusters, surfaces and interfaces *(Chair: Y. G. Smeyers)*
Reactive collisions and chemical reactions *(Chair: R. G. Woolley)*

A total of 37 lectures were scheduled over a 2½ day period. I express my gratitude to all of the speakers and the participants. They made the Workshop the stimulating and enjoyable experience that it was!

It is a pleasure to thank the members of the scientific organizing committee, Roy McWeeny (Pisa), Jean Maruani (Paris), and Yves G. Smeyers (Madrid), for their enthusiastic support and valuable advice throughout. I am especially grateful to Peter J. Grout (Oxford) for his help with the local organization of the Workshop.

Jesus College was founded in 1571 and is the only Oxford College to date from the Elizabethan period. Indeed, Queen Elizabeth I, who has the title of Foundress, granted timber for the College Buildings. The College provided a splendid venue for the Workshop at the heart of England's oldest University. It is a pleasure to thank the officers and staff of Jesus College, whose tireless attention to detail ensured the comfort of participants throughout the Workshop.

All contributions to this volume were refereed. I am most grateful to Erkki Brändas (Uppsala University) for organizing and executing the refereeing process with impressive proficiency.

Finally, the generous financial support of the European Union COST office is acknowledged. I particularly acknowledge the help with various "administrative details" given by Dr. S. Bénéfice of the COST office in Brussels.

S. WILSON
CHAIR, SCIENTIFIC
ORGANIZING COMMITTEE

Workshop Participants

J. Avery, Department of Chemistry, University of Copenhagen, DK-2100 Copenhagen, Denmark

P. Badger, Department of Chemistry, University of Sheffield, Sheffield, United Kingdom

M. Bylicki, Instytut Fizyki, Uniwersytet Mikolaja Kopernicka, 87-100 Torun, Poland

H. Chojnacki, Institute of Physical and Theoretical Chemistry, I-30, 50-370 Wroclaw, Poland

D. L. Cooper, Department of Chemistry, University of Liverpool, Liverpool L69 7ZD, United Kingdom

G. Day, Physical and Theoretical Chemistry Laboratory, University of Oxford, Oxford OX1 3QZ, United Kingdom

Ya. I. Delchev, Institute of Nuclear Research and Nuclear Energy, Bulgarian Academy of Sciences, 1784 Sofia, Bulgaria

J. Gerratt, School of Chemistry, University of Bristol, Cantocks Close, Bristol BS8 1TS, United Kingdom

E. Gianinetti, Dipartimento di Chimica Fisica ed Elettrochimica, Università di Milano, 20133 Milan, Italy

F. Gianturco, Department of Chemistry, The University of Rome, Città Universitaria, 00185 Rome, Italy

I. P. Grant, Mathematical Institute, University of Oxford, Oxford OX1 3LB, United Kingdom

P. J. Grout, Physical and Theoretical Chemistry Laboratory, University of Oxford, Oxford OX1 3QZ, United Kingdom

I. Hubač, Department of Chemical Physics, Faculty of Mathematics and Physics, Comenius University, 842 15 Bratislava, Slovakia

U. Kaldor, School of Chemistry, Tel Aviv University, 69978 Tel Aviv, Israel

I. G. Kaplan, Instituto de Física, Universidad Nacional Autónoma de México, 01000 México, D.F., Mexico

J. Karwowski, Instytut Fizyki, Uniwersytet Mikolaja Kopernicka, 87-100 Torun, Poland

G. J. A. Keith, Physical and Theoretical Chemistry Laboratory, University of Oxford, Oxford OX1 3QZ, United Kingdom

A. Khoudir, Laboratoire de Chimie Physique, Université Pierre et Marie Curie 75231 Paris Cedex 05, France

S. Kirkpekar, Department of Chemistry, Odense University, DK-5230 Odense M, Denmark

C. Kozmutza, Department of Theoretical Physics, Institute of Physics, Technical University of Budapest, Budapest, Hungary

J. Linderberg, Department of Chemistry, Aarhus University, DK-8000 Aarhus C, Denmark

N. O. J. Malcolm, Department of Chemistry, University of Manchester, Manchester M20 9PL, United Kingdom

A. Maquet, Laboratoire de Chimie Physique-Matière et Rayonnement, Université Pierre et Marie Curie, 75231 Paris Cedex 05, France

I. Martin, Departamento de Química Física, Facultad de Ciencias, 47005 Valladolid, Spain

J. Maruani, Laboratoire de Chimie Physique, Université Pierre et Marie Curie 75231 Paris Cedex 05, France

A. Mavridis, Department of Chemistry, Laboratory of Physical Chemistry, National and Kapodistrian University of Athens, 157 10 Zografou, Athens, Greece

R. McWeeny, Dipartimento di Chimica e Chimica Industriale, Università di Pisa, 56100 Pisa, Italy

A. K. Mohanty, IBM Corporation, Poughkeepsie, New York

T. van Mourik, Environmental Molecular Sciences Laboratory, Pacific Northwest Laboratory, Richland, Washington 99352

C. A. Nicolaides, Physics Department, National Technical University, Athens, Greece

J. M. Oliva, School of Chemistry, University of Bristol, Cantocks Close, Bristol BS8 1TS, United Kingdom

A. Papakondylis, Department of Chemistry, Laboratory of Physical Chemistry, National and Kapodistrian University of Athens, 157 10 Zografou, Athens, Greece

D. Parry, Department of Chemistry, University of Wales, Swansea, Singleton Park, Swansea SA2 8PP, United Kingdom

R. Pauncz, Department of Chemistry, Technion-Israel Institute of Technology, 32000 Haifa, Israel

C. Petrongolo, Dipartimento di Chimica, Università di Siena, I-53100 Siena, Italy

H. M. Quiney, Clarendon Laboratory, Department of Physics, University of Oxford, Oxford OX1 3PU, United Kingdom

M. Raimondi, Dipartimento di Chimica Fisica ed Elettrochimica, Università di Milano, 20133 Milan, Italy

T. T. Rantala, Department of Physical Sciences, University of Oulu, FIN-90571 Oulu, Finland

S. Rettrup, Department of Chemistry, Chemistry Laboratory IV, Copenhagen University, DK-2100 Copenhagen, Denmark

I. Roeggen, Institute of Mathematical and Physical Sciences, University of Tromsø, N-9037 Tromsø, Norway

J. Rothman, Department of Chemistry, Columbia University, New York City, New York 10027

J. Rychlewski, Department of Chemistry, A. Mickiewicz University, 60-780 Poznan, Poland

S. P. A. Sauer, Department of Chemistry, Odense University, DK-5230 Odense M, Denmark

L. Schulz, Institute of Physical and Theoretical Chemistry, I-30, 50-370 Wroclaw, Poland

H. Skaane, Mathematical Institute, University of Oxford, Oxford OX1 3LB, United Kingdom

Y. G. Smeyers, Instituto de Estructura de la Materia, CSIC, E-28006 Madrid, Spain

B. T. Sutcliffe, Department of Chemistry, University of York, Heslington, York YO1 5DD, United Kingdom

A. Szarecka, Department of Chemistry, A. Mickiewicz University, 60-780 Poznan, Poland

J. Tomasi, Dipartimento di Chimica e Chimica Industriale, Università di Pisa, 56100 Pisa, Italy

C. Valdemoro, Instituto de Matemáticas y Física Fundamental, Conséjo Superior de Investigacious Científicas, 28006 Madrid, Spain

I. Vandoni, Dipartimento di Chimica Fisica ed Elettrochimica, Università di Milano, 20133 Milan, Italy

S. Wilson, Rutherford Appleton Laboratory, Chilton, Oxfordshire OX11 0QX, United Kingdom

R. G. Woolley, Department of Chemistry and Physics, Nottingham Trent University, Nottingham NG11 8NS, United Kingdom

Quantum Systems in Chemistry and Physics: Some Hopes and Fears

B. T. Sutcliffe*

Department of Chemistry, University of York, Heslington, York YO1 5DD, England

Abstract

The topics to be discussed at this meeting are surveyed in an attempt to place them in the context of the considerations of our last meeting and of developments since then.

Contents

*bts1@york.ac.uk

1.   Introduction

I have been asked to introduce this, the Second European Work-
shop on *Quantum Systems in Chemistry and Physics*. Many of
you here will remember the first such Workshop which was held
in San Miniato in Tuscany in the spring of 1996. Roy McWeeny
provided the introductory lecture on that occasion and many
here will remember it well. It was a lovely evening, it was a
lovely place and it was a lovely lecture. So, even though the
weather here is good and the college is indeed lovely, I am nat-
urally pretty apprehensive about attempting to emulate him.
This is particularly so, since he is in the Chair of this session
and has so generously introduced me.

   In such circumstances I sometimes imagine myself in the po-
sition of the then Foreign Secretary who found himself subject
to the withering scorn of Aneurin Bevan who, in the Suez debate
in parliament in 1957, felt that the Foreign Secretary was not
in command of his material in the same way that his predeces-
sor (Anthony Eden. who was now Prime Minister) would have
been. Some of you may remember:

> I am not going to spend any time whatsoever at-
> tacking the Foreign Secretary. Quite honestly I am
> beginning to feel extremely sorry for him. If we com-
> plain about the tune, there is no reason to attack the
> monkey when the organ grinder is present.

I plead guilty to being the monkey and since I cannot hope to
carry the tune as well as Roy did, I shall not try. Rather I
shall attempt to dance a little by producing my "wish list" for
the topics that have been chosen for inclusion in our discussions
this week.

   I hope and believe that my wishes have a realistic chance
of fulfilment and I have not, at any rate consciously, wished for
anything quite ridiculous. But that is, of course, for my audience
to judge.

2. Density Matrices and Density Functionals

Simply to look at the literature is to convince yourself of the importance that density functional theory (DFT) methods have attained in molecular calculations. But there is among the molecular physics community, it seems to me, a widespread sense of unease about their undoubted successes. To many it seems quite indecent that such a "cheap and cheerful" approach (to employ Peter Atkins's wonderful phrase) should work at all, let alone often work very well indeed. I think that no-one in the community any longer seriously doubts the Hohenberg-Kohn theorem(s) and anxiety about this is not the source of the unease. As Roy reminded us at the last meeting, the $N-$ representability problem is still unsolved. This remains true and, even though the problem seems to be circumvented in DFT, it is done so by making use of a model system. He pointed out that "the connection between the model system and the actual system remains obscure and in practice DFT, however successful, still appears to contain empirical elements" And I think that is the source of our present unease.

We agree that the *exact* energy of the lowest state can be expressed as a universal functional of the electron density alone. We understand that we can approach an orbital form for this density through the Kohn-Sham ansatz. But there is, as yet, no convincing and useful variational formulation of the problem, which satisfies all the relevant constraints and is applicable when we don't know the exact density. This is not to say that the problem is not well understood: it is reviewed with insight in for example (1) and formal solutions to it have been proposed. But nothing of practical significance has yet emerged. In practice one chooses an exchange-correlation density functional from one of the large selection on offer and performs a self-consistent calculation. One allows orbital variations in much the same way that one would allow them in ordinary SCF calculations and

one feels free to attempt not only the ground state, but also
excited states. And usually, no trouble occurs. We have no
variational upper bound on the exact energy and usually this
doesn't seem to matter. But sometimes it does. Perhaps the
most celebrated and simple example is the failure of a gradient
corrected density functional approach (2) properly to describe
the dissociation of the ground state of He_2^+. In this case, you
will remember, the global energy minimum is *not* at R_e. This
behaviour is in stark contrast to that of an ordinary SCF calcu-
lation which may well dissociate incorrectly and may well give a
wrong dissociation energy but if there is a minimum in the po-
tential curve, it is always less than the energy of the separated
parts. The complete failure of any DFT approach to calculate
satisfactorily the energy and geometry of van der Waals com-
plexes is also well known. If binding is predicted, it is usually
at the level of excessive over-binding. Also well known are the
erratic results of attempts to calculate excited electronic states
and the difficulties of performing sensible property calculations.

Now I should stress that I do not think that it is failure of
DFT methods sometimes to get the "right" answer which is so
unsettling, rather it is that not yet can we always be sure that
we are using a functional that is suitable for the problem that
we have in hand. Unless we have some way of deciding this, then
a DFT approach has some of the same characteristics of general
semi-empirical approaches. Namely, one has to establish their
utility on a class of problems and one's confidence in the results
depends strongly on how closely the problem in hand fits into
the relevant class structure.

What would be nice is a development that enabled us make
in advance, an estimate of the sort of error that there might be in
a particular property when using a particular approach. Now I
certainly don't hope for the moon here. I don't expect a rigorous
variational result or even a perturbation estimate. Rather I hope
for the sort of knowledge that, for example, makes us confident of
a particular outcome for properties calculated using an LCAO-

SCF approach with a given basis. I accept too, that such a development may not take a strictly theoretical form, but could arise from extensive experience suitably codified. And if it does, and it is run up the flagpole, then I shall salute it. But I am not at present able to do that. And I very much want to be able to, for it seems to me that DFT approaches offer by far the best chance of constructing codes in which the effort scales only by N rather than as in conventional codes, by N^m with m at least 2 and usually 3 or 4.

I hope that I may be excused this excursion, for it may be without consequences at this meeting because there seem to be no contributions directly on DFT. However there are to be two talks on density matrix theory (DMT) and it is to this area that I shall turn next. As a graduate student I was fortunate enough to be a pupil of Roy McWeeny and to learn DMT from him and I must confess to a warm regard for DMT springing from that experience. It has always seemed to me to be much the most natural way in which to express results in classical quantum mechanics. The great advantage, in my view, is that it is often possible using DMT to exhibit usefully and in a non-trivial manner the basic structure of a result without assuming a particular approximate form for a wave function. As a consequence of this, it is always possible to regard the result in DMT form as a kind of master equation to be realised in any particular approximation for the wave function. One can therefore develop a systematic program of refinement of approach, if that is desired, or equally well a coarsening of approach if something quick and dirty will do, but all within a single well defined framework. Also from a DMT form for the expected energy, one can develop in well defined way, an effective Hamiltonian formulation of a problem in terms of a smaller number of electrons than in the full problem. I find the DMT approach to effective Hamiltonians more sympathetic than a direct second quantised approach (for a recent paper using this approach (3)) though I recognise that it sometimes helpful to cast the DMT approach in second quantised

form. Although over the years DMT has been used in effective Hamiltonian work, it seems to have failed to capture the general imagination and I regret this. I therefore look forward to the contributions by Roy McWeeny and by Carmela Valdemoro which, I hope will advance this area of endeavour further and hence make it more popular. I particularly hope to lean more of the work recently reviewed by Valdemoro and her coworkers (4).

3. Electron Correlation Effects: Many-Body Methods and Configuration Interaction

It is hard to avoid feeling that electron correlation problems are just like the biblical poor: they are always with us. Each new administration in Quantum Chemistry, just as each new administration in politics, hopes to have a solution to the problem. We have known since the 1970s much about the mathematical behaviour of electronic wave functions in terms of the relative separations between electrons and we know, at least for singlet states, that electronic wave functions should have cusps as electrons approach one another. (The behaviour for triplet states and those of higher multiplicity is not known, but cusp-like behaviour there seems plausible too.) But cusp-like behaviour is extremely difficult to build into approximate wave functions constructed from a discrete basis. A reasonable representation requires an extremely large basis and a very long expansion. It will therefore be extremely interesting to hear the contributions of those (Hubač, Roeggen, Avery, van Mourik, Pauncz) who offer approaches that attempt to mitigate these evils.

Of course the cusp can be represented by including the interparticle distances in a trial wave functions, most simply by means of Jastrow factors, exponentials of the inter-particle distances. But the problems of integral evaluation with such fac-

tors are such that the most that has been attempted directly are small (less than 10 electron) atoms while for molecules either a Monte Carlo method or a method that partially simulates the cusp for integration purpose, has had to be used. I wonder whether the time might not be ripe for another look at the old trans-correlated approach if it is hoped to do anything with cusped wave functions? Perhaps Dr Rychlewski intends to touch on this matter when he talks and I shall be most interested to see to what extent other speakers cover this ground.

But this section of our meeting gives me much unease. I seem to have heard so many talks on electron correlation over the years that now I feel rather like Omar Khayyam who said (in the Fitzgerald translation) you remember,

> Myself when young did eagerly frequent
> Doctor and Saint and heard great Argument
> About it and about: but evermore
> Came out by the same Door as in I went.

May I be proved too pessimistic by what we hear later.

4.   Relativistic Formulations

Methods for treating relativistic effects in molecular quantum mechanics have always seemed to me, if I may say so without appearing too impertinent to those who work in the field, a complete dog's breakfast. The difficulty is to know to what question they are supposed to be the answer, in the circumstances in which we find ourselves. We do not know what a relativistically invariant theory applicable to molecular behaviour might look like. As was pointed out to us at the last meeting, the Dirac equation certainly will not do to describe interacting electrons and even at the single particle level, where it seems to work, there is an inconsistency in interpreting its solutions in terms

of electron-positron pairs. But we have to do something, for we know that we have to take relativistic effects into account and not only for heavy atoms. The something that we have to do must use perturbation theory, but straightforward use of perturbation theory leads to divergences even when 4-component spinors are used. Much of the discussion at our last meeting was devoted to describing ways in which these divergences could be avoided, with notable contributions by Kutzelnigg, Snijders and Kellö. The talks at this meeting do not appear to be concerned with such technical problems. Can it be that all has been sorted out over the past year or so? Certainly that would be good news and I look forward greatly to the session in which these matters are to be discussed. My hopes here are that we are making progress, but I am afraid that, given the confused nature of the theory, progress might not be so easy to discern.

5. Valence Theory:Chemical Bonds and Bond Breaking

When I was an undergraduate I remember going to a lecture at which a distinguished visiting Professor explained to us all that the picture of bonds provided by valence bond (VB) theory was totally different from that provided by molecular orbital (MO) theory and that, any way, we were not to worry because both theories were utter rubbish. Even as a naive 19 year old, I did rather smell a rat. A couple of years later on I learned that the best way to look at the two theories was to regard them as limiting cases of a particular category of orbital approach. The difficulty with the VB approach was that it did not at all easily computable even using the digital computers that were then beginning to become available. It was thus hard to know whether or not a particular structural assertion made in the theory could be supported or if it had only a metaphysical significance. The MO approach on the other hand proved to be

eminently computable and thus came to dominate descriptions of valence and bonding, a dominance that has persisted until very recently. Among those who have been most responsible for the revival and development of VB type theories are Dr Gerratt and, following him, Dr Cooper and it is therefore with considerable interest that one anticipates their talks. And one wonders now, what approach Dr Mavridis is going to use in his calculation on ScB^+. Only a year or two ago one could have been absolutely certain that it would have been an MO one.

I hope that at the end of the session we shall have a clear view of what is now possible in valence theory, particularly when considering bond-breaking and that we are in possession of some new computational tools. And here my hopes are high.

6. Nuclear Motion, Vibronic Effects and Flexible Molecules

My hopes and fears here centre on the problems that arise in effectively defining a potential energy surface. Because I believe that this definition is central to thinking about reactive processes too, I shall defer most of my consideration for that section. That said however, there is no doubt that Dr Petrongolo has had great quantitative success in his treatment of flexible triatomics using a potential surface approach. And the idea of a single surface underlies the successful approach of Prof. Smeyers and his co-workers to the spectroscopy of flexible organic molecules. There can be no doubt that a potential surface view of this class of problems can be made to work but I am remain puzzled as to why it does. But perhaps that will turn out to be my failure to understand rather than any problems with the theory, that is the cause of my puzzlement.

7. Response Theory-Properties and Spectra: Atoms and Molecules in Strong Fields

It is usual to regard those who work using propagator theory and Green's function methods as the guardians of molecular response theory. However in this meeting, to judge from the titles of the talks, these approaches are not used in the work to be described. Could it be perhaps that other methods are beginning to find favour when considering molecular properties? For this, if for no other reason this promises to be an intriguing session. If I may, without seeming invidious, confess to my own special interests here. I'd like to learn of the methods used in core and the Rydberg calculations and those used in the non-linear optical work. The talk on H^- is also one to look forward to, for even in the absence of a field the system has only a single bound state and I simply do not know if it has any at all in the presence of a magnetic field. So I can't wait to find out what the states under investigation here are doubly excited *from*.

I suppose that in this area I am a bit like Mr Micawber in Charles Dickens's *David Copperfield*, I am always hoping that something will turn up, though I'm not too sure what it might be.

8. Condensed Matter Theory:Crystals and Clusters, Surfaces and Interfaces

In considering condensed matter I confess to being very pessimistic indeed. I suppose that if I hoped for anything here, it would be that it would go away. I simply see no way of dealing with the problems raised by the vast numbers of particles involved, with anything like the techniques that we can use for

small molecules. (Except perhaps in periodic systems where we might hope to use Hartree-Fock type approaches with suitable boundary conditions.) I see no chance of considering clusters of sufficient size for the results of calculations on them to yield spontaneously, condensed matter characteristics. I have even less hope of us dealing with liquids and with solvent-solute interactions by standard methods. So though I look forward with keen interest to this session, that interest is tinged with apprehension. It seems to me that we must simply face up to the fact that in this area we have no alternative but to build models that are plausibly connected with molecular quantum theory and do what we can with these. A reductionist program here is just out of the question.

9. Reactive Collisions and Chemical Reactions

In considering reactions (and, from above, flexible molecules) I shall simply stick my neck out. I am very doubtful that we shall get anywhere at all using molecular quantum mechanics, as long as we keep to the potential energy surface view of the problem. The assumption is that potential energy surfaces can be got from a sequence of clamped nuclei calculations and that the flexible molecule or the reacting molecule can be described in terms of nuclear motion on one or more of these surfaces. Now I have no doubt that one can get explanations of experimental phenomena in these terms, but I do not think that one can associate the underlying picture properly with the standard molecular Hamiltonian for the full problem. To see this one has only to realise that to perform a clamped nuclei calculation, one has to identify as separate entities, nuclei that are identical particles (the protons in ammonia, for example). The potential energy surface therefore carries nuclear labels and these are not usually removed by any symmetrising process in any subsequent

nuclear motion calculations. Thus one is solving an improperly posed problem in the vast majority of cases. This is not even to consider what might be the significance of solutions even to this ill-posed problem when surfaces cross.

I understand perfectly that if we are dealing with very large molecules or with complicated reacting systems, then we have no alternative but to deal with a model, as we must do in considering condensed matter. I also understand, as I mentioned above, that there is no doubt that the potential surface model can be used to account for experiment in a convincing and sometimes near quantitative way. However I don't think that we really know why this is and that we need to try and see, in some simple systems, if we can find out. So naturally it is my hope that some of the contributions in this session will try to deal with this.

10.   Postscript

In what has gone before, no alteration has been made from that which was said at the time. There are, of course, some things that I would wish to have changed and some statements that I would have wished not to have made. But since colleagues may in their presentations here, have included their responses to my un-wisdom, much as they were made in the discussion after the introduction and in their talks, it seemed honest if unflattering, to leave things as they were.

References

(1) E. Kryachko and E Ludeña, *Energy Density Functional Theory of Many-Electron Systems*, Kluwer, Dordrecht (1990).

(2) R. Merkle, A Savin and H. Preuss, *J. Chem. Phys* **97**, 9216-9221 (1992).

(3) S. Y. Lee and K. F. Freed, *J. Chem Phys*, **104**, 3260-3275 (1996)

(4) C. Valdemoro, L. M. Tel and E Pérez-Romero, *Adv. Quant. Chem.*, **28**, 33-46 (1997)

Separability of Quantum Systems: A Density Matrix Approach

Roy McWeeny

Dipartimento di Chimica e Chimica Industriale,
Via Risorgimento 35, 56100 Pisa, Italy

Abstract

The idea of 'separability' is concerned with the quantum mechanical description of systems in which it is possible to recognize experimentally the presence of certain 'structural units', each with a 'personal' identity. This idea is formulated mathematically in terms of 'group functions', each referring explicitly only to the electrons of one group in the field of the others. The density matrices for the whole system are expressible in terms of those of the separate groups and global optimization of the wavefunction is reduced to an iterative optimization involving only one group at a time: this provides a basis for many experimental 'additivity rules'. The feasibility of extending the approach to admit relativistic effects is also examined.

Contents

1   Introduction

A general quantum system may be described as 'separable' when the wavefunction can be represented , with high precision, as an antisymmetrized product of the form

$$\Psi_{A,B,\dots}(\mathbf{x}_1, \mathbf{x}_2, \dots \mathbf{x}_N) = M\hat{A}[\Phi_A(\mathbf{x}_1, \dots \mathbf{x}_{N_A})\Phi_B(\mathbf{x}_{N_A+1}, \dots \mathbf{x}_{N_A+N_B})\dots]. \quad (1)$$

Here $\hat{A}$ is the antisymmetrizer for all particles and any given factor Φ_R, for subsystem R, describes the state of a 'group' of N_R electrons. This *ansatz* is a 'generalized product function' [1] – analogous to a Slater determinant, but with each spin-orbital replaced by a many-electron function.

No *exact* wavefunction can be written in this way: neither electrons nor basis functions (i.e. the 'global set' from which the whole function Ψ is constructed) can be uniquely divided out among the subsystems (A,B,...R,...). Application of $\hat{A}$ ensures that the Pauli principle is satisfied and that no particular group of electrons 'belongs' to any specific subsystem; but the possibility of separating the *basis* into subsets which can each describe one subsystem with high accuracy raises delicate questions of overcompleteness. To avoid such problems it is desirable to *truncate* the function space associated with each group of particles, to eliminate excessive overlap between the functions of different groups. When the truncated sets describing different groups are mutually orthogonal, the subsystem wavefunctions will be *strong orthogonal*.

For separable systems with strong-orthogonal groups, with which this work is concerned, the density matrices of the whole system are readily expressed in terms of those for its component parts – the subsystems. In this way, calculations of the electronic structure and properties of a large many-electron system may be reduced to a series of similar calculations on the smaller subsystems. In the earliest work along such lines [1,2,3], the separation into subsystems was defined *a priori* by partitioning a global basis set into subsets, each considered adequate for the description of a particular part of the whole system. Such a procedure is often unsatisfactory (e.g. in the study of chemical reactions, where the subsystems representing reactants and products may have quite different forms, which change continuously during the reaction process): ideally, the definition of the subsystems should arise 'automatically' as a result of optimization of the wavefunction for the entire system.

The purpose of the present work is to show how global optimization of a wavefunction of group-function form can be achieved and to discuss some of the general implications of separability, particularly those that relate to so-called 'additivity rules'. A second aim is to sketch a generalization of the

approach to admit relativistic effects, which become very important when one or more of the groups contain heavy atoms. Density matrix theory provides a natural framework for all such developments and is fully reviewed elsewhere [2,4].

2 Density functions for separable systems

First let us recall the more important electron distribution functions and their origin in terms of corresponding density matrices. The electron probability density ('number' density in electrons/unit volume) is the best known distribution function: others refer to a pair of electrons, or a cluster of n electrons, simultaneously at given points in space.

For a completely general wavefunction, the electron density (P) is

$$P(\mathbf{r}) = N \int \Psi(\mathbf{x}, \mathbf{x}_2, \dots \mathbf{x}_N) \Psi^*(\mathbf{x}, \mathbf{x}_2, \dots \mathbf{x}_N) ds d\mathbf{x}_2 \dots d\mathbf{x}_N \qquad (2)$$

where $\mathbf{x}_i = \mathbf{r}_i, s_i$ and the spin variables have been 'integrated away'. $P(\mathbf{r})$ is in fact the 'diagonal element', $P(\mathbf{r}) = P(\mathbf{r}; \mathbf{r})$, of the (spinless) 1-electron density *matrix* $P(\mathbf{r}; \mathbf{r}')$, in which the $\mathbf{r}$ of Ψ^* in (2) is replaced by a second variable $\mathbf{r}'$.

$P(\mathbf{r}; \mathbf{r}')$ is derived from a density matrix $\rho(\mathbf{x}; \mathbf{x}')$ with spin included: namely

$$\rho(\mathbf{x}; \mathbf{x}') = N \int \Psi(\mathbf{x}, \mathbf{x}_2, \dots \mathbf{x}_N) \Psi^*(\mathbf{x}', \mathbf{x}_2, \dots \mathbf{x}_N) d\mathbf{x}_2 \dots d\mathbf{x}_N.$$

Thus, identifying s', s and integrating,

$$P(\mathbf{r}; \mathbf{r}') = \int_{s'=s} \rho(\mathbf{x}; \mathbf{x}') ds. \qquad (4)$$

An important property of the density matrices ρ and P, with and without spin, is that they provide simple and general expressions for the expectation values of all 1-electron quantities, for any type of system and any type of wavefunction: thus the total potential and kinetic energies (not depending on spin) are expressible as

$$V_{en} = <V> = \int V(\mathbf{r}) P(\mathbf{r}) d\mathbf{r}, \qquad <T> = \int_{\mathbf{r}'=\mathbf{r}} \frac{\hat{p}^2}{2m} P(\mathbf{r}; \mathbf{r}') d\mathbf{r}, \qquad (5)$$

where $V(\mathbf{r})$ and $\hat{p}^2/2m$ are the potential and kinetic energy operators for a single electron at point $\mathbf{r}$. When the 'operator' is merely a multiplicative factor, the off-diagonal quantity (with $\mathbf{r}' \neq \mathbf{r}$) is not required and $< V >$ is thus simply a *functional* of the electron density $P(\mathbf{r})$.

For operators that work also on spin variables, the expectation values are given by equations analogous to (5) except that P is replaced by ρ and the integrations are over $\mathbf{x}$ (i.e. both $\mathbf{r}$ and s) instead of $\mathbf{r}$ alone. Thus, the total spin z component has an expectation value

$$< \hat{S}_z >= \int_{\mathbf{x}'=\mathbf{x}} \hat{S}_z \rho(\mathbf{x}; \mathbf{x}') d\mathbf{x} = \int Q_z(\mathbf{r}; \mathbf{r}) d\mathbf{r}, \qquad (6)$$

where

$$Q_z(\mathbf{r}; \mathbf{r}') = \int [\hat{S}_z \rho(\mathbf{x}; \mathbf{x}')]_{s'=s} ds \qquad (7)$$

and only the diagonal element appears in (6) because no *spatial* operator is present and the variables $\mathbf{r}, \mathbf{r}'$ may thus be identified immediately. The function $Q_z(\mathbf{r}) = Q_z(\mathbf{r}; \mathbf{r})$ is usually referred to as the *spin density*, being the density of spin angular momentum around the z axis in units of $\hbar$; but it must be remembered that Q_z is only one component of a *pseudovector* density (angular momentum per unit volume), the other components $Q_x(\mathbf{r}), Q_y(\mathbf{r})$ being defined by equations analogous to (7).

It may be noted that the general form of $\rho(\mathbf{x}; \mathbf{x}')$ is

$$
\begin{aligned}
\rho(\mathbf{x}; \mathbf{x}') &= P_{\alpha,\alpha}(\mathbf{r}; \mathbf{r}')\alpha(s)\alpha^*(s') + P_{\alpha,\beta}(\mathbf{r}; \mathbf{r}')\alpha(s)\beta^*(s') \\
&+ P_{\beta,\alpha}(\mathbf{r}; \mathbf{r}')\beta(s)\alpha^*(s') + P_{\beta,\beta}(\mathbf{r}; \mathbf{r}')\beta(s)\beta^*(s'),
\end{aligned} \qquad (8)
$$

and that this may be regarded as the integral kernel representing the density *operator* $\hat{\rho}$, whose effect on any space-spin function $\psi(\mathbf{x})$ is determined by

$$\hat{\rho}\psi(\mathbf{x}) = \int \rho(\mathbf{x}; \mathbf{x}')\psi(\mathbf{x}') d\mathbf{x}'. \qquad (9)$$

For a system in a state of definite spin, with good quantum numbers S, M_S, only the first and last terms in (8) are non-zero; and in this case it follows that[1]

$$Q_z(\mathbf{r}) = \tfrac{1}{2}[P_\alpha(\mathbf{r}) - P_\beta(\mathbf{r})], \qquad (10)$$

---

[1] When the second variable $\mathbf{r}'$ is suppressed it is convenient also to omit the second spin index; thus $P_{\alpha\alpha} \rightarrow P_\alpha$, etc.

the components perpendicular to the axis of quantization (z) being everywhere zero.

One other 1-electron density is of great importance – the *current density* $\mathbf{J}(\mathbf{r})$, which is again a pseudovector density. This is everywhere zero until we apply an infinitely weak magnetic field, so as to define a quantization axis and to introduce an imaginary term in the wavefunction Ψ. The usual kinetic energy operator in the Hamiltonian is then replaced by

$$\hat{T} = (1/2m)\sum_i \hat{\pi}^2(i), \qquad \hat{\pi}_\lambda = \hat{p}_\lambda + eA_\lambda \qquad (\lambda = x, y, z), \qquad (11)$$

where $\hat{\pi}$ is the 'gauge invariant momentum' and contains the vector potential $\mathbf{A}$ of the field. The components of the *current density matrix* are then written most symmetrically as

$$J_\lambda(\mathbf{r}) = m^{-1}[\tfrac{1}{2}(\pi_\lambda + \pi'^\dagger_\lambda)P(\mathbf{r}; \mathbf{r}')]_{\mathbf{r}'=\mathbf{r}}, \qquad (12)$$

where the adjoint operator $\pi'^\dagger_\lambda$ works on the *primed* variables in the density matrix.

The diagonal element $J_\lambda(\mathbf{r})$, has all the properties of a *local* flux density at point $\mathbf{r}$, as defined in classical physics. In particular, for a wavefunction satisfying the time-dependent Schrödinger equation, it is easy to derive a conservation equation for the electron density:

$$\text{div } \mathbf{J}(\mathbf{r}) = -\frac{\partial \mathbf{P}(\mathbf{r})}{\partial t} \qquad (13)$$

– the rate of decrease of the probability of finding an electron in volume element $d\mathbf{r}$ at point $\mathbf{r}$ is the divergence of the current density at that point. For a system in a stationary state the currents must be *circulating* (div $\mathbf{J}$ = 0); and these induced currents (created by the external field) produce a secondary magnetic field, with components at point $\mathbf{r_0}$

$$B^{\text{ind}}_\lambda(\mathbf{r_0}) = \left(\frac{\mu_0}{4\pi}\right) \int \frac{[(\mathbf{r} - \mathbf{r_0}) \times \mathbf{J}(\mathbf{r})]_\lambda}{|\mathbf{r} - \mathbf{r_0}|^3} d\mathbf{r} \qquad (14)$$

– just as if the electron distribution were a conducting medium containing electric currents of density $-e\mathbf{J}(\mathbf{r})$.

Another interesting property of the current density is that the total electronic energy of an arbitrary system in the presence of any external field whatever, with vector potential $\mathbf{A}$, may be written [5]

$$E = E_0 - \int \mathbf{A} \cdot [-\mathbf{e}\mathbf{J_0}(\mathbf{r})]d\mathbf{r} - \tfrac{1}{2}\mathbf{A} \cdot [-e\mathbf{J}_{\text{ind}}(\mathbf{r})]d\mathbf{r} \qquad (15)$$

Here E_0 and $\mathbf{J_0}$ are the energy and current density in the zero-field limit ($\mathbf{J_0}$ vanishing except for systems of high symmetry in states with unquenched angular momentum e.g. paramagnetic atoms), while $\mathbf{J}_{\text{ind}}$ is the field-linear part of the current density and therefore describes the currents *induced* by the applied field. The two field-dependent terms in (15) represent, respectively, the potential energy of a system of 'permanent' electric currents, of density $-e\mathbf{J_0}(\mathbf{r})$, and that of a system of induced currents, of density $-e\mathbf{J}_{\text{ind}}(\mathbf{r})$, in a conducting medium in the presence of a field – as would be calculated from classical physics.

There are useful two- and many-electron analogues of the functions discussed above, but when the Hamiltonian contains only one- and two-body operators it is sufficient to consider the 'pair' functions: thus the analogue of $\rho(\mathbf{x}; \mathbf{x}')$ is the *pair* density matrix $\pi(\mathbf{x}_1, \mathbf{x}_2; \mathbf{x}_1', \mathbf{x}_2')$; while that of $P(\mathbf{r}; \mathbf{r}')$, which follows on identifying and integrating over spin variables as in (4), is $\Pi(\mathbf{r}_1, \mathbf{r}_2; \mathbf{r}_1', \mathbf{r}_2')$. When the electron-electron interaction is purely coulombic, only the diagonal element $\Pi(\mathbf{r}_1, \mathbf{r}_2)$ is required and the expression for the total interaction energy becomes

$$V_{\text{ee}} = \tfrac{1}{2}\int g(1,2)\Pi(\mathbf{r}_1, \mathbf{r}_2)d\mathbf{r}_1 d\mathbf{r}_2. \qquad (16)$$

As in (8), $\pi(\mathbf{x}_1, \mathbf{x}_2; \mathbf{x}_1', \mathbf{x}_2')$ can be expressed as a sum of terms corresponding to different spin situations:

$$
\begin{aligned}
\pi(\mathbf{x}_1, \mathbf{x}_2; \mathbf{x}_1', \mathbf{x}_2') = {} & \Pi_{\alpha\alpha,\alpha\alpha}(\mathbf{r}_1, \mathbf{r}_2; \mathbf{r}_1', \mathbf{r}_2')\alpha(s_1)\alpha(s_2)\alpha(s_1')\alpha(s_2') \\
& +\Pi_{\alpha\alpha,\alpha\beta}(\mathbf{r}_1, \mathbf{r}_2; \mathbf{r}_1', \mathbf{r}_2')\alpha(s_1)\alpha(s_2)\alpha(s_1')\beta(s_2') \\
& +\ldots\ldots\ldots+ \qquad\qquad\qquad\qquad\qquad\quad (17)\\
& +\Pi_{\beta\beta,\beta\beta}(\mathbf{r}_1, \mathbf{r}_2; \mathbf{r}_1', \mathbf{r}_2')\beta(s_1)\beta(s_2)\beta(s_1')\beta(s_2').
\end{aligned}
$$

Of the 16 terms, only 6 are non-zero in a state of definite spin and of these only 4 survive the spin integrations that lead to $\Pi(\mathbf{r}_1, \mathbf{r}_2; \mathbf{r}_1', \mathbf{r}_2')$. The spinless

pair density (diagonal element) is thus, omitting primed variables and the corresponding spin indices as in (10) *et seq.*,

$$\Pi(\mathbf{r}_1, \mathbf{r}_2) = \Pi_{\alpha\alpha}(\mathbf{r}_1, \mathbf{r}_2) + \Pi_{\alpha\beta}(\mathbf{r}_1, \mathbf{r}_2) + \Pi_{\beta\alpha}(\mathbf{r}_1, \mathbf{r}_2) + \Pi_{\beta\beta}(\mathbf{r}_1, \mathbf{r}_2), \qquad (18)$$

in which each term has a clear physical interpretation. For example, $\Pi_{\alpha\beta}(\mathbf{r}_1, \mathbf{r}_2)$ is a probability density for finding an 'up-spin' electron at point $\mathbf{r}_1$ and a 'down-spin' electron simultaneously at point $\mathbf{r}_2$. Other pair densities can be defined [6] and are useful for discussing spin-coupling effects [7], but are not required in the present work.

The beauty of the above results is that, apart from the use of a non-relativistic Born-Oppenheimer Hamiltonian, *no approximations have been made*: the density functions are all rigorously derivable, in principle, from an exact wavefunction containing no orbital approximations and remain valid for any system at any level of approximation.

The only approximation to be admitted at this stage will be that inherent in the separability *ansatz* (1) with the constraint of strong orthogonality. In this case there is a corresponding separability of the density functions, embodied in two theorems [1,2]: for a separable system, comprising subsystems A, B, .. R, .. , the one-body density matrix (spin included) takes the form

$$\rho(\mathbf{x}_1; \mathbf{x}_1') = \sum_R \rho_R(\mathbf{x}_1; \mathbf{x}_1'), \qquad (19)$$

while the corresponding two-body quantity becomes

$$\begin{aligned} \pi(\mathbf{x}_1, \mathbf{x}_2; \mathbf{x}_1', \mathbf{x}_2') &= \sum_R \pi_R(\mathbf{x}_1, \mathbf{x}_2; \mathbf{x}_1', \mathbf{x}_2') \\ &+ \tfrac{1}{2} {\sum_{R,S}}' [\rho_R(\mathbf{x}_1; \mathbf{x}_1')\rho_S(\mathbf{x}_2; \mathbf{x}_2') - \rho_R(\mathbf{x}_2; \mathbf{x}_1')\rho_S(\mathbf{x}_1; \mathbf{x}_2')]. \end{aligned} \qquad (20)$$

In dealing with quantities whose associated operators do not act on spin variables, we may use (4) and its two-electron analogue to derive parallel results for the spin-free densities. It is necessary only to change lower-case letters to upper-case ($\rho \to P$ and $\pi \to \Pi$), to replace variables $\mathbf{x}$ by $\mathbf{r}$, and (in the usual case where not more than one group is in a state of non-zero total spin), to put a factor $\tfrac{1}{2}$ before the exchange term in (20).

These results are of very general significance: in particular, the one-body density matrix for the whole system, with or without inclusion of spin, is a

sum of those for its constituent parts. As a consequence, the electron density becomes

$$P(\mathbf{r}) = \sum_R P_R(\mathbf{r}) \tag{21}$$

-- a simple superposition of the electron densities of the separate groups. The pair density, on the other hand,

$$\Pi(\mathbf{r}_1, \mathbf{r}_2) \;\; = \;\; \sum_R \Pi_R(\mathbf{r}_1, \mathbf{r}_2) \tag{22}$$

$$+\tfrac{1}{2}{\sum_{R,S}}'[P_R(\mathbf{r}_1)P_S(\mathbf{r}_2) - \tfrac{1}{2}P_R(\mathbf{r}_2; \mathbf{r}_1)P_S(\mathbf{r}_1; \mathbf{r}_2)].$$

-- a superposition of pair functions for the individual groups, plus inter-group terms which determine both a coulomb repulsion between their electron densities and an 'exchange' term which involves *off*-diagonal elements of the one-electron density matrices.

The significance of (18) is immediate: it provides a basis for a large number of additivity rules. Not only does it yield the electron density in the form (20), but also (by use of (7) and (12)) the spin density and the current density, all such functions being expressed as sums of strictly additive contributions from the separate electron groups. Observable molecular properties that depend only on these densities (including molecular electric moments, electric and magnetic fields due to charge and current distributions within the molecule, magnetic susceptibility, and many other properties) must all be expressible as sums of contributions from the separate groups.

Formally, the above results depend only on strong orthogonality; but separability is a valid and useful concept only when the ansatz (1) is variationally optimized. The optimization problem is considered in the next Section.

3   Optimization of the wavefunction

The possibility of a group-by-group optimization of the wavefunction of the whole system is a direct consequence of the reductions described in Sect.2. Thus, using (19) and (20), it follows that the contributions to $< T >, V_{en}, V_{ee}$ all comprise terms referring to groups (R) and pairs of groups (R,S). The total energy may then be written

$$E = \sum_R E_R + \tfrac{1}{2} \sideset{}{'}\sum_{R,S} E_{RS} = E_R^{\text{eff}} + \sum_{S(\neq R)} E_S, \qquad (23)$$

where, in the second form, all the interaction terms have been associated with one particular group R to give an 'effective' energy for that group in the field provided by all others. The wavefunction for the whole system may then be optimized by variation of each group function Φ_R, subject to orthogonality constraints, by minimizing each E_R^{eff} in turn – the final sum in (21) being independent of Φ_R. The procedure will of course be iterative: an 'improved' function Φ_R will be calculated for each group in turn, the *ansatz* (1) being revised at the end of the cycle; any slight loss of strong-orthogonality (the improved orbitals of different groups no longer being strictly orthogonal) may be eliminated by a symmetric orthogonalization; and the next cycle will begin. At convergence, the energy will be stationary with respect to variation of all Φ_R and all strong-orthogonality constraints will be satisfied. In this way the optimization of the wavefunction for a large number of particles (N) is reduced to a number of single-group optimizations, each involving only N_R electrons at a time.

Details of the effective Hamiltonian are available in the literature [2,4] and it is sufficient to put on record the key equations: the explicit form of the group energy E_R^{eff} is

$$\begin{aligned} E_R^{\text{eff}} &= \; < \hat{H}_R^{\text{eff}} > \qquad (24) \\ &= \; < |\sum_{i=1}^{N_R} \hat{H}_R^{\text{eff}}(i) + \tfrac{1}{2} \sum_{i,j=1}^{N_R} g(i,j) | >, \end{aligned}$$

and refers explicitly *only to the N_R electrons of group* R. The effective *one-electron* Hamiltonian $\hat{H}_R^{\text{eff}}$ in (24) is obtained by adding to the usual $\hat{H}$ the 'other-group' coulomb-exchange terms, thus:

$$\hat{H}_R^{\text{eff}}(i) = \hat{H}(i) + \sum_{S(\neq R)} [\hat{J}_S(i) - \hat{K}_S(i)], \qquad (25)$$

where the J and K operators have the general effect

$$\begin{aligned} \hat{J}_S \psi(\mathbf{x}_1) &= \left[\int g(1,1') \rho_S(\mathbf{x}_1'; \mathbf{x}_1') d\mathbf{x}_1' \right] \psi(\mathbf{x}_1) \qquad (26) \\ \hat{K}_S \psi(\mathbf{x}_1) &= \int g(1,1') \rho_S(\mathbf{x}_1; \mathbf{x}_1') \psi(\mathbf{x}_1') d\mathbf{x}_1'. \end{aligned}$$

In the preceding equations, $\psi(x)$ indicates a general function of space-spin variables ($\mathbf{x} = \mathbf{r}, s$): when the operators do not involve spin, the integrations over spin may be completed immediately to give similar results with ρ_S replaced by P_S and (in the usual case of a group with total spin zero) a factor $\frac{1}{2}$ in front of the exchange term. The term in square brackets in (23) then yields the potential energy of an electron at point $\mathbf{r}$ in the field of the electron distribution, of density $P_S(\mathbf{r}_1')$, of group S: the exchange term, involving an *off*-diagonal density matrix element, is usually rather small.

Let us consider a two-group system as a simple example, comprising a set of N_{val} 'valence' electrons in the presence of N_{val} 'valence' electrons. The practical implementation of the optimization will proceed as follows:

• Set up a 'global' basis $\{\chi_1, \chi_2, ...\}$ of N_b basis functions and divide the global space into three subspaces: (i) N_{cor} functions of a core space; (ii) N_{val} functions of a valence space; and N_{com} functions of a complementary subspace.

The initial separation is provisional and defines only a starting approximation, which will afterwards be systematically revised.

• Express the orbitals as $\phi = \chi\mathbf{T}$, where the transformation matrix $\mathbf{T}$ will take the block form

$$\mathbf{T} = (\mathbf{T}_{\text{cor}}|\mathbf{T}_{\text{val}}|\mathbf{T}_{\text{com}})$$

and use projection matrices to impose subspace orthogonality. The valence orbitals (represented by the columns of $\mathbf{T}_{\text{val}}$) then become orthogonal to the core orbitals (in the original ($\mathbf{T}_{\text{cor}}$); and, finally, orthogonalize the orbitals of the complementary space against both core and valence sets. The core and valence groups in $\Psi = \hat{A}[\Phi_{\text{cor}}\Phi_{\text{val}}]$ then become strong-orthogonal.

• Calculate the density matrices $\mathbf{p}_{\text{cor}}, \mathbf{p}_{\text{val}}$, and then construct the effective Hamiltonian for each group in the field of the other, using equation (23) and the spinless forms of (24)

• Optimize each group function, maintaining strong-orthogonality, and store the required corrections $\delta\mathbf{T}_{\text{cor}}, \delta\mathbf{T}_{\text{val}}$. It is evident that the constrained variation $\delta\mathbf{T}_{\text{cor}}$, must be orthogonal to the valence space and will thus arise by admixture of the columns of $\mathbf{T}_{\text{cor}}$ and $\mathbf{T}_{\text{com}}$; and that a similar variation $\delta\mathbf{T}_{\text{val}}$ may be obtained simply by reversing the roles of 'cor' and 'val'.

• At the end of the cycle update the full matrix $\mathbf{T}$ by making all corrections simultaneously, noting that this will result in a slight loss of strong-orthogonality.

• Start a new cycle, restoring strong-orthogonality, as above; and continue to convergence

This procedure is simple and robust and applies equally to a many-group system. Moreover, the group functions may be of arbitrary form: it is necessary only that the 1-electron density matrix can be calculated for each one. In the present context, for example, a core function of Hartree-Fock form may be used along with a valence function of VB form, thus allowing for correct dissociation of the system when its constituent groups are removed to infinity.

To illustrate the viability of the optimization procedure, two examples will suffice: both relate to molecular dissociation, in which the form of the valence group changes completely as the reaction proceeds, while the atomic cores of the various atoms (all comprised in the core group) are much less strongly affected.

Example 1. Dissociation of H_2O by symmetric stretch
Reference calculations are first performed at equilibrium geometry, using a simple basis of contracted gaussian functions [8]. The molecule is then dissociated by symmetric stretch, energies being calculated at bond length intervals of $\Delta R = 0.2R_e$ up to $R = 6.0R_e$ (where dissociation is effectively complete).

A standard closed-shell SCF calculation is used to obtain orbitals of type 1s and $2p_y$ (normal to the plane), which define an oxygen 'core'. In a 'frozen core' approximation, these orbitals are held fixed (i.e. no further optimization is performed. The remaining valence electrons are then described using a VB wavefunction consisting of just *two* covalent structures, these being sufficient in at least a qualitative sense [9] to describe dissociation in which the oxygen will be left in its triplet ground state. For every geometry, a global optimization of both core and valence orbitals is performed, using the method indicated above.
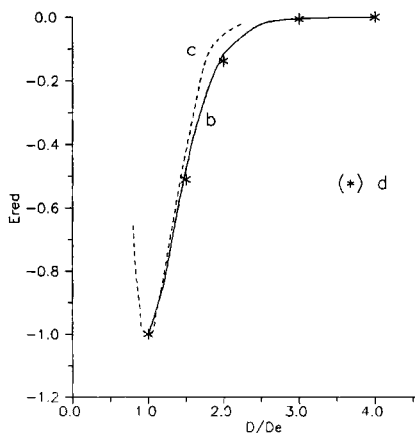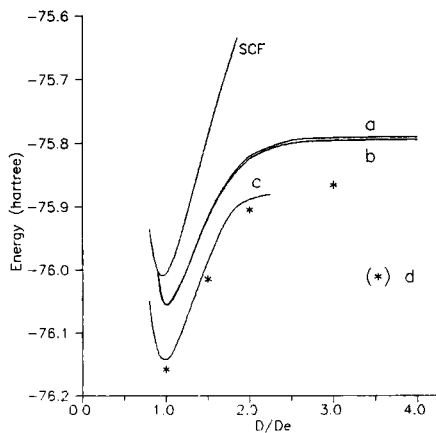
Fig.1:   PE curves for H_2O Fig.2:   Reduced curves for H_2O

Curve (a) in Fig.1 refers to the frozen core approximation; Curve (b) shows the effect of core optimization – which is evidently appreciable, though not large – as the core returns to its free-atom form. Another significant feature of both calculations is the growing importance, as R increases, of the second structure, in which the spin pairing in the bonds is replaced by that between the hydrogen atoms and within the oxygen atom; when the bonds are stretched to several times their normal length the structure coefficient ratio approaches 1:2. It is easily verified that the corresponding combination of structures then corresponds to the 'top' branching diagram function, the spins on the oxygen atom being *triplet*-coupled (as are those on the hydrogens), the two triplets being coupled to give total spin zero. Examination of the orbitals shows that, as dissociation proceeds, the oxygen hybrids shrink back into pure 2p orbitals and the atom thus reverts to its normal [3]P ground state.

Curve 1(c) shows the results of a rather accurate coupled-cluster calculation, while Curve (d) shows those of full CI calculations [10] (for all electrons outside a frozen 1s core), in which about 250 000 Slater determinants were employed.

It is well known that the slow convergence of large CI calculations is due to the difficulty of approximating the short-range correlation which inhibits the approach of two electrons as $r_{12} \to 0$. Most of the difference between Curves (b) and (d) results from this 'cusp' correlation error, which seems unlikely to be strongly dependent on molecular geometry. Owing to the difficulty of dealing with the correlation cusp, comparisons of potential energy curves are commonly made by introducing a 'reduced' curve [11]: the reduced PE curve results from a plot of

$$E_{\text{red}}(x) = \frac{E(x) - E(\infty)}{E(\infty) - E(1)}, \qquad x = R/R_e, \qquad (27)$$

which goes from -1 at equilibrium to 0 at infinity. The reduced curve obtained in this way from Curve (b) is compared with that from the full-CI and other results in Fig.2. The general shape of the two-structure VB energy curve is in excellent agreement with that obtained from the full-CI study.

Example 2. Dissociation of LiCl

Conventionally, the two atoms are regarded as possessing inert-gas cores, $Li[1s^2]$ and $Cl[1s^2 2s^2 2p^6]$, the remaining electrons belonging to the valence shell: the elementary textbook description assigns two electrons to a bond formed by overlap of the Li 2s orbital with a Cl 3p orbital ($3p\sigma$, say), the remainder forming lone pairs $Cl[3s^2\ 3p\pi^4]$. To study the bond-breaking process, it is convenient to adopt a VB description in which there are two electron pairs of sigma symmetry, the lone pair $Cl[3s^2]$ and the bond pair $Li(2s)-Cl(3p\sigma)$: the remaining electrons, whose orbitals are less strongly affected by bonding, will form an extended core. The orbitals used in describing the 16 core electrons and 4 valence electrons will not, of course, be simple AOs; they will be general linear combinations of the 'global' set of basis functions and their forms will be determined automatically in the constrained optimization that keeps the two groups strong orthogonal.

The global basis χ used in the calculations reported here is again of simple contracted gaussian form: it contains four contracted s functions and three sets of contracted p functions on the chlorine atom; three contracted s functions and two sets of contracted p functions on the lithium. When the orbitals are written in the matrix form $\phi = \chi T$, the first 8 columns of T, namely T_{cor}, define the doubly occupied core orbitals; the 3 columns of T_{val} define the sigma lone pair and the two orbitals of the bond pair; and the 11 columns of T_{com} provide the complementary (virtual) space.
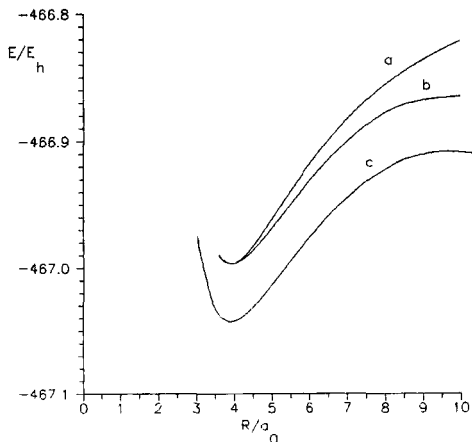
Fig. 3:   PE curves for LiCl

Curve (a) in Fig.3 displays the results of the frozen core approximation, the core orbitals being optimized (along with the valence orbitals) at the equilibrium geometry and then held fixed as dissociation proceeds. Curve (b) was obtained with global optimization at every geometry. For this system, with 20 electrons and 22 basis functions, a full-CI calculation is not yet feasible. Curve (c), from a coupled-cluster approach with the same basis, is expected to give a fairly good approximation near equilibrium geometry: but as dissociation is approached it becomes difficult to achieve convergence. With a VB-type valence function, on the other hand, no convergence problems are encountered, whatever the geometry. Again, the fully optimized VB curve and the coupled-cluster curve are roughly parallel: this is confirmed on plotting the reduced curves (cf. Fig. 2) which are found to be almost coincident. The most striking feature of Fig. 3, however, is the poor performance of the frozen-core approximation. This reflects the inability of the core to respond to great changes in the character of the bond: over much of the range the chlorine is almost a negative ion, but at very large R the atoms revert to their neutral ground states with the free spins coupled to $S = 0$.

4   Relativistic considerations

In any relativistic generalization of the formalism used so far, the 2-component spin-orbitals,

$$\psi_k = \phi_k^\alpha \alpha + \phi_k^\beta \beta, \tag{28}$$

used as building blocks in the construction of *non*-relativistic wavefunctions, will have to be replaced by the 4-component spinors that occur as solutions of the Dirac equation. A set of *non-interacting* Dirac electrons would be described using an antisymmetrized product of such spinors; and 'switching on' the interaction would lead to a function expressible as a linear combination of the totality of all possible antisymmetrized products. Instead of building the wavefunction from a complete set of spin-orbitals, we should then be using a complete set of 'Dirac spin-orbitals'.

The procedure just indicated would be consistent with the usual assumption [12] that the many-electron Hamiltonian can be written, to a well-defined order, as a sum of Dirac 1-electron Hamiltonians plus a sum of pairwise interaction terms. It must be remembered, however, that the Dirac equation refers essentially to a *one*-electron system; that its solutions fall into upper and lower sets, with positive and negative energies respectively; and that the conventional interpretation requires that all the lower energy states are filled by an infinite 'sea' of unobservable electrons. As Messiah [13] remarks "By postulating the occupation of the quasi-totality of negative energy states, the [Dirac] theory *ceases to be a one-electron theory*, even when it sets out to describe a single electron". Although the theory nicely accounts for such phenomena as electron-positron pair production, inconsistencies remain. Here we note only that the interpretation may at least be rationalized by treating the upper and lower energy electrons as two strong-orthogonal groups and employing a standard CI approximation to represent the system: provided no lower-to-upper (virtual) 'excitations' are admitted (i.e. no pair creation processes are envisaged), the negative-energy sea will play a purely passive role, while the N electrons of the upper-energy group may be described in terms of CI with only upper-to-upper excitations. In this way, contact is made with the conventional procedures of non-relativistic many-electron quantum mechanics.

Let us now write a typical Dirac spinor in the form

$$\psi_k = \phi_k^{(1)} e_1 + \phi_k^{(2)} e_2 + \phi_k^{(3)} e_3 + \phi_k^{(4)} e_4, \tag{29}$$

so as to preserve the analogy with usual 2-component spin-orbital (28). The Dirac 'spin space' is carried by the four basis vectors $\{e\mu\}$, orthogonal in the sense $< e\mu|e\nu >= \delta_{\mu\nu}$, which provide a representation of the Dirac operators. The solutions of the Dirac equation itself are of type (29), the negative and positive energy sets being separated by a gap of $2m_0c^2$, all solutions being orthogonal with the same metric.

A detailed study of the Dirac equation and its solutions will not be required: it will simply be assumed, as already indicated, that the system of N electrons 'above' the negative-energy sea may be described using a wavefunction constructed from antisymmetrized products of (positive energy) spin-orbitals of type (29). It is, however, necessary to know the basic properties of the operators $\alpha\mu$, which appear in the Dirac equation

$$(c\alpha \cdot \pi + V + m_0c^2\alpha_4)\psi = i\hbar(\partial\psi/\partial t). \tag{30}$$

Here the operator scalar product $\alpha \cdot \pi = \sum_{\mu=1}^3 \alpha_\mu\pi_\mu$ and the operators have the definitive properties

$$\alpha_\mu^2 = 1, \qquad (\alpha_\mu\alpha_\nu + \alpha_\nu\alpha_\mu) = 0, \ \mu \neq \nu. \tag{31}$$

The Dirac operators $\alpha_1, ...\alpha_4$, work on the basis vectors $e_1, ...e_4$ just as the Pauli spin operators work on the spin eigenvectors α, β. The only other property to be noted is that the Dirac spin-orbitals have two 'large components' and two 'small components', their ratio being of the order $(2m_0c)^{-1}$.

The first task is to generalize the density functions of Sect.2: thus, for example, using determinants of 4-component spin orbitals, the one-body density will become

$$\rho(\mathbf{x}; \mathbf{x}') = \sum_{i,j} \rho_{ij}\psi_i(\mathbf{x})\psi_j^*(\mathbf{x}'). \tag{32}$$

An alternative 'natural' expansion may also be found by choosing new linear combinations of the ψs, so as to diagonalize the density matrix: the result is then

$$\rho(\mathbf{x}; \mathbf{x}') = \sum_k n_k\psi_k(\mathbf{x})\psi_k^*(\mathbf{x}), \tag{33}$$

in which ψ_k is a 'natural' spin-orbital with occupation number n_k.

To maintain the parallel with 2-component theory, it is expedient to express the 'Dirac space' as a Kronecker product of two Pauli spaces. From

the alphas we find two operator sets with the same properties as the Pauli operators, namely

$$\hat{S}_1 = i\alpha_2\alpha_3, \qquad \hat{S}_2 = i\alpha_3\alpha_1, \qquad \hat{S}_3 = i\alpha_1\alpha_2 \qquad (34)$$

and

$$\hat{T}_1 = i\alpha_4\alpha_5, \qquad \hat{T}_2 = i\alpha_5, \qquad \hat{T}_3 = i\alpha_4, \qquad (35)$$

where $\alpha_5 = \alpha_1\alpha_2\alpha_3\alpha_4$. The 'spin operators' in the first set will correspond to twice the usual Pauli operators (with $x, y, z \to 1, 2, 3$). Let us now introduce basis vectors $u_1\ u_2$ and $v_1\ v_2$ to carry the two representations, supposing

$$\hat{S}_3 \begin{pmatrix} u_1 & u_2 \end{pmatrix} = \begin{pmatrix} u_1 & u_2 \end{pmatrix} \begin{pmatrix} 1 & 0 \\ 0 & -1 \end{pmatrix}, \qquad (36a)$$

$$\hat{T}_3 \begin{pmatrix} v_1 & v_2 \end{pmatrix} = \begin{pmatrix} v_1 & v_2 \end{pmatrix} \begin{pmatrix} 1 & 0 \\ 0 & -1 \end{pmatrix}. \qquad (36b)$$

The Dirac basis can then be expressed as

$$(e_1\ e_2\ e_3\ e_4) = (u_1v_1\ u_2v_1\ u_1v_2\ u_2v_2), \qquad (37)$$

where it follows from (33) that the basis vectors $e_1, \ldots e_4$ are simultaneous eigenvectors of $\hat{S}_3$ and $\hat{T}_3$ with eigenvalues $(+1, +1), (-1, +1), (+1, -1), (-1, -1)$, respectively.

On introducing two formal 'spin variables' s, t, so that $u_i \to u_i(s)$, $\qquad v_i \to v_i(t)$, the Dirac basis vectors become $e_1(s, t) = u_1(s)v_1(t)$, etc. and the 1-electron density matrix (26) takes the form

$$\begin{aligned} \rho(\mathbf{r}, s, t : \mathbf{r}', s', t') &= P_{11}(\mathbf{r}; \mathbf{r}')u_1(s)v_1(t)u_1^*(s')v_1^*(t') \\ &+ \ldots\ldots + \ldots\ldots + \ldots\ldots \\ &+ P_{44}(\mathbf{r}; \mathbf{r}')u_2(s)v_2(t)u_2^*(s')v_2^*(t') \end{aligned} \qquad (38)$$

– as in the familiar Pauli case, but now with 16 terms. When the non-spatial variables are removed by integration, in the usual way, we get the *spinless* density matrix

$$P(\mathbf{r}; \mathbf{r}') = \sum_{\mu} P_{\mu\mu}(\mathbf{r}; \mathbf{r}'), \qquad (39)$$

where the label $\mu = 1, ..4$ corresponds to the Dirac basis labelling and only terms with $\mu = \nu$ have survived the spin integrations. These are

$$P_{\mu\mu}(\mathbf{r}; \mathbf{r}') = \sum_{k} n_k \phi_k^{\mu}(\mathbf{r})\phi_k^{\mu\ *}(\mathbf{r}'). \qquad (40)$$

The terms $\mu = 1, 2$ are large, for $\mu = 3, 4$ they are small[2], and the spinless density (39) is thus

$$P(\mathbf{r}; \mathbf{r}') = P^L(\mathbf{r}; \mathbf{r}') + P^S(\mathbf{r}; \mathbf{r}'), \qquad (41)$$

a sum of the 'Large' and 'Small' terms

$$P^L(\mathbf{r}; \mathbf{r}') = \sum_k n_k [\phi_k^1(\mathbf{r})\phi_k^1 {}^*(\mathbf{r}') + \phi_k^2(\mathbf{r})\phi_k^2 {}^*(\mathbf{r}')], \qquad (42a)$$

$$P^S(\mathbf{r}; \mathbf{r}') = \sum_k n_k [\phi_k^3(\mathbf{r})\phi_k^3 {}^*(\mathbf{r}') + \phi_k^4(\mathbf{r})\phi_k^4 {}^*(\mathbf{r}')]. \qquad (42b)$$

Here we have used the natural expansion (33), with spin-orbitals written in the form (29). The second term in (41), absent in a Pauli-type approximation, contains the correction arising from the use of a 4-component formulation; it is of order $(2m_0c)^{-2}$ and is usually negligible except at singularities in the potential. As expected, for $N = 1$, (41) reproduces the density obtained from a standard treatment of the Dirac equation; but now there is no restriction on the particle number.

According to (12), the current density should also follow from (41): it should thus be

$$J_x(\mathbf{r}) = J_x^L(\mathbf{r}) + J_x^S(\mathbf{r}), \qquad (43)$$

with similar results for J_y, J_z, the 'L' and 'S' terms deriving from (39a) and (39b), respectively. Again, the Small terms are of order $(2m_0c)^{-2}$ relative to the Large. In this case, however, (40) does *not* reproduce the standard result for $N = 1$. This is because in the present approach the distributions of charge and spin are treated separately; the former leads to the 'conventional' current resulting from the circulation of point charges, while the latter leads to a 'spin current density' arising as the curl of a magnetization density associated with the spin magnetic dipoles. The conventional current is correctly given by (43), the spin current will be derived separately from the spin density.

The spin density should follow from the density matrix (38), which includes the spin variables. As in (42), $Q_x(\mathbf{x}; \mathbf{x}')$ will be a sum of terms containing the various spinor components, summed over all spin-orbitals in the natural expansion. A typical term will be

---

[2]The convention adopted here is that, for the positive-energy solutions of the Dirac equation, the 'large components' correspond to $\mu = 1, 2$ and the 'small components' to $\mu = 3, 4$. Some authors, notably Slater, use the opposite convention.

$$Q_x^k(\mathbf{r}; \mathbf{r}') = \int \left[\sum_{\mu\nu} \hat{S}_x \phi_k \mu(\mathbf{r}) e \mu(s,t) \phi_k^\nu{}^*(\mathbf{r}') e \nu^*(s',t') \right]_{\substack{s'=s \\ t'=t}} ds\,dt,$$

where the operator works on the unprimed variables. On expressing the Dirac basis vectors in the Kronecker product form (37) it follows that

$$
\begin{aligned}
\hat{S}_x(e_1 \; e_2 \; e_3 \; e_4) &= \hat{S}_x(u_1v_1, u_2v_1, u_1v_2, u_2v_2) \\
&= (u_2v_1, u_1v_1, u_2v_2, u_1v_2) \\
&= (e_2, e_1, e_4, e_3);
\end{aligned}
$$

and using these results in the previous equation we obtain

$$Q_x(\mathbf{r}; \mathbf{r}') = Q_x^L(\mathbf{r}; \mathbf{r}') + Q_x^S(\mathbf{r}; \mathbf{r}'), \tag{44}$$

where the Large and Small parts are given by

$$Q_x^L(\mathbf{r}; \mathbf{r}') = \sum_k n_k [\phi_k^2(\mathbf{r})\phi_k^1{}^*(\mathbf{r}') + \phi_k^1(\mathbf{r})\phi_k^2{}^*(\mathbf{r}')], \tag{45a}$$

$$Q_x^S(\mathbf{r}; \mathbf{r}') = \sum_k n_k [\phi_k^4(\mathbf{r})\phi_k^3{}^*(\mathbf{r}') + \phi_k^3(\mathbf{r})\phi_k^4{}^*(\mathbf{r}')]. \tag{45b}$$

There are corresponding results for Q_y, Q_z and again the 'L' and 'S' parts differ by two orders of magnitude, the large parts reproducing the densities obtained in 2-component Pauli approximation (cf. (9) *et seq.*). When the curl of the corresponding magnetization density is added to (43), for the case $N = 1$, we obtain the 'Dirac current density' which already includes the spin term.

In summary, although (to quote Slater [14]) " ... the Dirac wavefunction has the capability of giving complete information about the orientation of the spin in space..', the same is true for any number of electrons and for wavefunctions built from either 2-component or 4-component spin-orbitals. There is no need to invoke explicitly the Dirac equation or the expansion of small components in terms of large. The charge, current and spin densities defined in the conventional (2-component) approach, in terms of the usual density matrices, remain valid at the 'fully relativistic' (4-component) level. As a consequence, the possibility of 'separating' a large system into weakly interacting subsystems, as discussed in preceding Sections, should be quite independent of relativistic generalizations.

5   Conclusion

The main features of the present approach are

- Whenever an N-electron system is represented in terms of subsystems A, B,..., using a generalized product ansatz, the entire wavefunction can be optimized by repeated optimization of subsystem wavefunctions

- Any subsystem wavefunction, Φ_R, refers only to N_R electrons with an 'effective field' Hamiltonian, whose form depends on the forms of the 1-electron density matrices of all subsystems; all such functions can be optimized, in an iterative manner, by standard methods and without the constraints implied by any *a priori* partitioning of the global basis

- The resultant wavefunction provides an optimum 'separation' of the whole system, many of whose properties may then be expressed as sums of subsystem contributions

- Separability can be exploited even with admission of relativistic effects, by using the standard density matrix formalism with a simple extension to admit 4-component Dirac spin-orbitals: this opens up the possibility of performing *ab initio* calculations, with extensive CI, on systems containing heavy atoms.

References

[1] McWeeny, R. (1959) Proc. Roy. Soc. (Lond.) A253, 242.

[2] McWeeny, R. (1960) Rev. Mod. Phys. 32, 335.

[3] Klessinger, M. and McWeeny, R. (1965) J. Chem. Phys. 42, 3343.

[4] McWeeny, R. (1993) Methods of Molecular Quantum Mechanics 2nd ed. (Academic, London)

[5] McWeeny, R. (1986) Proc. Indian Acad. Sci. 96, 263

[6] McWeeny, R. and Mizuno, Y. (1961) Proc. Roy. Soc. (Lond.) A259, 554.

[7] McWeeny, R. (1965) J. Chem. Phys. 42, 1717.

[8] Dunning, T. H. (1970) J. Chem. Phys. 53, 2823.

[9] McWeeny, R. (1990) Int. J. Quantum Chem. Symp. 24, 733.

[10] Bendazzoli, G. (1997 – private communication)

[11] Sosa, C., Noga, J., Purvis, G. D. and Bartlett, R. J. (1988) Chem. Phys. Lett. 153, 139.

[12] Bethe, H. and Salpeter, E. (1957) Quantum Mechanics of One- and Two-Electron Atoms (Springer-Verlag, Berlin)

[13] Messiah, A. (1970) Quantum Mechanics Vol.II (North-Holland, Amsterdam)

[14] Slater, J. C. (1960) Quantum Theory of Atomic Structure Vol.II (McGraw-Hill, New York)

The first order contracted density equations: correlation effects.

C. Valdemoro, M. P. de Lara-Castells, E. Pérez-Romero* and L. M. Tel*

Instituto de Matemáticas y Física Fundamental
Consejo Superior de Investigaciones Científicas
Serrano 123. Madrid. 28006 Spain
*Dpto. de Química Física, Universidad de Salamanca
Salamanca. 37008 Spain

Abstract

The *many-body* problem is reformulated here by using a system of equations involving only first order Reduced Density Matrices. These matrices correspond to all the states of the spectrum of the system and to the transitions among the different states. Some results concerning the correlation effects are also reported here.

1. Introduction

2. General theoretical background

3. The structure of Reduced Density Matrices

4. Replacing the *many body* hierarchy of equations by a *single particle* set of equations

5. Is a global estimation of the correlation terms possible?

6. Some final remarks

7. Acknowledgments

References

1.   Introduction

By applying the general Matrix Contraction Mapping (MCM) [1-3] to the matrix representation of the Schrödinger Equation (SE) one obtains a hierarchy of Contracted Schrödinger Equations (CSE) [4] where the unknowns are the Reduced Density Matrix (RDM) elements. When the contraction is carried out from the N-electron space into the p-electron space, the solution of the p-CSE thus obtained depends not only on the p-RDM but also, assuming that the Hamiltonian only contains two-body interaction terms, on the $(p + 1)$-RDM and $(p + 2)$-RDM. An equivalent hierarchy of integro-differential equations was previously obtained [5-8] by integrating the SE over N-p variables. Although this work is closely related to and partially motivated by the research on the iterative solution of the 2-CSE [9-11], we look here at the *many body* problem from a different point of view.

Another important hierarchy of equations is obtained by applying the (MCM) to the matrix representation of the Liouville-von Neumann Equation ($LVNE$) [12,13]. In this way the p-order Contracted Liouville-von Neumann Equation (p-$CLVNE$) is obtained [4]. It will be shown here that: The structure of a particular **p**-CSE, that involves the higher order CSE's for a given state, can be replaced by an equivalent set of equations, 1-CSE and 1-$CLVNE$, but for the **whole spectrum**, i. e. involving all the states.

The second aim of this paper is to report a series of equations inter-relating in a global way what we define here as *correlation terms* and *particle-hole* terms.

This work is organized as follows: In the next section, the general theoretical background is described. Then in section three we show how the *many body* problem can be formally solved in terms of a *one-particle density* matrices. In this formalism the first order Transition Reduced Density Matrix (1-$TRDM$) plays an important role by describing how, due to the correlation effects, the particle, as an average, undergoes all possible virtual transitions. In section four, the relationship between the *particle-hole* terms, and the *correlation terms*, which appear in the decomposition of the high order Reduced Density Matrices (RDM), are reported. Some final comments are given in section five.

2.   General theoretical background

Let us start this section by recalling the general definition of a p-RDM in second quantization:

$$^pD^{\mathcal{LL}}_{i_1...i_p;j_1...j_p} = \frac{< \mathcal{L}|\, b^{\dagger}_{i_1} \ldots b^{\dagger}_{i_p}\, b_{j_p} \ldots b_{j_1}\, |\mathcal{L} >}{p!}$$

Similarly the complementary Holes Reduced Density Matrix (p-$HRDM$) is:

$$^{p}\bar{D}^{\mathcal{LL}}_{i_1...i_p;j_1...j_p} = \frac{< \mathcal{L}|\ b_{j_p}...b_{j_1}\ b^{\dagger}_{i_1}...b^{\dagger}_{i_p}|\mathcal{L} >}{p!}$$

Note, that the $p!$ factor will not appear if a unique ordering of the indices of the operators is imposed.

2.1.   The Matrix Contracting Mapping (MCM)

Let us consider the Density Matrix of an N-electron state $\mathcal{L}$. Its Λ, Ω element in the N-electron space representation is:

$$D^{\mathcal{LL}}_{\Lambda\Omega} = < \mathcal{L}|\Lambda >< \Omega|\mathcal{L} >$$

It has been shown [2-3] that a matrix contracting operation, exactly equivalent to the integration over (N-p) electron variables, can be performed in the following way:

$$^{p}D^{\mathcal{LL}}_{i_1...i_p;j_1...j_p} = \sum_{\Lambda\Omega} D^{\mathcal{LL}}_{\Lambda\Omega}\ ^{p}D^{\Lambda\Omega}_{i_1...i_p;\ j_1...j_p}$$

where $^{p}D^{\Lambda\Omega}_{i_1...i_p;\ j_1...j_p}$ is an element of the p-$TRDM$ involving the N-electron configurations Λ and Ω. It should be underlined that any matrix obtained by applying this MCM to a Density Matrix is by construction N-representable [14].

2.2.   The first order Contracted Schrödinger Equation in a spin-orbital representation

Let us consider the matrix representation of the Schrödinger equation:

$$\mathcal{E}_{\mathcal{L}}\ D^{\mathcal{LL}}_{\Lambda\Omega} = (\mathcal{H}\ D^{\mathcal{LL}})_{\Lambda\Omega}$$

where Λ, Ω are N-electron configurations and the $\mathcal{H}$ is the Full Configuration Interaction (FCI) Hamiltonian matrix. It can be shown that by applying the MCM to both sides of this equation in order to take it from the N-electron space into the 1-electron space one obtains.

$$\mathcal{E}_{\mathcal{L}}\ ^{1}D^{\mathcal{LL}}_{ik} = < \mathcal{L}|\hat{H}\ b^{\dagger}_i\ b_k|\mathcal{L} > \tag{1}$$

where i, k are spin-orbitals, $^1D^{\mathcal{LL}}$ is the 1-*RDM* corresponding to the N-electron eigenstate $\mathcal{L}$, and $\hat{H}$ is the usual spin-independent many-body Hamiltonian operator which may also be written as:

$$\hat{H} = \left\{ \begin{array}{l} \displaystyle\sum_{x<z;y<t} {}^0H^{\alpha\alpha}_{xz;yt}\, b^\dagger_x b^\dagger_z b_t b_y \\[2mm] + \displaystyle\sum_{uv;mn} {}^0H^{\alpha\beta}_{uv;mn}\, b^\dagger_u b^\dagger_{\bar{v}} b_{\bar{n}} b_m \\[2mm] + \displaystyle\sum_{x<z;y<t} {}^0H^{\beta\beta}_{xz;yt}\, b^\dagger_{\bar{x}} b^\dagger_{\bar{z}} b_{\bar{t}} b_{\bar{y}} \end{array} \right. \tag{2}$$

where the bar over the indices indicate that the spin function is a β one and the ^0H symbols represent the corresponding integral matrix elements [10].

After transforming relation (1) into its normal product form, one obtains:

$$\mathcal{E}\; {}^1D^{\mathcal{LL}}_{q;p} = \left\{ \begin{array}{l} \displaystyle\sum_k \left({}^0H^{\alpha\alpha}\, {}^2D^{\mathcal{LL}}\right)_{pk;qk} - \displaystyle\sum_k \left({}^0H^{\alpha\beta}\, {}^2D^{\mathcal{LL}}\right)_{p\bar{k};q\bar{k}} \\[2mm] + \displaystyle\sum_{i<j;x<k} \left({}^0H^{\alpha\alpha}_{ij;xk}\, {}^3D^{\mathcal{LL}}_{ijq;xkp} + {}^0H^{\beta\beta}_{ij;xk}\, {}^3D^{\mathcal{LL}}_{q\bar{i}\bar{j};p\bar{x}\bar{k}}\right) \\[2mm] + \displaystyle\sum_{i,j,x,k} {}^0H^{\alpha\beta}_{ij;xk}\, {}^3D^{\mathcal{LL}}_{q\bar{i}\bar{j};p\bar{x}\bar{k}} \end{array} \right. \tag{3}$$

and by interchanging β with α in the previous relation one obtains the equation for the β spin.

We have proposed a method for approximating a high order *RDM* in terms of the lower order ones [15] and we can use this approximation to replace the former ones, appearing on the *r.h.s.* of eq. (3) by the lower order ones forming a matrix M [9,10]. In this case, the trace of matrix M must be equal to $\mathcal{E}$ times N_α which provides a new value for $\mathcal{E}$. Then, by dividing M by this new value of $\mathcal{E}$, a new 1-*RDM* is found. The iterative procedure may then start again.

This equation has at least two exact solutions. Thus, both the set of *RDM*'s obtained in a Hartree-Fock (*HF*) calculation and that obtained from a *FCI* one fulfill exactly this effective one-body equation. Unfortunately, the iterative method sketched above converged to the *HF* solution in all the cases tested. This may be due to the fact that in our algorithm, the correlation effects are estimated through a renormalization procedure, which may not be sufficiently accurate in the first order case. To improve this aspect is one of the motivations of our present line of work.

2.3. The first order Contracted Liouville-von Neumann equation

In this paragraph, we consider the equation obtained by applying the same *MCM* to both sides of the matrix representation of the Liouville-von Neumann

equation:

$$(\mathcal{E}_{\mathcal{L}} - \mathcal{E}_{\mathcal{L}'})\ ^1D^{\mathcal{L}\mathcal{L}'}_{\Lambda\Omega} = \left[\mathcal{H},\ D^{\mathcal{L}\mathcal{L}'}\right]_{-\Lambda\Omega} \tag{4}$$

which gives:

$$(\mathcal{E}_{\mathcal{L}} - \mathcal{E}_{\mathcal{L}'})\ ^1D^{\mathcal{L}\mathcal{L}'}_{pq} = <\mathcal{L}|\left[\hat{H},\ b^\dagger_p b_q\right]_-|\mathcal{L}'> \tag{5}$$

This equation, after transforming the chain of operators into its normal product form, becomes:

$$(\mathcal{E}_{\mathcal{L}} - \mathcal{E}_{\mathcal{L}'})\ ^1D^{\mathcal{L}\mathcal{L}'}_{pq} = \left\{ \begin{array}{l} \displaystyle\sum_k \left[^0H^{\alpha\alpha},\ ^2D^{\mathcal{L}\mathcal{L}'}\right]_{-pk;qk} + \\[2mm] \displaystyle\sum_{\bar{k}} \left[^0H^{\alpha\beta},\ ^2D^{\mathcal{L}\mathcal{L}'}\right]_{-p\bar{k};q\bar{k}} \end{array} \right. \tag{6}$$

By interchanging β with α in relation (6) one obtains the equation for the β spin.

Note, that in the first term on the *r.h.s.* of equation (6) a unique ordering of the indices is assumed ($p < k$ and $q < k$), hence, when summing over all values of k, a factor -1 must multiply this term when: $p < k$ and $q > k$ or $p > k$ and $q < k$.

3.   The Structure of Reduced Density Matrices

Here, we will focus our attention on the 2-RDM and the 3-RDM which are the matrices appearing in the 1-CSE aiming at describing them in terms of a single particle density matrices.

3.1.   The 2-RDM

For the sake of simplicity, in what follows the superscript referring to the order of the RDM will be ommitted since the number of spin-orbital subscripts renders it redundant. Also the superscript referring to the state under study, $\mathcal{L}$, will be omitted whenever it can be inferred from the context.

Let us alter the normal order of the operators in an element of the 2-RDM in the following way:

$$2!\ D_{tv;yx} = <\mathcal{L}|b^\dagger_t\ b^\dagger_v\ b_x\ b_y|\mathcal{L}> = -\delta_{yv}\ d_{tx} + <\mathcal{L}|b^\dagger_t\ b_y\ b^\dagger_v\ b_x|\mathcal{L}> \tag{7}$$

A set of simple algebraic operations may now be applied to the r.h.s. of this relation:

$$2!\ D_{tv;yx} = -\delta_{yv}\ d_{tx} + \sum_{\mathcal{L}'} <\mathcal{L}|b^\dagger_t\ b_y|\mathcal{L}'> <\mathcal{L}'|b^\dagger_v\ b_x|\mathcal{L}>$$

$$2! \, D_{tv;yx} \;=\; -\delta_{yv} \, d_{tx} + d_{ty} \, d_{vx} + \sum_{\mathcal{L}' \neq \mathcal{L}} < \mathcal{L}|b_t^\dagger \, b_y|\mathcal{L}' > \, < \mathcal{L}'|b_v^\dagger \, b_x|\mathcal{L} > \qquad (8)$$

The 1-$TRDM$ elements appearing explicitly in this well known expression will be at the center of the following developments.

Recalling the basic relation obtained by taking the expectation value of the anticommutator of two fermion operators:

$$\delta_{yv} \;=\; d_{yv} + \bar{d}_{vy} \qquad (9)$$

and exploiting it in expression (8), one has:

$$2! \, D_{tv;yx} \;=\; \begin{cases} d_{ty} \, d_{vx} \;-\; d_{yv} \, d_{tx} \\[2mm] -\, \bar{d}_{vy} \, d_{tx} \;+\; \sum_{\mathcal{L}' \neq \mathcal{L}} < \mathcal{L}|b_t^\dagger \, b_y|\mathcal{L}' > \, < \mathcal{L}'|b_v^\dagger \, b_x|\mathcal{L} > \end{cases} \qquad (10)$$

The first two terms on the *r.h.s.* of equation (10) coincide with those obtained when evaluating the 2-RDM corresponding to a simple Slater determinant. Therefore, the only way in which these two terms may describe correlation effects is through the 1-RDM itself, when the state $\mathcal{L}$ is a correlated one. Note that in such a case the 1-RDM will not be an idempotent matrix.

The last two terms in relation (10) describe how the correlation effects, which in a wave function formalism are expressed through the interaction of excited configurations of a reference state, are expressed in an RDM oriented formalism. In our approximation of the 2-RDM in terms of the 1-RDM, these terms were partially taken into account through a renormalization of the 2-RDM [15].

In what follows, we will refer to the terms involving sums over the eigenstates $\mathcal{L}'$ of products of two $TRDM$ elements (similar to the last term of eq. (10)) as *correlation terms*. The terms involving $HRDM$'s elements also describe correlation effects. However, in order to distinguish them from the above mentioned sums, they will hereafted be referred to as *particle-hole terms*.

An intuitive physical interpretation of the *correlation terms* in the 2-RDM is that the two electrons undergo virtual excitations in such a way that when one goes from $\mathcal{L}$ into $\mathcal{L}'$, the other one undergoes the opposite transition.

3.1.1.   The 3-RDM

The same kind of arguments may be applied to the 3-RDM. Thus, one of the many possible ways of re-ordering the operators and of introducing the *unit operator*, gives:

$$3! \; D_{ijk;\ell rs} \; = \; < \mathcal{L}|b_i^\dagger \, b_j^\dagger \, b_k^\dagger \, b_s \, b_r \, b_\ell|\mathcal{L} > \; =$$

$$= \left\{ \begin{array}{l} 2! \; D_{ij;rs} \; \delta_{k\ell} \; - \; 2! \; D_{ik;rs} \; \delta_{j\ell} \; + \\[2mm] + \sum_{\mathcal{L}'} < \mathcal{L}|b_i^\dagger \, b_\ell|\mathcal{L}' > \; < \mathcal{L}'|b_j^\dagger \, b_k^\dagger \, b_s \, b_r|\mathcal{L} > \end{array} \right.$$

and isolating the case $\mathcal{L}' = \mathcal{L}$ we have

$$3! \; D_{ijk;\ell rs} \; = \left\{ \begin{array}{l} 2! \; D_{ij;rs} \; \delta_{k\ell} \; - \; 2! \; D_{ik;rs} \; \delta_{j\ell} \; + \; 2! \; d_{i\ell} \; D_{jk;rs} \; + \\[2mm] + \sum_{\mathcal{L}' \neq \mathcal{L}} < \mathcal{L}|b_i^\dagger \, b_\ell|\mathcal{L}' > \; < \mathcal{L}'|b_j^\dagger \, b_k^\dagger \, b_s \, b_r|\mathcal{L} > \end{array} \right. \tag{11}$$

As can be seen, the 3-RDM depends on the 2-RDM and on the 2-$TRDM$'s. Also, as in the 2-RDM case, the Kronecker δ's give rise to Hole terms which, however, will not be made explicit at this stage.

Let us now apply again the same arguments as previously to the last term:

$$\sum_{\mathcal{L}' \neq \mathcal{L}} < \mathcal{L}|b_i^\dagger \, b_\ell|\mathcal{L}' > \; < \mathcal{L}'|b_j^\dagger \, b_k^\dagger \, b_s \, b_r|\mathcal{L} > \; =$$

$$\sum_{\mathcal{L}' \neq \mathcal{L}} < \mathcal{L}|b_i^\dagger \, b_\ell|\mathcal{L}' > \; < \mathcal{L}'|b_j^\dagger \, b_r|\mathcal{L} > \; \delta_{ks}$$

$$- \sum_{\mathcal{L}' \neq \mathcal{L} \neq \mathcal{L}''} < \mathcal{L}|b_i^\dagger \, b_\ell|\mathcal{L}' > \; < \mathcal{L}'|b_j^\dagger \, b_s|\mathcal{L}'' > \; < \mathcal{L}''|b_k^\dagger \, b_r|\mathcal{L} > \tag{12}$$

$$- \sum_{\mathcal{L}' \neq \mathcal{L}} < \mathcal{L}|b_i^\dagger \, b_\ell|\mathcal{L}' > \; < \mathcal{L}'|b_j^\dagger \, b_s|\mathcal{L}' > \; < \mathcal{L}'|b_k^\dagger \, b_r|\mathcal{L} >$$

$$- \sum_{\mathcal{L}' \neq \mathcal{L}} d_{kr} \; < \mathcal{L}|b_i^\dagger \, b_\ell|\mathcal{L}' > \; < \mathcal{L}'|b_j^\dagger \, b_s|\mathcal{L} >$$

The previous relations show that the 3-RDM depends on:

- All the possible transitions that can occur in the system through the corresponding 1-$TRDM$'s.

- All the stationary states of the system through the corresponding 1-RDM's ($< \mathcal{L}'|b_j^\dagger \, b_s|\mathcal{L}' >$ in the third term on the r.h.s. of equation (12))

The interpretation of the correlation effects in the 3-RDM is slightly more complicated than in the 2-RDM case, although the electrons also avoid each other here by undergoing virtual excitations. In this case, two different correlation mechanisms contribute to the overall effect. In the first mechanism, one particle is in a stationary state – the ground or an excited state – while the two other particles undergo the same kind of virtual excitations as in the 2-RDM. In the second mechanism, the cycle of transitions involves three states instead of two. Finally the role played by the *hole* is more complex here, since the 1-$HRDM$ elements multiply a 2-RDM element and a cycle of two transitions.

4. Replacing the *Many Body* hierarchy equations by a *Single Particle* set of equations

We have just seen that, through the 2- and 3-RDM's, the 1-CSE depends, for a particular state $\mathcal{L}$, on the following matrices:

$$d,\ d^{\mathcal{L}'\mathcal{L}'},\ d^{\mathcal{L}\mathcal{L}'},\ d^{\mathcal{L}'\mathcal{L}''}$$

Now, in order to obtain the set of 1-$TRDM$'s, the corresponding set of 1-$CLVNE$'s must be solved. Since these equations involve the 2-$TRDM$ which also appear in the decomposition of the 3-RDM, it is clear that both the set of 1-$CLVNE$'s and the set of the 1-CSE **depend on the same variables.** Thus the system of equations

$$\mathcal{E}_{\mathcal{P}}\ d^{\mathcal{P}\mathcal{P}} = \mathcal{F}_{\mathcal{P}}\left(H^{\sigma\sigma'}, d^{11}, \ldots, d^{\mathcal{P}\mathcal{P}}, \ldots, d^{\mathcal{X}\mathcal{X}}, d^{12}, \ldots, d^{\mathcal{P}\mathcal{Q}}, \ldots d^{(\mathcal{X}-1)\mathcal{X}}\right)$$

$$(\mathcal{E}_{\mathcal{P}} - \mathcal{E}_{\mathcal{Q}})\ d^{\mathcal{P}\mathcal{Q}} = \mathcal{R}_{\mathcal{P}\mathcal{Q}}\left(H^{\sigma\sigma'}, d^{11}, \ldots, d^{\mathcal{P}\mathcal{P}}, \ldots, d^{\mathcal{X}\mathcal{X}}, d^{12}, \ldots, d^{\mathcal{P}\mathcal{Q}}, \ldots d^{(\mathcal{X}-1)\mathcal{X}}\right)$$

with $\mathcal{P}, \mathcal{Q}$ ranging over all states, together with the trace conditions for evaluating the energies, is well determined. The *many-body* problem can thus be transformed into a Single Particle one. However, the price to pay is high and, as can be appreciated, solving such a large system of equations is not feasible even for small systems and using small basis sets. Therefore we must investigate whether this development, apart from shedding a new light on the *many-body* problem, may lead to an useful way of obtaining approximate solutions.

The first question which arises is whether this system of equations can be truncated and whether some kind of approximation can be found for solving the truncated problem.

Let us assume that one is only interested in the results concerning a given state, say the ground state. Our initial working hypothesis, in order to assess whether a truncation of the system of equations is possible, has been to suppose that if a set of $TRDM$'s plays a relevant role in describing the *correlation terms* in the ground state 2-RDM, they will be relevant variables which must be taken into account. Therefore, the importance of the contribution of each $TRDM$ to the 2-RDM was examined. In all the trials performed, our test example was the Beryllium atom in a subspace spanned by a double zeta basis set [16]. This example allowed us to use the FCI eigenstates for evaluating the 1-RDM's and the 1-$TRDM$'s.

An analysis of the results obtained for the *correlation terms* showed that most of the 1-$TRDM$'s, considered individually, contributed significantly in

eq. (10), albeit by largely cancelling other 1-$TRDM$ contributions. It was also clear after this analysis that, in this case, the singlet-singlet and the single-triplet transitions played an equally important role. Therefore, according to our working hypothesis, a truncation will probably not be possible.

Alternatively, instead of looking for a significant truncation of the system of equations, one may try to perform multiple but simple calculations hoping for a favorable cancellation of errors. Thus, the idea tested was to start from a set of 2-$TRDM$'s, corresponding to the eigenstates of $\hat{S}^2$, and then to apply the $CLVNE$ in order to obtain a set of more accurate 1-$TRDM$'s . This kind of calculation was not only carried out for the Beryllium atom but also for the LiH molecule (also with a double zeta basis set). Unfortunately, the results were not encouraging either.

In these conditions, one may ask whether a global approach, where instead of determining each of the 1-$TRDM$'s one would look for the groups of elementary *correlation terms* as explained below, would not be a more suitable way of simplifying the problem.

In the following section we will report the first results obtained in our search for an averaged estimation of the *correlation terms*.

5. Is a global estimation of the correlation terms possible?

In this section, in order to classify the different kinds of *correlation terms* and to find the fundamental relations linking them, we will develop the following ideas:

− We will assume that the different states are pure spin ones and thus must obey well defined relations when the Spin operators act upon them. We will see that this analysis allows us to determine the global unknowns that must be evaluated.

− We will consider all the different, although equivalent, forms of decomposition of the 2-RDM (similarly to eq.(10)), for the different spin-blocks. In this way a set of relations linking the different kinds of correlation terms will be obtained.

From now on, whenever possible, we will use graphs instead of explicit formulae because the relations become more compact and their structure more transparent. The basic graphs are shown in Table 1.

Table 1: Graphs correspondence.

Matrix element	Graphs
d_{ip}	$\longrightarrow$ ... $\longrightarrow$ ...
$\bar{d}_{pi}$	$\longrightarrow$ ... $\longrightarrow$ ...
$D_{ij;pq}$	$\longrightarrow$ ... $\longrightarrow$ ...
$d_{i;p}^{\mathcal{L}\mathcal{L}'}$	$\longrightarrow$ ... $\longrightarrow$ ...
$\displaystyle\sum_{\mathcal{L}'\neq\mathcal{L}} d_{i;p}^{\mathcal{L}\mathcal{L}'}\, d_{j;q}^{\mathcal{L}'\mathcal{L}}$	$\longrightarrow$ ... $\longrightarrow$ ...
$\displaystyle\sum_{\substack{\mathcal{L}'\neq\mathcal{L}\\ \mathcal{L}'\epsilon\{S',M_s'\}}} d_{i;p}^{\mathcal{L}\mathcal{L}'}\, d_{j;q}^{\mathcal{L}'\mathcal{L}}$	$\longrightarrow$ ... $\longrightarrow$ ...
$\displaystyle\sum_{\mathcal{L}'\neq\mathcal{L}} d_{i;\bar{q}}^{\mathcal{L}\mathcal{L}'}\, d_{\bar{j};p}^{\mathcal{L}'\mathcal{L}}$	$\longrightarrow$ ... $\longrightarrow$ ...

5.1.   The Unknowns

In order to simplify the problem we will assume that the state, $\mathcal{L}$, in which we are interested is *singlet*. Then, the 1-$TRDM$, linking $\mathcal{L}$ to a quintuplet state vanishes. Therefore, the only cases that may arise come from *singlet-singlet* or *singlet-triplet* transitions. The cases that in principle have to be considered are:

- $S' = 0, M_s' = 0$: In this case, there will be two *correlation terms* acording to whether the spin functions of the two electrons involved in the 2-RDM are the same or one is α and the other β.

- $S' = 1, M_s' = 0$: The same argument applies here, therefore these spin quantum numbers give rise to two other *correlation terms*.

- $S' = 1, M_s' = 1$ and -1 : To each of the M_s' values corresponds another *correlation term*.

Therefore, in principle, there are six different kinds of elementary *correlation terms*. The relations linking some of these terms will now be investigated in order to reduce the number of unknowns.

5.1.1.   Action of the $\hat{S}^2$ operator

All the transitions considered involve eigenstates of the $\hat{S}^2$ operator. Therefore,

$$< \mathcal{L}|b_{t_\sigma}^\dagger \, b_{y_\sigma} \, \hat{S}^2|\mathcal{L}' > = \; S' \, (S' \, + \, 1) \; < \mathcal{L}|b_{t_\sigma}^\dagger \, b_{y_\sigma} \, |\mathcal{L}' > \qquad (13)$$

where the subcript σ stands for a generic spin function (either α or β) and $\bar{\sigma}$ would stand for its opposite. By developping eq. (13) one obtains the following results according to the value of S:

$$
\begin{aligned}
S_{\mathcal{L}'} &= 0 \; \longrightarrow \; d_{\alpha\alpha}^{\mathcal{L}\mathcal{L}'} &= \; d_{\beta\beta}^{\mathcal{L}\mathcal{L}'} \\
S_{\mathcal{L}'} &= 1 \; \longrightarrow \; d_{\alpha\alpha}^{\mathcal{L}\mathcal{L}'} &= \; - \, d_{\beta\beta}^{\mathcal{L}\mathcal{L}'}
\end{aligned}
\qquad (14)
$$

Hence

$$(15)$$

In those graphs, only the spin part of the four spin-orbitals appearing in eq. (10) is made explicit.

5.1.2. Action of the $\hat{S}_+$ operator

Let us consider

$$\sum_{\mathcal{L}'_{(M'_s=-1)}} <\mathcal{L}|b_i^\dagger b_{\bar{l}}|\mathcal{L}'> \, <\mathcal{L}'|b_{\bar{k}}^\dagger b_j|\mathcal{L}> =$$

$$= \sum_{\mathcal{L}''_{(M''_s=0)}} \frac{<\mathcal{L}|b_i^\dagger \, b_{\bar{l}} \, \hat{S}_-|\mathcal{L}''> \, <\mathcal{L}''|\hat{S}_+ \, b_{\bar{k}}^\dagger \, b_j|\mathcal{L}>}{S''\,(S''+1)\,-\,M''_s\,(M''_s-1)} \tag{16}$$

by moving the $\hat{S}_-$ to the left and the $\hat{S}_+$ to the right one finds:

$$\overset{\sigma \;\; \bar{\sigma}}{\underset{\sigma \qquad \bar{\sigma}}{\times}}{}^{1,-1} \;=\; 2 \; \overset{\sigma \;\; \sigma}{\underset{\sigma \qquad \sigma}{\times}}{}^{1,0} \tag{17}$$

Therefore, all the correlation terms may be expressed in terms of the elements of only two different matrices:

$$\overset{\sigma \;\;\; \sigma}{\underset{\sigma \qquad \sigma}{\sqcap\!\sqcap}}{}^{0,0} \quad \text{and} \quad \overset{\sigma \;\;\; \sigma}{\underset{\sigma \qquad \sigma}{\sqcap\!\sqcap}}{}^{1,0}$$

5.2. Two global relations

The question that will be addressed in this paragraph is whether the two correlation terms which are our global unknowns, can be evaluated or at least approximated with a sufficient accuracy.

Let us consider the equivalent expressions for the 2-*RDM* blocks, which may be derived by interchanging the fermion operators by following other options than the one used in eq. (7) which gave rise to eq. (10). For the $\sigma\sigma$ blocks one obtains:

$$2!\;\square \;=\; |\,| \,-\, \times \,-\, \times\!\!\!\!\!{}_{\circ}\!\!\!\!\!{}_{\circ} \,+\, \sqcap\!\sqcap{}^{0,0} \,+\, \sqcap\!\sqcap{}^{1,0} \tag{18}$$

$$2!\;\square \;=\; |\,| \,-\, \times \,+\, |\,{}_{\circ}^{\circ}\,| \,-\, \times{}^{0,0} \,-\, \times{}^{1,0} \tag{19}$$

For the $\sigma\bar{\sigma}$ blocks, the cross terms vanish and eqs. (18) and (19) become:

$$2!\;\square^{\sigma\bar{\sigma}} \;=\; \left(|\,| \,+\, \sqcap\!\sqcap{}^{0,0} \,-\, \sqcap\!\sqcap{}^{1,0} \right)^{\sigma\bar{\sigma}} \tag{20}$$

$$2!\,\square^{\sigma\bar{\sigma}} = \left(| \, | \; + \; |\,\substack{\circ\\\circ} \; - \; 2 \;\times^{1,-1} \right)^{\sigma\bar{\sigma}} \tag{21}$$

By applying relations (15) and (17) all terms on the *r.h.s.* of (20) and (21) may be expressed as $\sigma\sigma$ contributions as follows:

$$2!\,\square^{\sigma\bar{\sigma}} = \left(| \, | \; + \; \top\top^{0,0} \; - \; \top\top^{1,0} \right)^{\sigma\sigma} \tag{22}$$

$$2!\,\square^{\sigma\bar{\sigma}} = \left(| \, | \; + \; |\,\substack{\circ\\\circ} \; - \; 2 \;\times^{1,0} \right)^{\sigma\sigma} \tag{23}$$

Let us now substract relations (18) and (19) it follows that
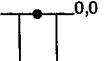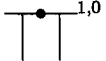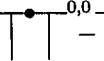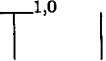
$$|\,\substack{\circ\\\circ} \; + \; \slashed{\times} \;=\; \top\top^{0,0} \; + \; \top\top^{1,0} \; + \; \times^{0,0} \; + \; \times^{1,0} \tag{24}$$

Similarly, by substracting relations (22) and (23) the following relation is obtained:

$$|\,\substack{\circ\\\circ} \;=\; \top\top^{0,0} \; - \; \top\top^{1,0} \; + \; 2 \;\times^{1,0} \tag{25}$$

It is interesting to notice the form in which the mixed products of 1-RDM and 1-$HRDM$ elements carry global information about the correlation effects. In our opinion (24) and (25) are important *Sum* relations. Unfortunately they are not independent relations since by adding up relation (25) for a given element to the relation obtained for the cross element one obtains relation (24). Therefore we have only **half** of the conditions needed for solving the global problem which thus remains open. The question is whether there is still possible to find new relations or whether we must think of an approximative approach which would complete the information needed.

Table 2: Numerical values of some terms.

Matrix element indices	^{0,0}	^{1,0}	^{0,0} ^{1,0}	
$2\,\bar 2;\ 2\,\bar 2$	0.0081	0.0063	0.0018	0.0145
$2\,\bar 3;\ 2\,\bar 3$	−0.0081	−0.0063	−0.0018	0.9707
$2\,\bar 3;\ 3\,\bar 2$	0.4877	0.4863	0.0014	−0.0112

6. Some final remarks

6.1. Magnitude of the correlation terms

It is interesting to analyse the magnitude of the correlation terms. We have calculated their value in our *test example* (the Beryllium atom ground state) and we report in table 2 an extract of the results.

As can be seen, although the complete correlation effect of the $\alpha\beta$ block is small, which seems to indicate that a perturbative treatment may be suitable for its estimation [11], this small quantity results from the cancellation between two large correlation matrices, which may render difficult the convergence of a perturbative treatment.

6.2. The Many-body effects in the 1-*RDM*

From the relations given in the previous section a vast number of equivalent relations can be obtained, each enlightening a different aspect of the problem. Here, as a conclusion, we wish to discuss how the many-body effects are averaged into the 1-*RDM*.

Obviously, relation (25) implies how we can express an 1-*RDM* element as a quotient of the *correlation terms* on the r.h.s. of (25) and of a corresponding 1-*HRDM* element.

Another way in which the 1-*RDM* contains correlation effects can be seen by summing over a common index belonging to different *TRDM*. Thus from relation (25), using the identity (9), one obtains:

$$ \qquad\qquad (26) $$

$$\text{(graph)} \quad = \quad (K - N_\alpha) \diagdown \quad = \quad 2 \; \text{(graph)}^1 \tag{27}$$

where the arc appearing in the graphs means that a sum over a common index is performed. The superscript 2 indicates that the line represents the square of the 1-RDM.

Relation (26) should be underlined since it describes the idempotency deffect of the 1-RDM which is the contraction of the complete *correlation term* corresponding to the $\alpha\beta$ block of the 2-RDM.

6.3. Concluding remarks

In this paper we have reported a series of theoretical results which contribute to clarify how the *many-body* effects can be expressed in terms of the single particle density matrices: 1-RDM and 1-$TRDM$. Whether it is possible to approximate a solution to this system of non-linear equations remains an open question after our initial study of this problem.

Our analysis of the elementary *correlation terms* has lead to three *Sum* relations, eqs. (25), (26) and (27), which express new RDM properties of general interest. The question whether the missing relation connecting the two unknown elementary *correlation terms* exists and can be found or at least approximated is being now investigated in our group.

7. Acknowledgements

References

(1) H. Kummer, J. Math. Phys. **8**, 2063 (1967).

(2) C. Valdemoro, Anales de la Real Soc. Fis. **a79**, 95 (1983).

(3) C. Valdemoro, Phys. Rev.A **31**, 2114 (1985).

(4) C. Valdemoro, pg. 275 in *Density Matrices and Density Functionals* Proceedings of the A.J. Coleman Symposium, Kingston, Ontario, 1985, edited by R. Erdahl and V. Smith (Reidel, Dordrecht, 1987).

(5) S. Cho, Sci. Rep. Gumma Univ. **11**, 1 (1962).

(6) H. Nakatsuji, Phys. Rev. A **14**, 41 (1976).

(7) L. Cohen and C. Frishberg, Phys. Rev. A **13**, 927 (1976).

(8) H. Schlosser, Phys. Rev. A **15**, 1349 (1977).

(9) F. Colmenero and C. Valdemoro, Int. J. Quantum Chem., **51**(6), 369 (1994).

(10) C. Valdemoro, L. M. Tel, E. Pérez-Romero, in *Recent Advances in Computational Quantum Chemistry*, J. Karwowski and M. Karelson, eds. *Advances in Quantum Chemistry*, **28**, 33. Academic Press, 1997.

(11) H. Nakatsutji, K. Yasuda, Phys. Rev. Let. **76**, 1039 (1996).

(12) see for instance pg. 18 and pg. 225 in M. Toda, R Kubo, N. Saito *Statistical Physics I* Springer (1995)

(13) P. O. Löwdin, pg. 1 in *Density Matrices and Density Functionals*, Proceedings of the A.J. Coleman Symposium, Kingston, Ontario, 1985, R. Erdahl and V. Smith, eds. (Reidel, Dordrecht, 1987).

(14) A. J. Coleman, Rev. Mod. Phys. **35**, 668 (1963).

(15) C. Valdemoro, Phys. Rev. A **45**, 4462 (1992).

(16) E. Clementi, C. Roetti, At. Data and Nucl. Data Tables **14**, 428 (1974).

A Consistent Calculation of Atomic Energy Shell Corrections Strutinsky's Method in the Hartree-Fock-Roothaan Scheme

Ya. I. DELCHEV,[a,b] A. I. KULEFF,[a] Jean MARUANI,[b,a] and R. L. PAVLOV[a]

[a] Institute of Nuclear Research and Nuclear Energy, Bulgarian Academy of Sciences, 72 Tsarigradsko Chaussee, 1784 Sofia, Bulgaria

[b] Laboratoire de Chimie Physique, CNRS and UPMC, 11 rue Pierre et Marie Curie, 75005 Paris, France

Abstract

Strutinsky's method for performing a consistent decomposition of the binding energy of a quantum system into averaged and oscillating parts is presented and used to derive a self-consistent averaging procedure (SCAP) in the Hartree-Fock-Roothaan (HFR) scheme. This procedure is applied to atoms from Be to Zn, using their HFR one-electron energies, which shows that the application of Strutinsky's method to atoms requires an accurate determination of that part of the energy spectrum responsible for shell effects. It is shown that SCAP would be a precise tool for splitting an energy space into core and valence parts and for defining and extracting shell effects in such energetic properties as ionization potentials.

1. Introduction
2. Strutinsky's averaging method in the Hartree-Fock scheme
    2.1. Decomposition of the energy into averaged and oscillating parts
    2.2. Strutinsky's averaging technique
    2.3. The self-consistent averaging procedure (SCAP)
3. Formulation of Strutinsky's method in the Hartree-Fock-Rooothaan scheme
4. Results and Discussion
    4.1. Determination of the first-order shell-effect terms
    4.2. Core-valence division of the coordinate space
    4.3. The role of second-order terms in the oscillating part of the energy
5. Conclusion
    Acknowledgments
    References

1. Introduction

Due to Heisenberg's uncertainty and Pauli's exclusion principles, the properties of a multifermionic system correspond to fermions being grouped into shells and subshells. The "shell structure" of the one-particle energy spectrum generates so-called shell effects, at different hierarchical levels (nuclei, atoms, molecules, condensed matter) [1-3].

Shell-structure effects can be divided in two types. The first type is related to the pattern of variation of global properties in specific systems (nuclei, atoms, molecules, clusters) with increasing complexity, revealing a shell-filling process. In atoms, global shell effects are manifested as peculiarities in the variations of elemental properties such as ionization energies, electron affinity, binding energy or polarizabilities, with increasing atomic number [1-6]. The other type of shell effects is related to oscillations, within a system, of local properties such as the one-particle charge, spin or momentum distributions, manifesting a shell structure [7].

The idea of splitting in a systematic manner properties characterizing a Fermi system into a smoothly varying (averaged) part and an oscillating (shell-structure) part originates from results of the semiclassical approach to the many-body problem (Thomas-Fermi treatment and its TFW improvement), which show a complete lack of structure [8, 9]. On the other hand, even the lowest semiclassical (WKB) approximation involving a wave-function, which contains more information on the system, allows recovering of shell corrections in the one-particle density and total binding energy [1, 10]. Other approximations to the problem of extracting shell effects, applicable to many-electron systems [11], are based on a semiclassical description of the one-electron motion: Kohn and Sham [12] and Kirzhnits and Shpatakovskaya [10] have used a semiclassical Green's function approach; Light, Yuang and Lee [13] have introduced a directly determined single-density matrix in the path integral formulation; Englert and Schwinger [4, 5] have incorporated the radial and angular quantizations into an improved statistical model.

The use of these two semiclassical levels of description - the statistical (e.g. TFW) model and the semiclassical (e.g. WKB) treatment - of the one-body motion shows that the main, global or local, properties of a quantum system can be split into two terms: the first, largest one is a smoothly varying term, where shell effects are averaged out, and the second one is an oscillating correction, which contains the information on the system specificity. The question now arises of the relevance and accuracy of such a decomposition.

A method allowing a consistent decomposition of the total binding energy of a quantum system into averaged and oscillating parts was earlier proposed by Strutinsky [14] for nuclear structure theory. This approach was further developed [15, 16] and applied to atomic nuclei [16-22] and metal clusters [3]. In a previous paper [6] we have used a semiclassical energy functional with a model density function for evaluating the smoothly varying part of the binding energy in atoms, and derived shell corrections by substracting the resulting energies from calculated HF energies. However, this procedure does not yield a perfect description of the HF smooth contribution (and could even introduce some spurious correlation) whereas Strutinsky's averaging method is genuinely self-consistent. In the present paper we propose a procedure based on this method within the Hartree-Fock-Roothaan scheme and apply it to some atoms from the 2nd and 3rd rows of the periodic table.

2. Strutinsky's averaging method in the Hartree-Fock scheme

2.1. Decomposition of the energy into averaged and oscillating parts

We consider a system made up of N fermions (nucleons or electrons) interacting through two-body forces and with an external field, with respective potentials $\upsilon(r, r')$ and $V(r)$. We assume there exists a possibility of decomposing the one-particle density matrix into an averaged part and an oscillating part, i.e.:

$$\rho = \tilde{\rho} + \delta\rho, \tag{1}$$

this leading to the decomposition:

$$E = \tilde{E} + \delta E. \tag{2}$$

In what follows we shall, for simplicity, consider HF densities and energies, but the treatment could easily be extended to other levels of approximation.

In matrix notation, the total energy of the system, as a functional of the one-particle density function, takes the form:

$$E_{HF}[\rho] = tr\{h\rho\} + \frac{1}{2} tr.\,tr\{\rho\upsilon_A\rho\}, \tag{3}$$

where $h = -\Delta/2 + V(r)$ is the one-particle energy operator and υ_A is the antisymmetrized matrix operator of the two-particle interaction. The corresponding HF equations take the form:

$$H_{HF}[\rho]\varphi_i(r) = \varepsilon_i\varphi_i(r), \tag{4}$$

where

$$H_{HF}[\rho] = h + tr\{\upsilon_A\rho\} \tag{5}$$

is the one-particle HF effective Hamiltonian. Inserting Eqn (1) into Eqn (3) yields the following decomposition:

$$E_{HF}[\rho] = \tilde{E}_{HF} + \delta_1 E_{HF} + \delta_2 E_{HF} \equiv \tilde{E}_{HF} + \delta E_{HF}, \tag{6}$$

which has the same form as Eqn (2) and where:

$$\tilde{E}_{HF} = E_{HF}[\tilde{\rho}] = tr\{h\tilde{\rho}\} + \frac{1}{2} tr.\,tr\{\tilde{\rho}\upsilon_A\tilde{\rho}\}, \tag{7a}$$

$$\delta_1 E_{HF} = tr\{H_{HF}[\tilde{\rho}]\delta\rho\} = tr\{[h + tr(\upsilon_A\tilde{\rho})]\delta\rho\}, \tag{7b}$$

$$\delta_2 E_{HF} = \frac{1}{2} tr.\,tr\{\delta\rho\upsilon_A\delta\rho\}. \tag{7c}$$

Using a representation of the one-particle density matrix in position space:

$$\rho \equiv \rho(r;r') = \sum_{i=1}^{N} \varphi_i(r)\varphi_i^*(r') = \sum_{\alpha=1}^{\infty} n_\alpha \varphi_\alpha(r)\varphi_\alpha^*(r'), \qquad (8)$$

where n_α may take on fractional values for natural orbitals, and introducing averaged occupation numbers $\tilde{n}_\alpha$, one can express $\tilde{\rho}$ and $\delta\rho$ through these numbers:

$$\tilde{\rho} \equiv \tilde{\rho}(r;r') = \sum_{\alpha=1}^{\infty} \tilde{n}_\alpha \varphi_\alpha(r)\varphi_\alpha^*(r'), \qquad (9)$$

$$\delta\rho \equiv \delta\rho(r;r') = \sum_{\alpha=1}^{\infty} \delta n_\alpha \varphi_\alpha(r)\varphi_\alpha^*(r'), \qquad (10)$$

where

$$\delta n_\alpha = n_\alpha - \tilde{n}_\alpha. \qquad (11)$$

One can rewrite the first-order shell-correction term given by Eqn (7b) by using the self-consistent energies ε_i and the above decomposition:

$$\delta_1 E_{HF} = \sum_\alpha \varepsilon_\alpha n_\alpha - \sum_\alpha \varepsilon_\alpha \tilde{n}_\alpha = \Sigma - \tilde{\Sigma}, \qquad (12)$$

which leads to the following expression of Strutinsky's energy theorem (SET):

$$E_{HF}[\rho] = E_{HF}[\tilde{\rho}] + \sum_\alpha \varepsilon_\alpha \delta n_\alpha + \Theta(\delta^2\rho). \qquad (13)$$

Equations (7) can be viewed as a formal Taylor-series expansion, around the averaged part of the one-particle density matrix, of the HF energy functional $E[\rho]$ [16, 18], this defining a "shell-correction series". In Eqn (13) the first-order term of this expansion is expressed in terms of the single-particle energies ε_i.

In order to device an effective averaging procedure one still has to specify formulas for the average occupation numbers $\tilde{n}_\alpha$.

2.2. Strutinsky's averaging technique

This approach to the averaging problem rests on the idea that shell effects in the ground-state energy stem from the shell structure of the one-particle energy-level distribution g(E):

$$g(E) = \sum_i \delta(E - \varepsilon_i). \qquad (14)$$

A smoothing of the spectrum $\{\varepsilon_i\}$ would lead to an averaging of the total energy.

The smoothed energy level distribution $\tilde{g}(E)$ is defined through a convolution of g(E) with an averaging function $f(x)$:

$$\tilde{g}(E) = \frac{1}{\gamma} \int_{-\infty}^{+\infty} g(E') f\left(\frac{E-E'}{\gamma}\right) dE' = \frac{1}{\gamma} \sum_i f\left(\frac{E-\varepsilon_i}{\gamma}\right), \qquad (15)$$

where γ is the width of the averaging function. The choice of this latter is a widely discussed problem [20-22] and it turns out that there exists a whole class of appropriate functions giving identical results [21]. One may use the first M terms of a series expansion of the sharp distribution (14) in terms of Hermite polynomials to define the smoothed distribution $\tilde{g}(E)$ beyond a simple sum of Gaussians:

$$\tilde{g}(E) = \frac{1}{\gamma\sqrt{\pi}} \sum_i \left\{ e^{-((E-\varepsilon_i)/\gamma)^2} + \sum_{n=1}^{M} a_{2n} \gamma^{2n} \frac{d^{2n}}{dE^{2n}} e^{-((E-\varepsilon_i)/\gamma)^2} \right\}, \quad a_{2n} = (-1)^n / 2^{2n}(2n)!,$$

this yielding the modified Gaussian form for the averaging function of order M:

$$f_M(x) = \frac{1}{\sqrt{\pi}} \sum_{n=0}^{M} \frac{(-1)^n}{2^{2n}(2n)!} \frac{d^{2n}}{dx^{2n}} e^{-x^2}. \qquad (16)$$

This expression includes the curvature corrections to the Gaussian function, which play an important role in the averaging procedure: they ensure the smoothed spectrum $\tilde{g}(E)$ to be approximated, through the above definition, by its own truncated Taylor expansion. This smoothing procedure of the one-electron spectrum is an application of the method of moments, also used in other systems [23].

The conservation of the number of particles introduces a new Fermi level and helps to define the averaged occupation numbers, e.g., in the HF case:

$$N = \int_{-\infty}^{\tilde{\lambda}} \tilde{g}_{HF}(E)dE = \sum_i \int_{-\infty}^{\tilde{\lambda}} \tilde{g}_{i\,HF}(E)dE = \sum_i \tilde{n}_i. \qquad (17)$$

The averaged occupation numbers $\tilde{n}_i$ are a formal ingredient in Strutinsky's averaging method. Combining Eqs (15) and (17) yields their explicit form:

$$\tilde{n}_i = \int_{-\infty}^{t_i} f(x)dx, \quad t_i = (\tilde{\lambda} - \varepsilon_i)/\gamma. \qquad (18)$$

By analogy with the obvious expression for the term Σ introduced in Eqn (12):

$$\Sigma = \int_{-\infty}^{\lambda} Eg_{HF}(E)dE = \sum_i \varepsilon_i n_i, \qquad (19)$$

one can define an averaged term $\tilde{\Sigma}'$ by replacing the energy level distribution g_{HF} in Eqn (19) with the averaged $\tilde{g}_{HF}$ and the Fermi level λ by $\tilde{\lambda}$. The result, which is valid for a whole class of averaging functions, is [16, 21]:

$$\widetilde{\Sigma}' = \sum_i \varepsilon_i \widetilde{n}_i + A(\gamma) = \widetilde{\Sigma} + A(\gamma), \tag{20}$$

where:

$$A(\gamma) = \gamma^2 \sum_i \int_{-\infty}^{t_i} x \widetilde{g}_{i\,HF}(x) dx. \tag{21}$$

It can also be shown that [16, 21]:

$$\frac{d\widetilde{\Sigma}'}{d\gamma} = \gamma \sum_i \int_{-\infty}^{t_i} x \widetilde{g}_{i\,HF}(x) dx \equiv \frac{1}{\gamma} A, \tag{22}$$

and hence $\widetilde{\Sigma}'$ can be written in the form:

$$\widetilde{\Sigma}' = \sum_i \varepsilon_i \widetilde{n}_i + \gamma \frac{d}{d\gamma} \widetilde{\Sigma}'. \tag{23}$$

Imposing the plateau condition [21]

$$\frac{d}{d\gamma} \widetilde{\Sigma}' \bigg|_{\gamma = \gamma_0} = 0 \tag{24}$$

brings $\widetilde{\Sigma}'$ in the desired form $\widetilde{\Sigma}' = \sum_i \varepsilon_i \widetilde{n}_i$ at the values of the smearing parameter γ_0 that satisfy Eqn (24). The stationary condition (24) also leads to the elimination of γ as a free parameter. The explicit expression of $\widetilde{\Sigma}'$ - see Eqs (19-21) - is a highly non-linear function of γ and also depends on the order M of the smearing function in Eqn (16): $\widetilde{\Sigma}' = \widetilde{\Sigma}'(\gamma, M)$. All this leads to the following:

1) There may exist a whole interval of solutions for that equation; these solutions must satisfy the constraint (19) to ensure particle number conservation.
2) When performing the iterative search for γ_0, the condition

$$\widetilde{\Sigma}'(\gamma_0, M) = \widetilde{\Sigma}'(\gamma_0, M+1) \tag{25}$$

must be fulfilled, as the optimum value $M = M_{opt}$ is the smallest for which this equality holds.

With the determination of γ_0 the above-described averaging procedure can be performed, yielding the averaged value $\widetilde{E}_{HF}$ and the shell corrections $\delta_1 E_{HF}$ and $\delta_2 E_{HF}$ for the energy, as well as the averaged and fluctuating parts $\widetilde{\rho}$ and $\delta\rho$ of the one-particle density matrix.

2.3. The self-consistent averaging procedure (SCAP)

By analogy with Eqn (4), let us introduce the new HF-like equations:

$$H_{HF}[\tilde{\rho}]\,\tilde{\varphi}_i(r) = \tilde{\varepsilon}_i\tilde{\varphi}_i(r), \tag{26}$$

where the complete matrix ρ has been replaced with the averaged matrix $\tilde{\rho}$. The first step of the iterative procedure is to solve Eqn (26) with the averaged matrix given by Eqs (9) and (18). In terms of the resulting $\tilde{\varepsilon}_i$ and $\tilde{\varphi}_i$, one can then build the new matrix:

$$\overline{\rho} \equiv \overline{\rho}(r, r') = \sum_i \overline{n}_i \tilde{\varphi}_i(r)\tilde{\varphi}_i^*(r'), \tag{27}$$

where the factors $\overline{n}_i = \theta(\tilde{\varepsilon}_F - \tilde{\varepsilon}_i)$ are the new occupation numbers, $\tilde{\varepsilon}_F$ being the Fermi level of the new spectrum $\{\tilde{\varepsilon}_i\}$. The second step is to average the resulting matrix $\overline{\rho}$, applying Strutinsky's technique described above, and to determine the new occupation numbers related to $\tilde{\overline{\rho}}$.

This process is repeated until self-consistency is reached, the final values $\tilde{\overline{\rho}}_{opt}$ and $\tilde{\overline{n}}_{i\,opt}$ being noted $\tilde{\rho}$ and $\tilde{n}_i$. Using these values the first-order shell correction to the energy can be written:

$$\delta_1 E = \sum_i \tilde{\varepsilon}_i \delta \overline{n}_i, \tag{28}$$

where $\delta \overline{n}_i = \overline{n}_i - \tilde{n}_i$. Involving the so-determined quantities $\tilde{E}_{HF}$ and $\delta_1 E_{HF}$ in Eqn (6) one can reformulate Strutinsky's energy theorem, expressing the total energy in the form:

$$E_{HF}[\rho] = \tilde{E}_{HF} + \delta_1 E_{HF} + \delta_2 E'_{HF} + \delta_2 E''_{HF}, \tag{29}$$

where the last two terms, expressing the second-order corrections, are given by:

$$\delta_2 E' = tr\{h + tr\{\rho \upsilon_A\}\}(\rho - \overline{\rho}), \tag{30a}$$

$$\delta_2 E'' = \frac{1}{2} tr.tr\{\delta \rho \upsilon_A \delta \rho\} - tr.tr\{\delta \rho \upsilon_A (\rho - \overline{\rho})\}. \tag{30b}$$

The analysis of Eqs (29) and (30) shows that the self-consistent treatment of the *averaged part* of the energy tends to minimize the second-order terms [16]. Thus we arrive to the approximate form of the SET:

$$E_{HF} \approx \tilde{E}_{HF} + \delta_1 E, \tag{31}$$

which tells us that all first-order contributions to the fluctuating part of the density matrix are contained in the quantity $\delta_1 E$ given by Eqn (28).

3. Formulation of Strutinsky's method in the Hartree-Fock-Roothaan scheme

The Hartree-Fock-Roothaan (HFR) scheme [24] consists in approximating the one-particle orbitals $\varphi_i(r)$ with linear combinations of suitable basis functions $\chi_p(r)$:

$$\varphi_i = \sum_p \chi_p c_{pi} = \chi \cdot c_i. \tag{32}$$

Then the familiar HF equations (4) take the matrix form:

$$Fc_i = \varepsilon_i Sc_i, \tag{33}$$

where F is the Fockian matrix of the system, S the overlap matrix: $S_{pq} = \langle \chi_p | \chi_q \rangle$, and ε_i and c_i are eigenvalues and eigenvectors defining the system states.

For systems with an open shell, one can express the closed-shell (C), open-shell (O) and total (T) density matrices through the coefficients vectors c_i as:

$$D_C = \sum_k c_k c_k^+, \quad D_O = \sum_m c_m c_m^+, \quad D_T = D_C + D_O. \tag{34}$$

The Fockian matrix can then be written in the form [24]:

$$F = h + P - Q + R, \tag{35}$$

where:

$$\left.\begin{array}{l} h: \ h_{pq} = \langle \chi_p | h | \chi_q \rangle, \\ P = (2J - K)D_T, \\ Q = (2\alpha J - \beta K)D_O, \\ R = SD_T Q + QD_T S. \end{array}\right\} \tag{36}$$

In Eqn (36) J and K are the Coulomb repulsion and exchange supermatrices:

$$J_{pq,rs} = \iint \chi_p^*(1)\chi_r^*(2)\frac{1}{r_{12}}\chi_q(1)\chi_s(2)dr_1 dr_2, \tag{37a}$$

$$K_{pq,rs} = \iint \chi_p^*(1)\chi_r^*(2)\frac{1}{r_{12}}\chi_s(1)\chi_q(2)dr_1 dr_2. \tag{37b}$$

Finally, the total energy of the system can be written in the form [24]:

$$E = (h+F)^t D_T - Q^t (D_C - f D_O),\tag{38}$$

where f is the (generally fractional) occupation number of the open shell.

For our purposes it is convenient to express the closed-shell, open-shell and total density matrices, D_C, D_O, D_T, in terms of closed-shell, open-shell and total occupation numbers, n_i^C, n_i^O, n_i^T, respectively:

$$\left.\begin{aligned}
D_C &= \sum_k c_k c_k^+ = \sum_{i,p} n_i^C c_{pi} c_{ip}^+, \\
D_O &= \sum_m c_m c_m^+ = \sum_{i,p} n_i^O c_{pi} c_{ip}^+, \\
D_T &= D_C + D_O = \sum_{i,p} n_i^T c_{pi} c_{ip}^+.
\end{aligned}\right\}\tag{39}$$

Introducing the averaged occupation numbers $\tilde{n}_i^C$, $\tilde{n}_i^O$, $\tilde{n}_i^T$ from Eqn (17) into Eqn (39), one obtains the averaged parts of the above:

$$\left.\begin{aligned}
\tilde{D}_C &= \sum_{i,p} \tilde{n}_i^C c_{pi} c_{ip}^+, \\
\tilde{D}_O &= \sum_{i,p} \tilde{n}_i^O c_{pi} c_{ip}^+, \\
\tilde{D}_T &= \sum_{i,p} \tilde{n}_i^T c_{pi} c_{ip}^+.
\end{aligned}\right\}\tag{40}$$

Substituting these averaged density matrices into Eqn (36), then into Eqn (35), one obtains the Fockian matrix as a functional of the averaged density matrices:

$$F\big[\tilde{D}\big] = h + P\big[\tilde{D}_T\big] - Q\big[\tilde{D}_O\big] + R\big[\tilde{D}_O, \tilde{D}_T\big],\tag{41}$$

where:

$$\left.\begin{aligned}
P\big[\tilde{D}_T\big] &= B\tilde{D}_T = (2J - K)\tilde{D}_T, \\
Q\big[\tilde{D}_O\big] &= L\tilde{D}_O = (2\alpha J - \beta K)\tilde{D}_O, \\
R\big[\tilde{D}_O, \tilde{D}_T\big] &= S\tilde{D}_T L\tilde{D}_O - L\tilde{D}_O \tilde{D}_T S.
\end{aligned}\right\}\tag{42}$$

The corresponding HFR system of equations is:

$$F\big[\tilde{D}\big] c_i' = \varepsilon_i' S c_i'.\tag{43}$$

Solving the HFR problem yields new coefficients c_i', which define a new density matrix $\tilde{D}'$ according to Eqs (40). With this new matrix and using Eqs (7) and (38), one can express the averaged energy as:

$$\tilde{E}_{HFR} = \left(h + F[\tilde{D}']\right)^{t} \tilde{D}'_{T} - Q[\tilde{D}'_{O}]^{t}\left(\tilde{D}'_{C} + f\tilde{D}'_{O}\right). \qquad (44)$$

As we have satisfied the plateau condition (24) and the condition (25) for reaching the optimal value of M, we have defined a self-consistent procedure leading to the optimal averaged density matrix $\tilde{D}^{opt}$.

We can now give the explicit forms of the self-consistent averaged and first-order oscillating parts of the ground-state energy of the open-shell system:

$$\left.\begin{array}{l} \tilde{E}_{HFR} = tr\left\{\left(h + F[\tilde{D}^{opt}]\right)^{t} \tilde{D}_{T}^{opt} - Q[\tilde{D}_{O}^{opt}]^{t}\left(\tilde{D}_{C}^{opt} + f\tilde{D}_{O}^{opt}\right)\right\}, \\ \\ \delta_{1}E_{HFR} = tr\left\{\left[\left(h + F[\tilde{D}^{opt}]\right)^{t} \tilde{D}_{T}^{opt} - Q[\tilde{D}_{O}^{opt}]^{t}\left(\tilde{D}_{C}^{opt} + f\tilde{D}_{O}^{opt}\right)\right]\delta D_{T}^{opt}\right\}, \end{array}\right\} \quad (45)$$

where: $\delta D_{T}^{opt} = \sum_{i,p} \delta n_{i}^{T} c_{pi}^{opt}\left(c_{ip}^{opt}\right)^{+}$. Using these expressions for $\tilde{E}_{HFR}$ and $\delta_{1}E_{HFR}$ and the non-averaged optimal density matrices $\overline{D}_{C}$, $\overline{D}_{O}$ and $\overline{D}_{T}$ (obtained through the first step of the SCAP), one can express the total energy E_{HFR} in the form given by Eqn (29).

4. Results and Discussion

In Section 3 we have formulated Strutinsky's shell-correction method in the framework of the analytic HFR scheme, for single open-shell atoms and molecules in their ground state. The consideration of two or many open-shell systems could be performed following the same pattern. Both the averaged part of the energy, $\tilde{E}_{HFR}$, and its first-order shell-correction part, $\delta_{1}E_{HFR}$, have been derived in analytic form, and the self-consistent process for determining them has been described.

4.1. Determination of the first-order shell-effect terms

In Subsections 2.2 and 2.3 it was shown that Strutinsky's energy theorem can be formulated in two different forms, Eqs (13) and (29). The first form is relevant after the first step of the SCAP (the first averaging of the HFR results) is performed, whereas the second form comes in after the final step. Actual calculations in nuclear physics [16-22] have shown that the values obtained for $E[\tilde{\rho}]$ and $\tilde{E}[\tilde{\rho}]$ are rather close. The SCAP stationarity essentially leads to the gathering of all fluctuations of the total energy in the first-order term, $\delta_{1}E(\tilde{\varepsilon}_{i})$, minimizing the sum of the second-order terms in Eqn (29).

We have performed calculations aimed at testing the applicability of Strutinsky's shell-correction method to atoms and also at investigating the main features of the irregular part $\delta_{1}E_{HFR}$ of E_{HFR} as a function of the atomic number Z. For this

purpose we have performed the non-self-consistent computation of the first-order shell-correction term $\delta_1 E_{HFR} = \sum_i \varepsilon_i \delta n_i$ using the one-particle HFR spectra $\{\varepsilon_i\}$ from Clementi and Roetti [25].

In order to determine the averaged occupation numbers $\tilde{n}_i$ for the considered atoms ($3 \leq Z \leq 30$), we have solved numerically the system of highly non-linear equations composed from the particle number conservation condition (17) and the plateau condition (24). It was found that the condition (25) is fulfilled with desired accuracy (with less than 1% discrepancy for $\delta_1 E_{HFR}$) for values of M $\geq$ 35, and the roots γ_0 and $\tilde{\lambda}$ found at M = 35 allow a correct determination of the $\tilde{n}_i$.

It turns out there are increasing roots, γ_0^i, of the parameter γ that lead to successive (shell after shell) smoothing of the discrete spectrum g(E). In this investigation, we have chosen the first roots $\gamma = \gamma_0^i$ that fulfill the successive smearing of the different main shells and for which a well pronounced plateau is observed. Fig. (1a) displays the smoothed energy level distribution $\tilde{g}_{HFR}$ (E) for atom Zn (Z = 30), which has four shells ($1s^2 2s^2 2p^6 3s^2 3p^6 3d^{10} 4s^2$), for the plateau values of γ: γ_0^{min} (continuous line) and γ_0^{mid} (dotted line). We see that the root γ_0^{min} corresponds to complete smoothing (in energy space) of the two outer-shell electrons $4s^2$ but that the spectrum $\tilde{g}_{HFR}$ (E, γ_0^{min}) preserves a clear information on the existence of the first two shells. For the root γ_0^{mid} such information is still kept only about the deeply bonded $1s^2$ electrons. Fig. (1b) displays the function $\tilde{g}_{HFR}$ (E, γ_0^{max}), which shows that for $\gamma = \gamma_0^{max}$ the one-particle spectrum is completely smoothed out.
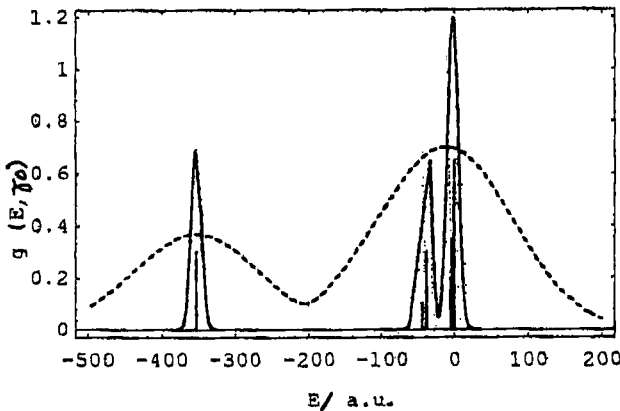
Fig. (1a) Smoothed energy-level distribution $\tilde{g}_{HFR}$ (E) for the Zn atom (Z = 30) with plateau values of γ: γ_0^{min} (continuous line) and γ_0^{mid} (dotted line).
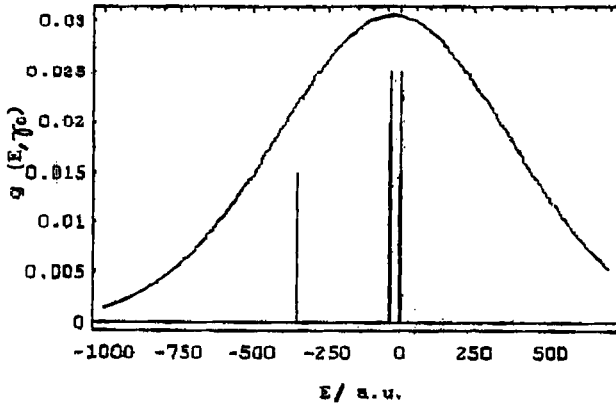
Fig. (1b) Smoothed energy-level distribution $\tilde{g}_{HFR}$ (E) for the Zn atom (Z = 30) with the plateau value $\gamma = \gamma_0^{max}$.

In accordance with these observations one can completely smooth an atomic spectrum with some optimal value of γ, γ_0^{max}. The two-shell, second-row atoms ($3 \leq Z \leq 10$) have only one stationary value: $\gamma = \gamma_0^{max}$ (the first that smoothes the whole spectrum). The three-shell, third-row atoms ($11 \leq Z \leq 18$) have two such values of γ: the first one, γ_0^{mid}, corresponds to complete smoothing of the two-shell upper part of the discrete spectrum, and the second one, γ_0^{max}, leads to total smoothing of the whole spectrum. In the case of four-shell, fourth-row atoms, as it was illustrated on Zinc, there exist three such roots: γ_0^{min}, γ_0^{mid}, γ_0^{max}. The use of the second one (γ_0^{mid}) results in complete smoothing of g_{HFR}(E) beyond the K-shell region. The same role was played by the first root in the case of three-shell atoms (that is why we denote these two different roots with the same symbol).

An important feature of SCAP is that in regions of level energies for which the condition $|\varepsilon_i - \lambda| \gg \gamma_0$ is fulfilled, the occupation numbers $\tilde{n}_i \rightarrow 1$ ($\delta n_i \rightarrow 0$) and the contributions from these levels are practically negligible. Thus, when $\gamma = \gamma_0^{mid}$ the contribution from the K-shell electrons to $\delta_1 E_{HFR}$ is averaged out and when $\gamma = \gamma_0^{min}$ the same holds true for contributions from the K- and L-shell electrons.

In Figures (2a), (2b) and (2c) there are displayed the calculated functions $\delta_1 E_{HFR}(\gamma_0^{max})$, $\delta_1 E_{HFR}(\gamma_0^{mid})$ and $\delta_1 E_{HFR}(\gamma_0^{min})$, respectively. The first curve shows no visible peculiarity. The second curve is still monotonous but displays an inflection

point. The third curve shows a typical shell-effect pattern. We shall now analyze the behaviour of these three curves, taking into account the specificity of atomic energy level distributions compared to those in nuclei, where the proposed SCAP works remarkably well.
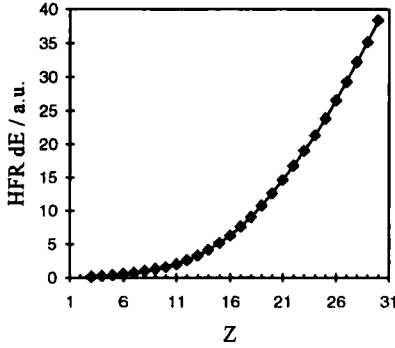
Fig. (2a) Graphic of $\delta E_{HFR}(\gamma_0^{max})$ as a function of Z.
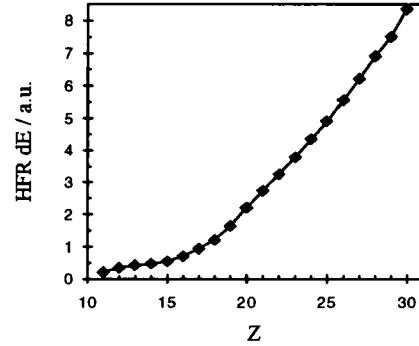
Fig. (2b) Graphic of $\delta E_{HFR}(\gamma_0^{mid})$ as a function of Z.
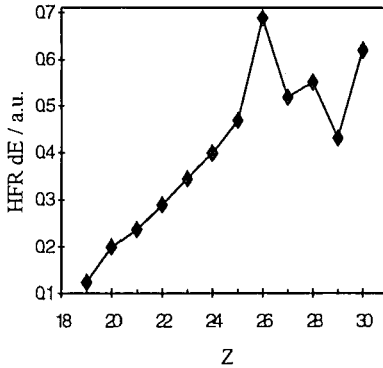
Fig. (2c) Graphic of $\delta E_{HFR}(\gamma_0^{min})$ as a function of Z.
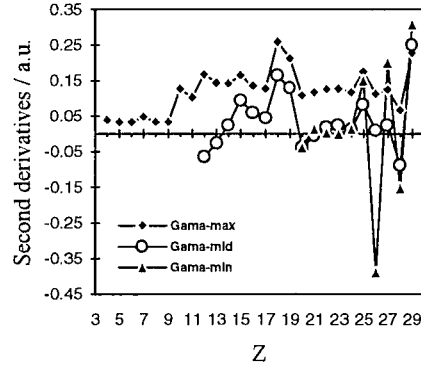
Fig. (3) Graphics of the second derivatives of the curves shown in Figs (2a,b,c).

A typical feature of one-particle level distributions in atomic nuclei is that, the shells being roughly at a distance Ω apart, a value of $\gamma_0 \geq \Omega$ smoothes out the whole spectrum, though only the region around the Fermi level participates in real calculations. This suggests that one could smooth an n-shell energy spectrum using

(n-1) values γ'_0 (i = 1, ..., n-1). The question then arises about which of these values γ'_0 eventually leads to a smoothing of the spectrum that allows a decomposition of the ground-state energy into regular and irregular parts.

We have shown in a previous paper [6] that the second (finite-difference) discrete derivative can be used to enhance (and make visible) tiny irregularities in an energy variation and that the curve $d^2E_{HFR}(Z) / dZ^2$ bears a striking resemblance with that of first ionisation energies, where shell effects appear connected with electrons near the Fermi level. Therefore, in order to analyze the functions displayed in Figs (2a), (2b) and (2c), we have calculated their second discrete derivatives, which are displayed in Fig. (3). It appears the three curves follow a similar trend, excepting the points for Z = 12 (Mg), Z = 13 (Al) and Z = 14 (Sc). This latter peculiarity can be explained by noticing that for the first third-row atoms ($11 \leq Z \leq 14$) those values $\gamma_0^{mid}(Z)$ that smooth their spectrum for $\varepsilon_i > \varepsilon_{1s}$ fulfill the following inequality: $|\varepsilon_{2s} - \varepsilon_F| \geq \gamma_0^{mid}$. This means the contribution of the 2s-electrons to $\delta_1 E_{HFR}(Z, \gamma_0^{mid})$ is partly eliminated. This defect comes from the application of the standard averaging procedure to atoms, and may be overcome by performing a more precise averaging, as is discussed below.

It can be seen on Fig. (3) that, excepting the mentioned three points, the second derivatives $\dfrac{d^2(\delta_1 E_{HFR}(Z, \gamma_0^{mid}))}{dZ^2}$ and $\dfrac{d^2(\delta_1 E_{HFR}(Z, \gamma_0^{max}))}{dZ^2}$ are almost parallel. The parallelism of these curves, which differ only by the contribution of the K-shell electrons to $\delta_1 E_{HFR}(Z, \gamma_0^{max})$, shows this contribution is practically regular, and can be included in $\widetilde{E}_{HFR}(Z, \gamma_0^{max})$. The similar conclusion that the L-electrons do not contribute to the fluctuating part of the energy can be made by comparing the derivatives $\dfrac{d^2(\delta_1 E_{HFR}(Z, \gamma_0^{mid}))}{dZ^2}$ and $\dfrac{d^2(\delta_1 E_{HFR}(Z, \gamma_0^{min}))}{dZ^2}$ in their common interval $19 \leq Z \leq 29$. It turns out that the complete smoothing of the highest two bunches (shells) of energy levels is sufficient to evaluate the first-order correction in the ground-state energy:

$$\delta_1 E_{HFR}(Z) \approx \begin{cases} \delta_1 E_{HFR}(Z, \gamma_0^{max}), & 3 \leq Z \leq 10 \\ \delta_1 E_{HFR}(Z, \gamma_0^{mid}), & 11 \leq Z \leq 18 \\ \delta_1 E_{HFR}(Z, \gamma_0^{min}), & 19 \leq Z \leq 30. \end{cases} \tag{46}$$

The shape of this function, displayed in Fig. (4), resembles that of the first ionization potentials. It should be stressed that a more precise determination of the levels involved in the averaging procedure should allow a more exact extraction of the irregular component of the energy [26]. As we have seen, the standard Strutinsky technique gives the possibility of smoothing out an atomic spectrum, shell after shell, beginning with those shells outermost in energy space. But it cannot help determine in advance the region in energy space corresponding specifically to the irre-

gular component of the binding energy. That is why Eqn (46) is only approximate, and must be improved. In particular, the values of $\delta_1 E_{HFR}(Z, \gamma_0^{mid})$ in the interval $11 \leq Z \leq 14$ should be corrected. A precise splitting of the ground-state energy into regular and irregular parts using Strutinsky's method would eventually lead to a consistent core-valence separation in the energy space.
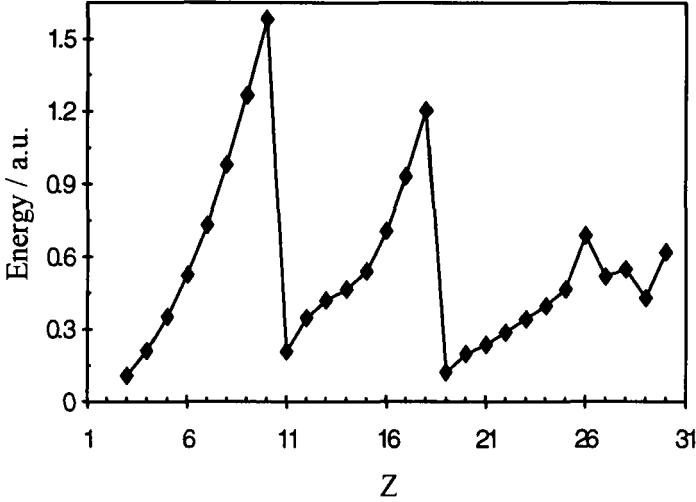
Fig. (4) Graphic of $\delta_1 E_{HFR}$, Eqn (46), as a function of Z.

4.2. Core-valence division of the coordinate space

Using Eqs (9) and (10) for the smooth and oscillating parts of the one-body density matrix in the configuration space, one can calculate the averaged and shell-correction parts of all single-particle operators, particularly the respective charge densities. Figure (5a) displays the radial density distribution for the Argon atom: $D(r) = 4\pi r^2 \rho(r, r')\big|_{r=r'}$, and its smoothed part: $\tilde{D}(r) = 4\pi r^2 \tilde{\rho}(r, r')\big|_{r=r'}$, for $\gamma = \gamma_0^{max}$. Figure (5b) displays the oscillating part $\delta D(r) = D(r) - \tilde{D}(r) = 4\pi r^2 \delta\rho(r, r')\big|_{r=r'}$ for $\gamma = \gamma_0^{max}$ and $\gamma = \gamma_0^{mid}$. As it can be seen on Fig. (5a), averaging in energy space, even when the spectrum is completely smoothed, does not imply an essential change in the radial charge distribution. Taking into account Eqn (17), it follows from Eqn (11) that $\sum_i \delta n_i = 0$, which gives $\int \delta D(r) dr = 0$. So the effect of Strutinsky's averaging shows up in the charge redistribution (Fig. 5b). Obviously $-\int_0^{r_c} \delta D(r) dr = \int_{r_c}^{\infty} \delta D(r) dr = \Delta N$, where

r_C is the point at which $\delta D(r)$ crosses the r-axis and ΔN is the number of electrons transferred from the outermost to the inner levels, all belonging to the interval $\varepsilon_F - \gamma_0$ $< \varepsilon_i \leq \varepsilon_F$. The dependence of ΔN on Z should be a completely irregular function reflecting the peculiarities of the shell structure. For actual smoothing ($\gamma = \gamma_0^{mid}$) of the Argon spectrum, $r_C(\gamma_0^{mid}) = 0.798$ and $\Delta N = 1.447$. The corresponding core radius r_C for Ar, determined through an averaged potential function [27], is 0.737. The behaviour of the valence electrons [27] with respect to the atomic number Z has, in general, the same shape as the function $\delta_1 E_{HFR}(Z)$ plotted in Fig. (4).
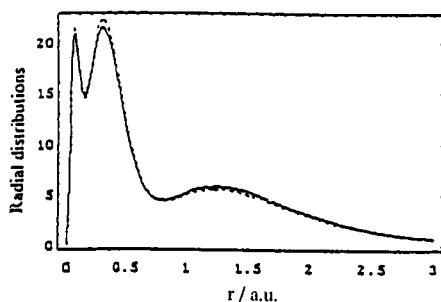
Fig. (5a) Radial charge density distribution in Argon. Total density $D(r)$ (solid) and its smoothed part $\tilde{D}(r)$ for $\gamma = \gamma_0^{max}$ (dotted).
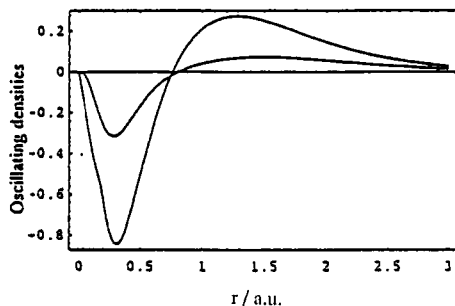
Fig. (5b) Oscillating part of the radial density $\delta D(r) = D(r) - \tilde{D}(r) = 4\pi r^2 \delta\rho(r, r')\big|_{r=r'}$ for $\gamma = \gamma_0^{max}$ (broad) and $\gamma = \gamma_0^{mid}$ (sharp).

Thus, dividing the energy space into core and valence parts generates a core valence partition of the density distribution. This shows that a careful application, as discussed above, of the considered method should allow to define, in a systematic way, a division of the coordinate space into a chemically relevant valence region and a more physical core region. The absolute value of the total energy of the isolated atoms is of little importance for understanding the diverse aspects of molecular structure and chemical reactivity [8, 28]. Properties which are extremely useful in such investigations are the electronegativity μ and hardness η. These are defined as the first and second discrete derivatives of E with respect to the electron number N at constant nuclear charge Z. From this it follows that the peculiarities of μ and η along the periodic table should be determined by the shell-effect part δE of the total energy and their smooth behaviour from the averaged part $\tilde{E}$.

4.3. The role of second-order terms in the oscillating part of the energy

Let us assume that a strict decomposition of the HF energy is performed in the framework of Strutinsky's method: $E_{HFR}(Z) = \tilde{E}_{HFR}(Z) + \delta_1 E_{HFR}(Z) + \delta_2 E_{HFR}(Z)$.

By hypothesis, the regular term $\tilde{E}_{HFR}(Z)$ is a (smooth) monotonic function without peculiarities. Hence, the second derivative $\dfrac{d^2}{dZ^2}\tilde{E}_{HFR}(Z)$ (assuming Z varies continuously) is a function of the same type containing information about the curvature of $\tilde{E}_{HFR}(Z)$ but not its values. Therefore, a mathematical smoothing of $\dfrac{d^2}{dZ^2}E_{HFR}(Z)$ through a suitable smoothing function should yield a reasonable evaluation of the second derivative of $\tilde{E}_{HFR}(Z)$: $\dfrac{d^2}{dZ^2}\tilde{E} \approx \left\langle \dfrac{d^2}{dZ^2}E \right\rangle$. We have calculated $\dfrac{d^2}{dZ^2}E_{HFR}(Z)$ by taking the discrete (finite-difference) second derivative of $E_{HFR}(Z)$ and smoothing it with the second derivative of the Thomas-Fermi-Schwinger (TFS) binding energy expression [5]:

$$\frac{d^2}{dZ^2}E_{TFS} = aZ^{-1/3} + bZ^{1/3} + c, \tag{47}$$

where a, b, c were treated as free parameters. Performing a least-squares fit of the calculated values of the discrete second derivative $\dfrac{d^2}{dZ^2}E_{HFR}(Z)$ to Eqn (47), we obtain an approximation of the second derivative of the smooth part of the energy: $\left\langle \dfrac{d^2}{dZ^2}E_{HFR}(Z) \right\rangle = -1.23104Z^{-1/3} - 2.74327Z^{1/3} + 2.12069$. Subtracting the values obtained using this expression from those calculated for $\dfrac{d^2}{dZ^2}E_{HFR}(Z)$ yields an estimate for the second derivative of the full shell-effects in the energy, $\delta E_{HFR} = \delta_1 E_{HFR} + \delta_2 E_{HFR}$:

$$\frac{d^2}{dZ^2}\delta E_{HFR}(Z) \approx \frac{d^2}{dZ^2}E_{HFR}(Z) - \left\langle \frac{d^2}{dZ^2}E_{HFR}(Z) \right\rangle. \tag{48}$$

Figures (6a) and (6b) display this function together with the finite-difference second derivatives $\dfrac{d^2}{dZ^2}\delta_1 E_{HFR}(Z, \gamma_0^{max})$ and $\dfrac{d^2}{dZ^2}\delta_1 E_{HFR}(Z, \gamma_0^{mid})$ in their relevant domains. The function $\dfrac{d^2}{dZ^2}\delta E_{HFR}(Z)$ is a sum of two irregular functions: $\dfrac{d^2}{dZ^2}\delta_1 E_{HFR}(Z)$ and $\dfrac{d^2}{dZ^2}\delta_2 E_{HFR}(Z)$, which are mathematical approximations to the corresponding functions computable using Strutinsky's energy averaging method. The function $\dfrac{d^2}{dZ^2}\delta_1 E_{HFR}(Z, \gamma_0^{max})$ involves, besides the finite-difference second derivative of the first-order shell-correction term, $\dfrac{d^2}{dZ^2}\delta_1 E_{HFR}(Z)$, an unknown regular function (see

Subsection 4.1). This tells us that the irregularities in both functions should have the same character if the second-order term derivative $\frac{d^2}{dZ^2}\delta_2 E_{HFR}(Z)$ is negligible.
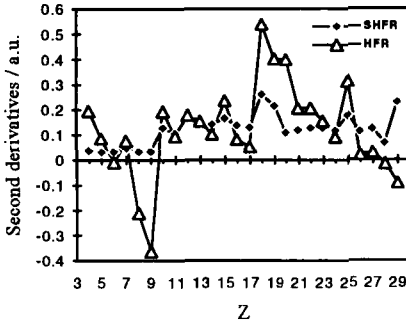
Fig. (6a) Comparison of the second derivatives of $\delta_1 E_{HFR}(\gamma_0^{max})$ (SHFR) and δE_{HFR} (HFR) as functions of Z.
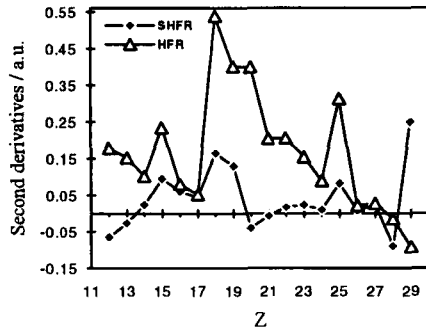
Fig. (6b) Comparison of the second derivatives of $\delta_1 E_{HFR}(\gamma_0^{mid})$ (SHFR) and δE_{HFR} (HFR) as functions of Z.

It turns out that for the second and third rows of elements the variations of the functions presented in Fig. (6a) are roughly similar, whereas some exceptions appear for the fourth row. One of these occurs in the subinterval $Z = 20\text{-}23$, and is obviously due to the influence of the second-order term $\frac{d^2}{dZ^2}\delta_2 E_{HFR}(Z)$ when the subshell 3d starts filling. The opposite variations of the two recorded functions in the $Z = 22\text{-}23$ interval are due to the fact that in the calculation of finite-difference second derivatives the values of two neighbouring left points are involved. In other words, the unconformity in the $Z = 22\text{-}23$ interval is a result of the larger discrepancy due to irregular shell filling between $Z = 20$ and 21. A similar exception occurs in the subinterval $Z = 28\text{-}29$, which again stresses the role of the second-order term when shell filling is irregular: Ni $(3d^8 4s^2) \rightarrow$ Cu $(3d^{10} 4s^1) \rightarrow$ Zn $(3d^{10} 4s^2)$.

Another difference between $\frac{d^2}{dZ^2}\delta_1 E_{HFR}(Z, \gamma_0^{max})$ and $\frac{d^2}{dZ^2}\delta E_{HFR}(Z)$ is the enhancement of the peaks at $Z = 10$ (Ne) and 18 (Ar), where the shells are filled, and at $Z = 15$ (P) and 25 (Mn), where the 3p and 3d subshells, respectively, are half-filled. We have shown in a previous paper [6] that these values correspond to peaks in the second derivative of the Hartree-Fock energy as well as of the first ionization potential. It can also be noticed that, contrary to the situation in the third and fourth rows, the variations of the functions $\frac{d^2}{dZ^2}\delta_1 E_{HFR}(Z, \gamma_0^{max})$ and $\frac{d^2}{dZ^2}\delta E_{HFR}(Z)$ in the sec-

ond row, although quite similar in shape, are very different in amplitude. These differences obviously result from the behaviour of the second-order shell-effect component $\frac{d^2}{dZ^2}\delta_2 E_{HFR}(Z)$ within $\frac{d^2}{dZ^2}\delta E_{HFR}(Z)$. This does not mean, however, that the second-order correction itself, $\delta_2 E_{HFR}$, is very large for second-row elements, but it testifies that the role of this corrective term must be carefully investigated.

To summarize this subsection one can state that: i) The role of second-order shell-effect terms can be determined by investigating the discrepancies between the discrete second derivatives of the functions $\delta E_{HFR}(Z)$ and $\delta_1 E_{HFR}(Z, \gamma_0)$. ii) For the second row of elements these terms determine the whole pattern of the oscillating part of the energy. iii) They also play an important role in critical regions of shell filling (i.e., around shells fully, half, or irregularly filled).

5. Conclusion

The basic feature of semiclassical approaches is that Thomas-Fermi (TF) or TF-like model distributions of the one-fermion spectrum obtained in this manner are continuous. The result is a complete smoothing of all (global and local) properties of the TF systems, i.e., an averaging out of shell-structure effects. Using a TF model in the framework of a semiclassical independent-particle approach, Englert and Schwinger (ES) [5] incorporated angular and radial quantization effects into the statistical treatment. The physical meaning of the quantum correction E_{qu} obtained in this manner is that it improves the TF description of the energy - restoring its missing irregular ingredient - as well as of the one-electron density and all other properties [4]. As the ES approach is less accurate than the HF model and as in our treatment shell effects are considered at the HF level, we must compare the ES correction E_{qu} with the HF oscillations [5]: $E_{osc} = E_{HF} - E_{TF}$. It turns out that, to a large extent, E_{qu} qualitatively reflects the pattern of E_{osc}, but not its magnitude.

The idea that there exists a smoothly varying part in the ground-state energy which is of a statistical nature has been used to extract the shell-effect part of atomic properties [28]. This approach applied to the investigation of the tiny irregular variations of atomic energies with atomic number Z presents some uncertainty [6], due to the hypothetical nature of the statistical description of the large smooth variation. In fact, the problem of performing a consistent separation of the oscillating component of the atomic energies is still open. The results of Subsection 4 make us believe that this problem could be solved in the framework of Strutinsky's energy averaging method. However, it turns out that a proper application of this method requires a more accurate formulation, involving only that region of actual definition of the irregular property [26]. This implies averaging that part of the spectrum which generates the fluctuations in the energy, which can be done by applying a modification [26] of the original method or through the standard procedure, by freezing the core region and smearing out only the outermost part of the property.

Such an investigation of the irregular components of physical properties caused by the outermost electrons should give the possibility to check to what extent the core-valence splitting hypothesis is fulfilled and to investigate the existence of shell-effects due to the bulk electrons. It would be particularly interesting to study diatomics in this framework, as this might give critical information about the specific character of chemical bonds.

In conclusion it can be said that the self-consistent averaging procedure presented in this paper could be a precise tool for splitting the energy space into core and valence parts, and extracting the smooth and oscillating variations in such energetic properties as ionisation potential, electron affinity, electronegativity or hardness, and for defining the splittings in atomic spectra in terms of core and valence contributions in the energy space.

References

1. D.A. Kirzhnits, Yu.E. Lozovik, and G.V. Shpatakovskaya, Sov. Phys. Usp. **18**, 649 (1976).

2. P. Ring and P. Schuck, *The Nuclear Many-Body Problem* (Springer Verlag, New York, 1980).

3. M. Brack, Rev. Mod. Phys. **65**, 677 (1993).

4. B.-G. Englert, *Lecture Notes in Physics* **300** (Springer Verlag, Berlin, 1988).

5. B.-G. Englert and J. Schwinger, Phys. Rev. A **32**, 47 (1985).

6. Ya.I. Delchev, R.L. Pavlov, K.A. Pavlova, L.P. Marinova, and J. Maruani, Int. J. Quantum Chem. **52**, 1349 (1994).

7. C. Sarasola, L. Dominguez, M. Aguado, and J.M. Ugalbe, J. Chem. Phys. **96**, 6778 (1992) and references therein.

8. R.G. Parr and W. Yang, *Density-Functional Theory of Atoms and Molecules* (Oxford University Press, New York, 1989).

9. I.Zh. Petkov and M.V. Stoitsov, *Nuclear Density-Functional Theory* (Clarendon Press, Oxford, 1991).

10. D.A. Kirzhnits and G.V. Shpatakovskaya, J.E.T.P. **62**, 2082 (1972); **66**, 1828 (1974).

11. Because of the near constancy of the density distributions in the nuclear volume, the separation of shell effects is easier there and part of the methods deviced in the nuclear field are not applicable to electronic structure.

12. W. Kohn and J.L. Sham, Phys. Rev. A **137**, 1697 (1965).

13. J.C. Light and J.-M. Yuang, J. Chem. Phys. **58**, 660 (1973); J.-M. Yuang, S.-Y. Lee and J.C. Light, J. Chem. Phys. **61**, 3394 (1974).

14. V.M. Strutinsky, Nucl. Phys. A **95**, 420 (1967); A **122**, 1 (1968).

15. M. Brack, O. Gezken, and K. Hansen, Z. Phys. D **21**, 65 (1991).

16. M. Brack and P. Quentin, Nucl. Phys. A **361**, 35 (1981).

17. M. Brack, "Physics and Chemistry of Fission", Jülich 1979 (IAAE, Vienna, 1980), vol. 1, p 227.

18. M. Brack and P. Quentin, in G. Ripka and M. Porneuf (eds), *Nuclear Self-Consistent Field* (North-Holland, Amsterdam, 1975), p. 353.

19. M. Brack, in R.M. Dreizler and J. da Providencia (eds), *Density Functional Methods in Physics*, NATO ASI Series B **123** (Plenum, New York, 1985), p. 331.

20. M. Brack, J. Damgaard, A.S. Nilsen, H.C. Pauli, V.M. Strutinsky, and C.Y. Wong, Rev. Mod. Phys. **44**, 320 (1973).

21. M. Brack and H.C. Pauli, Nucl. Phys. A **207**, 401 (1973).

22. G.G. Bunatian, V.M. Kolomietz, and V.M. Strutinsky, Nucl. Phys. A **188**, 225 (1972).

23. J.C. Parikh, J. Phys. B **11**, 1881 (1978). M. Bancewicz, G.H.F. Dierksen and J. Karwowski, Phys. Rev. A **40**, 5507 (1989). Other references can be found in: T.A. Broody, J. Flowers, J.B. French, *et al.*, Rev. Mod. Phys. **53**, 385 (1982).

24. C.C.J. Roothaan, Rev. Mod. Phys. **23**, 69 (1951); **32**, 179 (1960).

25. E. Clementi and C. Roetti, Atomic and Nuclear Data Tables **14**, 177 (1974).

26. V.M. Strutinsky and F.A. Ivanjyk, Nucl. Phys. A **255**, 405 (1975).

27. K.D. Sen, T.V. Gayatri, R. Krishnaveni, *et al.*, Int. J. Quantum Chem. **56**, 399 (1995).

28. A. Vela, M. Galván and J. L. Gázquez, Int. J. Quantum Chem. **22**, 329 (1988). I.K. Dimitrieva and G.I. Plindov, J. Physique **43**, 1599 (1982).

Multireference Brillouin-Wigner Coupled-Cluster Theory.

Single-root approach.

Jozef Mášik and Ivan Hubač

Department of Chemical Physics, Faculty of Mathematics and Physics,

Comenius University, 842 15 Bratislava, Slovakia

Abstract

Recently developed Brillouin-Wigner coupled-cluster theory [I. Hubač and P. Neogrády, Phys. Rev. A **50**, 4558 (1994)] is extended to a multireference case using the Hilbert space approach. We formulate the so-called single-root (one-state or state-specific) version which deals with one state at a time while employing a multiconfigurational reference wave function. Employing the Hilbert space approach to the wave operator, we present an explicit form for cluster amplitudes in a spin-orbital form within the CCSD approximation; i.e. coupled-cluster method truncated at the single and double excitation level. The method is applied to a trapezoidal H4 model system with the use of a two-determinant reference space and the results are compared with the full configuration interaction as well as other correlated multireference techniques. The method provides a balanced description of the ground state in both quasidegenerate and nondegenerate regions and deviations from the full configuration interaction energies do not exceed 0.6 mHartree.

Contents:

1. INTRODUCTION.

In the past two decades, the single-reference coupled-cluster (CC) method, based on the exponential expansion of the wave function, has become one of the most efficient and reliable methods to account for many-electron correlation effects in the closed-shell nondegenerate ground states [1–9]. Attraction of the CC method lies in its size-extensive character (linear dependence of the energy on the number of particles) and computational feasibility. As is well-known, size-extensivity of the CC method and related Rayleigh-Schrödinger perturbation theory (RSPT) or alternatively referred to as many-body perturbation theory (MBPT) that employs a perturbation expansion of the wave function is guaranteed by the linked cluster theorem [10] which results in a full cancellation of the so-called unlinked diagrams. This property is achieved by the use of the Rayleigh-Schrödinger type of resolvent in perturbation theories and the Baker-Campbell-Hausdorff (BCH) formula in the case of CC theories. In contrast to the CC method, the use of MBPT is computationally more demanding and the alternative truncated configuration interaction (CI) method, based on the variational expansion of the wave function, does not provide us with size-extensive energies and, moreover, its convergence is very slow.

Nevertheless, an extension of the CC method to a multireference case, that is necessary when handling quasi-degenerate or general open-shell systems, has proven far from being straightforward, both theoretically and computationally. Depending on the form of an exponential ansatz employed, existing multireference coupled-cluster (MR CC) theories can be divided into two broad types, namely the Fock space approach (also referred to as valence universal) which employs a single (valence universal) exponential wave operator [11–22] and the Hilbert space approach (also referred to as state universal) based on the exponential ansatz of Jeziorski and Monkhorst [23] who represent the wave operator as a superposition of exponential operators, one for each configuration spanning the reference space. While the Fock space formalism is suitable for the calculation of the "differential" properties, such as excitation or ionization energies, and has seen an increasing number of applications in recent years, the Hilbert space formalism is preferred in determination of potential energy surfaces and, unlike the Fock space approach, has seen rather limited number of applications, mostly oriented to the H4 and H8 model systems exploiting a two-determinant reference space.

The main reason why existing MR CC methods as well as related MR MBPT cannot be considered as standard or routine methods is the fact that both theories suffer from the intruder state problem or generally from the convergence problems. As is well known, both MR MBPT/CC theories are built on the concept of the effective Hamiltonian that acts in a relatively small model or reference space and provides us with energies of several states at the same time by diagonalization of the effective Hamiltonian. In order to warrant size-extensivity, both theories employ the complete model space formulations. Although conceptually simpler, the use of the complete model space makes the calculations rather

complex since too large model spaces are more likely to be plagued by intruder states and even singularities may appear on the potential energy surfaces. This situation is more pronounced to the Rayleigh-Schrödinger MR MBPT where the use of various shifting techniques (with an averaging of orbital energies in the active space, as a rule) is necessary in order to eliminate singularities, see e.g. [24]; while in the case of the MR CC methods we encounter a system of nonlinear equations which may be cumbersome to converge. The alternative MR CI method, a posteriori corrected for the size-extensivity error by the application of various Davidson-type corrections [25,26] is nowadays regarded as a routine and superior method to be applied to general states of an arbitrary multiplicity in the case of smaller molecular systems (no intruder states, small or almost negligible size-extensivity error), but its use for larger systems becomes computationally very demanding and tedious in view of its small convergence.

For these reasons, it is worthwhile to explore alternative methods which would deal with one state at a time while employing a multiconfigurational reference and assuming that the size-extensivity is not significantly violated. Such approaches, representing somewhat heterogeneous group, are often called as one-state or state-selective or state-specific or single-root methods. The first state-selective CC approaches were proposed by Harris [27], Paldus et al. [28], Saute et al. [29] and Nakatsuji and Hirao [30]. Next, we should mention works of Banerjee and Simons [31], Baker and Robb [32], Takana and Terashima [33], Laidig et al. [34,35] and Hoffmann and Simons [36] that are based the multiconfigurational self-consistent-field (MC SCF) wave function as a reference. Very recently, Li and Paldus developed a size-extensive, spin-free open-shell CC theory based on the unitary group approach (UGA) formalism [37] and successfully applied to several open-shell systems, see e.g. [38]. It is beyond the scope of this article to give an exhausting review of all these methods but it is worth noting that many of them have to face the size-extensivity problem what seems to be an inevitable tax paid on their conceptual simplicity (except the latter approach, of course).

In our recent articles [39–41] we have studied the Brillouin-Wigner type of the coupled cluster (BWCC) theory in the nondegenerate case. We have shown that the BWCC theory is fully equivalent to the standard CC theory, but it differs by the fact that it does not employ the BCH formula and therefore it does not employ the linked cluster theorem. Nonetheless, the nondegenerate BWCC theory is a size-extensive method since the disconnected diagrams are cancelled out by the iterative procedure. In this article we study the multireference formulation of the BWCC theory. We start from the multireference Brillouin-Wigner perturbation theory (MR BWPT); however, instead of a perturbative treatment, we exploit an exponential ansatz for the wave operator. The question, we ask, is whether the multireference Brillouin-Wigner coupled cluster (MR BWCC) theory can bring more advantages over the standard MR CC methods; especially with respect to the intruder state problem. In the past, BWPT was intensively studied by several authors; here we should mention the series of articles by Löwdin [42] and also by Brandow [43] who employed MR BWPT to develop

the size-extensive MR RSPT. Needless to say, BWPT alone is not often used in quantum molecular physics because it is not size-extensive, its convergence is believed to be slow and it has to be solved iteratively. On the other hand, MR BWPT is formally very simple; in contrast to MR RSPT it does not contain the so-called renormalization terms and, moreover, provides us with one energy at a time. This feature enables us to formulate two different MR BWCC approaches, namely the "multi-root" version if one is interested in a manifold of states and the "single-root" one. The multi-root formulation of the MR BWCC method leads to existing MR CC approaches and is the subject of our previous article [44]. In this paper we focus on the single-root version of the MR BWCC theory which represents a new approach in this respect. Using the Hilbert space approach to the wave operator, we derive the basic equations for cluster amplitudes in a spin-orbital form within the MR BWCCSD approximation; i.e. coupled-cluster method with the inclusion of singly and doubly excited cluster components. The performance of the method is tested on the trapezoidal H4 model system with a two-dimensional reference space spanned by two closed-shell type configurations and the results are compared with the full configuration interaction (FCI) method as well as other correlated multireference techniques.

2. MULTIREFERENCE BWPT.

In this section, we briefly recall the basic notation and formalism of the MR BWPT. As is usual in perturbation theory, let us assume that the exact Hamiltonian H can be split into two parts, namely

$$H = H_0 + V \tag{1}$$

where H_0 is the zeroth-order Hamiltonian and V is a perturbation. Our task is to find a solution of the Schrödinger equation for the exact Hamiltonian H

$$H \Psi_\alpha = \mathcal{E}_\alpha \Psi_\alpha \tag{2}$$

while we know the solution of the characteristic problem of the zeroth-order Hamiltonian H_0

$$H_0 \Phi_\mu = E_\mu \Phi_\mu \tag{3}$$

In general, we do not need to know the whole energy spectrum, but we are interested in several low lying states, say, Ψ_α where $\alpha = 1, 2, \ldots, d$. Let us further assume that the most important contributions to d exact wave functions Ψ_α come from d configurations Φ_μ represented by Slater determinants in the spin-orbital formalism, where $\mu = 1, 2, \ldots, d$. Given dominant configurations span the so-called model or reference space. To simplify

our derivation, we use Greek indices α, β to denote exact wave functions, indices μ, ν for configurations spanning the model space and the Latin index q for configurations from the complementary space. If we separate the complete configuration space into the d-dimensional model space P and its orthogonal complement Q, the projection operators associated with these subspaces will have the form

$$P = \sum_{\mu=1}^{d} |\Phi_\mu\rangle\langle\Phi_\mu| = \sum_{\mu \in P} |\Phi_\mu\rangle\langle\Phi_\mu| \tag{4}$$

$$Q = \sum_{q>d} |\Phi_q\rangle\langle\Phi_q| = \sum_{q \in Q} |\Phi_q\rangle\langle\Phi_q| \tag{5}$$

$$P + Q = 1 \tag{6}$$

Projections of the exact wave functions onto the model space (sometimes denoted as model functions)

$$\Psi_\alpha^P = P\Psi_\alpha; \qquad \alpha = 1,\ldots,d \tag{7}$$

are, in general, nonorthogonal but they are assumed linearly independent.

Within the multireference BWPT [45], the exact wave functions Ψ_α for $\alpha = 1,\ldots,d$ can be expanded in the Brillouin-Wigner (BW) perturbation series as follows

$$\Psi_\alpha = (1 + B_\alpha V + B_\alpha V B_\alpha V + \ldots)\Psi_\alpha^P \tag{8}$$

where Ψ_α^P is the projection of the exact wave function onto the model space and B_α is the BW type of propagator

$$B_\alpha = \sum_{q \in Q} \frac{|\Phi_q\rangle\langle\Phi_q|}{\mathcal{E}_\alpha - E_q} \tag{9}$$

At this place it should be mentioned that the BW expansion (8) at the same time prescribes the normalization of the exact wave functions, i.e.

$$\langle\Psi_\alpha^P|\Psi_\alpha\rangle = \langle\Psi_\alpha^P|\Psi_\alpha^P\rangle = 1 \tag{10}$$

which is referred to as an intermediate normalization. If we introduce a new operator Ω_α to denote the operator expansion inclosed in parenthesis

$$\Omega_\alpha = 1 + B_\alpha V + B_\alpha V B_\alpha V + \ldots \tag{11}$$

Eq. (8) will read

$$\Psi_\alpha = \Omega_\alpha \Psi_\alpha^P \tag{12}$$

As one can see, the operator Ω_α has a property of the wave operator (it transforms the projection of the exact wave function into the exact wave function), however, it should be stressed that the operator Ω_α converts just one projected wave function into the corresponding exact wave function; so we will denote it as a "state-specific" wave operator in contrast to the so-called Bloch wave operator [46] that transforms all d projections Ψ_α^P into corresponding exact states. From definition (11) it is immediately seen that the state-specific wave operators obey the following system of equations for $\alpha = 1, \ldots, d$

$$\Omega_\alpha = 1 + B_\alpha V \Omega_\alpha \tag{13}$$

that may be viewed as a Bloch equation [45–49] in the Brillouin-Wigner form.

3. SINGLE-ROOT FORMULATION OF THE MULTIREFERENCE BWPT.

As mentioned in Introduction, the simultaneous calculation of several states within the existing MR CC approaches (referred to as "multi-root" approaches in next) may be computationally very demanding or even impossible in view of the intruder state problems, convergence difficulties or multiple solutions. In addition, if the model space does not contain all necessary configurations to describe all states, it is rather probable that a worsened description of one state due to the insufficient reference space (or truncation of the cluster operator) may worsen the convergence of other states or even destroy the convergence alone. To a lesser extent, different electronic states may have different orbital requirements. Therefore, it is highly desirable to develop such a theory which would aim at one state while employing a multiconfigurational reference. In this section we formulate a single-root version of the MR BWPT. To this end, let us assume that we are interested in one state, say, for simplicity, the ground state Ψ_0. As shown in Section II, within the MR BWPT one can introduce a state-specific wave operator $\tilde{\Omega}$, acting on states from the model space, in the following way

$$\tilde{\Omega} = 1 + B_0 V + B_0 V B_0 V + \ldots \tag{14}$$

or, equivalently

$$\tilde{\Omega} = 1 + B_0 V \tilde{\Omega} \tag{15}$$

where B_0 is the BW type of a propagator

$$B_0 = \sum_{q \in Q} \frac{|\Phi_q\rangle\langle\Phi_q|}{\mathcal{E}_0 - E_q} \tag{16}$$

and $\mathcal{E}_0$ is the exact energy of the ground state. It should be noted, however, that Eqs. (14) and (15) are equivalent only in the case when the BW perturbation expansion converges. Then, in accordance with (8), the wave operator $\tilde{\Omega}$ has the property

$$\Psi_0 = \tilde{\Omega}\left(P\Psi_0\right) = \tilde{\Omega}\,\Psi_0^P \tag{17}$$

that means, it transforms the projection Ψ_0^P of the ground state back into the exact wave function. In contrast to the Bloch wave operator that is used in multi-root approaches, the wave operator $\tilde{\Omega}$ does not convert projections of other exact wave functions Ψ_α^P into corresponding exact states; so in order to avoid any confusion it will be referred to as a single-root wave operator and we use a tilde for a better distinction.

If we denote the "action" of the wave operator $\tilde{\Omega}$ on the model space configurations as $\tilde{\Psi}_\mu$, i.e.

$$\tilde{\Psi}_\mu = \tilde{\Omega}\Phi_\mu \tag{18}$$

it is very easy to show that the operator $\tilde{\Omega}$ is a bijection (one-to-one mapping). Using the BW perturbation expansion (14) gives us

$$\tilde{\Psi}_\mu = \Phi_\mu + B_0\left(V + VB_0V + \ldots\right)\Phi_\mu \tag{19}$$

which implies that the resulting states $\tilde{\Psi}_\mu$ are linearly independent and the operator $\tilde{\Omega}$ represents a bijection (it transforms d linear independent states into d linear independent states). Since the states $\tilde{\Psi}_\mu$ are not necessarily orthogonal, the single-root wave operator $\tilde{\Omega}$ is, in general, non-Hermitian (like the Bloch wave operator). The only bottleneck of such an approach is the existence the wave operator $\tilde{\Omega}$ alone, or, in other words, the convergence of the BW perturbation expansion (14). In the case of the ground state, it is quite reasonable to assume that the convergence can be achieved in view of expected larger differences $(\mathcal{E}_0 - E_q)$, but in general, we are not able to ensure convergence for excited states, when the exact energy $\mathcal{E}_\alpha$ of our interest becomes close to some zeroth-order energy E_q. In that case one can start from Eq. (15) which prescribes an explicit form of the operator $\tilde{\Omega}$ to be the inverse of $(1 - B_0V)$; i.e.

$$\tilde{\Omega} = (1 - B_0V)^{-1} \tag{20}$$

The inverse operator may exist even in the case when the corresponding power series in terms of B_0V does not converge; therefore, in next we will start from Eq. (15) instead of (14). Now, we can introduce the "effective" Hamiltonian, acting within the model space, in the same way as in the multi-root theory, i.e.

$$\tilde{H}_{eff} = PH\tilde{\Omega}P \tag{21}$$

Employing Eq. (17) one can write

$$\tilde{H}_{eff}\Psi_0^P = PH\Psi_0 = \mathcal{E}_0\Psi_0^P \tag{22}$$

which implies that the exact energy of the ground state can be obtained as one of eigenvalues of the effective Hamiltonian $\tilde{H}_{eff}$ and, likewise, the projection of the ground state onto the

model space Ψ_0^P can be found as one of eigenvectors of $\tilde{H}_{eff}$. As concerns remaining eigenvalues and eigenvectors of $\tilde{H}_{eff}$, these are uniquely determined by definition of the single-root wave operator (14) even though they do not represent any physical meaningful solution. Likewise in the multi-root approach, the effective Hamiltonian $\tilde{H}_{eff}$ is a non-Hermitian operator (due to the non-hermicity of $\tilde{\Omega}$). For a better distinction from the multi-root theory, it would be possibly desirable to put some adjective in front of the term "effective Hamiltonian" but we think that the use of a tilde is fully sufficient. We recall that in both "multi-root" as well as "single-root" approaches the effective Hamiltonian acts within the same d-dimensional reference space, but within the "multi-root" approach all eigenvalues (roots) of the effective Hamiltonian are physically meaningful in contrast to the "single-root" approach where just one eigenvalue (root) possesses physical meaning. And this was also the reason why we decided to prefer notation "multi-root" and "single-root" approaches. Moreover, using the name "single-root" rather than "state-selective" or "state-specific" we would like to highlight the fact that the weights of intervening single determinantal configurations are not a priori fixed as is often the case of the state-selective MR theories based on the MC SCF reference wave function (i.e. MR techniques with prediagonalization).

In order to obtain the wave operator $\tilde{\Omega}$ in a form suitable for practical calculations, we project Eq. (15) onto configurations from the Q and P subspaces

$$\langle \Phi_q | \tilde{\Omega} | \Phi_\mu \rangle = (\mathcal{E}_0 - E_q)^{-1} \langle \Phi_q | V \tilde{\Omega} | \Phi_\mu \rangle \tag{23}$$

which brings us

$$(\mathcal{E}_0 - E_q) \langle \Phi_q | \tilde{\Omega} | \Phi_\mu \rangle = \langle \Phi_q | V \tilde{\Omega} | \Phi_\mu \rangle \tag{24}$$

If we use the Schrödinger equation for the zeroth-order Hamiltonian (3), we get the system of coupled equations for $\mu = 1, 2, \ldots, d$

$$\mathcal{E}_0 \langle \Phi_q | \tilde{\Omega} | \Phi_\mu \rangle = \langle \Phi_q | H \tilde{\Omega} | \Phi_\mu \rangle \tag{25}$$

that determines the wave operator $\tilde{\Omega}$ in the single-root case. Note, that the splitting of the exact Hamiltonian H is now eliminated (which is advantageous from the computational point of view) but the wave operator $\tilde{\Omega}$ still depends on the exact energy. One can thus conclude, that within the multireference BWPT we were able to construct a single-root wave operator $\tilde{\Omega}$ as well as the effective Hamiltonian $\tilde{H}_{eff}$ that determine the exact wave function as well as energy just for one state exploiting a multiconfigurational reference. Second, we derived an analogue of the Bloch equation for the single-root wave operator (15), but in contrast to multi-root theories, such an equation is dependent on the exact energy of our interest and it must be solved simultaneously with the eigenvalue problem for the effective Hamiltonian.

4. SINGLE-ROOT MR BWCC THEORY: HILBERT SPACE APPROACH.

So far, we have specified the wave operator $\tilde{\Omega}$ in the BW form (15). If we adopt an exponential ansatz for the wave operator $\tilde{\Omega}$, we can speak about the single-root multireference Brillouin-Wigner coupled-cluster (MR BWCC) theory. The simplest way how to accomplish the idea of an exponential expansion is to exploit the so-called state universal or Hilbert space exponential ansatz of Jeziorski and Monkhorst [23]

$$\tilde{\Omega} = \sum_{\mu \in P} e^{T^\mu} |\Phi_\mu\rangle\langle\Phi_\mu| \qquad (26)$$

where T^μ is a cluster operator defined with respect to the μ-th configuration involving, in general, one-body (T_1^μ), two-body (T_2^μ) up to the N-body (T_N^μ) cluster components

$$T^\mu = T_1^\mu + T_2^\mu + \ldots + T_N^\mu \qquad (27)$$

with N being the total number of electrons. Substituting the cluster ansatz (26) into (17) leads to the following cluster expansion for the ground state

$$\Psi_0 = \sum_{\mu \in P} c_{\mu 0} e^{T^\mu} |\Phi_\mu\rangle \qquad (28)$$

where the coefficients $c_{\mu\alpha}$ are obtained by diagonalization of the effective Hamiltonian. Needless to say, the resulting wave function represents a generalization of the cluster expansion previously introduced by Silverstone and Sinanoğlu for open-shell wave functions with an empty set of core orbitals [50]. As mentioned in Introduction, despite a great progress achieved in the MR CC methods, there have been reported only a few applications of the Hilbert space approach, mostly oriented to simple H_4 and H_8 model systems exploiting a two-determinant model space (more precisely speaking, systems involving two active orbitals of different symmetry) at the level of the CCSD approximation; see e.g. [51–63]. Existing Hilbert space approaches can be divided into two groups depending on whether they exploit the BCH formula or not. Now, we describe both groups in outline.

The first approach, taking the advantage of the BCH formula, was initiated by Jeziorski and Monkhorst [23] and, so far, it has been intensively developed within Paldus's group [5,51–55] who formulated an orthogonally spin-adapted Hilbert space MR CC method for a special case of a two-dimensional model space spanned by closed-shell-type reference configurations. The unknown cluster amplitudes are obtained by the solution of the Bloch equation [45–49]

$$H\Omega P = \Omega P H \Omega P \qquad (29)$$

that determines the wave operator Ω in the multi-root case. The use of the BCH formula causes that only connected diagrams survive which results in great freedom when doing

various approximations without the loss of size-extensivity. Disadvantage of such an approach lies in a somewhat complicated structure of coupling terms containing the product of exponentials $\exp(-T^\mu)\exp(T^\nu)$.

Amongst the applications, first we should mention the linear MR CCSD (MR L-CCSD) approximation of Jeziorski and Paldus [52] that was first applied to the H_4 model system by Paldus et al. [54] exploiting a two-dimensional reference space. This approximation neglects all terms nonlinear in T^μ when calculating the effective Hamiltonian as well as cluster amplitudes. Although such a linear theory is size-extensive and works well in highly quasidegenerate region, it undergoes singular behaviour in the nondegenerate region. Moreover, it is remarkable, that while the lowest root of the effective Hamiltonian always describes the ground state, the second root successively approximates higher and higher excited states. As a next step, we should mention quadratic MR CCSD-1, MR CCSD-2 and MR CCSD-3 approximations developed by Paldus et al. [55] and tested on the H_4 system. These approximations differ by sequential addition of quadratic terms to direct and coupling terms; the first approximation contains just the quadratic $(T_2^\mu)^2$ term involved in the direct term while the MR CCSD-3 method represents a fully quadratic MR CCSD approximation considering all bilinear terms (in fact, the first two approximations were designed in order to better assess the importance of various nonlinear terms). The inclusion of quadratic terms eliminates singular behaviour of the linear MR CCSD approximation (even at the MR CCSD-1 level) and the inclusion bilinear components usually further improves the results.

At the same time, Meissner, Kucharski and others [56,57] developed the quadratic MR CCSD method in a spin-orbital form which does not exploit the BCH formula. The unknown cluster amplitudes are calculated from the so-called generalized Bloch equation [45–47,49,64,65] (or in our language the Bloch equation in the Rayleigh-Schrödinger form)

$$[\Omega, H_0]P = V\Omega P - \Omega P V \Omega P \qquad (30)$$

and the word "quadratic" denotes that only linear and quadratic (bilinear) terms are retained in coupling terms whereas the full expansion of the direct term is taken into account. This method is very close to the MR CCSD-3 approximation but differs by a simpler structure of the coupling terms which no more contain the product of exponentials. Even though some disconnected diagrams persist, the quadratic MR CCSD method is size-extensive and nowadays is amply employed by Bartlett's group; see e.g. [56–61]. The spin-orbital formulation also enables us to obtain some open-shell (although spin-contaminated) energies in a special case of the model space spanned by two open-shell Slater determinants that combine into a singlet and triplet states. Such an approach was proposed by Balková and Bartlett [60] and successfully applied to several open-shell systems [61]. As is well known, the spin-orbital formulation of the Hilbert space approach scales as the number of reference determinants times the cost of a single-reference CCSD calculation, so the use of too large model spaces becomes rather demanding. Although recently formulated incomplete model

space formulations also provide us with size-extensive results [62], the use of a complete model spaces is still conceptually simpler. Needless to say, all nonlinear approximations presented so far employ the full expansion of the effective Hamiltonian.

Turning now back to the single-root MR BWCC approach, we derive the basic equations for the effective Hamiltonian and cluster amplitudes in the spin-orbital form without the use of the BCH formula. We limit ourselves to a complete model space which implies that amplitudes corresponding to internal excitations (i.e. excitations within the model space) are equal to zero. In our derivation we shall work with the Hamiltonian in the normal-ordered-product form, i.e.

$$H = \langle \Phi_\mu | H | \Phi_\mu \rangle + H_N(\mu) = H_{\mu\mu} + H_N(\mu) \tag{31}$$

with the μ-th configuration being the Fermi vacuum. In general, we work with different Fermi vacua for different reference configurations when calculating matrix elements containing the wave operator $\tilde{\Omega}$; in our derivation the role of the Fermi vacuum is always played by the configuration with the μ-th subscript. Using the exponential ansatz (26), the off-diagonal matrix elements of the effective Hamiltonian (21) can be expressed in the form

$$\tilde{H}^{eff}_{\nu\mu} = \langle \Phi_\nu | H \tilde{\Omega} | \Phi_\mu \rangle = \langle \Phi_\nu | H_N(\mu) e^{T^\mu} | \Phi_\mu \rangle \tag{32}$$

and the diagonal elements are given by

$$\tilde{H}^{eff}_{\mu\mu} = \langle \Phi_\mu | H \tilde{\Omega} | \Phi_\mu \rangle = H_{\mu\mu} + \langle \Phi_\mu | H_N(\mu) e^{T^\mu} | \Phi_\mu \rangle = H_{\mu\mu} + \langle H_N(\mu) e^{T^\mu} \rangle_\mu \tag{33}$$

Obviously, we gain precisely the same expressions as in the multi-root theory since we postulated the same form of the effective Hamiltonian. We recall that all matrix elements of the effective Hamiltonian are expressed by means of connected diagrams only; in the case of diagonal elements just connected vacuum diagrams may come into consideration and in the case of off-diagonal elements at least one part of a disconnected diagram would correspond to an internal excitation.

As concerns cluster amplitudes, if we employ the exact Hamiltonian in the normal-ordered-product form (31) with the μ-th configuration as a Fermi vacuum, the basic equation for the single-root wave operator (25) takes the form

$$(\mathcal{E}_0 - H_{\mu\mu}) \langle \Phi_q | \tilde{\Omega} | \Phi_\mu \rangle = \langle \Phi_q | H_N(\mu) \tilde{\Omega} | \Phi_\mu \rangle \tag{34}$$

If we substitute the Hilbert space exponential ansatz (26) for the wave operator $\tilde{\Omega}$, we obtain the system of equations

$$(\mathcal{E}_0 - H_{\mu\mu}) \langle \Phi_q | e^{T^\mu} | \Phi_\mu \rangle = \langle \Phi_q | H_N(\mu) e^{T^\mu} | \Phi_\mu \rangle \tag{35}$$

that can be used for the calculation of cluster amplitudes in the single-root MR BWCC theory. Using the Hilbert space approach to the wave operator, the single-root MR BWCC

method offers several advantages over the existing "multi-root" Hilbert space MR CC approaches. First of all, it does not contain the so-called coupling terms. Second, equations for cluster amplitudes (35) do not mix various sets of amplitudes (i.e. amplitudes belonging to various reference configurations) and the coupling among them is provided indirectly through the exact energy $\mathcal{E}_0$; that means through the off-diagonal matrix elements of the effective Hamiltonian. Third, it is relatively simple; all necessary diagrams are already present in the single-reference CC theory (with the only modification being that the cluster amplitudes corresponding to internal excitations are equal to zero). On the other hand, the method is not fully size-extensive due to the fact that it does not work with a "genuine" Bloch equation for the wave operator.

For the sake of completeness, we recall that the idea of the single-root formalism exploiting the Hilbert space approach was also proposed by Banerjee and Simons [31] and Laidig and Bartlett [34,35]. In both approaches they start from the complete active space MC SCF wave function, however, in order to eliminate redundant cluster amplitudes they approximate the wave operator by

$$\Omega \simeq e^T \tag{36}$$

with the exact energy being

$$\mathcal{E} = \langle \Psi_{MCSCF} | e^{-T} H e^T | \Psi_{MCSCF} \rangle \tag{37}$$

While Banerjee and Simons take into account only the valence correlations (obtained by exciting valence electrons into particle orbitals) which may be not justified in many cases, Laidig et al. also incorporate core excitations including semi-internal ones with all contributions being considered at the linear level in T. The latter approach is referred to by its authors as the MR linearized coupled-cluster method (MR LCCM), however, it should not be confused with the linear MR CC method by Paldus at al. [52–55] which is size-extensive and does not employ "prediagonalization" of the effective Hamiltonian. Later on, Hoffmann and Simons developed a UGA based formalism [36]. To our knowledge, the MR LCCM of Laidig et al. has been applied to study potential energy curves of F_2 and N_2 diatomics at the CCSD level [35]; in view of the approximations involved it is not surprising that it yields spectroscopic constants very similar to the MR CISD method (i.e. configuration interaction truncated at the single and double excitation level).

5. SINGLE-ROOT MR BWCCSD APPROXIMATION.

In this section, we derive basic equations for the monoexcited and biexcited cluster amplitudes at the CCSD level of approximation, i.e. with the cluster operators T^μ being approximated by their singly and doubly excited cluster components

$$T^\mu = T_1^\mu + T_2^\mu \tag{38}$$

in a spin-orbital form. To this end, let us assume that the q-th configuration is a monoexcited configuration with respect to the μ-th configuration, i.e.

$$\Phi_q(\mu) = \Phi_I^A(\mu) \tag{39}$$

In that case, Eq. (35) reduces to

$$(\mathcal{E}_0 - H_{\mu\mu}) \, t_I^A(\mu) = \langle \Phi_I^A(\mu) | H_N(\mu) \, e^{T^\mu} | \Phi_\mu \rangle \tag{40}$$

where we used the well-known fact

$$\langle \Phi_I^A(\mu) | e^{T^\mu} | \Phi_\mu \rangle = t_I^A(\mu) \tag{41}$$

In accordance with [41,66], the direct term on the right hand side of Eq. (40) can be split into connected (subscript C) and disconnected parts as follows

$$\langle \Phi_I^A(\mu) | H_N(\mu) \, e^{T^\mu} | \Phi_\mu \rangle = \langle \Phi_I^A(\mu) | H_N(\mu) \, e^{T^\mu} | \Phi_\mu \rangle_C + t_I^A(\mu) \, \langle H_N(\mu) \, e^{T^\mu} \rangle_\mu \tag{42}$$

If we take into account the expression for diagonal elements of the effective Hamiltonian (33), we get a system of nonlinear equations

$$(\mathcal{E}_0 - \tilde{H}_{\mu\mu}^{eff}) \, t_I^A(\mu) = \langle \Phi_I^A(\mu) | H_N(\mu) \, e^{T^\mu} | \Phi_\mu \rangle_C \tag{43}$$

that can be used for the calculation of singly excited cluster amplitudes within the single-root MR BWCCSD approximation.

In the case of biexcited amplitudes we proceed in a similar way. Assuming the q-th configuration to be a biexcited configuration with respect to the μ-th configuration, i.e.

$$\Phi_q(\mu) = \Phi_{IJ}^{AB}(\mu) \tag{44}$$

Eq. (35) can be expressed in the form (for simplicity, we omit subscript μ at individual amplitudes)

$$(\mathcal{E}_0 - H_{\mu\mu}) \, (t_{IJ}^{AB} + t_I^A t_J^B - t_J^A t_I^B)_\mu = \langle \Phi_{IJ}^{AB}(\mu) | H_N(\mu) \, e^{T^\mu} | \Phi_\mu \rangle \tag{45}$$

where we used the well-known fact

$$\langle \Phi_{IJ}^{AB}(\mu) | e^{T^\mu} | \Phi_\mu \rangle = (t_{IJ}^{AB} + t_I^A t_J^B - t_J^A t_I^B)_\mu \tag{46}$$

Then, according to [41,66], the direct term on the right hand side of Eq. (45) can be split into connected and disconnected parts in a following way

$$\langle \Phi_{IJ}^{AB}(\mu) | H_N(\mu) \, e^{T^\mu} | \Phi_\mu \rangle = \langle \Phi_{IJ}^{AB}(\mu) | H_N(\mu) \, e^{T^\mu} | \Phi_\mu \rangle_C + (t_{IJ}^{AB} + t_I^A t_J^B - t_J^A t_I^B)_\mu \langle H_N(\mu) \, e^{T^\mu} \rangle_\mu$$
$$+ \, \mathcal{P}_{IJ} \mathcal{P}_{AB} \left[t_I^A(\mu) \langle \Phi_J^B(\mu) | H_N(\mu) \, e^{T^\mu} | \Phi_\mu \rangle_C \right] \tag{47}$$

where $\mathcal{P}_{IJ}$ and $\mathcal{P}_{AB}$ are antisymmetrizers of the form

$$\mathcal{P}_{IJ} = 1 - P(I \leftrightarrow J) \tag{48}$$

If we take into account the expression for diagonal elements of the effective Hamiltonian (33), we obtain a system of nonlinear equations

$$
\begin{aligned}
(\mathcal{E}_0 - \tilde{H}_{\mu\mu}^{eff}) \left(t_{IJ}^{AB} + t_I^A t_J^B - t_J^A t_I^B \right)_\mu &= \langle \Phi_{IJ}^{AB}(\mu) | H_N(\mu) \, e^{T^\mu} | \Phi_\mu \rangle_C \\
&\quad + \mathcal{P}_{IJ}\mathcal{P}_{AB} \left[t_I^A(\mu) \langle \Phi_J^B(\mu) | H_N(\mu) \, e^{T^\mu} | \Phi_\mu \rangle_C \right]
\end{aligned}
\tag{49}
$$

that can be used for the calculation of doubly excited cluster amplitudes within the single-root MR BWCCSD approximation. Of course, no extra calculation is required for the matrix element $\langle \Phi_J^B(\mu) | H_N(\mu) \, e^{T^\mu} | \Phi_\mu \rangle_C$. The configuration $\Phi_J^B(\mu)$ either represents an external monoexcitation, so the matrix element can replaced from the equation for monoexcited amplitudes (43) or an internal monoexcitation, so the matrix element is an off-diagonal matrix element of the effective Hamiltonian (32). Hence, the coupling between various sets of amplitudes is also provided directly through the "coupling terms" containing off-diagonal elements of the effective Hamiltonian that explicitly enter the equation for biexcited amplitudes (like in the multi-root theories). The above equation can be further simplified for a special case of a two-determinant model space spanned by two active orbitals of different symmetry. Since the internal monoexcitations cannot contribute for symmetry reasons, we can exploit Eq. (43) even for the case of internal excitations, which gives us

$$
(\mathcal{E}_0 - \tilde{H}_{\mu\mu}^{eff}) \, t_{IJ}^{AB}(\mu) = \langle \Phi_{IJ}^{AB}(\mu) | H_N(\mu) \, e^{T^\mu} | \Phi_\mu \rangle_C + (\mathcal{E}_0 - \tilde{H}_{\mu\mu}^{eff})(t_I^A t_J^B - t_J^A t_I^B)_\mu
\tag{50}
$$

Equations (43) and (49) can be used for the calculation of monoexcited and biexcited cluster amplitudes in the single-root MR BWCCSD approximation in a general case. In the case of a two-determinant model space the equation for biexcited cluster amplitudes (49) can be replaced by its simpler, two-determinant version (50). As already spoken, these equations do not mix various sets of cluster amplitudes and the coupling among amplitudes is provided through the off-diagonal elements of the effective Hamiltonian (if the off-diagonal elements were zeroes, the coupling would vanish). On the other hand, the equations explicitly depend on the exact energy of our interest and they must be solved simultaneously with the eigenvalue problem for the effective Hamiltonian. Hence, the set of Eqs. (43) and (49) is solved iteratively and after each iteration we compute the effective Hamiltonian (32–32). Diagonalization of the effective Hamiltonian provides us with several eigenvalues; the lowest one is taken as a new exact energy $\mathcal{E}_0$, while remaining ones (not physically meaningful) are thrown away. The computational cost of the method scales as the number of reference determinants times the cost of one single-reference CCSD calculation.

Finally, let us pay attention to the convergence of the presented single-root Hilbert space MR BWCCSD approximation. When calculating the ground state energy, the denominators appearing in Eqs. (43) and (49) are always negative, so one could not expect problems

with vanishing denominators or intruder states. Moreover, as the coupling between cluster amplitudes is mediated through the off-diagonal elements of $\tilde{H}_{eff}$, one may expect good convergence over the whole potential energy curve, because the off-diagonal elements enable us "to switch" in a continuous manner between the single-reference and multireference approaches. To be more precise, in the nondegenerate case, when the coupling between the reference configurations is weak, the off-diagonal elements of $\tilde{H}_{eff}$ are negligible (in fact, the off-diagonal elements would correspond to amplitudes of internal excitations divided by pertinent denominators), which implies that the difference $(\mathcal{E}_0 - \tilde{H}_{\mu\mu}^{eff})$ approaches zero for the ground state configuration Φ_μ and Eqs. (43) and (49) reduce to standard nondegenerate CCSD equations for the ground state. In the quasi-degenerate case, when the coupling between the reference configurations is getting large, the coupling between Eqs. (43) and (49) becomes stronger and these equations correspond to the multireference case.

From the above discussion one may expect that the single-root MR BWCCSD approximation is well suited to the calculation of the ground state energy. As concerns the calculation of excited states, the convergence problems can not be excluded in view of unknown behaviour of denominators. Moreover, the choice of the correct eigenvalue amongst several eigenvalues of the effective Hamiltonian may not seem so unambiguous matter as in the case of the ground state.

6. RESULTS AND DISCUSSION.

To get a better idea about the performance of the presented single-root MR BWCC approach, we carried out single-root MR BWCCSD calculations for the ground state and first excited state of the H_4 model system with the use of minimal and DZP basis sets. As is well known, the H_4 model system was introduced by Jankowski and Paldus [67] and nowadays is widely used to explore the performance of various single-reference and MR approaches in quasidegenerate situations. In this work, we limit ourselves to a trapezoidal H4 model consisting of two stretched hydrogen molecules in an isosceles trapezoidal arrangement. All the nearest-neighbour internuclear separations are fixed and equal to 2 a.u. The geometry of the H4 model is uniquely specified by a single parameter α defining the trapezoidal angle $\varphi = \alpha * \pi$. The given model enables us to vary the degree of quasidegeneracy in a continuous manner from a fully degenerate case in the square arrangement ($\alpha = 0.0$) to a non-degenerate one in the linear arrangement ($\alpha = 0.5$) and such an "opening" of the trapezoid may be viewed as a breaking of a single chemical bond.

The H4 model shows a configurational degeneracy in the square arrangement; that means the weights of the ground state configuration $|1\bar{1}2\bar{2}\rangle$ and the first biexcited configuration $|1\bar{1}3\bar{3}\rangle$ in the FCI expansion become equal. Therefore, in order to obtain reliable potential energy surfaces, both closed-shell-type configurations should be included in the reference

space. The corresponding active orbital space is spanned by two orbitals: ϕ_2 being the highest occupied molecular orbital (HOMO) and ϕ_3 being the lowest unoccupied molecular orbital (LUMO). The lowest totally symmetric orbital ϕ_1 plays the role of a core orbital. Since the active orbitals ϕ_2 and ϕ_3 are of different spacial symmetry, the monoexcited configurations $|1\bar{1}2\bar{3}\rangle$ and $|1\bar{1}3\bar{2}\rangle$ do not contribute for symmetry reasons which implies that our two-determinant model space is complete. Moreover, one can take advantage of Eq. (50) when calculating doubly excited cluster amplitudes. The orbital HOMO-LUMO degeneracy is not observed in this model; however the orbital degeneracy alone is of less concern in the CC approaches. The H4 model has been studied in a great detail using various single-reference [67–70] as well as MR methods [54,55,58,71,72] at the level of minimal as well as DZP basis sets. For the sake of comparison, we employ the same minimal basis set (MBS) as Jankowski and Paldus [67] and, analogously, the same DZP basis set as Paldus et al. [69]. Molecular orbitals are taken from the restricted Hartree-Fock (RHF) calculations for the ground state.

Examining the H4 MBS model first, we performed the single-root MR BWCCSD calculations for the ground state and first excited state of the H4 MBS model exploiting a two-determinant model space spanned by the ground state configuration $|1\bar{1}2\bar{2}\rangle$ and first biexcited configuration $|1\bar{1}3\bar{3}\rangle$. In Table I we present the FCI correlation energies for the lowest three totally symmetric singlet states as well as correlation energies for the ground state obtained by the single-root MR BWCCSD method, including expansion coefficients within the model space. We also add results for the second (nonphysical) root of the effective Hamiltonian. The expansion coefficient c_0 corresponds to the ground state configuration and c_1 to the biexcited one. Of course, the use of the intermediate normalization implies

$$c_0^2 + c_1^2 = 1$$

In Table II we compare correlation energies for the ground state of the H4 MBS model obtained by the single-root MR BWCCSD method with other multireference techniques exploiting the same two-determinant model space. The linear MR CCSD (MR L-CCSD) approximation neglects all terms nonlinear in T^μ when calculating the effective Hamiltonian as well as cluster amplitudes. The MR CCSD-3 approximation introduced by Paldus et al. [55] incorporates all linear $(T_i^\mu; \ i = 1, 2)$ and bilinear $(T_i^\mu T_j^\nu; \ i,j = 1, 2)$ terms in the direct as well as coupling terms when calculating cluster amplitudes. The "quadratic" MR CCSD method by Balková et al. [58] considers all linear and bilinear terms in the coupling term while the full expansion of the direct term is taken into account. All nonlinear approximations employ the full expansion of the effective Hamiltonian. For easier comparison, instead of correlation energies we present their differences from the corresponding FCI values, i.e. $\Delta = X$ - FCI.

As one can see, the single-root MR BWCCSD correlation energies for the ground state are in perfect agreement with the FCI values with deviations not exceeding 0.6 mHartree.

Needless to say, the single-root MR BWCC approach is devoid of the intruder state problem in contrast to the linear MR CCSD approximation which undergoes a singular behaviour and completely fails in the nondegenerate region (no convergence is achieved when the ground and first biexcited states are to be calculated simultaneously). As already spoken, the inclusion of the quadratic $(T_2^\mu)^2$ term entirely heals the singular behaviour of the linear MR CCSD approximation and considerably improves the agreement with FCI results. As may be expected, there are only slight differences between the MR CCSD-3 and "quadratic" MR CCSD methods. In the degenerate region; i.e. for $\alpha \leq 0.05$ both methods give almost identical results which are in the best agreement with the FCI method whereas in the non-degenerate region ($\alpha > 0.05$) this agreement steadily deteriorates with the largest deviation being 2.015 mHartree for $\alpha = 0.5$. The "quadratic" MR CCSD method does somewhat better job what may be attributed to the presence of cubic and quartic terms involved in the direct term.

On the other hand, the single-root MR BWCCSD approach provides a balanced description of the potential energy surface over the whole spectrum of studied geometries. More detailed look at the expansion coefficients within the model space for the ground state (Table I) confirms that the ground state configuration dominates in the nondegenerate region ($\alpha > 0.05$) while in the degenerate region ($\alpha \leq 0.05$) the importance of the biexcited configuration monotonously increases and in the square arrangement both weights become equal. As concerns the nonphysical root, it is able to describe neither the first excited state nor the second one (in fact, it cannot be associated with a physically meaningful eigenstate across the whole range of geometries). To some extent it is interesting that the non-hermicity is relatively small; the eigenvectors of the effective Hamiltonian are almost orthogonal, even in a highly nondegenerate region.

Analogous results for the first biexcited state of the H4 MBS model are collected in Tables III and IV. In Table III we present correlation energies for the first biexcited state obtained by the single-root MR BWCCSD method, including expansion coefficients as well as nonphysical root, and Table IV compares correlation energies for the first biexcited state obtained by various multireference techniques. Two facts are immediately apparent when comparing correlation energies. First, the single-root MR BWCCSD method gives correlation energies at the level of the MR CCSD-3 and "quadratic" MR CCSD approximations across the whole region of studied geometries (a slight improvement in the case of the single-root MR BWCCSD method is not essential). This fact indicates that the single-root MR BWCC method can be successfully applied even to excited states; even though, in general, we are not able to predict the behaviour of denominators of the type $(\mathcal{E}_i - E_q)$. Of course, there is a freedom in the choice of the zeroth-order Hamiltonian since the equations for cluster amplitudes are invariant as to the choice of the zeroth-order energies E_q, but this choice affects the rate of convergence.

Second, the description of the first biexcited state worsens with an increasing value of the

parameter α. While in the degenerate region the correlation energies are very close to the FCI ones, in the highly nondegenerate region we encounter differences of about 7 mHartree what can be probably attributed to the lack of important configurations in the model space. In fact, for $\alpha \geq 0.4$ a predominant configuration in the FCI expansion is not the biexcited configuration $|1\bar{1}3\bar{3}\rangle$ but the monoexcited configuration $|1\bar{3}2\bar{2}\rangle$; so the model space contains only a minor part of the exact wave function. We recall that a similar worsening is also observed for the first biexcited state of the Li_2 molecule studied by a two-determinant "quadratic" MR CCSD by Balková et al. [59] (for this state, a predominant configuration in the nondegenerate region is not the biexcited configuration $1\sigma_g^2 1\sigma_u^2 2\sigma_u^2$ but the monoexcited configuration $1\sigma_g^2 1\sigma_u^2 2\sigma_g 3\sigma_g$). As concerns a nonphysical root, it cannot sufficiently describe the ground state and, likewise, the overall non-hermicity is small.

Since the minimal basis set provides us with a configurational space spanned by a very few configurations (only one tetraexcitation), we also carried out the single-root MR BWCCSD calculations in a DZP basis set, providing thus much more tetraexcited configurations in the Q space. In Table V we compare correlation energies for the ground state of the H4 DZP model obtained by various multireference techniques in a two-determinant model space and in Table VI we compare correlation energies for the first biexcited state. Besides the above mentioned linear MR CCSD and "quadratic" MR CCSD approximations, we also present correlation energies for the MR CISD method [69] and the third-order MR Rayleigh-Schrödinger MBPT (MR MBPT3) method [72]. However, it should be stressed that in the case of the MR MBPT3 calculations the RHF orbital energies of two active orbitals had to be averaged in order to eliminate intruder states. Such a shifting technique does not destroy size-extensivity and is denoted as a forced degeneracy partitioning; see e.g. [24].

As one can see, the DZP basis set gives qualitatively the same results and confirms our previous findings for the MBS model. As concerns the ground state, it is undisputable, that the superior approximation to the FCI method is again provided by the single-root MR BWCCSD method. In comparison to the MR CISD method, the single-root MR BWCCSD approach also includes the effect of higher than single and double excitations. In the nondegenerate region, the single-root MR BWCCSD method remains at the level of the nondegenerate CCSD method (in fact, it gives slightly better results) supporting thus our idea of a smooth transition between the degenerate and nondegenerate regions. As concerns the first biexcited state, its description remains at the level of the "quadratic" MR CCSD method. It is interesting that the MR MBPT3 method can sufficiently describe this state only in the highly degenerate region while completely fails in nondegenerate region; despite the absence of intruders. This fact indicates that a proper choice of a model space (i.e. spanned by all relevant configurations) is essential for the third-order MR MBPT calculations. Remarkable enough, the single-root MR BWCCSD as well as MR CCSD approaches do well in this situation.

7. SUMMARY AND CONCLUSIONS.

In our recent articles [39–41] we have analyzed the coupled-cluster theory based on the Brillouin-Wigner perturbation expansion. To our knowledge, BWPT is not often used in quantum molecular physics because it is not size-extensive and its convergence is believed to be slow. Moreover, the BW perturbation series has to be solved iteratively. With the coupled-cluster formulation of BWPT the situation is different. Although the BWCC equations must be solved iteratively anyway and we do not employ the BCH formula, the single-reference BWCC theory is size-extensive and provides us with equivalent results as the standard CC theories. In this article, we extend the BWCC theory to a multireference case using the Hilbert space approach. We formulate the so-called single-root version which deals with one state at a time and we present the basic equations for cluster amplitudes within the CCSD approximation.

The single-root MR BWCC method employs a state-specific wave operator which leads to only one root of the quasidegenerate energy spectrum. Such an approach has many advantages over the existing multi-root Hilbert space MR CC approaches; it does not contain the so-called coupling terms and it is relatively very simple (all necessary diagrams are already present in the standard single-reference CC theories). Equations for cluster amplitudes do not mix various sets of amplitudes and the coupling among amplitudes is provided through the presence of the exact energy in denominators. The principal property of the single-root MR BWCC method is its ability of a continuous transition between the single-reference and multireference approaches. Of course, one must employ a typical Brillouin-Wigner-like scheme of calculation: equations for amplitudes have to be solved simultaneously with the eigenvalue problem for the effective Hamiltonian. Diagonalization of the effective Hamiltonian provides us with several eigenvalues; one is taken as a new exact energy and remaining ones are thrown away (they do not represent a physical meaningful solution). On the other hand, the method is not fully size-extensive in view of the fact that it does not work with the "genuine" Bloch equation for the wave operator. A question of the size-extensivity will be discussed in our next article.

In order to better assess performance of the presented approach, we carried out single-root MR BWCCSD calculations for the ground state and the first biexcited state of the trapezoidal H4 model system exploiting a two-determinant model space and results were compared with other multireference techniques, including the FCI method. We have found that in the case of the ground state the single-root MR BWCCSD method provides the best approximation to the FCI energies of all presented methods with a balanced description in the quasidegenerate and nondegenerate regions. Moreover, it does not suffer from intruder states what was another reason for doing this work. In spite of the fact, that our results are limited to a simple H4 model system, the single-root MR BWCC method seems to be a viable approach for the calculation of the ground state energy over the whole potential

energy surface and should deserve our future attention.

REFERENCES

[1] F. Coester, Nucl. Phys. **7**, 421 (1958); F. Coester and H. Kümmel, Nucl. Phys. **17**, 477 (1960).

[2] J. Čížek, J. Chem. Phys. **45**, 4256 (1966); Adv. Chem. Phys. **14**, 35 (1969).

[3] J. Čížek and J. Paldus, Int. J. Quantum Chem. **5**, 359 (1971).

[4] J. Paldus, J. Čížek, and I. Shavitt, Phys. Rev. A **5**, 50 (1972).

[5] J. Paldus, in *Methods in Computational Molecular Physics*, NATO ASI Series, S. Wilson and G. H. F. Diercksen, Eds. (Plenum, New York, 1992), pp. 99–194; in *Relativistic and Correlation Effects in Molecules and Solids*, NATO ASI Series, G. L. Malli, Ed. (Plenum, New York, 1994), pp. 207–282.

[6] R. J. Bartlett, Ann. Rev. Phys. Chem. **32**, 359 (1981); J. Chem. Phys. **93**, 1697 (1989).

[7] R. J. Bartlett, C. E. Dykstra, and J. Paldus, in *Advanced Theories and Computational Approaches for the Electronic Structure of Molecules*, C. E. Dykstra, Ed. (Reidel, Dordrecht, 1984), pp. 127–159.

[8] K. Jankowski, in *Methods in Computational Chemistry*, Vol. 1, S. Wilson, Ed. (Plenum, New York, 1987), pp. 1–116; M. Urban, I. Černušák, V. Kellö, and J. Noga, *ibid.*, pp. 117–250.

[9] S. Wilson, *Electron Correlation in Molecules* (Clarendon, Oxford, 1984).

[10] K. A. Brueckner, Phys. Rev. **100**, 36 (1955); J. Goldstone, Proc. R. Soc. London, Ser. A **239**, 267 (1957).

[11] F. Coester, in *Lectures in Theoretical Physics*, Vol. 11B, K. T. Mahanthappa and W. E. Brittin, Eds. (Gordon and Breach, New York, 1966), pp. 157-186.

[12] D. Mukherjee, R. K. Moitra, and A. Mukhopadhyay, Pramana **4**, 247 (1975); Mol. Phys. **30**, 1861 (1975); Mol. Phys. **33**, 955 (1977); A. Haque and D. Mukherjee, J. Chem. Phys. **80**, 5058 (1984).

[13] R. Offermann, W. Ey, and H. Kümmel, Nucl. Phys. A **273**, 349 (1976); R. Offermann, Nucl. Phys. A **273**, 368 (1976); W. Ey, Nucl. Phys. A **296**, 189 (1978).

[14] I. Lindgren, Int. J. Quantum Chem. Symp. **12**, 33 (1978).

[15] L. Z. Stolarczyk and H. J. Monkhorst, Phys. Rev. A **32**, 725 (1985); *Ibid.* 743 (1985); Phys. Rev. A **37**, 1908 (1988); *Ibid.* 1926 (1988).

[16] W. Kutzelnigg, J. Chem. Phys. **80**, 822 (1984).

[17] A. Haque and U. Kaldor, Chem. Phys. Lett. **117**, 347 (1985); Chem. Phys. Lett. **120**, 261 (1985); Int. J. Quantum Chem. **29**, 425 (1986).

[18] U. Kaldor, J. Chem. Phys. **87**, 467 (1987); Theor. Chim. Acta **80**, 427 (1991) and references therein.

[19] I. Lindgren and D. Mukherjee, Phys. Rep. **151**, 93 (1987).

[20] D. Mukherjee and S. Pal, Adv. Quantum Chem. **20**, 292 (1989) and references therein.

[21] L. Meissner, J. Chem. Phys. **103**, 8014 (1995); L. Meissner, Chem. Phys. Lett. **255**, 244 (1996).

[22] M. Nooijen and R. J. Bartlett, J. Chem. Phys. **104**, 2652 (1996); M. Nooijen, J. Chem. Phys. **104**, 2638 (1996).

[23] B. Jeziorski and H. J. Monkhorst, Phys. Rev. A **24**, 1668 (1981).

[24] K. F. Freed, in Many-Body Methods in Quantum Chemistry, Lecture Notes in Chemistry, Vol. 52, U. Kaldor, Ed. (Springer, Berlin, 1989), pp. 1–21 and references therein; J. P. Finley, R. K. Chaudhuri, and K. F. Freed, J. Chem. Phys. **103**, 4990 (1995) and references therein.

[25] E. R. Davidson, *The World of Quantum Chemistry*, R. Daudel and B. Pullman, Eds. (Reidel, Dordrecht, 1974).

[26] L. Meissner, Chem. Phys. Lett. **146**, 204 (1988).

[27] E. F. Harris, Int. J. Quantum Chem. Symp. **11**, 403 (1977).

[28] J. Paldus, J. Čížek, M. Saute, and A. Laforgue, Phys. Rev. A **17**, 805 (1978).

[29] M. Saute, J. Paldus, and J. Čížek, Int. J. Quantum Chem. **15**, 463 (1979).

[30] M. Nakatsuji and K. Hirao, J. Chem. Phys. **68**, 2053 (1978); *Ibid.* 4279 (1978); M. Nakatsuji, Chem. Phys. Lett. **59**, 362 (1978); Chem. Phys. Lett. **67**, 329 (1979); Int. J. Quantum Chem. Symp. **17**, 241 (1983) and references therein.

[31] A. Banerjee and J. Simons, Int. J. Quantum Chem. **19**, 207 (1981); J. Chem. Phys. **76**, 4548 (1982); Chem. Phys. **81**, 297 (1983); Chem. Phys. **87**, 215 (1984).

[32] H. Baker and M. A. Robb, Mol. Phys. **50**, 1077 (1983).

[33] R. Takana and H. Terashima, Chem. Phys. Lett. **106**, 558 (1984).

[34] W. D. Laidig and R. J. Bartlett, Chem. Phys. Lett. **104**, 424, (1984).

[35] W. D. Laidig, P. Saxe, and R. J. Bartlett, J. Chem. Phys. **86**, 887 (1987).

[36] M. R. Hoffmann and J. Simons, J. Chem. Phys. **88**, 993 (1988).

[37] J. Paldus and X. Li, in *Symmetries in Science* VI, B. Gruber, Ed. (Plenum, New York, 1993), pp. 573–591; X. Li and J. Paldus, Int. J. Quantum Chem. Symp. **27**, 269 (1993); J. Chem. Phys. **101**, 8812 (1994); B. Jeziorski, J. Paldus, and P. Jankowski, Int. J. Quantum Chem. **56**, 129 (1995).

[38] X. Li and J. Paldus, J. Chem. Phys. **102**, 2013 (1995); **102**, 8059 (1995); **103**, 1024 (1995); **103**, 6536 (1995).

[39] I. Hubač and P. Neogrády, Phys. Rev. A **50**, 4558 (1994).

[40] I. Hubač, in *New Methods in Quantum Theory*, NATO ASI Series, C. A. Tsipis, V. S. Popov, D. R. Herschbach, and J. S. Avery, Eds. (Kluwer, Dordrecht, 1996), pp. 183–202.

[41] J. Mášik and I. Hubač, Coll. Czech. Chem. Commun. **62**, 829 (1997).

[42] P.-O. Löwdin, *Perturbation Theory and its Applications in Quantum Mechanics*, C. H. Wilcox, Ed. (Wiley, New York, 1966); Int. J. Quantum Chem. **2**, 867 (1968).

[43] B. H. Brandow, Rev. Mod. Phys. **39**, 771 (1967).

[44] J. Mášik and I. Hubač, in *Quantum Systems in Chemistry and Physics: Trends in Methods and Applications*, R. McWeeny, J. Maruani, Y. G. Smeyers, and S. Wilson, Eds. (Kluwer Academic Publishers, Dordrecht, 1997).

[45] I. Lindgren, J. Phys. B **7**, 2441 (1974).

[46] C. Bloch, Nucl. Phys. **6**, 329 (1958).

[47] V. Kvasnička, Czech. J. Phys. B **24**, 605 (1974).

[48] V. Kvasnička, Czech. J. Phys. B **27**, 599 (1977); Adv. Chem. Phys. **36**, 345 (1977).

[49] I. Lindgren, Int. J. Quantum Chem. Symp. **12**, 33 (1978).

[50] H. J. Silverstone and O. Sinanoğlu, J. Chem. Phys. **44**, 3608 (1966).

[51] J. Paldus, in *New Horizons of Quantum Chemistry*, P.-O. Löwdin and B. Pullman, Eds. (Reidel, Dordrecht, 1983), pp. 31–60.

[52] B. Jeziorski and J. Paldus, J. Chem. Phys. **88**, 5673 (1988).

[53] K. Jankowski, J. Paldus, and J. Wasilewski, J. Chem. Phys. **95**, 3549 (1991).

[54] J. Paldus, L. Polypow, and B. Jeziorski, in *Many-Body Methods in Quantum Chemistry*, Lecture Notes in Chemistry, Vol. 52, U. Kaldor, Ed. (Springer, Berlin, 1989), pp. 151–170.

[55] J. Paldus, P. Piecuch, L. Polypow, and B. Jeziorski, Phys. Rev. A **47**, 2738 (1993).

[56] L. Meissner, K. Jankowski, and J. Wasilewski, Int. J. Quantum Chem. **34**, 535 (1988).

[57] S. A. Kucharski and R. J. Bartlett, J. Chem. Phys. **95**, 8227 (1991); S. A. Kucharski, A. Balková, P. G. Szalay, and R. J. Bartlett, J. Chem. Phys. **97**, 4289 (1992).

[58] A. Balková, S. A. Kucharski, L. Meissner, and R. J. Bartlett, Theor. Chim. Acta **80**, 335 (1991).

[59] A. Balková, S. A. Kucharski, and R. J. Bartlett, Chem. Phys. Lett. **182**, 511 (1991).

[60] A. Balková and R. J. Bartlett, Chem. Phys. Lett. **193**, 364 (1992).

[61] A. Balková, S. A. Kucharski, L. Meissner, and R. J. Bartlett, J. Chem. Phys. **95**, 4311 (1991); A. Balková and R. J. Bartlett, J. Chem. Phys. **99**, 7907 (1993); *Ibid.* **101**, 4936 (1994); *Ibid.* **102**, 7116 (1995).

[62] L. Meissner, S. A. Kucharski, and R. J. Bartlett, J. Chem. Phys. **91**, 6187 (1989); L. Meissner and R. J. Bartlett, J. Chem. Phys. **92**, 561 (1990).

[63] S. Berkovic and U. Kaldor, Chem. Phys. Lett. **199**, 42 (1992); J. Chem. Phys. **98**, 3090 (1993).

[64] V. Kvasnička, Chem. Phys. Lett. **79**, 89 (1981).

[65] I. Lindgren and J. Morrison, *Atomic Many-Body Theory* (Springer-Verlag, Berlin, 1982).

[66] J. Paldus, J. Čížek, and B. Jeziorski, J. Chem. Phys. **90**, 4356 (1989).

[67] K. Jankowski and J. Paldus, Int. J. Quantum Chem. **18**, 1243 (1980).

[68] S. Wilson, K. Jankowski, and J. Paldus, Int. J. Quantum Chem. **23**, 1781 (1983).

[69] J. Paldus, P. E. S. Wormer, and M. Bénard, Coll. Czech. Chem. Commun. **53**, 1919 (1988).

[70] S. A. Kucharski, A. Balková, and R. J. Bartlett, Theor. Chim. Acta **80**, 321 (1991).

[71] S. Zarrabian and J. Paldus, Int. J. Quantum Chem. **38**, 761 (1990).

[72] J. Mášik, I. Hubač, and P. Mach, Int. J. Quantum Chem. **53**, 207 (1995).

TABLES

TABLE I. Comparison of the single-root two-determinant BWCCSD correlation energies for the ground state of the H4 MBS model with FCI data. We also present correlation energies for the nonphysical root as well as corresponding expansion coefficients within the model space. The FCI correlation energies (relative to the ground state RHF energy) are listed for the lowest three totally symmetric singlet states. All energies are in mHartree.

	FCI			1st root (ground state)			2nd root (nonphysical root)		
alpha	$\Delta\mathcal{E}_0$	$\Delta\mathcal{E}_1$	$\Delta\mathcal{E}_2$	$\Delta\mathcal{E}_0$	c_0	c_1	$\Delta\mathcal{E}_1$	c_0	c_1
0.0	-117.621	-7.268	446.325	-117.190	0.7071	-0.7071	0.992	0.7071	0.7071
0.005	-109.196	2.863	447.394	-108.759	0.7612	-0.6485	11.492	0.6483	0.7614
0.01	-102.307	14.250	448.304	-101.872	0.8065	-0.5912	23.519	0.5907	0.8069
0.015	-96.711	26.591	449.122	-96.281	0.8427	-0.5384	36.734	0.5375	0.8433
0.02	-92.147	39.577	449.912	-91.721	0.8708	-0.4917	50.809	0.4904	0.8715
0.05	-76.429	118.950	456.798	-75.981	0.9452	-0.3264	140.108	0.3235	0.9462
0.1	-65.321	221.428	482.682	-64.792	0.9706	-0.2407	269.172	0.2369	0.9715
0.12	-62.776	249.491	496.482	-62.229	0.9739	-0.2269	310.302	0.2231	0.9748
0.15	-60.040	280.303	517.306	-59.480	0.9767	-0.2144	361.347	0.2107	0.9775
0.2	-57.260	310.816	545.685	-56.696	0.9789	-0.2042	422.384	0.2007	0.9797
0.3	-54.775	333.480	575.126	-54.225	0.9803	-0.1977	483.278	0.1945	0.9809
0.4	-53.905	337.503	585.372	-53.369	0.9805	-0.1964	502.209	0.1933	0.9811
0.5	-53.690	337.643	587.722	-53.160	0.9806	-0.1962	505.935	0.1932	0.9812

TABLE II. Correlation energies for the ground state of the H4 MBS model obtained using various multireference correlation techniques within a two-dimensional model space spanned by the ground state configuration $|1\bar{1}2\bar{2}\rangle$ and the first biexcited configuration $|1\bar{1}3\bar{3}\rangle$. For simplicity, we present only differences from corresponding FCI values (Δ = X - FCI) in mHartree.

alpha	FCI	MR L-CCSD[a]	MR CCSD-3[b]	MR CCSD[c]	single-root MR BWCCSD
0.0	-117.621	-1.131	0.046	0.046	0.431
0.005	-109.196	-1.171	0.035	0.035	0.437
0.01	-102.307	-1.220	0.020	0.021	0.435
0.015	-96.711	-1.270	–	0.006	0.430
0.02	-92.147	-1.315	-0.005	-0.006	0.426
0.05	-76.429	-1.462	-0.044	-0.044	0.448
0.1	-65.321	-2.833	-0.217	-0.209	0.529
0.12	-62.776	-6.582	–	-0.344	0.547
0.15	-60.040	NC	-0.625	-0.604	0.560
0.2	-57.260	NC	-1.103	-1.070	0.564
0.3	-54.775	NC	-1.747	-1.704	0.550
0.4	-53.905	NC	-1.971	-1.929	0.536
0.5	-53.690	NC	-2.015	-1.974	0.530

[a] Linear MR CCSD approximation. Symbol "NC" indicates that no convergence is achieved when the ground and first biexcited states are calculated simultaneously.

[b] MR CCSD-3 approximation; taken from [55]. Missing values were not present.

[c] "Quadratic" MR CCSD approximation [58]. Since not all geometries were present, we recomputed the whole curve again.

TABLE III. Comparison of the single-root two-determinant BWCCSD correlation energies for the first biexcited state of the H4 MBS model with FCI data. We also present correlation energies for the nonphysical root as well as corresponding expansion coefficients within the model space. The FCI correlation energies (relative to the ground state RHF energy) are listed for the lowest three totally symmetric singlet states. All energies are in mHartree.

alpha	FCI			1st root (nonphysical root)			2nd root (biexcited state)		
	$\Delta\mathcal{E}_0$	$\Delta\mathcal{E}_1$	$\Delta\mathcal{E}_2$	$\Delta\mathcal{E}_0$	c_0	c_1	$\Delta\mathcal{E}_1$	c_0	c_1
0.0	-117.621	-7.268	446.325	-123.628	0.7071	-0.7071	-7.262	0.7071	0.7071
0.005	-109.196	2.863	447.394	-115.448	0.7617	-0.6479	2.880	0.6476	0.7620
0.01	-102.307	14.250	448.304	-108.984	0.8075	-0.5899	14.295	0.5893	0.8079
0.015	-96.711	26.591	449.122	-103.961	0.8439	-0.5364	26.670	0.5354	0.8446
0.02	-92.147	39.577	449.912	-100.078	0.8722	-0.4892	39.697	0.4876	0.8731
0.05	-76.429	118.950	456.798	-89.246	0.9472	-0.3207	119.242	0.3169	0.9485
0.1	-65.321	221.428	482.682	-84.717	0.9734	-0.2293	221.336	0.2247	0.9744
0.12	-62.776	249.491	496.482	-83.760	0.9769	-0.2137	248.905	0.2097	0.9778
0.15	-60.040	280.303	517.306	-82.381	0.9799	-0.1997	278.705	0.1974	0.9803
0.2	-57.260	310.816	545.685	-80.036	0.9817	-0.1904	307.410	0.1918	0.9814
0.3	-54.775	333.480	575.126	-76.208	0.9818	-0.1900	327.940	0.1968	0.9804
0.4	-53.905	337.503	585.372	-74.094	0.9813	-0.1924	331.399	0.2013	0.9795
0.5	-53.690	337.643	587.722	-73.433	0.9811	-0.1933	331.464	0.2026	0.9793

TABLE IV. Correlation energies for the first biexcited state of the H4 MBS model obtained using various multireference correlation techniques within a two-dimensional model space spanned by the ground state configuration $|1\bar{1}2\bar{2}\rangle$ and the first biexcited configuration $|1\bar{1}3\bar{3}\rangle$. For simplicity, we present only differences from corresponding FCI values (Δ = X - FCI) in mHartree.

alpha	FCI	MR L-CCSD[a]	MR CCSD-3[b]	MR CCSD[c]	single-root MR BWCCSD
0.0	-7.268	-3.629	0.002	0.001	0.006
0.005	2.863	-3.817	0.007	0.007	0.017
0.01	14.250	-4.033	0.021	0.023	0.045
0.015	26.591	-4.302	–	0.039	0.079
0.02	39.577	-4.640	0.054	0.058	0.120
0.05	118.950	-9.443	0.050	0.060	0.292
0.1	221.428	-54.959	-0.686	-0.660	-0.092
0.12	249.491	-131.222	--	-1.280	-0.586
0.15	280.303	NC	-2.484	-2.445	-1.598
0.2	310.816	NC	-4.440	-4.389	-3.406
0.3	333.480	NC	-6.581	-6.522	-5.540
0.4	337.503	NC	-7.056	-6.999	-6.104
0.5	337.643	NC	-7.093	-7.038	-6.179

[a] Linear MR CCSD approximation. Symbol "NC" indicates that no convergence is achieved when the ground and first biexcited states are calculated simultaneously.

[b] MR CCSD-3 approximation; taken from [55]. Missing values were not present.

[c] "Quadratic" MR CCSD approximation [58]. Since not all geometries were present, we recomputed the whole curve again.

TABLE V. Correlation energies for the ground state of the H4 DZP model obtained using various multireference correlation techniques within a two-dimensional model space spanned by the ground state configuration $|1\bar{1}2\bar{2}\rangle$ and the first biexcited configuration $|1\bar{1}3\bar{3}\rangle$. For simplicity, we present only differences from corresponding FCI values (Δ = X - FCI) in mHartree.

alpha	FCI	nondeg. CCSD	MR MBPT3[a]	MR CISD[b]	MR L-CCSD[c]	MR CCSD[d]	single-root MR BWCCSD
0.0	-131.361	5.508	2.172	–	-3.685	-0.687	-0.100
0.005	-123.831	4.474	2.234	1.794	-3.670	-0.664	-0.074
0.01	-117.956	3.603	2.295	1.771	-3.610	-0.594	-0.012
0.015	-113.412	2.928	2.348	1.741	-3.527	-0.503	0.065
0.02	-109.870	2.431	2.386	1.706	-3.436	-0.408	0.146
0.05	-98.647	1.262	2.373	1.507	-3.120	-0.084	0.454
0.1	-91.006	0.911	2.155	1.277	-5.027	-0.172	0.582
0.12	-89.169	0.860	2.106	–	-13.442	-0.322	0.591
0.15	-87.121	0.811	2.073	–	NC	-0.714	0.590
0.2	-84.953	0.770	2.079	1.039	NC	-1.186	0.579
0.3	-83.042	0.749	2.136	–	NC	-1.995	0.559
0.4	-82.460	0.751	2.161	–	NC	-2.305	0.551
0.5	-82.333	0.753	2.166	0.895	NC	-2.375	0.548

[a] Third-order MR MBPT calculation; taken from [72].
Intruder state problem is obviated by averaging of active orbital energies.

[b] MR CISD approximation; taken from [69]. Missing values were not present.

[c] Linear MR CCSD approximation. Symbol "NC" indicates that no convergence is achieved when the ground and first biexcited states are calculated simultaneously.

[d] "Quadratic" MR CCSD approximation; taken from [58].

TABLE VI. Correlation energies for the first biexcited state of the H4 DZP model obtained using various multireference correlation techniques within a two-dimensional model space spanned by the ground state configuration $|1\bar{1}2\bar{2}\rangle$ and the first biexcited configuration $|1\bar{1}3\bar{3}\rangle$. For simplicity, we present only differences from corresponding FCI values ($\Delta = X - FCI$) in mHartree.

alpha	FCI	MR MBPT3[a]	MR L-CCSD[b]	MR CCSD[c]	single-root MR BWCCSD
0.0	-49.683	5.975	-1.499	3.370	3.115
0.005	-40.119	6.148	-1.730	3.356	3.109
0.01	-29.192	6.351	-2.044	3.299	3.078
0.015	-17.275	6.600	-2.429	3.228	3.037
0.02	-4.729	6.899	-2.879	3.160	3.004
0.05	71.152	10.071	-7.724	3.060	3.085
0.1	168.217	21.819	-51.385	3.491	3.744
0.12	194.947	28.667	-132.149	3.585	3.919
0.15	224.624	39.942	NC	3.462	3.903
0.2	254.831	57.217	NC	2.767	3.329
0.3	279.104	76.350	NC	1.721	2.329
0.4	284.609	81.839	NC	1.652	2.207
0.5	285.262	82.797	NC	1.723	2.250

[a] Third-order MR MBPT calculation; taken from [72]. Intruder state problem is obviated by averaging of active orbital energies.

[b] Linear MR CCSD approximation. Symbol "NC" indicates that no convergence is achieved when the ground and first biexcited states are calculated simultaneously.

[c] "Quadratic" MR CCSD approximation; taken from [58].

The Effect of Basis Set Superposition Error (BSSE) on the Convergence of Molecular Properties Calculated with the Correlation Consistent Basis Sets.

TANJA VAN MOURIK,[a] ANGELA K. WILSON, KIRK A. PETERSON,[b]
DAVID E. WOON,[c] AND THOM H. DUNNING, JR.[d]
*Environmental Molecular Sciences Laboratory[e] Pacific Northwest National
Laboratory, Richland, Washington 99352, U.S.A.*

Abstract

It is shown that, in many cases, the convergence behavior of molecular properties computed with the correlation consistent basis sets (both standard and augmented sets) is significantly improved if basis set superposition error (BSSE) is taken into account. The effects are most pronounced for pure van der Waals systems like the helium or argon dimers. For these systems the uncorrected D_e, r_e, and ω_e behave very irregularly with increasing basis set size, with the convergence behavior being dramatically improved by use of the counterpoise procedure. Even for strongly bound diatomics like N_2, HF, and HCl, the counterpoise correction often significantly improves the convergence behavior of r_e and ω_e. Similar behavior is observed in the weakly bound molecular complexes, ArHF, HCO⁻, and $(HF)_2$, as well as for the more strongly bound HCO molecule. For HCO⁻, because of the pronounced lengthening of the CO bond upon molecular formation, the deformation energy must also be taken into account.

---

[a] Current address: Department of Chemistry, University College London, 20 Gordon Street, London WC1H 0AJ, U.K.

[b] Department of Chemistry, Washington State University

[c] Current address: Molecular Research Institute, 845 Page Mill Road, Palo Alto CA 94304, USA

[d] Electronic mail addresses: t_vanmourik@pnl.gov, ak_wilson@pnl.gov, ka_peterson@pnl.gov, woon@hecla.molres.gov, and th_dunning@pnl.gov

I. INTRODUCTION

In the last few years significant advances in the computation of potential energy surfaces have led to accurate *ab initio* predictions of molecular properties as well as interaction energies of weakly bonded complexes that in some cases rival the accuracy of experimental data. This is in part a result of progress in developing quantum mechanical methodologies that account for the effects of electron correlation, which is critical for an accurate description of molecules and, in particular, for the computation of the interaction energies of molecular complexes [see, *e.g.*, (Yarkony, 1995)]. Another key to this success is the development of basis sets that can provide accurate solutions of the equations describing electron correlation, *e.g.*, the atomic natural orbital (ANO) basis sets of Taylor and Almöf (Taylor and Almlöf, 1987) and Widmark *et al.*, (Widmark, et al., 1990; Widmark, et al., 1991) and the correlation consistent basis sets of Dunning and coworkers (Dunning Jr., 1989; Kendall, et al., 1992; Woon and Dunning Jr., 1993c; Woon and Dunning Jr., 1994b; Woon and Dunning Jr., 1995; Wilson, et al., 1996; van Mourik, et al., 1997). Unlike most sets in use today, these sets were specifically designed and optimized to describe electron correlation effects.

Of particular interest here are the standard and augmented correlation consistent basis sets (cc-pVnZ and aug-cc-pVnZ, n = D, T, Q, ...). As n increases, these sets systematically expand the coverage of the atomic radial and angular spaces and provide a means of converging both wave functions and properties to the complete basis set (CBS) limit. In fact, the convergence behavior observed for many properties is often so regular that simple functions, *e.g.*, exponentials, can be used to estimate the CBS limits. In a series of benchmark calculations (Woon and Dunning Jr., 1993b; Peterson, et al., 1993b; Peterson, et al., 1993a; Peterson, et al., 1994; Woon, 1994; Woon and Dunning Jr., 1994a; Peterson and Dunning Jr., 1995a; Woon and Dunning Jr., to be published), and in a number of other studies (Feller, 1992; Xantheas and Dunning Jr., 1992; Woon, 1993; Xantheas and Dunning Jr., 1993b; Feller, 1993; Xantheas and Dunning Jr., 1993a; Woon and Dunning Jr., 1993a; Xantheas and Dunning Jr., 1993c; Peterson and Dunning Jr., 1995b; Peterson, 1995; Wilson, et al., 1996; Woon, et al., 1996; Xantheas, 1996; van Mourik and Dunning Jr.) it has been convincingly demonstrated that the correlation consistent basis sets are capable of accurately describing the wave functions and properties of strongly, as well as weakly bound, molecular systems.

One problem in the computation of interaction energies of weakly bonded systems is the uncertainty caused by basis set superposition errors (BSSE). Boys and Bernardi (Boys and Bernardi, 1970) have proposed the counterpoise procedure to correct for this, and although this approach is still regarded with some skepticism, there is nowadays common agreement that the counterpoise procedure is a useful procedure for correcting for BSSE. In the limit of a complete basis, BSSE would, of course, be zero, and it can therefore be expected that the counterpoise-corrected and uncorrected interaction energies computed with increasingly larger basis sets

will converge to the same limit. A point of interest is whether BSSE causes erratic behavior in the convergence of the uncorrected results, which, if so, would greatly complicate the determination of CBS limits for the uncorrected calculations. Studies on the water dimer by Feller *et al.* (Feller, 1992; Feyereisen, et al., 1996) show generally smooth convergence of both the corrected and uncorrected MP2 interaction energies for $(H_2O)_2$ computed with the cc-pVnZ and aug-cc-pVnZ sets, although the uncorrected results computed with the aug-cc-pVnZ sets do not converge smoothly. However, the interaction energies were not computed with basis sets beyond aug-cc-pVQZ, and minor irregularities in the convergence behavior might only be evident if more data are available. Xantheas (Xantheas, 1996) computed counterpoise-corrected and uncorrected interaction energies for the hydrogen-bonded systems $(H_2O)_2$, F$^-$-(H_2O), and Cl$^-$-(H_2O) with basis sets from aug-cc-pVDZ through aug-cc-pV5Z. It was found that the counterpoise-corrected interaction energies converge nearly exponentially, while the uncorrected results do not. Studies on more weakly bonded systems (Woon, 1993; Woon, 1994; Peterson and Dunning Jr., 1995a; Woon, et al., 1996) indicate that the uncorrected results sometimes behave very irregularly and unpredictably. Recently, Jensen (Jensen, 1996) investigated the effect of BSSE on energy differences between two configurations of the same molecule using the correlation consistent basis sets. For the quantities investigated, *i.e.*, the barrier to linearity in H_2O, the inversion barrier in NH_3, and the rotational barrier in CH_3CH_3, the BSSE ranged from a few kcal/mol (or 5 to 15% of the total energy difference) for cc-pVDZ to about 0.1 kcal/mol for cc-pV5Z. The counterpoise-corrected results appeared to be slightly better behaved, and the CBS limit obtained by extrapolation of the counterpoise-corrected values is probably more accurate.

In this work we primarily assemble the results of previous studies (van Mourik, et al., 1997; Wilson, et al., 1996; van Mourik and Dunning Jr., 1997; Peterson and Dunning Jr., 1995a) in order to investigate the effect of BSSE on the convergence behavior of quantities computed with the correlation consistent basis sets. We investigate the effect of BSSE not only on computed interaction energies but also on other spectroscopic constants, specifically, the equilibrium bond length, R_e, and harmonic frequency, ω_e. In the next section we briefly review the basic concepts related to the counterpoise correction. Section III describes the basis sets and wave functions used. In Section IV we present results on the helium and argon dimers as well as on N_2, HF, and HCl. He$_2$ and Ar$_2$ are simple rare-gas pairs, and are classic examples of pure van der Waals systems. The well depths are very shallow (7.6 and 99 cm^{-1}, respectively), and it is well-recognized that the counterpoise procedure is critical for obtaining accurate results for these systems. We also investigate BSSE effects on the computed properties of strongly bound diatomics, including N_2, HF and HCl. Section V discusses the effects of BSSE on the interaction between an atom and a molecule, using Ar-HF and H-CO$^-$ as examples, as well as the strongly bound HCO molecule. The Ar-HF system is bound by less than 0.6 kcal/mol (211 cm^{-1}) and the binding in H-CO$^-$ is only 5 kcal/mol; however, formation of HCO$^-$ leads to large changes in r_e(CO). The H-CO bond strength is approximately 15 kcal/mol, substantially smaller than conventional CH bonds but significantly larger

than the binding energies of the other atom-diatom systems considered. Section VI analyzes the results on the HF dimer, which is bound by slightly less than 5 kcal/mol, as an example of the interaction between two molecules. Finally, Section VII summarizes our results.

II. THEORY

Quantum mechanical methods for calculating the interaction energy between two weakly interacting systems can be divided into two main approaches, *viz.* methods based on symmetry-adapted perturbation theory (SAPT) (Jeziorski and Kolos, 1982; Jeziorski, et al., 1994), in which the interaction energy is calculated directly as a sum of distinct energy terms, and methods based on the supermolecular approach, in which the interaction energy is obtained as the difference of the energy of the supermolecule AB and the sum of the energies of the separated fragments A and B. Each approach has its advantages and disadvantages. SAPT is only applicable for weak interactions, but analysis of the different energy contributions can provide valuable insights in the various factors contributing to the strength of the molecular interaction. [For a recent review of the SAPT approach see (Jeziorski, et al., 1994).] An advantage of the supermolecular approach is that it can be applied not only to weakly interacting systems, but to strongly bound systems as well. Consequently, one can exploit the vast experience of using widely available, and efficiently implemented, standard quantum mechanical software.

In the supermolecular approach, the interaction energy ΔE is given by:

$$\Delta E(\mathbf{R}) = E_{AB}(\mathbf{R}) - E_A - E_B \qquad (1)$$

where $E_{AB}(\mathbf{R})$ is the energy of the AB dimer at geometry $\mathbf{R}$ and E_A and E_B are the energies of the separate monomers, *i.e.*, when $\mathbf{R} = \infty$. One problem with the supermolecular approach is that the interaction energy computed according to Eq. (1) is subject to basis set superposition error (BSSE). At large intermolecular distances the two monomers, A and B, do not interact, and (assuming the employed quantum mechanical method is size-consistent) $E_{AB}(R)$ reduces to the sum $E_A + E_B$. At smaller separations, however, one of the monomers in the complex AB can make use of the basis set of the other monomer, thereby providing an unphysical lowering of the dimer energy. The problem is basically a balancing error, resulting from the fact that one compares the energy of AB at finite distances where the monomers can make use of the basis set of their partner in the complex, to AB at infinity, where the monomers have only their own basis sets to use.

The term BSSE was first introduced in 1973 by Liu and McLean (Liu and McLean, 1973). However, as early as 1970 Boys and Bernardi (Boys and Bernardi, 1970) had proposed the function counterpoise procedure (CP) as a strategy to correct for BSSE. In this procedure the monomer calculations are given the same flexibility that is available to the monomers in the dimer calculation, namely, the monomer energies are evaluated in the complete dimer basis set. The counterpoise-corrected interaction energy then becomes:

$$\Delta E^{CP}(\mathbf{R}) = E_{AB}(\mathbf{R}) - E_A^{\{AB\}}(\mathbf{R}) - E_B^{\{AB\}}(\mathbf{R}) \tag{2}$$

The superscripts $\{AB\}$ indicate that the monomer energies are computed in the dimer basis set, $A \cup B$. The $\{B\}$ basis in the $E_A^{\{AB\}}$ calculation and the $\{A\}$ basis in the $E_B^{\{AB\}}$ calculation are usually referred to as "ghost" basis sets. Eq. (1) represents the uncorrected interaction energy, which subsequently will be referred to as $\Delta E^{no\ CP}$. ΔE_{BSSE} is usually defined as the difference between ΔE^{CP} and $\Delta E^{no\ CP}$, *i.e.*,

$$\Delta E_{BSSE} = E_A^{\{AB\}}(\mathbf{R}) + E_B^{\{AB\}}(\mathbf{R}) - E_A^{\{A\}} - E_B^{\{B\}} \tag{3}$$

Eq. (2) is generally valid for the interaction between two fragments A and B, with interfragment geometrical parameters $\mathbf{R}$. When A and B are molecules, Eq. (2) represents the counterpoise-corrected energy gained by bringing these two molecules, *with their geometry deformed to the same geometry as they have in the particular complex geometry one is studying*, together to the complex geometry $\mathbf{R}$, *i.e.*, Eq. (2) yields a vertical interaction energy. The energy required to bring monomer A to a particular intramolecular geometry $\mathbf{r}_A$ is given by the deformation energy:

$$\Delta U_A^{def}(\mathbf{r}_A) = E_A^{\{A\}}(\mathbf{r}_A) - E_A^{\{A\}}(\mathbf{r}_e) \tag{4}$$

with a similar expression for B. Here, $\mathbf{r}_e$ represents the equilibrium geometry of molecule A. (In the remainder of the paper, we will denote interfragment distances with $\mathbf{R}$ and intrafragment distances with $\mathbf{r}$). The deformation energy is a monomer property, and is therefore computed in the monomer basis set, indicated by the superscripts $\{A\}$ in Eq. (4). The total counterpoise-corrected interaction energy, with intermolecular geometrical parameters $\mathbf{R}$ and intramolecular parameters $\mathbf{r}_A$ and $\mathbf{r}_B$ can then be written as:

$$\Delta E^{CP}(\mathbf{R},\mathbf{r}_A,\mathbf{r}_B) = E_{AB}(\mathbf{R},\mathbf{r}_A,\mathbf{r}_B) - E_A^{\{AB\}}(\mathbf{R},\mathbf{r}_A,\mathbf{r}_B) - E_B^{\{AB\}}(\mathbf{R},\mathbf{r}_A,\mathbf{r}_B)$$
$$+ \Delta U_A^{def}(\mathbf{r}_A) + \Delta U_B^{def}(\mathbf{r}_B) \tag{5}$$

At the equilibrium geometry of the molecular complex AB, the gain in energy due to relaxing the monomer geometry from $\mathbf{r}_e$ to the optimal complex geometry $\mathbf{r}_A$ is termed the monomer relaxation energy. It can be calculated as the difference in interaction energy of AB with all geometrical parameters at their equilibrium values and AB with the monomers fixed at the monomer geometry.

In many cases the deformation energy is very small at the complex's optimized geometry, and neglect of it will only introduce a small error in the computed binding energy. However, if one considers (intramolecular) geometries further away from the equilibrium structure, as will be the case if the interaction is strong, the deformation energy must be taken into account. Formally, it must also be taken into account whenever the geometry of the complex is fully optimized even if the molecules are little perturbed by the interaction.

A counterpoise-corrected geometry optimization (with concurrent optimization of the intramolecular geometry) requires minimization of Eq. (5). To date, no automated counterpoise-corrected optimization algorithms based on Eq. (5) have

been implemented (outside of straightforward numerical finite-difference methods). Alternatively, the structure of two interacting molecules can be optimized by computing the interaction energy via Eq. (5) at a selection of geometries, whereupon analytical functions in the to-be-optimized geometrical parameters can be determined from the computed interaction energies. Any known technique can then be used to extract the desired information (equilibrium geometry, spectroscopic constants) from the computed surface.

One may argue that the basis set that is actually available to a monomer in the complex is *not* the full dimer basis set, but rather only the virtual orbitals of the partner molecule, since its occupied orbitals are not available to the other monomer because of the Pauli exclusion principle. If this were true, it would imply that the counterpoise procedure overestimates the BSSE. This has led to the proposal of the "virtuals-only" counterpoise scheme (Daudey, et al., 1974), in which the monomer energies are calculated in the monomer basis augmented only with the virtual orbitals of the partner molecule. However, since then, conclusive numerical evidence (Gutowski, et al., 1986; Gutowski, et al., 1993) has been presented in support of the "full" counterpoise procedure. In addition, it has been recognized (Gutowski, et al., 1986; Gutowski, et al., 1993; Gutowski and Chalasinski, 1993) that the non-availability of the occupied orbitals of the partner molecule in the dimer calculation is directly related to the intermolecular exchange repulsion energy. The "to-be-occupied" orbitals must be fully included in the monomer calculation, otherwise one risks underestimating the repulsive Pauli exclusion effect resulting from having these orbitals occupied in the dimer calculation. In 1994 Van Duijneveldt *et al.* (van Duijneveldt, et al., 1994) presented a theorem for full CI wavefunctions, showing that the full counterpoise procedure yields BSSE-free interaction energies.

As an alternative to the counterpoise procedure, methods have been proposed (Cullen, 1991; (Sadlej, 1991; Mayer and Surján, 1989; (Mayer, et al., 1989; Mayer and Vibók, 1991; Noga and Vibók, 1991; Vibók and Mayer, 1992; Valiron, et al., 1993) that are designed to *a priori* eliminate BSSE by restricting the monomers in the complex in such a way that usage of the partner basis set is avoided. These methods however were found to give unsatisfactory results (Gutowski and Chalasinski, 1993; van Duijneveldt, et al., 1994).

Although it is generally believed that the counterpoise recipe is the most reasonable procedure for correcting for BSSE, there is still a widespread belief that counterpoise overcorrects, and that interaction energies computed according to Eq. (5) are artificially too repulsive. The discussion has a long history [for a recent review on the counterpoise method see (van Duijneveldt, et al., 1994)]. In the present paper we show examples of cases for which counterpoise improves the convergence behavior of properties computed with the correlation consistent basis sets, thus facilitating extrapolation to the complete basis set (CBS) limit. Since BSSE is zero at the CBS limit, regular convergence is more important than absolute numbers, as it allows a more exact estimate of the CBS limit. In this paper, we will not concern ourselves with the rigor of the counterpoise procedure, but will illustrate the merits of applying the counterpoise correction with respect to the convergence behavior of properties computed with the correlation consistent basis sets.

III. COMPUTATIONAL METHODOLOGY

In the present work, the correlation consistent (cc-pVnZ) basis sets of Dunning and coworkers (Dunning Jr., 1989; Woon and Dunning Jr., 1993c; Wilson, et al., 1996) have been used. Since diffuse functions are known to be essential for an accurate description of weak atomic and molecular interactions, the augmented correlation consistent (aug-cc-pVnZ) basis sets (Kendall, et al., 1992; Woon and Dunning Jr., 1994b; van Mourik, et al., 1997) were used for most of the systems discussed in the present paper. The aug-cc-pVnZ sets contain an additional diffuse function for each angular symmetry present in the standard cc-pVnZ sets. The doubly (d-aug-cc-pVnZ) and triply (t-aug-cc-pVnZ) augmented sets are derived from the singly augmented sets by addition of a second (for d-aug-cc-pVnZ) or third (for t-aug-cc-pVnZ) diffuse function for each angular symmetry. The exponents of the additional diffuse functions are given by $\alpha\beta$ and $\alpha\beta^2$ for the d-aug-cc-pVnZ and t-aug-cc-pVnZ sets, respectively, where α is the exponent of the most diffuse function in the aug-cc-pVnZ set and β is the ratio between the two most diffuse functions in this set (with $\beta < 0$); α was obtained from calculations on the atomic negative ions. The original hydrogen aug-cc-pV5Z set has recently been modified, by changing the most diffuse s-exponent from 0.0138 to 0.0207, because it was found that the original s-exponent was incorrect. We have used the "new" hydrogen aug-cc-pV5Z set (with diffuse s-exponent 0.0207) in this work.

All calculations were carried out with the CCSD(T) method (Raghavachari, et al., 1989; Hampel, et al., 1992; Deegan and Knowles, 1994) as implemented in the MOLPRO Program Package (Werner and Knowles, 1994). For the open-shell systems the partially spin-restricted coupled cluster method of Knowles et $al.$ (Knowles, et al., 1994) was employed. Only the valence electrons were correlated, and spherical harmonics were used for the angular parts of the Gaussian functions. The counterpoise-corrected and uncorrected dissociation energy D_e^{CP} and D_e^{noCP} is defined as the negative of the interaction energy ΔE at the optimized geometry.

It is generally observed (Feller, 1992; Peterson, et al., 1993b; Peterson, et al., 1993a; Woon and Dunning Jr., 1993b; Woon, 1993; Xantheas and Dunning Jr., 1993b; Xantheas and Dunning Jr., 1993c; Peterson, et al., 1994; Peterson and Dunning Jr., 1995a; Peterson, 1995; Wilson, et al., 1996; Xantheas, 1996; Wilson and Dunning, 1997; van Mourik, et al., 1997; van Mourik and Dunning Jr., 1997) that many molecular properties computed with a series of correlation consistent basis sets of increasing n converge regularly toward an apparent complete basis set limit. In the present study the basis set dependence is approximated by a simple exponential function of the form:

$$A(n) = A(\infty) + Be^{-Cn} \tag{6}$$

where n is the cardinal number of the basis set ($n = 2$ for DZ, $n = 3$ for TZ, and so on), and $A(\infty)$ is the estimated complete basis set (CBS) limit for the molecular property A. $A(\infty)$, B, and C are adjustable parameters in a least-squares fit to Eq. (6).

For the weakly bonded diatomic He_2, the interaction energy ΔE was calculated using the aug-, d-aug-, and t-aug-cc-pVnZ basis sets through sextuple zeta quality; for Ar_2 only the results with the d-aug-cc-pVnZ sets are reported here. For He_2, the energies were computed at 15 interatomic separations around the minimum, with the He-He distance ranging from 5.1 to 8.4 bohr. For Ar_2, the energies were computed at 14 points with the Ar-Ar distance ranging from 6.1 to 11.0 bohr [for more details see (van Mourik, et al., 1997).] For the more strongly bound diatomics; N_2, HF and HCl, the interaction energy was computed with the standard cc-pVnZ (N_2, HF, and HCl) and the aug-cc-pVnZ (HF and HCl) basis sets through sextuple zeta quality at 7 interatomic distances, over the range -0.3 $a_0 \leq (r - r_{expt}) \leq +0.5$ a_0 [see (Wilson, et al., 1996), (Peterson and Dunning Jr., 1995a) and (van Mourik and Dunning Jr., to be published)]. Potential energy functions were obtained by fitting polynomials of eighth (He_2 and Ar_2) or sixth (N_2, HF, HCl) degree in $(R-R_e)$ through the computed interaction energies. A standard Dunham analysis (Dunham, 1932) was used to derive the spectroscopic constants via second-order perturbation theory.

For ArHF both the intermolecular Ar-H distance and the intramolecular HF distance have been explicitly optimized. The molecule is linear. The interaction energy as defined by Eq. (5) was calculated at a total of 93 symmetry-unique geometries with the aug-cc-pVDZ and aug-cc-pVTZ sets, and at a set of 73 geometries with the aug-cc-pVQZ basis. The HF distance was varied from 1.46 to 2.23 bohr, the Ar-H distance from 4.2 to 7.5 bohr, the Ar-F distance from 5.5 to 8.8 bohr, and the Ar-H-F angle from 180° to 100°. Polynomials in the two bond lengths and the bending angle were fitted through the computed interaction energies. The fits were carried out with the program SURFIT (Senekowitz, 1988). Additionally, the interaction energy was computed with the aug-cc-pV5Z basis set. In these calculations, only the Ar-H distance was optimized by fitting 5 or 6 points to polynomials in $(R-R_e)$. The Ar-H-F angle was held fixed at 180°, and the HF bond length was kept fixed at the estimated aug-cc-pV5Z distance. [For further details see (van Mourik and Dunning Jr., 1997).]

The H-CO and H-CO⁻ interaction energies were computed at a total of 59 geometries, employing the aug-cc-pVDZ through aug-cc-pVQZ basis sets. For HCO, the CH distance was varied from 1.76 to 2.72 bohr, the CO distance from 2.05 to 2.53 bohr, and the HCO angle from 94° to 154°. For HCO⁻, the CH distance was varied from 1.97 to 2.77 bohr, the CO distance from 2.23 to 2.55 bohr, and the HCO angle from 95° to 125°. Single point calculations at the estimated aug-cc-pV5Z geometries of HCO and HCO⁻ were carried out with the aug-cc-pV5Z basis set. As for ArHF, polynomials in the two bond lengths and the bending angle were fitted through the computed interaction energies with the program SURFIT (Senekowitz, 1988). [For further details see (van Mourik and Dunning Jr., 1997).]

For $(HF)_2$ full geometry optimizations in all internal coordinates have been carried out with the aug-cc-pVDZ and aug-cc-pVTZ basis sets. With the aug-cc-pVQZ set just the F-F distance was optimized by fitting 5 points to polynomials in $(R-R_e)$. In these calculations, the two intermolecular angles were held fixed at their optimized aug-cc-pVTZ values, and the two HF bond lengths were held fixed at

estimated aug-cc-pVQZ values. [For further details see (Peterson and Dunning Jr., 1995a).]

IV. DIATOMIC MOLECULES

We first consider two very weakly bound molecules, He_2 and Ar_2, for which BSSE is a well recognized problem and then consider the impact of the counterpoise correction on the strongly bound N_2, HF, and HCl molecules.

A. Very Weakly Bound Molecules: He_2 and Ar_2

Figure 1 shows the counterpoise-corrected and uncorrected binding energies, D_e, for the helium dimer (van Mourik and Dunning Jr., to be published), computed with the aug-cc-pVnZ, d-aug-cc-pVnZ, and t-aug-cc-pVnZ basis sets. Clearly, the uncorrected results do not smoothly converge. This is a discouraging observation, because it implies that the uncorrected results cannot be used to estimate the complete basis set (CBS) limits of various correlation methods despite the fact that at the CBS limit the BSSE is zero. In fact, it is not even clear that the sequence is converging, e.g., ΔD_e from V5Z to V6Z is approximately the same as ΔD_e from VQZ to V5Z. In striking contrast to the uncorrected D_e's, the corrected results converge smoothly to a well-defined limit, and therefore can be used to estimate CBS limits.

The convergence behavior of the aug-cc-pVnZ sets might give rise to the illusion that the uncorrected D_e's converge to the CBS limit faster than the counterpoise-corrected values. This is, however, due to a fortuitous cancellation of errors: BSSE which increases D_e *versus* basis set incompleteness which decreases D_e. The plots of the results obtained with the d-aug-cc-pVnZ and t-aug-cc-pVnZ sets (for which BSSE is larger than for the singly augmented sets) show that, for these sets, the uncorrected D_e's can be at least as far away from the CBS limit as the counterpoise-corrected results. It is well-recognized (Gutowski, et al., 1993; van Duijneveldt, et al., 1994) that the counterpoise correction may not produce results that are closer to the CBS limit than the uncorrected results. As in the present case, basis set incompleteness may compensate for the spurious attractive interaction caused by BSSE. The criterion for judging a counterpoise-corrected result should be whether it is close to (or perhaps identical to) the result that one can expect to obtain with the basis set and computation method employed.
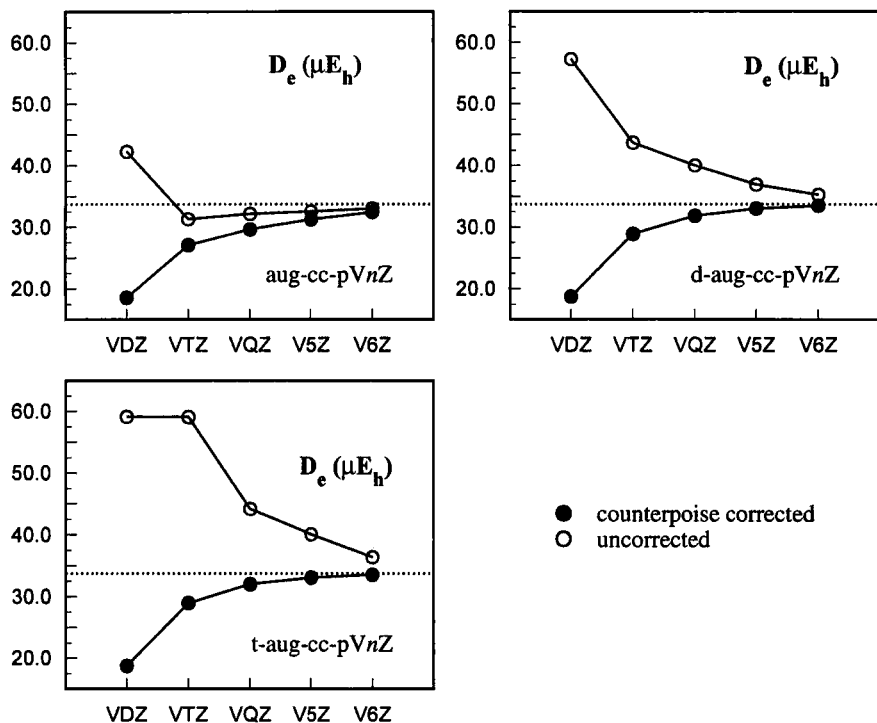
Fig. 1. Counterpoise-corrected and uncorrected D_e for the helium dimer. The dashed lines represent the estimated CBS limit.

The BSSE at the counterpoise-corrected equilibrium bond length (optimized for each basis set), as defined by Eq. (3), is depicted in Figure 2. It is clear that BSSE cannot simply be eliminated by increasing the size of the basis set. While BSSE decreases with increasing n (from x-aug-cc-pVDZ to x-aug-cc-pV6Z), it increases when the basis set is improved along the x-coordinate (from aug-cc-pVnZ to t-aug-cc-pVnZ). This is not surprising, since it well-known that BSSE can either increase or decrease with increasing basis set size (Gutowski, et al., 1986). Compact (high-exponent) functions tend to improve the intramolecular correlation energy, and thereby reduce BSSE, while diffuse (low-exponent) functions tend to increase BSSE, because their large spatial extent makes them more accessible to the other atom.
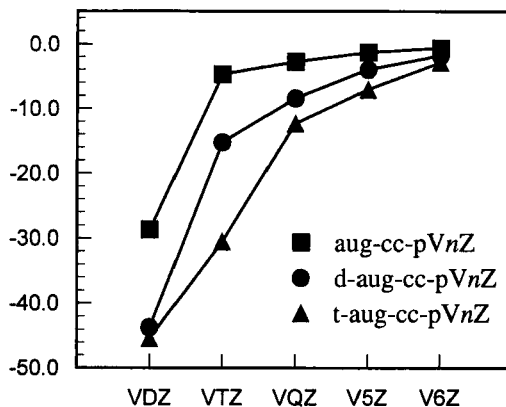
Fig. 2. ΔE_{BSSE} (in μE_h) for He_2 at 5.6 bohr, computed at the equilibrium distance optimum for each basis set.

Naturally, in the limit of using a complete basis set BSSE should vanish, and the BSSE curves in Figure 2 gradually approach zero for all sets considered. However, Figure 2 shows that, even for fairly large basis sets, BSSE may be non-negligible. At the t-aug-cc-pV6Z basis set level, BSSE is still 2.88 μE_h, which is 8.6% of the total He_2 interaction energy. The increase in BSSE due to an additional set of diffuse functions decreases when the basis set is improved from TZ toward 6Z quality. For the DZ quality sets however, BSSE increases by 12.7 μE_h when the basis set is improved from aug-cc-pVDZ to d-aug-cc-pVDZ, but then increases by only 3.4 μE_h when the basis is further improved to t-aug-cc-pVDZ, indicating a saturation effect with increasing shells of diffuse functions. This effect is related to the zigzag pattern from t-aug-cc-pVDZ to t-aug-cc-pVQZ observed for the uncorrected D_e's.

It is well-recognized that the counterpoise correction is essential in the calculation of interaction energies of weakly bonded systems. However, D_e is not the only molecular property affected by BSSE, other spectroscopic constants, like R_e and ω_e, may be contaminated with BSSE. Van Duijneveldt *et al.* (van Duijneveldt, et al., 1994) have observed that the effect of BSSE on computed vibrational frequencies can be avoided by applying the counterpoise procedure. For AH...B hydrogen-bonded systems for example, BSSE tends to increase the ν_{AH} stretching frequency mode (Newton and Kestner, 1983; Bouteiller and Behrouz, 1992; Bouteiller, 1992; van Duijneveldt-van de Rijdt and van Duijneveldt, 1992b), and leads to an imprecise prediction of the position of certain combination transitions (Bouteiller and Behrouz, 1992; Bouteiller, 1992). Figure 3 shows the counterpoise-corrected and uncorrected R_e and ω_e of He_2, computed with the t-aug-cc-pVnZ basis sets through sextuple zeta quality. Again, the counterpoise-corrected R_e and ω_e converge regularly, while the uncorrected values do not. Here we again see the typical zigzag pattern that is often observed for properties that are

substantially affected by BSSE. The differences between the counterpoise-corrected and uncorrected R_e and ω_e do not decrease gradually with increasing basis set quality–for both R_e and ω_e the differences first decrease from t-aug-cc-pVDZ to t-aug-cc-pVTZ, then increase when the basis is improved to t-aug-cc-pVQZ, and then decrease monotonically when the basis is further improved to t-aug-cc-pV6Z. Figure 3 does show that the corrected and uncorrected values do appear to be converging to approximately the same limit.
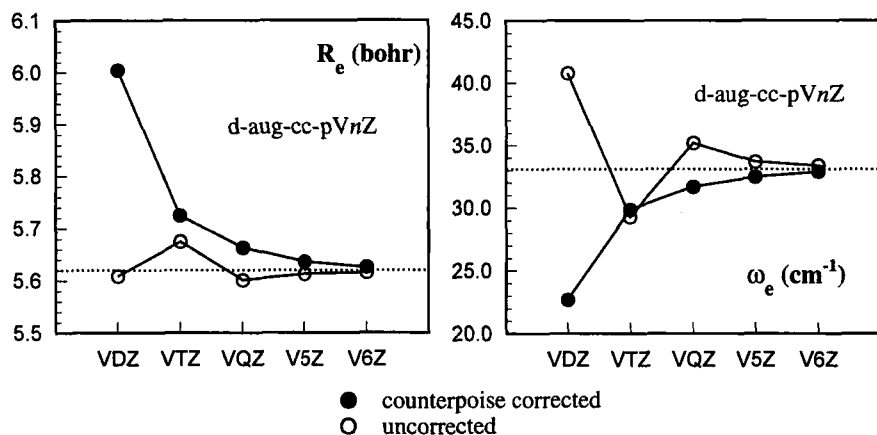

Fig. 3. Counterpoise-corrected and uncorrected R_e and ω_e for the helium dimer, computed with the t-aug-cc-pVnZ sets. The dashed lines represent the estimated CBS limit.

D_e, R_e, and ω_e for the argon dimer (van Mourik and Dunning Jr., to be published) are plotted in Figure 4. The results are similar to the corresponding He_2 curves (see Figures 1 and 3), although there are now easily recognized oscillations in the uncorrected results. As in He_2, the counterpoise-corrected curves are well behaved and can be used to establish the CBS limit with some confidence.
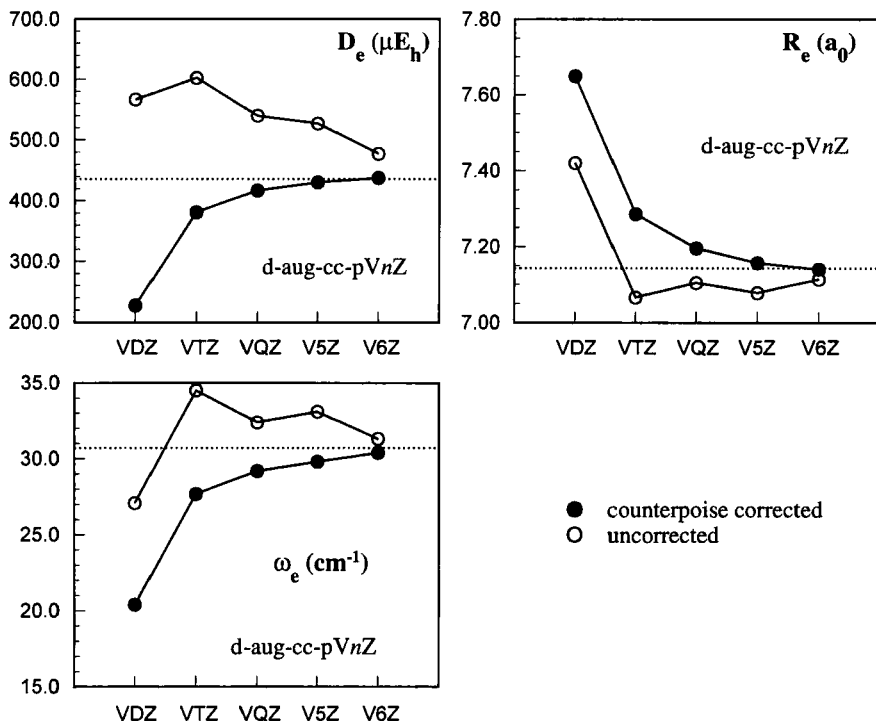
Fig. 4. Counterpoise-corrected and uncorrected R_e and ω_e for the argon dimer, computed with the d-aug-cc-pVnZ sets. The dashed lines represent the estimated CBS limit.

B. Strongly Bound Molecules: N_2, HF, and HCl

For strongly bound molecules, it is frequently stated that BSSE has an insignificant effect on the computed binding energies. However, we have found (Wilson, et al., 1996) that, even for strongly bound molecules like N_2 and HF, BSSE may be non-negligible, particularly for the smaller sets (cc-pVDZ and cc-pVTZ). For N_2, for example (Wilson, et al., 1996), BSSE is about 5 kcal/mol at the cc-pVDZ basis set level, compared to a total D_e of 196 kcal/mol. Although BSSE is certainly significant in N_2, it is small compared to the basis set effect, which is the difference betweeen the computed value for the cc-pVDZ set and the CBS limit. For N_2, D_e for the cc-pVDZ set is 31 kcal/mol from the CBS limit. However, for estimating the CBS limit of the N_2 binding energy, BSSE causes no problem, because it decreases rapidly with increasing basis set size and both the counterpoise-corrected and uncorrected D_e converge smoothly to the same limit. At the cc-pV6Z basis set level, BSSE is just 0.3 kcal/mol, and the CBS limits obtained by extrapolation of the corrected or uncorrected D_e's are 226.9 and 227.0 kcal/mol,

respectively, well within the error limits of the extrapolation procedure itself. The D_e, R_e and ω_e of N_2, computed with the cc-pVnZ sets through sextuple zeta quality, are depicted in Figure 5.
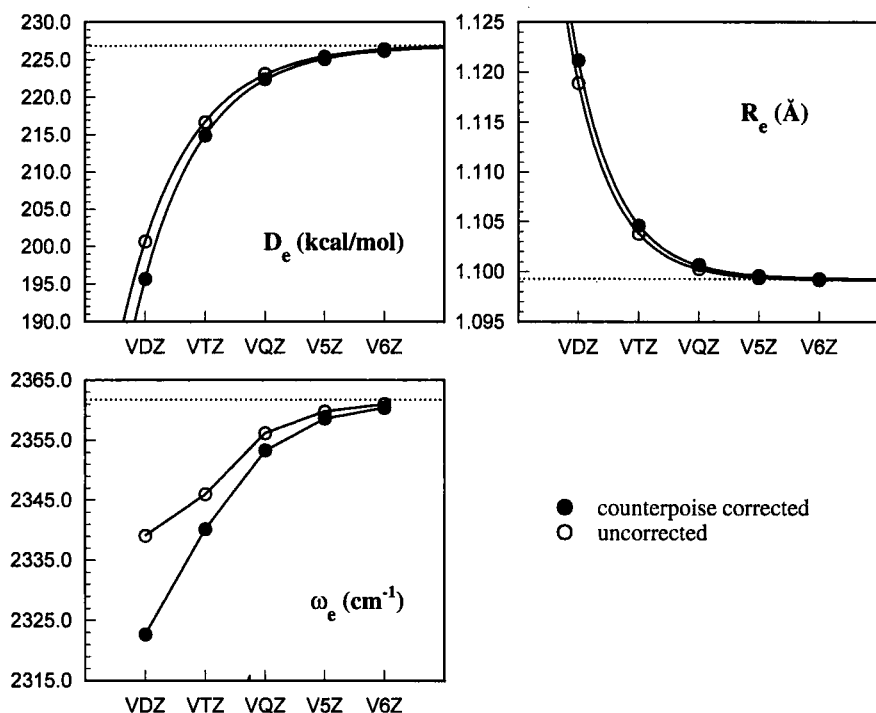

Fig. 5. Counterpoise-corrected and uncorrected D_e, R_e, and ω_e for N_2, computed with the cc-pVnZ basis sets. The dashed lines represent the estimated CBS limit.

The effect of BSSE on the computed R_e's is very small as well, and, again, both the counterpoise-corrected and uncorrected R_e converge smoothly to the same limit. The uncorrected ω_e's, on the other hand, do not converge regularly. This is not unexpected, since it has been observed before (Woon and Dunning Jr., 1993b; Peterson, et al., 1993b; Peterson, et al., 1993a) that harmonic frequencies do not always converge regularly. Generally, the convergence behavior of computed properties becomes less regular as the quantities become less related to energies (Woon and Dunning Jr., 1993b). However, Figure 5 also shows that the counterpoise correction markedly improves the convergence behavior of the frequencies. The counterpoise-corrected ω_e's converge smoothly to a well-defined limit (which is the same as the uncorrected limit), although the variation is not well represented by a simple exponential function like Eq. (6).

For HF the situation is slightly different (Wilson, et al., 1996), see Figure 6. As for N_2, the effect of BSSE on the computed D_e is small, and both the counterpoise-corrected and uncorrected results converge smoothly to essentially the same limit. The uncorrected R_e's, however, do not. The uncorrected R_e's first decrease from cc-pVDZ to cc-pVQZ, and then increase if the basis set is further improved to cc-pV5Z and cc-pV6Z. The convergence behavior is again much improved by applying the counterpoise procedure, though the variation is not strictly exponential. The counterpoise-corrected R_e's decrease rapidly from cc-pVDZ to cc-pVQZ and then remain essentially constant from cc-pVQZ to cc-pV6Z, *i.e.*, R_e is apparently converged at the cc-pVQZ basis set level and the variations observed in the uncorrected R_e's beyond this level are due to BSSE.
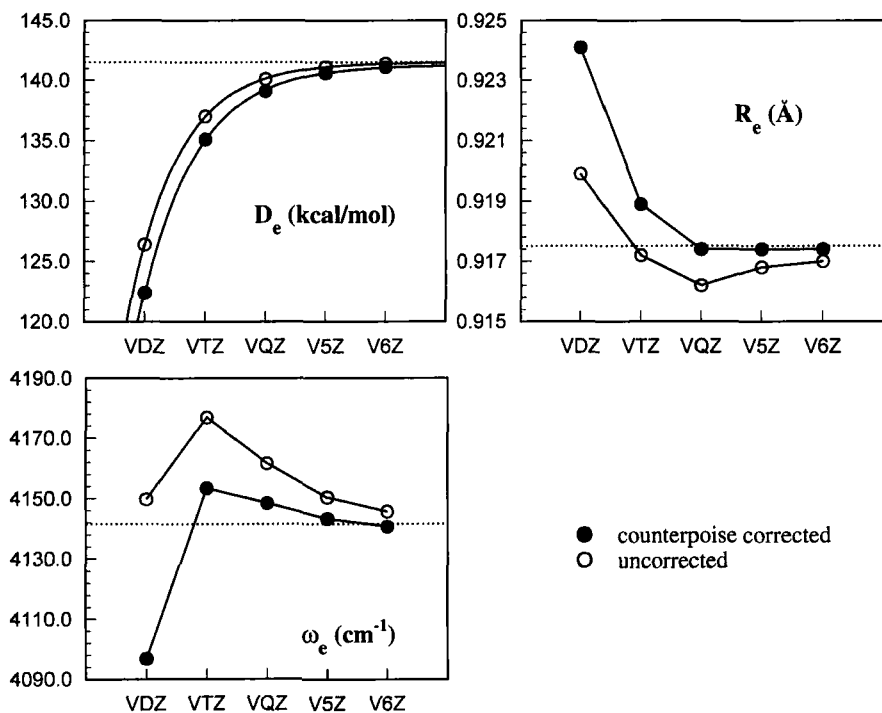

Fig. 6. Counterpoise-corrected and uncorrected D_e, R_e, and ω_e for HF, computed with the cc-pVnZ basis sets. The dashed lines represent the estimated CBS limit.

Turning to the basis set dependence of the harmonic frequencies of HF, we see that the uncorrected ω_e's first increase, and then decrease with increasing basis set quality. Although the frequencies are improved by applying the counterpoise correction, the counterpoise-corrected results show the same general convergence behavior as the uncorrected results. Note the fortuitous cancellation of errors in the

uncorrected ω_e with the cc-pVDZ set. Because the basis set superposition error approximately cancels the basis set convergence error for this set, ω_e(cc-pVDZ) is closer to the CBS limit than those from the calculations with the cc-pVTZ, cc-pVQZ, and cc-pV5Z sets

We also computed the HF potential energy curve with the augmented correlation consistent basis sets through sextuple zeta quality. Because of the highly ionic nature of HF, use of the augmented sets substantially improves the convergence with n (Peterson, et al., 1993b; Martin and Taylor, 1994; Wilson, et al., 1996). The counterpoise-corrected and uncorrected D_e, R_e, and ω_e are shown in Figure 7.
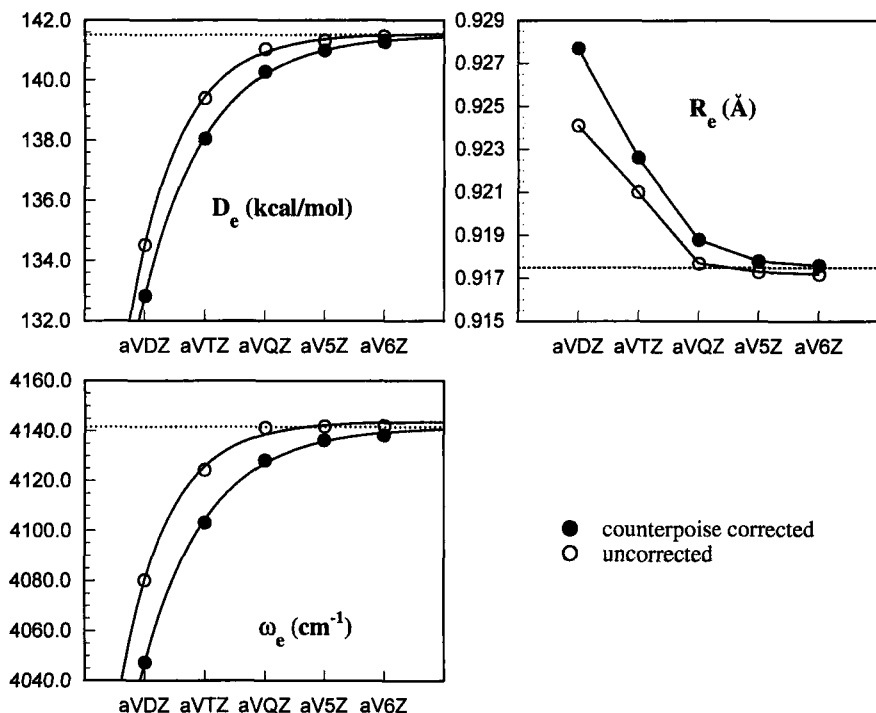

Fig. 7. Counterpoise-corrected and uncorrected D_e, R_e, and ω_e for HF, computed with the aug-cc-pVnZ basis sets. The dashed lines represent the estimated CBS limit.

The "dip" in the uncorrected R_e (as observed for the cc-pVnZ sets) has disappeared, but the results still do not converge very regularly: the change in R_e is 0.0031 Å when the basis set is increased from aug-cc-pVDZ to aug-cc-pVTZ, and this change gets slightly *larger* (0.0033 Å) when the basis is further improved to aug-cc-pVQZ. The counterpoise-corrected R_e are better behaved, although the

variation is still not well represented by a simple exponential function. In addition, R_e now decreases by an additional 0.0012 Å as the set is expanded from QZ to 6Z.

The convergence behavior of the uncorrected as well as the corrected ω_e is improved substantially by including diffuse functions in the basis set. The counterpoise-corrected values are again slightly better behaved.

Figure 8 shows the BSSE in D_e for HF, computed at the counterpoise-corrected equilibrium bond length (optimized for each individual basis set). While for He_2 the BSSE increases with the addition of diffuse functions to the basis set (see previous section), for HF the BSSE is slightly smaller for the aug-cc-pVnZ sets than for the cc-pVnZ sets.
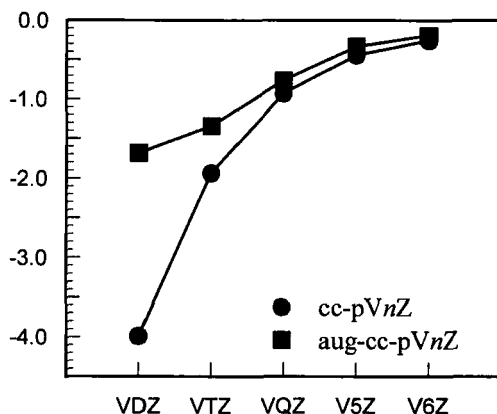

Fig. 8. BSSE for HF (in kcal/mol), computed at the equilibrium distance optimum for each basis set.

As seen above, application of the counterpoise procedure or the addition of diffuse functions may result in $R_e(nZ)$ or $\omega_e(nZ)$ curves which are better behaved. As another example, Figure 9 shows the harmonic frequency of HCl, computed with the cc-pVnZ and aug-cc-pVnZ basis sets. As for HF, application of the counterpoise correction improves the convergence behavior of ω_e computed with the regular sets, although the convergence behavior of the corrected ω_e's is far from simple. Addition of the set of diffuse functions to the basis as well as use of the counterpoise correction results in a very smooth dependence of ω_e on basis set.
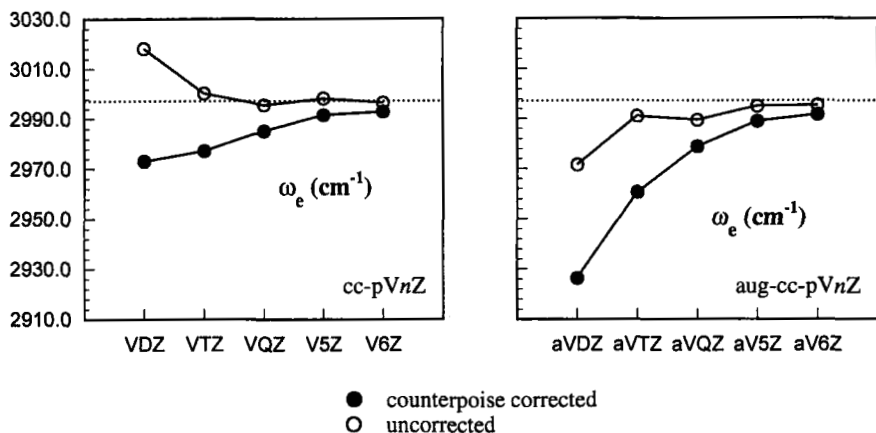
Fig. 9. Counterpoise-corrected and uncorrected ω_e for HCl, computed with the cc-pVnZ and aug-cc-pVnZ basis sets. The dashed lines represent the estimated CBS limit.

As mentioned earlier in this section, the convergence behavior of computed properties generally becomes less exponential as the quantities become less related to energies. By way of illustration, neither the application of the counterpoise procedure nor the addition of diffuse functions to the basis set improves the convergence behavior of the computed anharmonicities $\omega_e x_e$ of the HF molecule (see Figure 10). Even in this case, however, both the uncorrected and corrected curves appear to be converging to the same limits.
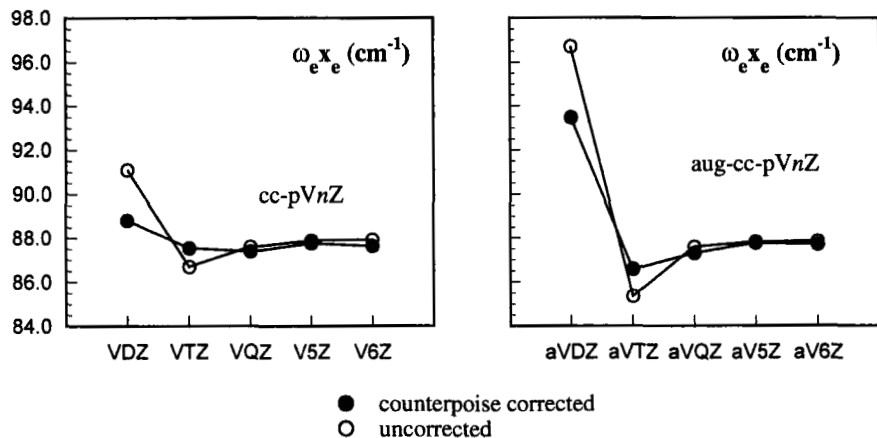
Fig. 10. Counterpoise-corrected and uncorrected $\omega_e x_e$ for HF, computed with the cc-pVnZ and aug-cc-pVnZ basis sets. The dashed lines represent the estimated CBS limit.

V. TRIATOMIC MOLECULES

We now turn our attention to the interaction of an atom with a diatomic molecule. We consider three examples: (*i*) Ar-HF, which is a traditional weakly bound system with a binding energy D_e(Ar-HF) of just 211 cm^{-1} (0.6 kcal/mol); (*ii*) H-CO$^-$, which is also weakly bound, D_e(H-CO$^-$) $\approx$ 8 kcal/mol, but results in large changes in the CO distance; and (*iii*) H-CO, a molecule whose bond strength is intermediate between the other atom-diatom systems considered and more traditional, strongly bound molecules (the H-CO bond strength is just 19 kcal/mol).

A. Weakly Bound Triatomic Molecules: ArHF and HCO$^-$

Figure 11 shows the counterpoise-corrected and uncorrected D_e, R_e(Ar-H) and r_e(HF) of the primary minimum of the ArHF complex. (van Mourik and Dunning Jr., 1997) Again, the uncorrected D_e and R_e(ArH) do not show regular convergence, while the counterpoise-corrected results converge smoothly to well-defined limits. The convergence behavior of the uncorrected D_e and R_e is reminescent of the zigzag convergence patterns observed for the rare-gas dimers [see (van Mourik, et al., 1997) and Figs. 1 and 3]. The uncorrected results obviously cannot be used for extrapolation to the complete basis set limit. Except for the results with the aug-cc-pVDZ set, the uncorrected values are further from the empirical results than the counterpoise-corrected values. In the present case there is no cancellation of basis set incompleteness and basis set superposition errors as observed for the aug-cc-pVnZ results for He$_2$ (see Fig. 1) In this case the BSSE is larger than the basis set incompleteness.
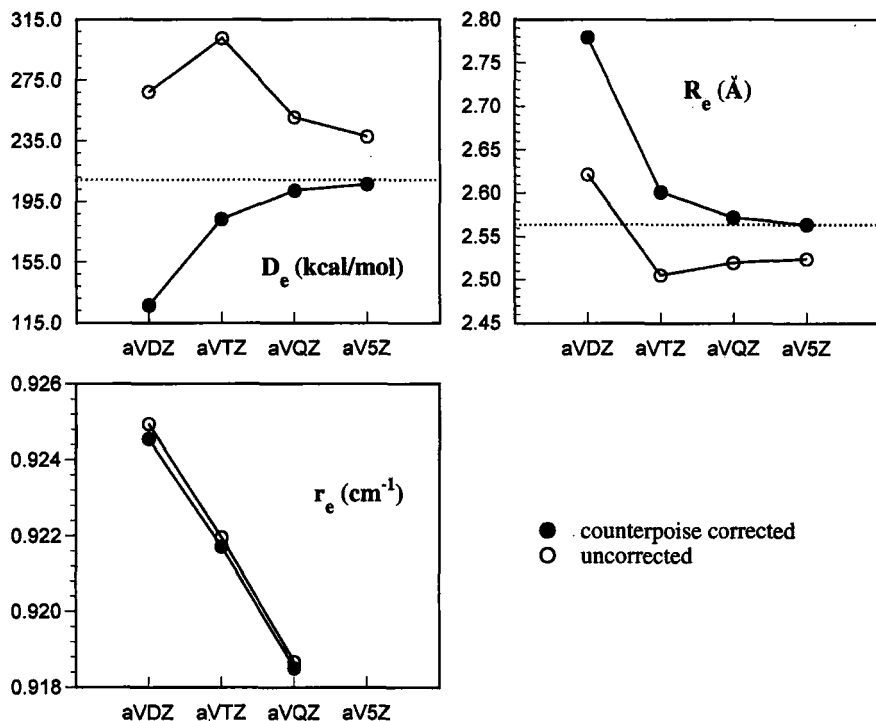
Fig. 11. Counterpoise-corrected and uncorrected D_e, R_e(ArH) and r_e(HF) for ArHF, computed with the aug-cc-pVnZ basis sets. The dashed lines represent the estimated CBS limit.

Often the counterpoise correction for D_e is only applied at the uncorrected geometry. Figure 11 shows that the Ar-H distance will be significantly too short if BSSE is not corrected for. This is in agreement with our results on the diatomics, where BSSE also leads to equilibrium distances that are too short (see Figs. 4, 5, 6, and 7). Similar errors have been reported for other molecular complexes, like $(CO)_2$ (Eggenberger, et al., 1991), and the water dimer (Newton and Kestner, 1983; van Duijneveldt-van de Rijdt and van Duijneveldt, 1992a; Xantheas, 1996). The intramolecular HF bond length in ArHF, on the other hand, is slightly shortened upon applying the counterpoise correction. Generally, intermolecular distances are increased and intramolecular distances are decreased by the counterpoise procedure (see for example (Bouteiller and Behrouz, 1992; Bouteiller, 1992; Peterson and Dunning Jr., 1995a). However, it must be noted that Eq. (5) only describes the effect of the "ghost functions" positioned on Ar on the intramolecular HF distance r. The effect of BSSE on the HF distance would normally refer to the placement of ghost functions on the H and F atoms (as in the previous section). Therefore, the

changes with basis set of the HF distance in ArHF are more similar to the uncorrected than to the counterpoise-corrected r_e of a free HF (compare Figs. 7 and 11). In HF itself, BSSE decreases the bond distance (see Figures 6 and 7).

Table I shows the HF deformation energy ΔU^{def} [as defined by Eq. (4)] as a function of the HF distance r. Also listed are the counterpoise-corrected and uncorrected interaction energies, ΔE^{CP} [cf. Eq. (5)] and $\Delta E^{no\ CP}$ [Eq. (1)], respectively. The energy term labeled ΔE_{def}^{CP} is the energy gained to bring an HF molecule (deformed to the same HF distance as in the particular Ar-HF geometry one is studying) and an Ar atom together. ΔU^{def} is the energy required to bring HF to this deformed geometry. The sum of ΔU^{def} and ΔE_{def}^{CP} is the total counterpoise-corrected interaction energy. All energy terms are computed with the CCSD(T) method and the aug-cc-pVTZ basis set. The Ar-HF molecule was kept linear, and the Ar-H distance was kept fixed at the CCSD(T)/aug-cc-pVTZ optimized value (*i.e.*, 2.602 Å).

<div align="center">

TABLE I.

CONTRIBUTIONS TO THE COUNTERPOISE-CORRECTED AR-HF
INTERACTION ENERGY, CALCULATED WITH CCSD(T) AND AUG-CC-PVTZ
(IN CM^{-1}).

</div>

r (Å)	ΔE^{CP}	$\Delta E^{no\ CP}$	ΔE_{def}^{CP}	ΔU^{def}
0.773	7670.72	7551.68	-131.69	7802.40
0.810	3826.08	3710.33	-143.89	3969.97
0.847	1446.71	1333.12	-156.63	1603.33
0.884	196.98	84.81	-169.74	366.73
0.921	-183.09	-294.33	-183.10	0.01
0.92171	-183.31	-294.52	-183.44	0.14
0.958	103.96	-6.61	-196.55	300.51
1.032	2078.87	1969.21	-223.08	2301.96
1.106	5214.51	5105.95	-248.17	5462.68
1.180	8942.52	8835.87	-270.50	9213.02

By its very definition, the ΔU^{def} potential has the same shape as the potential energy curve of a free HF. At the equilibrium distance of a free HF molecule (which is 0.9210 Å for the present method and basis set) ΔU^{def} equals zero. If HF is distorted from its optimal distance, the deformation energy increases steeply. ΔE_{def}^{CP} gradually becomes more attractive with increasing HF distance, but this energy term changes at a much slower rate than ΔU^{def}. Thus, the interaction of the HF molecule with the Ar atom has only a minor effect on the HF distance, and the optimal HF distance in Ar-HF is mainly determined by the deformation energy. At the equilibrium ArHF geometry [r_e(HF) = 0.92171 Å], ΔU^{def} equals 0.14 cm^{-1}, which is only about 0.1% of the total interaction energy. Neglect of the deformation energy at the equilibrium ArHF geometry therefore will not affect the computed

interaction energy substantially. However, as noted in Section II, the deformation energy is essential in counterpoise-corrected geometry optimizations (if one also optimizes the intramolecular structural parameters), because then HF distances further from the equilibrium value are considered.

The deformation energy will be larger if the monomer geometry is substantially different in the complex than in the free monomer. We have encountered this in studies of HCO⁻ (van Mourik and Dunning Jr.). Although the C-H bond is weak (the equilibrium bond dissociation energy, D_e, is approximately 8.2 kcal/mol (Berkowitz, private communication), the addition of H⁻ to CO has a pronounced effect on the CO distance. The CO distance in HCO⁻ is calculated [CCSD(T)/aug-cc-pVQZ] to be 1.2403 Å, while it is 1.1318 Å in a free CO molecule.

Figure 12 shows ΔU^{def}, ΔE^{CP}, and ΔE_{def}^{CP}, computed with the aug-cc-pVDZ basis set, as a function of the CO distance. The CH distance and the HCO angle are kept at the aug-cc-pVDZ optimized values (1.2544 Å and 109.26°, respectively).
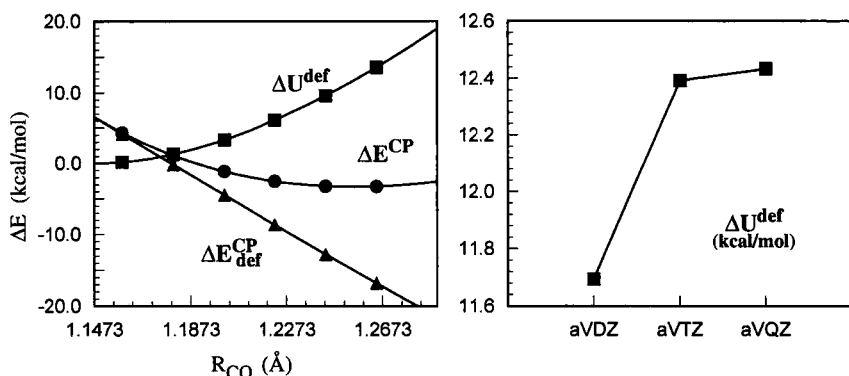

Fig. 12. Dependence on the CO distance of ΔU^{def}, ΔE^{CP}, and ΔE_{def}^{CP}, computed with aug-cc-pVDZ, for the HCO⁻ molecule. Also shown is the basis set dependence of ΔU^{def}.

The deformation energy increases rapidly if the CO molecule is distorted from its optimal distance (which is 1.1473 Å for aug-cc-pVDZ) to the distance it has in HCO⁻ (1.2552 Å). ΔE_{def}^{CP} on the other hand becomes more attractive with increasing CO distance and now varies at a similar rate as ΔU^{def}, partially outweighing the energy loss related to the elongation of CO. The minimum value of ΔE^{CP} is therefore at a significantly longer CO distance than the equilibrium distance of a free CO molecule, as can be clearly seen in Figure 12. The deformation energy is 11.7 kcal/mol at the aug-cc-pVDZ optimized geometry, several times larger than the total counterpoise-corrected interaction energy of 3.33 kcal/mol [computed with CCSD(T) and aug-cc-pVDZ]. Also shown in Figure 12 is the variation of ΔU^{def} with increasing basis set size. The deformation energy increases when the basis set is improved from the aug-cc-pVDZ set to the aug-cc-pVQZ set, and appears to be nearly converged for the aug-cc-pVQZ set.

Figure 13 shows the counterpoise-corrected and uncorrected D_e, $R_e(CH)$ and $r_e(CO)$ of HCO^- as a function of basis set size. Also shown in Figure 13 is the difference of the uncorrected and counterpoise-corrected D_e's, previously (Wilson, et al., 1996) termed $BSSE(D_e)$, which is a measure of the basis set superposition error. [As explained in (Wilson, et al., 1996), $BSSE(D_e)$ differs slightly from the commonly employed definition of BSSE, *i.e.*, Eq. (3).] Although the effect of BSSE on the computed D_e and $R_e(CH)$ is certainly not negligible, both the counterpoise-corrected and uncorrected curves smoothly converge to the same limit. $BSSE(D_e)$ decreases regularly with increasing basis set quality. It decreases from -1.60 kcal/mol for aug-cc-pVDZ to only -0.16 kcal/mol for aug-cc-pV5Z. As for ArHF, BSSE slightly elongates the intramolecular CO bond length.

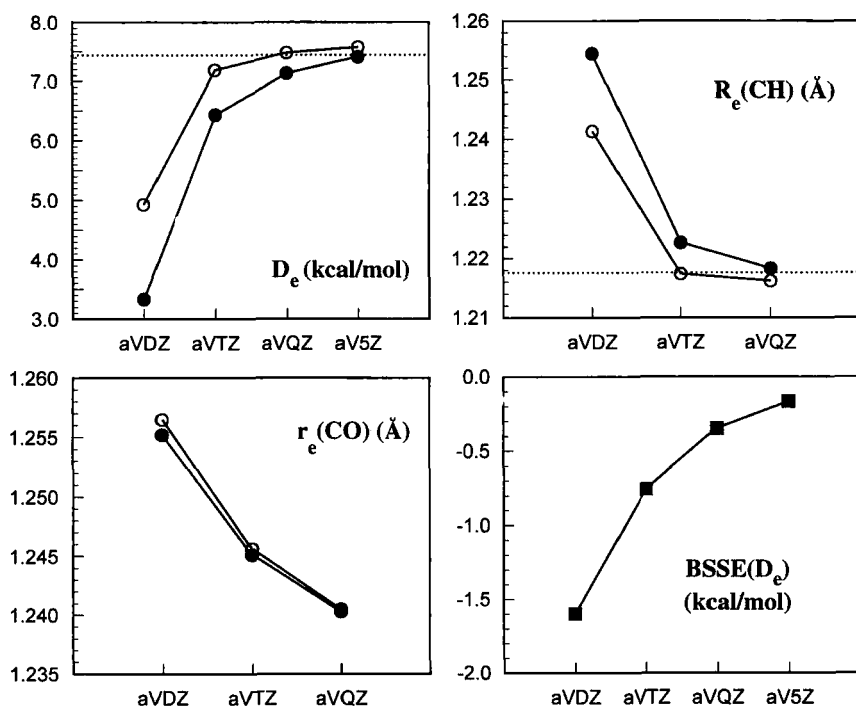**Fig. 13.** Counterpoise-corrected and uncorrected D_e, R_e, and ω_e for HCO^-, as well as $BSSE(D_e)$, computed with the aug-cc-pVnZ basis sets. The dashed lines represent the estimated CBS limit.

B . More Strongly Bound Molecules: HCO

The convergence behavior of D_e, $R_e(CH)$, $r_e(CO)$, and $BSSE(D_e)$ of the HCO molecule (van Mourik and Dunning Jr.) is illustrated in Figure 14.

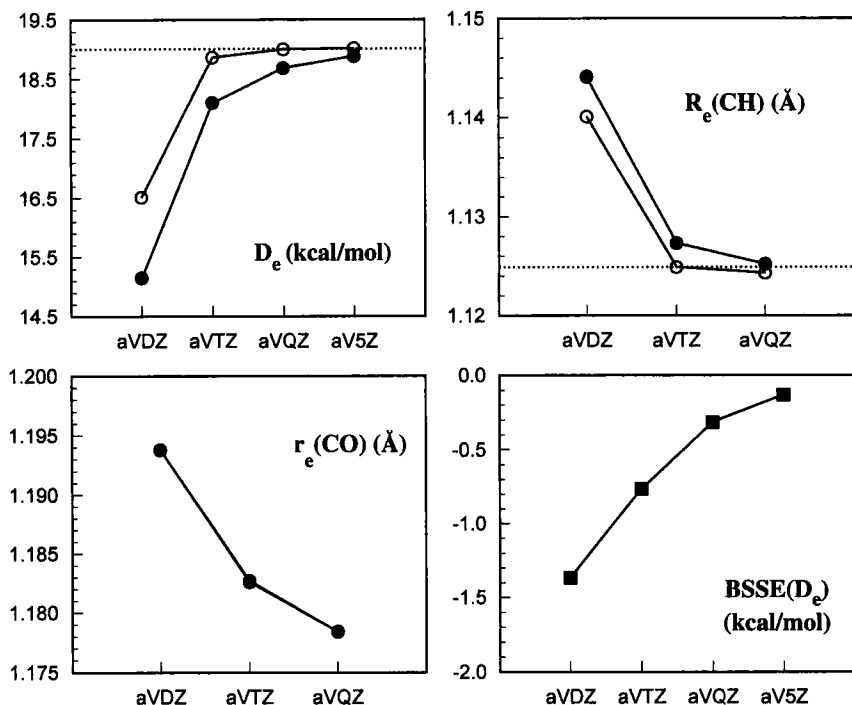**Fig. 14.** Counterpoise-corrected and uncorrected D_e, R_e, and ω_e for HCO, computed with the aug-cc-pVnZ basis sets. The dashed lines represent the estimated CBS limit.

At the aug-cc-pVQZ basis set level, the counterpoise-corrected CH bond energy is calculated to be 18.7 kcal/mol, approximately 10 kcal/mol larger than the CH bond energy in HCO⁻, but several times smaller than the CH bond energy in more traditional, strongly bound molecules. In spite of the small CH bond strength in HCO, the CH bond distance (computed to be 1.120 Å with aug-cc-pVQZ) is not all that different than the CH bond length in strongly bound molecules.

As in the case of HCO⁻, both the counterpoise-corrected and the uncorrected properties converge smoothly towards the same limit. Although the CH bond energy in HCO is nearly twice as large as in HCO⁻, the convergence patterns of the counterpoise-corrected and uncorrected D_e, R_e(CH), and r_e(CO) are very similar for HCO and HCO⁻. BSSE(D_e) is of the same order of magnitude as for HCO⁻, decreasing from -1.37 kcal/mol for aug-cc-pVDZ to -0.13 kcal/mol for aug-cc-pV5Z. BSSE has only a very small effect on the CO bond length, hardly visible in Figure 14.

At the aug-cc-pVQZ optimized geometry, ΔU^{def} equals 2.64 kcal/mol, substantially smaller than ΔU^{def} in HCO⁻, but still a significant fraction of the total

D_e of 18.65 kcal/mol. The CO distance equals 1.178 Å, shorter by 0.06 Å than the CO distance in HCO⁻.

VI. TETRATOMIC MOLECULES

In this section we focus on the weakly bound HF dimer (Peterson and Dunning Jr., 1995a), a prototypical hydrogen-bonded system. Figure 15 depicts the counterpoise-corrected and uncorrected D_e, R_e(FF) and r_e(HF) of the HF dimer. [The r_e(HF) shown is the HF distance for the proton donor monomer and is labeled r_1 in (Peterson and Dunning Jr., 1995a).] The D_e's obtained by applying the counterpoise procedure at the uncorrected geometry are shown as well.
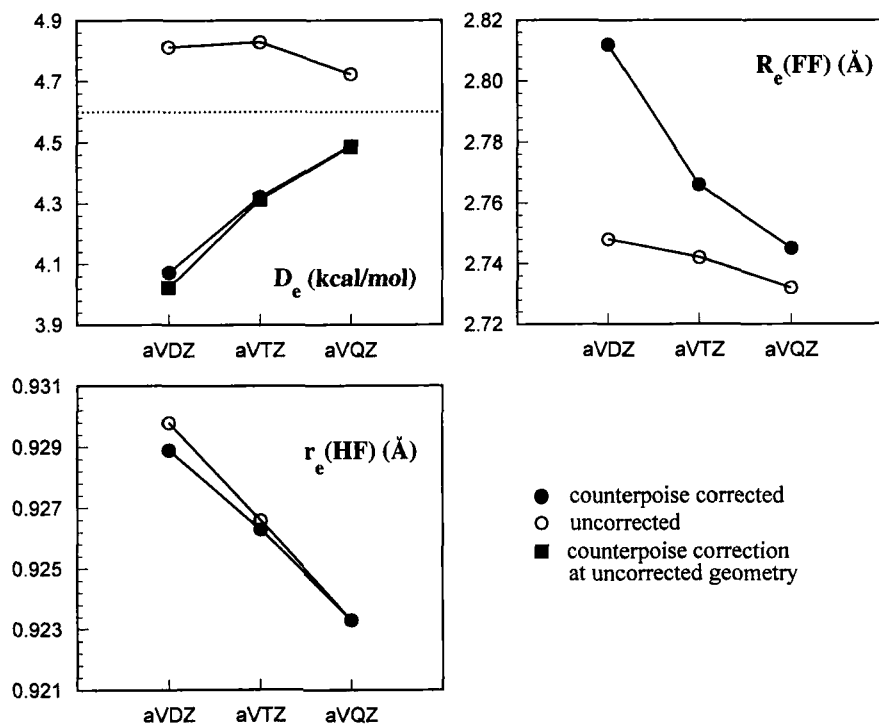
Fig. 15. Counterpoise-corrected and uncorrected D_e, R_e(FF) and r_e(HF) for the HF dimer, computed with the aug-cc-pVnZ basis sets. The dashed lines represent the estimated CBS limit.

As expected, the F-F distance is too short if the geometry optimization is not carried out on the counterpoise-corrected surface. The corrected and uncorrected R_e(FF) are much different at the aug-cc-pVDZ basis set level, but the differences

decrease dramatically with increasing basis set size, becoming 0.013 Å for the QZ set. Although the uncorrected distances do not show exponential convergence, the corrected and uncorrected R_e(FF) seem to be converging to approximately the same limit.

As in the case of ArHF, the uncorrected D_e first increases and then decreases when the basis set is improved from aug-cc-pVDZ to aug-cc-pVQZ. The corrected results converge much more regularly. Similar patterns have been observed for other systems as well, including $F^-(H_2O)$ and $Cl^-(H_2O)$ (Xantheas, 1996). The posthoc counterpoise-corrected D_e's are very close to the results obtained by optimizing the dimer geometry on the counterpoise-corrected surface; only for the aug-cc-pVDZ set is the result significantly different. This is due to the fact that the uncorrected F-F distances are too short, an effect that is largest for the aug-cc-pVDZ set.

The convergence behavior of the corrected and uncorrected intramolecular r_e(HF) is very similar to ArHF (see previous section). The monomer deformation energies are small for this system as well. At the CCSD(T)/aug-cc-pVQZ level, $\Delta U_A^{def}(r_A) + \Delta U_B^{def}(r_B)$ is just 0.03 kcal/mol. However, as we have seen in the previous section, for systems in which the monomers are strongly distorted from their uncomplexed geometries the deformation energy can be significantly larger [see also (Xantheas, 1996)].

VII. CONCLUSIONS

We have investigated the effect of BSSE on the convergence of molecular properties calculated with the correlation consistent basis sets (for both standard and augmented cc-pVnZ sets). It is shown that in a number of cases BSSE destroys the well behaved convergence patterns of the computed quantities. Not surprisingly, the effects are largest for pure van der Waals systems. Our results on He_2 and Ar_2 show a dramatic improvement in the convergence behavior of D_e, r_e, and ω_e by application of the counterpoise correction. While the uncorrected values behave erratically and cannot be reliably extrapolated to the complete basis set (CBS) limit, the counterpoise-corrected results converge smoothly towards well-defined limits. Although BSSE decreases upon improving the basis across the n coordinate (from DZ, TZ, ... to 6Z), it increases by the addition of more diffuse functions to the basis set (from aug-cc-pVnZ to d-aug-cc-pVnZ to t-aug-cc-pVnZ), and is small, but non-negligible even for fairly large basis sets like the t-aug-cc-pV6Z set.

For strongly bound diatomics like N_2, HF, and HCl, the counterpoise procedure can improve the convergence behavior of r_e and ω_e (although the counterpoise-corrected values are not always well represented by a simple exponential formula). For highly ionic molecules like HF and HCl, it was found that addition of diffuse functions to the basis set in addition to the counterpoise correction also improves the convergence of r_e and ω_e.

In some cases the uncorrected results seem to converge more rapidly to the estimated CBS limit than the counterpoise-corrected values. For example, this is

observed for the well depth of the helium dimer computed with the aug-cc-pVnZ sets. However, this is due to a fortuitous cancellation of errors–the basis set superposition error counterbalancing the basis set convergence error. For He$_2$ we have shown that improving the basis set by addition of diffuse functions (thereby increasing the BSSE and decreasing the basis set incompleteness) causes the uncorrected D$_e$ to overestimate the exact value, and results in differences relative to the CBS limit that are as large as those for the counterpoise-corrected results.

Potential energy surfaces of polyatomic molecules may also be distorted if BSSE is not corrected for, especially for weakly bound systems. For ArHF and (HF)$_2$ we found that the uncorrected binding energies as well as the equilibrium structures varied erratically with basis set and could not be directly used to estimate the complete basis set limit; the corrected values were much better behaved. Optimizing the structure of these complexes without the counterpoise correction yields intermolecular distances that are too short, while the intramolecular bond lengths are slightly too long. These distortions will affect other spectroscopic constants as well. Although the deformation energy was found to be small for ArHF and (HF)$_2$, this energy term is essential in counterpoise-corrected geometry optimizations. For systems in which the monomer structure is strongly distorted from the uncomplexed geometry [HCO$^-$, see also (van Mourik and Dunning Jr.,) or F$^-$(H$_2$O) (Xantheas, 1996)], the deformation energy may be large, even at the equilibrium geometry of the complex.

ACKNOWLEDGMENTS

REFERENCES

Berkowitz, J. (private communication).

Bouteiller, Y. (1992). *Chem. Phys. Lett.* 198, 491.

Bouteiller, Y. and Behrouz, H. (1992). *J. Chem. Phys.* 96, 6033.

Boys, S. F. and Bernardi, F. (1970). *Mol. Phys.* 19, 553.

Cullen, J. M. (1991). *Int. J. Quant. Chem. Symp.* 23, 193.

Daudey, J. P., Claverie, P. and Malrieu, J. P. (1974). *Int. J. Quant. Chem.* 8, 1.

Deegan, M. J. O. and Knowles, P. J. (1994). *Chem. Phys. Lett.* 227, 321.

Dunham, J. L. (1932). *Phys. Rev.* 41, 713.

Dunning Jr., T. H. (1989). *J. Chem. Phys.* 90, 1007.

Eggenberger, R., Gerber, S., Huber, H. and Searles, D. (1991). *Chem. Phys. Lett.* 183, 223.

Feller, D. (1992). *J. Chem. Phys.* 96, 6104.

Feller, D. (1993). *J. Chem. Phys.* 98, 7059.

Feyereisen, M. W., Feller, D. and Dixon, D. A. (1996). *J. Phys. Chem.* 100, 2993.

Gutowski, M. and Chalasinski, G. (1993). *J. Chem. Phys.* 98, 5540.

Gutowski, M., van Duijneveldt-van de Rijdt, J. G. C. M., van Lenthe, J. H. and van Duijneveldt, F. B. (1993). *J. Chem. Phys.* 98, 4728.

Gutowski, M., Van Lenthe, J. H., Verbeek, J. and Van Duijneveldt, F. B. (1986). *Chem. Phys. Lett.* 124, 370.

Hampel, C., Peterson, K. A. and Werner, H.-J. (1992). *Chem. Phys. Lett.* 190, 1.

Jensen, F. (1996). *Chem. Phys. Lett.* 261, 633.

Jeziorski, B. and Kolos, W. (1982), in*Molecular Interactions* (Wiley, Chichester).

Jeziorski, B., Moszynski, R. and Szalewitz, K. (1994). *Chem. Rev.* 94, 1887.

Kendall, R. A., Dunning Jr., T. H. and Harrison, R. J. (1992). *J. Chem. Phys.* 96, 6796.

Knowles, P. J., Hempel, C. and Werner, H.-J. (1994). *J. Chem. Phys.* 99, 5219.

Liu, B. and McLean, A. D. (1973). *J. Chem. Phys.* 59, 4557.

Martin, J. R. L. and Taylor, P. R. (1994). *Chem. Phys. Lett.* 225, 473.

Mayer, I., Surján, P. J. and Vibók, A. (1989). *Int. J. Quant. Chem. Symp.* 23, 281.

Mayer, I. and Surján, P. R. (1989). *Int. J. Quant. Chem.* 36, 225.

Mayer, I. and Vibók, A. (1991). *Int. J. Quant. Chem.* 40, 139.

Newton, M. D. and Kestner, N. R. (1983). *Chem. Phys. Lett.* 94, 198.

Noga, J. and Vibók, A. (1991). *Chem. Phys. Lett.* 180, 114.

Peterson, K. A. (1995). *J. Chem. Phys.* 102, 262.

Peterson, K. A. and Dunning Jr., T. H. (1995a). *J. Chem. Phys.* 102, 2032.

Peterson, K. A. and Dunning Jr., T. H. (1995b). *J. Phys. Chem.* 99, 3898.

Peterson, K. A., Kendall, R. A. and Dunning Jr., T. H. (1993a). *J. Chem. Phys.* 99, 9790.

Peterson, K. A., Kendall, R. A. and Dunning Jr., T. H. (1993b). *J. Chem. Phys.* 99, 1930.

Peterson, K. A., Woon, D. E. and Dunning Jr., T. H. (1994). *J. Chem. Phys.* 100, 7410.

Raghavachari, K., Trucks, G. W., Pople, J. A. and Head-Gordon, M. (1989). *Chem. Phys. Lett.* 157, 479.

Sadlej, A. J. (1991). *J. Chem. Phys.* 95, 6707.

Senekowitz, J. (1988), Ph.D. Thesis, Universität Frankfurt, Germany.

Taylor, P. R. and Almlöf, J. (1987). *J. Chem. Phys.* 86, 4070.

Valiron, P., Vibók, A. and Mayer, I. (1993). *J. Comput. Chem.* 14, 401.

van Duijneveldt, F. B., van Duijneveldt-van de Rijdt, J. G. C. M. and van Lenthe, J. H. (1994). *Chem. Rev.* 94, 1873.

van Duijneveldt-van de Rijdt, J. G. C. M. and van Duijneveldt, F. B. (1992a). *J. Chem. Phys.* 97, 5019.

van Duijneveldt-van de Rijdt, J. G. C. M. and van Duijneveldt, F. B. (1992b). *J. Comput. Chem.* 13, 399.

van Mourik, T. and Dunning Jr., T. H. (1997). *J. Chem. Phys 107, 2451.*

van Mourik, T. and Dunning Jr., T. H. (to be published).

van Mourik, T. and Dunning Jr., T. H. (to be published).

van Mourik, T., Wilson, A. K. and Dunning, J., T.H. (to be published).

Vibók, A. and Mayer, I. (1992). *Int. J. Quant. Chem.* 43, 801.

MOLPRO94 is a suite of *ab initio* programs written by Werner, H.-J. and Knowles, P. J., with contributions by J. Almlöf, R. D. Amos, M. Deegan, S. T. Elbert, C. Hampel, W. Meyer, K. A. Peterson, R. M. Pitzer, E.-A. Reinsch, A. J. Stone and P. R. Taylor.

Widmark, P.-O., Joakim, B. and Roos, B. O. (1991). *Theor. Chim. Acta* 79, 419.

Widmark, P.-O., Malmquist, P.-A. and Roos, B. O. (1990). *Theor. Chim. Acta* 77, 291.

Wilson, A. K. and Dunning, T. H., Jr. (1997). *J. Chem. Phys.* 106, 8718.

Wilson, A. K., van Mourik, T. and Dunning Jr., T. H. (1996). *J. Mol. Struct. (Theochem)* 388, 339.

Woon, D. E. (1993). *Chem. Phys. Lett.* 204, 29.

Woon, D. E. (1994). *J. Chem. Phys.* 100, 2838.

Woon, D. E. and Dunning Jr., T. H. (1993a). *J. Chem. Phys.* 99, 3730.

Woon, D. E. and Dunning Jr., T. H. (1993b). *J. Chem. Phys.* 99, 1914.

Woon, D. E. and Dunning Jr., T. H. (1993c). *J. Chem. Phys.* 98, 1358.

Woon, D. E. and Dunning Jr., T. H. (1994a). *J. Chem. Phys.* 101, 8877.

Woon, D. E. and Dunning Jr., T. H. (1994b). *J. Chem. Phys.* 100, 2975.

Woon, D. E. and Dunning Jr., T. H. (1995). *J. Chem. Phys.* 103, 4572.

Woon, D. E. and Dunning Jr., T. H. (to be published).

Woon, D. E., Dunning Jr., T. H. and Peterson, K. A. (1996). *J. Chem. Phys.* 104, 5883.

Xantheas, S. S. (1996). *J. Chem. Phys.* 104, 8821.

Xantheas, S. S. and Dunning Jr., T. H. (1992). *J. Phys. Chem.* 96, 7505.

Xantheas, S. S. and Dunning Jr., T. H. (1993a). *J. Phys. Chem.* 97, 8037.

Xantheas, S. S. and Dunning Jr., T. H. (1993b). *J. Phys. Chem.* 97, 18.

Xantheas, S. S. and Dunning Jr., T. H. (1993c). *J. Phys. Chem.* 97, 6616.

Yarkony, D. R. (1995) *Modern Electronic Structure Theory, Parts I and II*, (World Scientific, London).

Role of electron correlation in nonadditive forces and *ab initio* model potentials for small metal clusters

I. G. Kaplan

Instituto de Física, Universidad Nacional Autónoma de México
Apartado Postal 20-364, 01000 México, D.F., MEXICO

Abstract. The physical nature of nonadditivity in many-particle systems and the methods of calculations of many-body forces are discussed. The special attention is devoted to the electron correlation contributions to many-body forces and their role in the Be_N and Li_N cluster formation. The procedure is described for founding a model potential for metal clusters with parameters fitted to *ab initio* energetic surfaces. The proposed potential comprises two-body, three-body, and four body interation energies each one consisting of exchange and dispersion terms. Such kind of *ab initio* model potentials can be used in the molecular dynamics simulation studies and in the analysis of binding in small metal clusters.

I. Physical nature of nonadditivity and the definition of m-body forces

II. Many-body interaction energies and correlation contributions in the PT formalism

III. Results of calculations for Be_N and Li_N clusters

IV. *Ab initio* model potentials for small metal clusters

References

I. Physical nature of nonadditivity and the definition of m-body forces

Most physical laws established for many-particle systems are additive. The well-known examples are the Coulomb law:

$$V = \sum_{a<b} \frac{q_a q_b}{r_{ab}} \tag{1}$$

and the Newton gravitational law:

$$V = \gamma \sum_{a<b} \frac{m_a m_b}{r_{ab}}, \tag{2}$$

where r_{ab} is the distance between two interacting objects. These laws imply that the charges or bodies can be described as point objects. The interaction of point objects is always characterized by the pair additivity. We also have an additivity for space-extented objects if they are rigid. In general, the potential energy of a rigid-particle system can be always represented as a sum of pair potentials g_{ab}

$$V = \sum_{a<b} g_{ab}, \tag{3}$$

irrespectively of an interaction law.

However, in quantum mechanics, the charges are not point and not rigid. The interacting atoms (molecules) have an internal electronic structure which is modified in different environments. There are two kinds of interatomic forces which lead to nonadditivity: polarization and exchange forces[1].

The nonadditivity arising from the polarization forces is the most evident. The interaction energy of two atoms depends upon the location of other atoms because the latter polarize the electronic charge distribution of both interacting atoms. For a three-atom system each pair interaction depends on coordinates of all three atoms,

$$V(\mathbf{r}_1, \mathbf{r}_2, \mathbf{r}_3) = V_{12}(r_{12}, r_{13}, r_{23}) + V_{13}(r_{13}, r_{12}, r_{23}) + V_{23}(r_{23}, r_{12}, r_{13}). \tag{4}$$

So, V_{ij} in Eq. (4) cannot be considered as a pure two-body interaction. But we can always represent the energy (4) as a sum of two-body interactions of isolated pairs and a remainder depending upon coordinates of three atoms,

$$V(\mathbf{r}_1, \mathbf{r}_2, \mathbf{r}_3) = V_{12}(r_{12}) + V_{13}(r_{13}) + V_{23}(r_{23}) + V_{123}(r_{12}, r_{13}, r_{23}). \tag{5}$$

This additional to the two-body interaction energies term originates from three-body interactions and is called the three-body interaction energy.

A second type of interparticle forces which leads to nonadditivity comprises exchange forces of two kinds. The first kind has its origin in the Pauli principle which requires the antisymmetrization of the many-electron wave function. The exchange of electrons belonging to three or more atoms results in nonadditive terms in the interaction energy. The second kind is connected with the direct exchange through transverse photons. It results in the nonadditivity of electrodynamical interactions in many-atom systems (the Casimir-Polder retardation forces [2]). The physical picture in the case of three atoms is the following: atom A emits a photon which is scattered by atom B and then absorbed by atom C.

One of the necessary conditions for a many-body description is the validity of the decomposition of the system under consideration on separate subsystems. In the case of very large collective effects we cannot separate the individual parts of the system and only the total energy of the system can be defined. However, in atomic systems the inner-shell electrons are to a great extent localized. Therefore, even in metals with strong collective valence-electron interactions, atoms (or ions) can be identified as individuals and we can define many-body interactions. The important role in this separation plays the validity for atom- molecular systems the adiabatic or the Born-Oppenheimer approximations which allow to describe the potential energy of an N-atom system as a functional of the positions of atomic nuclei.

The interaction energy of N-atom (N-molecule) system can be presented as a finite sum of m-body interaction energies [1,3]

$$E_{int}(N) = E_2(N) + E_3(N) + \ldots + E_N(N). \qquad (6)$$

In the general case, we cannot expect that the terms in Eq. (6) have diminishing values and we must not be surprised if the decomposition (6) not converges entirely, as was shown by Heine et al [4] in the case of solids. For metal clusters, as was shown some time ago [5,6], the 3-body and even the 4-body interaction energies can be larger then the 2-body ones. This was confirmed recently in more precise calculations [7,8]. Nevertheless, instead of the full decomposition (6), the truncated (to the 3-body or even only to the 2-body terms) decomposition of semiempirical potentials is successfully used. The reason is that the potentials of such kind have fitting parameters. So it is not real potentials but effective ones.

There are many empirical and semi-empirical pair potentials which describe quite satisfactorily the properties of liquids and solids, see chapter 5 in book [1]. The parameters in these potentials are not real parameters of a true two-body interaction, their values depend upon properties of a medium. So these effective two-body potentials include nonadditive interactions through their parameters. The latter can not be directly related to the definite physical

properties [9]. For instance, the coefficient of the term R^{-6} in the Buckingham or the Lennard-Jones potentials is not equal to the dispersion constant C_6. In many cases for obtaining a good agreement with experimental data the effective potentials for clusters and liquids, must be constructed with 3-body terms. [10,11] Effective potentials which take into account many-body interactions and satisfactorily describe properties of solid materials, are discussed in the review by Carlsson.[12]

Note that the decomposition (6) is exact, but the relative weights of m-body contributions are method-dependent. For obtaining the reliable values of m-body interaction energies, the calculation method must be as precise as possible.

The analytical expressions for many-body interaction energies are defined in a recurrence manner:

$$E_2(N) = \sum_{a<b}^{\{N\}} \epsilon_{ab}, \tag{7}$$

where

$$\epsilon_{ab} \equiv E_{int}(ab). \tag{8}$$

The notation $\{N\}$ in Eq. (7) means that the summation is carried over all pairs of the N-atom system. The number of pairs is equal to $C_N^2 = N(N-1)/2$.

$$E_3(N) = \sum_{a<b<c}^{\{N\}} \epsilon_{abc}, \tag{9}$$

$$\epsilon_{abc} = E_{int}(abc) - E_2(abc), \tag{10}$$

etc. up to $E_N(N)$. In Eqs. (7) and (9), $E_m(N)$ designates the sum of m-body interactions for all $C_N^m = N!/(N-m)!m!$ m-atom clusters, which can be separated in the original N-atom cluster; $\epsilon_{ab...m}$ is the m-body interaction energy in a concrete m-atom cluster. These m-atom clusters are treated as isolated with the geometry taken from the original N-atom cluster.

For $N \geq 4$ the recurrence procedure becomes rather cumbersome. Instead of the algorithm (7)-(10) a closed recurrence formula for the energy of m-body interactions can be obtained[7]:

$$E_m(N) = \sum_{a<b<...<m}^{\{N\}} E(ab...m) - \sum_{k=1}^{m-1} a_{mN}^k E_k(N), \tag{11}$$

$$a_{mN}^k = \frac{(N-k)!}{(N-m)!(m-k)!}. \tag{12}$$

The expressions (11), (12) were used in variational calculations of the many-body partition in the case of $Ag_N(N = 2$ to $6)$ [7,13] and Be_N, Li_N $(N = 2$ to $4)$ [8] clusters.

II. Many-body interaction energies and correlation contributions in the PT formalism

At distances where the magnitude of the interaction energy of a system under consideration can be considered small in comparison with the sum of the energies of the isolated subsystems, the interaction energy may be decomposed in a series over various orders of the perturbation theory (PT):

$$E_{int} = \epsilon_{el}^{(1)} + \epsilon_{exch}^{(1)} + \sum_{n=2}^{\infty} \left[\epsilon_{pol-exch}^{(n)} + \epsilon_{pol}^{(n)} \right]. \qquad (13)$$

The first order energy, $\epsilon_{el}^{(1)}$, is the classical electrostatic energy for an interaction of space-distributed charges,

$$\epsilon_{el}^{(1)} = \langle \psi_a^{(o)} \psi_b^{(o)} \dots \psi_N^{(o)} | V | \psi_a^{(o)} \psi_b^{(o)} \dots \psi_N^{(o)} \rangle. \qquad (14)$$

It is evidently additive: the additive operator V is calculated over unperturbed wave functions, which means that at this approximation the interacting charges are rigid. The exchange energy, $\epsilon_{exch}^{(1)}$, is nonadditive for all exchanges mixing electrons of three or more atoms.

As the exchange energy, the polarization-exchange energy $\epsilon_{pol-exch}$ is also nonadditive. The standard PT cannot be applied to the calculation of the $\epsilon_{pol-exch}$. The reason is that the antisymmetrized functions of zeroth order $(\hat{A}\psi_0^A \psi_0^B \dots)$ are not eigenfunctions of the unperturbed Hamiltonian H_0 as long as the operator H_0 does not commute with the antisymmetrizer operator $\hat{A}$. Many successful approaches for the symmetry adapted perturbation theory (SAPT) have been developed; for a detailed discussion see chapter 3 in book[1], the modern achievements in the SAPT are described in reviews [14–16].

At large distances where the overlap of interacting charges becomes negligible, the expression for E_{int} (13) reduces to

$$E_{int.asymp} = \epsilon_{el}^{(1)} + \sum_{n=2}^{\infty} \epsilon_{pol}^{(n)} \equiv \epsilon_{el}^{(1)} + E_{pol}. \qquad (15)$$

$\epsilon_{pol}^{(n)}$ is the polarization energy of the nth order of the standard PT, it comprises the induction, $\epsilon_{ind}^{(n)}$, and the dispersion, $\epsilon_{disp}^{(n)}$, energies. These energies are nonadditive in all orders of PT; the only exception is $\epsilon_{disp}^{(2)}$, see proofs in books [1,3]. For example, for a three-atom system

$$\epsilon_{disp}^{(2)}(abc) = \epsilon_{disp}^{(2)}(ab) + \epsilon_{disp}^{(2)}(ac) + \epsilon_{disp}^{(2)}(bc). \qquad (16)$$

Thus, in the energy partition (13) only two terms are additive: $\epsilon_{el}^{(1)}$ and $\epsilon_{disp}^{(2)}$. If we subtract them from E_{int}, the remaining part will contain only

nonadditive contributions, E_{int}^{nonadd},

$$E_{int}^{nonadd} = \epsilon_{exch}^{(1)} + E_{pol-exch} + E_{pol}^{nonadd}, \tag{17}$$

where

$$E_{pol-exch} = \sum_{n=2}^{\infty} \epsilon_{pol-exch}^{(n)}, \qquad E_{pol}^{nonadd} = E_{pol} - \epsilon_{disp}^{(2)}. \tag{18}$$

Now we can decompose the m-body interaction energies, defined in previous section, into the PT series. For the two-body interaction energy, the expression directly follows from Eqs. (7), (8) and (13).

$$E_2(N) = \sum_{a<b}^{\{N\}} \epsilon_{ab};$$

$$\epsilon_{ab} = \epsilon_{e\ell}^{(1)}(ab) + \epsilon_{exch}^{(1)}(ab) + \sum_{n=2}^{\infty} \left[\epsilon_{pol-exch}^{(n)}(ab) + \epsilon_{pol}^{(n)}(ab) \right]. \tag{19}$$

For $m \geq 3$, the expressions for m-body energies contain only E_{int}^{nonadd} as all additive terms are cancelled. For example, in Eq. (10)

$$\epsilon_{abc} = E_{int}^{nonadd}(abc) - \sum_{a<b}^{\{abc\}} E_{int}^{nonadd}(ab)\;^{17}. \tag{20}$$

The sum in the right-hand side of Eq. (20) contains $C_3^2 = 3$ terms, the sum in Eq. (9) contains $C_N^3 = N!/(N-3)!3!$ terms. If we substitute Eq. (20) into Eq. (9) and subdivide $C_N^3 \cdot C_3^2$ 2-body terms on C_N^2 -membered sets, each corresponding to the nonadditive part of the 2-body interaction energy of N-atom system (denote it as $\tilde{E}_2(N)$), we obtain

$$E_3(N) = \sum_{a<b<c}^{\{N\}} E_{int}^{nonadd}(abc) - (N-2)\tilde{E}_2(N), \tag{21}$$

where

$$\tilde{E}_2(N) = \sum_{a<b}^{\{N\}} E_{int}^{nonadd}(ab). \tag{22}$$

In Eq. (19) and (21) the atom-atom distances in two- and three-atom clusters are taken the same as in the original N-atom cluster.

In the general case, the energy of m-body interactions in a PT approach is expressed through the energy of k-body ($k \leq m-1$) ones by the following recurrence formula [18]:

$$E_m(N) = \sum_{a<b<...<m}^{\{N\}} E_{int}^{nonadd}(ab...m) - a_{mN}^2 \tilde{E}_2(N) - \sum_{k=3}^{m-1} a_{mN}^k E_k(N). \tag{23}$$

The term $\tilde{E}_2(N)$ is separated, in so far as it differs from the energy of 2-body interactions in a N-atom system, given by Eq. (19). The expression for the coefficients a_{mN}^k is giving by Eq. (12). For clusters with number of monomers $N \geq 4$ formula (23) is more convenient and efficient than the ordinary recurrence procedure.

Let us turn to the electron correlation energy. According to its definition [19], the correlation energy is the difference between the exact eigenvalue of the Hamiltonian describing the system under consideration and the Hartree-Fock (SCF) value. But except for the smallest systems, we cannot obtain the exact energy. So, the magnitude of the computed correlation energy depends upon the approximation used. For the energy of m-body interactions, the correlation contribution is defined as

$$\Delta E_m^{corr}(N) = E_m(N) - E_m^{SCF}(N) \tag{24}$$

and depends upon the method which is applied for a calculation of $E_m(N)$. The SCF interaction energy can be decomposed as [20,21]

$$E_{int}^{SCF} = \epsilon_{el}^{(1)} + \epsilon_{exch}^{(1)} + E_{def}^{SCF}. \tag{25}$$

The deformation energy, E_{def}^{SCF}, is the correction to the first order of PT due to the relaxation of orbitals in the self-consistent field. It originates from the induction-exchange interactions. On the distances where exchange effects can be neglected, E_{def}^{SCF} is the classical induction energy.

Certainly, we can took into account only a finite number of terms in the perturbation series (13). Let us assume that we perform calculations to the pth order of PT. If we use the Møller-Plesset PT then $p \leq 4$. The expression for $\Delta E_2^{corr}(N)$ is easily obtained from Eqs. (19), (24), and (25)

$$\Delta E_2^{corr}(N) = \sum_{a<b}^{\{N\}} \left[\sum_{n=2}^{p} [\epsilon_{pol-exch}^{(n)}(ab) + \epsilon_{pol}^{(n)}(ab)] - E_{def}^{SCF}(ab) \right]. \tag{26}$$

Eq. (26) can be written in a more compact notations:

$$\Delta E_2^{corr}(N) = \sum_{a<b}^{\{N\}} \left[E_{pol-exch}(ab) + E_{pol}(ab) - E_{def}^{SCF}(ab) \right]. \tag{27}$$

The contributions of the induction energy to the energy difference in brackets in Eq. (27) are almost cancelled. To some degree the same happens to the exchange energy. At large distances, the exchange terms can be totally neglected and the main contribution to ΔE_2^{corr} will be given by the dispersion energy to second order,

$$\Delta E_{2,asymp}^{corr}(N) = \sum_{a<b}^{\{N\}} \epsilon_{disp}^{(2)}(ab). \tag{28}$$

The expression for the correlation contribution to the energy of 3-body interactions can be represented as follows:

$$\Delta E_3^{corr}(N) = \sum_{a<b<c}^{\{N\}} \left[E_{pol-exch}(abc) + E_{pol}^{nonadd}(abc) - E_{def}^{SCF}(abc) \right]$$

$$- (N-2) \sum_{a<b}^{\{N\}} \left[E_{pol-exch}(ab) + E_{pol}^{nonadd}(ab) - E_{def}^{SCF}(ab) \right]. \qquad (29)$$

Similar expressions can be obtained for the correlation contribution to the m-body energy for $m > 3$. At large distances, the exchange terms can be neglected and, as in the case of ΔE_2^{corr}, the expression for ΔE_3^{corr} will contain only the dispersion terms in which the leading terms are the III order dispersion energies: the Axilrod-Teller dispersion energy, $\epsilon_{disp}^{(3)}(abc)$, and the III order dispersion energy for dimers, $\epsilon_{disp}^{(3)}(ab)$,

$$\Delta E_{3,asymp}^{corr}(N) = \sum_{a<b<c}^{\{N\}} \epsilon_{disp}^{(3)}(abc) - (N-2) \sum_{a<b}^{\{N\}} \epsilon_{disp}^{(3)}(ab). \qquad (30)$$

III. Results of calculations for Be_N and Li_N clusters

The interaction energy and its many-body partition for Be_N and $Li_N(N = 2$ to 4) were calculated in[8] by the SCF method and by the Møller-Plesset perturbation theory up to the fourth order (MP4), in the frozen core approximation. The calculations were carried out using the triply split valence basis set [6-311+G(3df)].

In Table I, the calculated m-body energy decomposition (6) of the interaction energy of Be_N and Li_N clusters is presented. For an estimation of the convergence of the m-body expansion, the latter is often expressed as the ratios of m-body to 2-body energies

$$E_{int}(N) = |E_2(N)| \Big(\alpha_2(2, N) + (\alpha_3(2, N) + \ldots + \alpha_N(2, N) \Big), \qquad (31)$$

where

$$\alpha_m(2, N) = \frac{E_m(N)}{|E_2(N)|}. \qquad (32)$$

From Table I, the following decompositions (31) for Be_N clusters are obtained

$$E_{int}(Be_3) = |E_2(Be_3)|(-1 - 53.9) \qquad (33)$$

$$E_{int}(Be_4) = |E_2(Be_4)|(1 - 6.69 + 1.03). \qquad (34)$$

Table I

Many-body energy decomposition of the interaction energy of Be_N and Li_N clusters, calculated at the MP4 level[8], in $a.u.$.

A_N	$E_{int}(N) = -E_{bind}$	$E_2(N) = E_{add}$	$E_3(N)$	$E_4(N)$	$E_{nonadd} = \sum\limits_{m=3}^{4} E_m(N)$
Be_2	-0.00289	-0.00289			
Be_3	-0.04115	-0.00075	-0.04040		-0.04040
Be_4	-0.14672	0.03150	-0.21080	0.03258	-017822
Li_2	-0.03509	-0.03509			
Li_3	-0.04842	-0.08846	0.04004		0.04004
Li_4	-0.10166	-0.16342	0.17882	-0.11706	0.06176

It is evident that for Be_3 and Be_4 clusters the 3-body energy is not only the dominant term of the m-body decomposition but it is the single stabilization factor. The extremely large magnitude of $\alpha_3(2,3)$ for Be_3 does not follow from physics of many-body interactions. It is due to the almost zero value of $E_2(Be_3)$ because the equilibrium distance in the Be_3 triangle is located in the vicinity of the intersection of the Be_2 potential curve and the abscissa axis. The fact that the Be_3 and Be_4 clusters are stabilized by the three-body interactions and the flatness of the two-body potential explain the decrement in the interatomic distances as the size of the cluster increases[22]: the attractive three-body forces become larger with decreasing Be-Be distance while the two-body forces undergo small changes until the Be-Be distance becomes smaller than $4a_0$ (a_0 is the Bohr radius).

For Li_N clusters the decompositions (31) are the following:

$$E_{int}(Li_3) = |E_2(Li_3)|(-1 + 0.45) \qquad (35)$$
$$E_{int}(Li_4) = |E_2(Li_4)|(-1 + 1.03 - 0.74) \qquad (36)$$

The physical picture is opposite to the beryllium cluster case. The 2-body interaction energies are large and stabilizing while the 3-body forces play a destabilizing role. The attractive 4-body forces are decisive for formation the Li_4 cluster since the 2-body attraction in the Li_4 is smaller than the 3-body repulsion. It means that all terms in the m-body decomposition of the Li_4 interaction energy are important. The same was demonstrated in the accurate calculation of the He_4 and Ne_4 clusters by Wells and Wilson[23,24].

The calculations at the SCF and the MP4 levels, performed in[8] allow to estimate the role of the electron correlation in the cluster formation and in many-body interactions.

It is well known [25,5] that in the SCF approximation the Be_N clusters are stable only for $N \geq 4$. The inclusion of the electron correlation makes stable the $Be_2(E_b^{MP4} = 1.8$ kcal/mol) and the $Be_3(E_b^{MP4} = 25.8$ kcal/mol) clusters and increases the binding energy of the Be_4 cluster from $E_b^{SCF} = 41.9$ kcal/mol to $E_b^{MP4} = 92.0$ kcal/mol. Although for Li_N clusters, the inclusion of the electron correlation does not lead to qualitative changes, the quantitative changes even larger then in the Be_N case: the ratio E_b^{MP4}/E_b^{SCF} is equal to 5.65 (Li_2), 2.55 (Li_3), and 3.26(Li_4).

For calculations at the MP4 level, the correlation contributions to the m-body interaction energy, according to Eq. (24), is equal to

$$\Delta E_m^{corr}(N) = E_m^{MP4}(N) - E_m^{SCF}(N). \tag{37}$$

Table II

Relative contributions of electron correlation into many-body interaction energies for Be_N and Li_N clusters; β_m and γ_m are defined by Eqs. (38) and (39), respectively.

A_N	β_3, %	γ_3, %	β_4, %	γ_4, %
Be_3	40	28		
Be_4	55	36	171	63
Li_3	63	168		
Li_4	122	549	93	1280

The relative correlation contribution is defined as

$$\beta_m(N) = \left| \frac{\Delta E_m^{corr}(N)}{E_m^{MP4}(N)} \right|. \tag{38}$$

In the cases when the correlation contributions are much larger than E_m^{SCF}, as for Li_4 clusters, $\beta_m(N)$ will be close to 1 and it is more instructive to use the relative correlation contribution to the E_m^{SCF},

$$\gamma_m(N) = \left| \frac{\Delta E_m^{corr}(N)}{E_m^{SCF}(N)} \right| \tag{39}$$

In Table II we present for comparison both kinds of correlation contributions. As follows from these data, the contributions of the electron correlation is essential for both Be_N and Li_N cluster. In particular for Li_4 cluster its magnitude is surprisingly large.

As was shown by Habitz et $al.$ [26] and confirmed recently in more precise calculations [27,28], for finding the nonadditive contribution to the interaction energy of $(H_2O)_N$ clusters it is enough to perform calculations at the SCF level. The electron correlation corrections to many-body interaction energies of water clusters are very small. For example, according to the data[27], $\gamma_3((H_2O)_3)=4\%$ and becomes even smaller, $\sim 1\%$, if we use the data of Ref. [28]. For small metal clusters, the situation is contrary to the $(H_2O)_N$ case, nonadditive interactions in Be_N and Li_N clusters cannot be studied without taking into account the electron correlation. It is interesting to note that the contributions of the electron correlation to nonaddittive energies of rare-gas atom clusters is also large[29,30]: $\gamma_3(He_3) =49\%$ for the D_{3h} symmetry conformation and 100% for the linear geometry[29].

IV. Ab $initio$ model potentials for small metal clusters

In this section we discuss model potentials for small metal clusters with parameters fitted to ab $initio$ calculated potential surfaces. We named such potentials as ab $initio$ model potentials [31]. This approach was first elaborated by Clementi and coworkers [32-34] and used for the Monte-Carlo simulation of biological systems in liquid water [35,36].

As was shown in previous section, the many-body forces play a crucial role in metal cluster stability. So, a model potential must include many-body terms, at least 3- and, sometimes, 4-body ones. For clusters of larger size, the fitted parameters in these terms will include ("absorb") many-body effects of higher orders.

The model potential composed of 2-, 3-, and 4-body terms was elaborated in[31,37] for study of the Ag_N clusters. The same form of potential can be recommended for other small metal clusters with atoms having only s-type valence electrons. The atoms with closed electronic shells and the ns valence subshell do not possess any multipole moments. In this case, the electrostatic and induction interactions contribute only in the overlap region and decrease exponentially with the interatomic distance. So, they can be included into exchange terms. This allows to represent the m-body interaction energy as a sum of the exchange and dispersion terms:

$$V = \sum_{m=2}^{4} V_m = \sum_{m=2}^{4} \left(V_m^{exch} + V_m^{disp} \right), \tag{40}$$

$$V_2^{exch} = \sum_{a<b}^{\{N\}} A_2 \exp(-\alpha_2 r_{ab}), \tag{41}$$

$$V_2^{disp} = -\sum_{a<b}^{\{N\}} \left[C_6 \frac{D_6(r_{ab})}{r_{ab}^6} + C_8 \frac{D_8(r_{ab})}{r_{ab}^8} + C_{10} \frac{D_{10}(r_{ab})}{r_{ab}^{10}} \right], \tag{42}$$

$$V_3^{exch} = \sum_{a<b<c}^{\{N\}} A_3 \exp\left(-\alpha_3 \sum_{a<b}^{\{abc\}} r_{ab} \right), \tag{43}$$

$$V_3^{disp} = \sum_{a<b<c}^{\{N\}} C_9 \frac{D_3(r_{ab})D_3(r_{ac})D_3(r_{bc})}{r_{ab}^3 r_{ac}^3 r_{bc}^3} (1 + 3\cos\Theta_a \cos\Theta_b \cos\Theta_c), \tag{44}$$

$$V_4^{exch} = \sum_{a<b<c<d}^{\{N\}} A_4 \exp(-\alpha_4 \sum_{a<b}^{\{abcd\}} r_{ab}), \tag{45}$$

$$V_4^{disp} = \sum_{a<b<c<d}^{\{N\}} C_{12} \Big[f(abcd)D(abcd) + f(abdc)D(abdc)$$
$$+ f(acbd)D(acbd) \Big], \tag{46}$$

$$\begin{aligned} f(abcd) = & (r_{ab}r_{bc}r_{cd}r_{da})^{-3}[-1 + (\mathbf{u}_{ab} \cdot \mathbf{u}_{bc})^2 + (\mathbf{u}_{ab} \cdot \mathbf{u}_{cd})^2 \\ & + (\mathbf{u}_{ab} \cdot \mathbf{u}_{da})^2 + (\mathbf{u}_{bc} \cdot \mathbf{u}_{cd})^2 + (\mathbf{u}_{bc} \cdot \mathbf{u}_{da})^2 \\ & + (\mathbf{u}_{cd} \cdot \mathbf{u}_{da})^2 - 3(\mathbf{u}_{ab} \cdot \mathbf{u}_{bc})(\mathbf{u}_{bc} \cdot \mathbf{u}_{cd})(\mathbf{u}_{cd} \cdot \mathbf{u}_{ab}) \\ & - 3(\mathbf{u}_{ab} \cdot \mathbf{u}_{bc})(\mathbf{u}_{bc} \cdot \mathbf{u}_{da})(\mathbf{u}_{da} \cdot \mathbf{u}_{ab}) \\ & - 3(\mathbf{u}_{ab} \cdot \mathbf{u}_{cd})(\mathbf{u}_{cd} \cdot \mathbf{u}_{4a})(\mathbf{u}_{da} \cdot \mathbf{u}_{ab}) \\ & - 3(\mathbf{u}_{bc} \cdot \mathbf{u}_{cd})(\mathbf{u}_{cd} \cdot \mathbf{u}_{da})(\mathbf{u}_{da} \cdot \mathbf{u}_{bc}) \\ & + 9(\mathbf{u}_{ab} \cdot \mathbf{u}_{bc})(\mathbf{u}_{bc} \cdot \mathbf{u}_{cd})(\mathbf{u}_{cd} \cdot \mathbf{u}_{da})(\mathbf{u}_{da} \cdot \mathbf{u}_{ab})], \end{aligned} \tag{47}$$

$\mathbf{u}_{ab}$ is the unit vector in the direction from atom a to atom b. The damping functions were taken in the form:

$$D_n(r_{ab}) = \begin{cases} \exp\left[-\mu_n(\beta_n \frac{r_o}{r_{ab}} - 1)^2 \right] & r_{ab} \le \beta_n r_o \\ 1 & r_{ab} > \beta_n r_o \end{cases} \tag{48}$$

where μ_n and β_n are free parameters and r_0 is the equilibrium distance for the dimer. In some cases it is useful to construct a two-exponential exchange potentials, which can change sign for certain geometries.

The expression of the three-body exchange energy was proposed in[38,39]. For the four-body exchange energy we used a similar term. The analytical form of the dispersion terms was taken from perturbation theory up to fourth order. For the two-body dispersion energy, the dipole-dipole (r^{-6}), dipole-quadrupole

(r^{-8}), and dipole- octopole plus quadrupole-quadrupole (r^{-10}) interactions were taken into account. For the three- body dispersion energy, we used the well-known Axilrod-Teller expression[40], whereas for the four- body dispersion energy the expression derived by Bade [41] was incorpored. The angular part of the V_4^{disp}, Eq. (47), contains many terms which have a strong tendency to cancel each other because of the nature of their angular dependence. So, in some cases it is sufficient to use only V_4^{exch}.

We included to all dispersion terms the damping function $D_n(r_{ab})$. The reason for this is the following. At intermediate distances, the expressions for the dispersion energy given by standard perturbation theory are not valid. At these distances, the exchange effects must be taken into account. Also, the multipole expansion is not valid at distances where the overlap of the wave functions of interacting atoms becomes important [1]. As was shown in Refs. [42-44], the corrections are large enough. For V_2^{disp}, the dipole-dipole expression, C_6/r_{ab}^6, overestimates the SAPT values calculated in[42] for the $H - H$ system by 2.8 times at $r = 4a_0$ and by 1.6 times at $r = 5a_0$. For the H_3 trimer, in the equilateral triangle structure with sides equal to $5a_0$, the Axilrod-Teller energy is more than two times larger than in calculations taking into account the overlap effect [44]. The damping functions have to improve the behavior of dispersion terms at intermediate and short distances.

In[31,37], the two-step optimization procedure was elaborated for a construction of the *ab initio* model potential for the Ag_6 cluster. On the first step, the parameters in the 2-body, V_2, and the 3-body, V_3, potentials are optimized separately, using for V_2 the calculated *ab initio* potential curve of Ag_2 and for V_3 the calculated *ab initio* potential surfaces of Ag_3. On the second step, the sum $V_3 + V_4$ is fitted to the nonadditive *ab initio* energy $E_{nonadd}(Ag_N)$,

$$E_{nonadd}(Ag_N) = E_{int}(Ag_N) - V_2(Ag_N), \qquad (49)$$

For V_3, the parameters found at the first step are used as the initial set. In the fit of $V_3 + V_4$, for the better reproduction of the three-body energy it was found more effective to add to the $E_{nonadd}(Ag_N)$, the $E_3(Ag_3)$ for triangles not presented in the Ag_N geometry.

The *ab initio* model potential for Ag_6 was used in molecular dynamics (MD) simulation of the thermal behavior of different isomers of Ag_6 in our studies[31,37]. The advantages of using such kind of potential in MD simulation studies are related to the reliability of the quantitative predictions obtained, due to the use of an accurate model potential at the electron correlation level and to the extended length of the simulation time (comparing with other *ab initio* MD approaches) during which a good statistics is collected.

The *ab initio* model potentials is useful not only for a MD simulation. When the model potential is found, we obtain the explicit expressions for the

interaction energy and its many-body decomposition via exchange and disper-
sion energies. We have possibility to study the dependence of all these physical
quantities via atom-atom distances and cluster geometry. We illustrate this
on the example of the *ab initio* model potential for the Be_3 cluster, obtained
in[45].

In a three-atom clusters, the nonadditive effects are completely described
by the 3-body forces,

$$V(Be_3) = \sum_{a<b} V_{ab} + V_{abc} = V_2^{exch} + V_2^{disp} + V_3^{exch} + V_3^{disp}. \qquad (50)$$

The analytical expressions for all terms in Eq. (50), except V_3^{exch}, were used
as for Ag_N, see Eqs. (41), (42) and (44). For 3-body exchange potential, a
more sophisticated form was used. It is expressed in symmetry coordinates
(Q_1, Q_2, Q_3) originally developed for elemental solids by Murrel and coworkers
[47,48]. These coordinates are related to the three sides of a triangle by

$$
\begin{aligned}
Q_1 &= \frac{1}{\sqrt{3}}(r_{ab} + r_{ac} + r_{ca}), \\
Q_2 &= \frac{1}{\sqrt{2}}(r_{bc} - r_{ca}), \\
Q_3 &= \frac{1}{\sqrt{6}}(r_{ab} - r_{bc} - r_{ca}).
\end{aligned}
\qquad (51)
$$

The 3-body exchange potential contains 16 parameters and has the follow-
ing form:

$$
\begin{aligned}
V_3^{exch}(Q_1, Q_2, Q_3) &= [(b_2 + b_3 Q_1 + b_4 Q_1^2) + \\
&(Q_2^2 + Q_3^2)(b_5 + b_6 Q_1 + b_7 Q_1^2) + \\
&(Q_3^3 - 3Q_3 Q_2^2)(b_8 + b_9 Q_1 + b_{10} Q_1^2) + \\
&(Q_2^2 + Q_3^2)^2(b_{11} + b_{12} Q_1 + b_{13} Q_1^2) + \\
&(Q_2^2 + Q_3^2)(Q_3^3 - 3Q_3 Q_2^2)(b_{14} + b_{15} Q_1 + b_{16} Q_1^2) \times e^{-b_1 Q_1}. \qquad (52)
\end{aligned}
$$

The parameters of the model potential (52) have been fitted (separately
for V_2 and V_3) to *ab initio* energy surfaces calculated at the MP4 level and
corrected for the basis set superposition error. The parameters of the additive
potential V_2 were fitted to 65 calculated points on the potential curve of Be_2,
the parameters of the 3-body potential V_3 were fitted to the $E_3(Be_3)$ potential
surface with total number of calculated points equal to 108. It is important to
note that in the fitting procedure we find the sum (or difference) of exchange
and dispersion terms for each m-body potentials V_n. This sum is correct for
all distances considered. But we cannot expect the same from the absolute

Table III

Physical contributions to the m-body interaction energies (in $a.u.$) of the Be_3 cluster for different distances in the equilateral triangle geometry, according to the model potential (50).

$r, \overset{\circ}{A}$	V	V_2	V_2^{exch}	V_2^{disp}	V_3	V_3^{exch}	V_3^{disp}
1.8	0.010	0.103	1.251	-1.147	-0.093	-0.221	0.128
2.0	-0.029	0.032	0.791	-0.759	-0.061	-0.174	0.113
2.2	-0.041	0.002	0.501	-0.498	-0.043	-0.126	0.083
2.4	-0.037	-0.007	0.317	-0.324	-0.030	-0.085	0.055
2.6	-0.029	-0.009	0.200	-0.209	-0.020	-0.055	0.034
2.8	-0.020	-0.008	0.127	-0.134	-0.013	-0.034	0.021
3.0	-0.013	-0.006	0.080	-0.086	-0.007	-0.020	0.013
3.2	-0.009	-0.005	0.051	-0.056	-0.004	-0.012	0.008
3.4	-0.006	-0.004	0.032	-0.036	-0.002	-0.007	0.005
3.6	-0.005	-0.004	0.020	-0.024	-0.001	-0.004	0.003
3.8	-0.004	-0.003	0.013	-0.016	0.000	-0.002	0.002
4.0	-0.003	-0.003	0.008	-0.011	0.000	-0.001	0.001

values of exchange and dispersion terms. They can differ from the exact E_m^{exch} and E_m^{disp}, see[48]. However, because of a reliable distance behavior of exchange and dispersion parts of m-body model potentials, the decomposition (50) is useful for a comparative study of the distance dependence of different terms in it and their relative contributions to the binding energy of different cluster isomers.

The dependence of distance of the m-body interaction energies and their physical contributions into the *ab initio* model potential (50) for an equilateral triangle geometry of the Be_3 cluster are presented in Table III. For intermediate and equilibrium distances $|V_2|$ is less or much less than $|V_3|$, however the main contribution to the total exchange, V^{exch}, and dispersion, V^{disp}, energies

$$V^{exch} = V_2^{exch} + V_3^{exch}, \quad V^{disp} = V_2^{disp} + V_3^{disp}, \tag{53}$$

comes from the 2-body interactions. On the other hand, V_2^{exch} and V_2^{disp} have opposite sign (V_2^{exch} is repulsive and V_2^{disp} is attractive potentials) which leads to a compensation.

In the case of the 3-body forces, the physical picture is opposite: V_3^{exch} is attractive and V_3^{disp} is repulsive. It is important to note that for all calculated

distances $|V_3^{exch}| > |V_3^{disp}|$. Thus, in contrary to the Barker approach[49], for the Be_3 cluster the 3-body forces cannot be approximated solely by the Axilrod-Teller term. The reasons for the satisfactory approximation of many-body energy by the Axilrod-Teller term in the bulk phases of the rare gases were discussed by Meath and Aziz[50]. As follows from precise calculations of the 3-body interaction energy in the He_3[29], Ne_3[30] and Ar_3 [20] trimers, both the Axilrod-Teller and the exchange energies are important. Nevertheless, in some studies of many-body interactions, the exchange effects are still neglected and the many-body contribution is approximated by only dispersion terms, for example see [51].

Table IV

The physical contributions to the binding energy of Be_3 and Ar_3 clusters, equilateral triangle geometry.

E, mh	V	V_2	V_2^{exch}	V_2^{disp}	V_3	V_3^{exch}	V_3^{disp}
Be_3, $r_0 = 2.24\mathring{A}$ the model potential (50).	-41.0	-1.0	457	-458	-40.0	-117	77.0
	E_{int}	E_2^{MP4}	$E_2^{exch a)}$	$E_2^{disp a)}$	E_3^{MP4}	$E_3^{exch a)}$	$\epsilon_{disp}^{(30)}$
Ar_3, $r_0 = 3.7\mathring{A}$ SAPT [20,53,54]	-0.339	-0.350	0.305	-0.655	0.0108	-0.0088	0.0196

a) $E_2^{disp} = \epsilon_{disp}^{(20)} + \epsilon_{disp}^{(21)}$, $E_2^{exch} = E_2^{MP4} - E_2^{disp}$, $E_3^{exch} = E_3^{MP4} - \epsilon_{disp}^{(30)}$

The discussion of the Be_3 formation within the scope of m-body forces leads to the conclusion that it is the 3-body forces that stabilize the Be_3 cluster and it is right. The attractive part of the 3-body potential is V_3^{exch} and we could make a conclusion that it is the exchange 3-body forces that stabilize the Be_3 cluster. But this conclusion would be wrong. We must consider all physical contributions to the model potential (50). In total, we have two contributions to the repulsive part: V_2^{exch} and V_3^{disp}, and two contributions to the attractive part: V_2^{disp} and V_3^{exch} [52]. Hence, we should conclude that there are two sources of the binding in the Be_3 cluster: the additive (2-body) dispersion forces and the nonadditive (3-body) exchange forces.

In Table IV, the results of the decomposition of the model potential (50) for the equilibrium triangle geometry of the Be_3 cluster is presented. For comparison, the SAPT results for the Ar_3 cluster are also included. As follows from Table IV, the main contribution to the Be_3 binding energy give the 2-body dispersion interactions although about 20% of the total attraction interaction comes from the 3-body exchange interactions (according to the SAPT calculations, see[48], E_3^{exch} contributes 35% to the total attraction energy). In the Ar_3 cluster, E_3^{exch} contributes only 1.3% to the total attraction energy. So, the Ar_3 is a pure van der Waals molecule while the binding in the Be_3 cluster has a mixed nature: it is provided by the additive local van der Waals forces and the nonadditive delocalized exchange forces. These kind of forces have to be responsible for the formation of more large Be_N clusters. The binding energy for the Be_3 cluster is equal to 41.2 mh=25.8 kcal/mol. This is not much less than in some covalent molecules. In the Be_4 cluster the binding energy becomes even larger, 92.0 kcal/mol[8], as in tightly bound covalent molecules. In spite of that, in the Be_N case (as in the case of rare-gas atom clusters) we cannot speak about the covalent bonding because the latter means that the formation of a bond is caused by the 2-body exchange interaction, while in the Be systems, the 2-body exchange interactions are always repulsive.

References

1. I. G. Kaplan, Theory of Molecular Interactions, Elsevier, Amsterdam 1986.

2. H. B. Casimir and D. Polder, *Phys. Rev.* **73**, 360 (1948).

3. H. Margenau and N. R. Kestner, Theory of Intermolecular Forces, Pergamon, New York, 1971.

4. V. Heine, I.G. Robertson, and M.C. Payne, *Phil. Trans. Roy. Soc., London* **A334**, 393 (1991).

5. O. Novaro and W. Kołos, *J. Chem. Phys.* **67**, 5066 (1977).

6. J. García-Prieto, W.L. Feng, and O. Novaro, *Surf. Sci.* **147**, 555 (1984).

7. I.G. Kaplan, R. Santamaría, and O. Novaro, *Mol. Phys.* **84**, 105 (1995).

8. I. G. Kaplan, J. Hernández-Cobos, I. Ortega-Blake, and O. Novaro *Phys. Rev. A***53**, 2493 (1996).

9. I.G. Kaplan and O.B. Rodimova, *Dokl. AN SSSR* **265**, 1179 (1982).

10. W.J. Meath and R.A. Aziz, *Mol. Phys.* **52**, 225 (1984).

11. T.R. Horn, R.B. Gerber, J.J. Valentini, and M.A. Ratner, *J. Chem. Phys.* **94**, 6728 (1991).

12. A.E. Carlsson, in Solid State Physics (Eds. H. Ehrenreich and D. Turnbull, Academic: New York) **43**, 1 (1990).

13. I. G. Kaplan, R. Santamaría, and O. Novaro, *Int. J. Quantum Chem.* **55**, 237 (1995).

14. T. Cwiok, B. Jeziorski, W. Koĺos, R. Moszynski, and K. Szalewicz, *J. Mol. Structure (Theochem)* **307**, 135 (1994).

15. B. Jeziorski, R. Moszynski, and K. Szalewicz, *Chem. Rev.* **94**, 1887 (1994).

16. G. Chaĺasiński and M.M. Szcześniak, *Chem. Rev.* **94**, 1793 (1994).

17. We denoted by the same notation (17) the energies for dimers which cannot be nonadditive. It means that the energy becomes nonadditive for system with number of monomers ≥ 3.

18. I. G. Kaplan, CAM-94 Physics Meeting, AIP Conference Proceedings 342, Woodbury, New York, 1995, p. 154.

19. P.O. Löwdin, *Adv. Chem. Phys.* **2**, 207 (1959).

20. G. Chaĺasiński, M.M. Szcześniak, and S. M. Cybulski, *J. Chem. Phys.* **92**, 2481 (1990).

21. M. M. Szcześniak, G. Chaĺasiński, and P. Piecuch, *J. Chem. Phys.* **99**, 6732 (1993).

22. The equilibrium Be-Be distance is decreasing from 4.9 a_0 in Be_2 and 4.2 a_0 in Be_3 to 3.9 a_0 in Be_4, see Table I in[8].

23. B. H. Wells and S. Wilson, *Mol. Phys.* **65**, 1363 (1988).

24. B. H. Wells and S. Wilson, *Mol. Phys.* **66**, 457 (1989).

25. W. Koĺos, F. Nieves, and O. Novaro, *Chem. Phys. Lett.* **41**, 431 (1976).

26. P. Habitz, P. Bagus, P. Siegbahn, and E. Clementi, *Int. J. Quantum Chem.* **23**, 1803 (1983).

27. G. Chaĺasiński, M.M. Szcześniak, P. Cieplak, and S. Scheiner, *J. Chem. Phys.* **94**, 2873 (1991).

28. W. Klopper, M. Schutz, H. Luthi, and S. Leutwyler, *J. Chem. Phys.* **103**, 1 (1995).

29. B. H. Wells and S. Wilson, *Mol. Phys.* **55**, 199 (1985).

30. B. H. Wells and S. Wilson, *Mol. Phys.* **57**, 21 (1986).

31. I. G. Kaplan, I. Garzón, R. Santamaria, B. S. Vaisberg, and O. Novaro, *J. Mol. Structure (Theochem)* **398-399**, 333 (1997).

32. H. Popkie, M. Kistenmacher and F. Clementi, *J. Chem. Phys.* **59**, 1325 (1973).

33. E. Clementi, F. Cavalone and R. Scordamaglia, *J. Amer. Chem. Soc.* **99**, 5531 (1977).

34. G. Corongiu and E. Clementi, *Gazzeta Chimica Italiana,* **108**, 273 (1978).

35. E. Clementi and G. Corongiu, *Int. J. Quantum Chem.* **16**, 897 (1979).

36. U. Niesar, G. Corongiu, E. Clementi, G. R. Kneller and D. K. Bhattacharya, *J. Phys. Chem.* **94**, 7949 (1990).

37. I. L. Garzón, I. G. Kaplan, R. Santamaría, B. S. Vaisberg and O. Novaro, *Z. Phys. D* **40**, 202 (1997).

38. L. Bruch and I. G. Mc. Gee, *J. Chem. Phys.* **59**, 409 (1973).

39. L. Bruch, E. Blaisten-Barojas, and O. Novaro, *J. Chem. Phys.* **67**, 4701 (1977).

40. B.M. Axilrod and E. Teller, *J. Chem. Phys.* **11**, 299 (1943) .

41. W. L. Bade, *J. Chem. Phys.* **28**, 282 (1958).

42. J.N. Murrell and G. Shaw, *J. Chem. Phys.* **49**, 4731 (1968).

43. M. Kreek and M. J. Meath, *J. Chem. Phys.* **50**, 2289 (1969).

44. S. F. O'Shea and M. J. Meath, *Mol. Phys.* **28**, 1431 (1974); **31**, 515 (1976).

45. J. Hernández-Cobos, I. G. Kaplan, and J. Murrel, *Mol. Phys.* **92**, N6 (1997).

46. J.N. Murrell and R.E. Mottram, *Mol. Phys.* **69**, 571 (1990).

47. A.K. Al-Derzi, R.L. Johnston, J.N. Murrell, and J.A. Rodríguez-Ruíz, *Mol. Phys.* **73**, 265 (1991).

48. I. G. Kaplan, *Polish J. Chem.,* (in press).

49. J. A. Barker, *Mol. Phys.* **57**, 755 (1986); **60**, 887 (1987).

50. W.J. Meath and R.A. Aziz, *Mol. Phys.* **52**, 225 (1984).

51. C. A. Parish, and D. E. Dykstra *J. Chem. Phys.* **98**, 437 (1993); **101**, 7618 (1994).

52. Note that the values of V_2^{disp} and V_3^{disp} do not coincide with the real dispersion energies not only because they contain fitting parameters, but also because of the damping function corrections. The latter take into account the influence of exchange effects.

53. M.M. Szcześniak and G. Chałasiński, *J. Mol. Structure (Theochem)* **261**, 37 (1992).

54. G. Chałasiński, M.M. Szcześniak and R. A. Kendall, *J. Chem. Phys.* **101**, 8860 (1994)

Distributed Gaussian basis sets in correlation energy studies: the second order correlation energy for the ground state of the hydrogen molecule

D. Moncrieff[†] and S. Wilson[‡]

[†] *Supercomputer Computations Research Institute,*
Florida State University,
Tallahassee, FL 32306, U.S.A.
[‡] *Rutherford Appleton Laboratory,*
Chilton, Oxfordshire OX11 0QX, England

Abstract

The use of distributed basis sets of s-type Gaussian functions in electron correlation energy studies is investigated for the ground state of the hydrogen molecule at its equilibrium nuclear geometry. Empirical schemes are developed both to generate the exponents defining the basis functions and to define their distribution in space. The matrix Hartree-Fock reference energy obtained with the largest distributed basis set developed in this work is in error by less than ~ 0.1 μHartree. The second-order many-body perturbation theory correlation energy component is determined and, for the largest of the distributed basis sets studied in the present work, is in error by ~ 0.6 mHartree. Our previous study of the hydrogen molecule ground state has demonstrated that the error in the matrix Hartree-Fock and second-order correlation energies can be reduced to ~ 3 μHartree and ~ 0.15 mHartree, respectively, by using a systematically generated sequence of atom-centred, even-tempered basis sets containing functions of s, p, d and f symmetry.

Contents
1. Introduction
2. Basis set development
   2.1 Basis subsets
   2.2 Distribution of basis subsets

1   Introduction

The aim of this paper is ascertain whether it is possible to determine the ground
state second-order correlation energy of the hydrogen molecule to sub-millihartree
accuracy using a basis set containing only s-type Gaussian functions with expo-
nents and distribution determined by an empirical, but physically motivated,
procedure.

   Almost all contemporary *ab initio* molecular electronic structure calculations
employ basis sets of Gaussian-type functions in a pragmatic approach in which no
error bounds are determined but the accuracy of a calculation is assessed by com-
parison with quantities derived from experiment[1] [2]. In this quasi-empirical[3]
approach each basis set is calibrated[4] for the treatment of a particular range of
atoms, for a particular range of properties, and for a particular range of methods.
Molecular basis sets are almost invariably constructed from atomic basis sets. In
1960, Nesbet[5] pointed out that molecular basis sets containing only basis sets
necessary to reach to atomic Hartree-Fock limit, the isotropic basis set, cannot
possibly account for polarization in molecular interactions. Two approaches to
the problem of constructing molecular basis sets can be identified:

> *i)* the addition of atom-centred polarization functions to the atomic
> basis sets,
> *ii)* the addition of off-centre functions of the same symmetry as
> the atomic Hartree-Fock basis set.

In the early sixties, Reeves et al[6]−[8] established important elements of current
"mainstream" usage of Gaussian basis sets. They concluded that[9] *no significant
advantage was gained by letting the basis functions float away from the nuclear
centres.* These conclusions were drawn from matrix Hartree-Fock calculations
using small basis sets. Today, it is recognized that large basis sets are required
for accurate studies particularly when the effects of electron correlation are con-
sidered. Calculations using in excess of 10^3 basis functions can be carried out on
a present day workstation and calculations using basis sets of a size approaching
10^4 can be seriously contemplated. The "direct" algorithms[10] avoid the need to
store integrals over two-electron integrals and thereby facilitate the use of such
large basis sets. It is, therefore, timely to consider approaches *i)* and *ii)* in the

light of recent algorithmic and technical developments. In the present work approach *ii)* is considered. Approach *i)* has been elsewhere[11]. It should be noted that these two approaches are not mutually exclusive[11].

Building on atomic studies using even-tempered basis sets, universal basis sets and systematic sequences of even-tempered basis sets, recent work has shown that molecular basis sets can be systematically developed until the error associated with basis set truncation is less that some required tolerance. The approach has been applied first to diatomic molecules within the Hartree-Fock formalism[12] [13] [14] [15] [16] [17] where finite difference[18] [19] [20] [21] and finite element[22] [23] [24] [25] calculations provide benchmarks against which the results of finite basis set studies can be measured and then to polyatomic molecules and in calculations which take account of electron correlation effects by means of second order perturbation theory. The basis sets employed in these calculations are even-tempered and distributed, that is they contain functions centred not only on the atomic nuclei but also on the midpoints of the line segments between these nuclei and at other points. Functions centred on the bond centres were found to be very effective in approaching the Hartree-Fock limit but somewhat less effective in recovering correlation effects.

The concept of the distributed basis set has been introduced. For the hydrogen molecular ion a total electronic energy of sub-μHartree accuracy has been determined by employing a distributed basis set of s-type Gaussian functions in three different approaches:- *(i)* based on a physically motivated distribution of the functions along the internuclear axis[26] [27] [28] [29], *(ii)* using a generalization of the Gaussian cell model[30] [31] [32] of Haines *et al*[33], and *(iii)* by means of a distribution generated by exploiting a Laplace transform[34] [35].

The exact Hartree-Fock energy for the ground state of the hydrogen molecule with a nuclear separation of 1.4 bohr is -1.13362957 Hartree[36]. An estimate of the exact second order correlation energy component at the same geometry is -0.033877731 Hartree[11]. Kolos and Wolniewicz[37] find the exact non-relativistic electronic energy for the ground state of the hydrogen molecule at a nuclear separation of 1.4 bohr to be -1.17447 Hartree so that the exact electron correlation energy is -0.04084 Hartree. The exact second order energy corresponds to $\sim 83\%$ of the exact electron correlation energy and is in error by -6.96 mHartree.

Traditionally, electron correlation in diatomic molecules in general and the hydrogen molecule in particular are analyzed in terms of longitudinal, axial and angular correlation effects[38]. Qualitatively, longitudinal correlation in the hydrogen molecule ground state describes the tendency of the two electrons to assume positions at the opposite ends of the internuclear axis. Axial correlation arises from the tendency for one electron to be far from the internuclear axis when the other is close. The term angular correlation describes the tendency for the two electrons to adopt a configuration which increases the angle between the perpendiculars drawn from the electrons to the internuclear axis when viewed along

the internuclear axis. The qualitative concepts of longitudinal, axial and angular correlation effects provide a physical motivation for the spatial distribution of the basis set.

2 Basis set development

2.1 Basis subsets

The total distributed molecular basis set, χ, is constructed from M basis subsets, χ_p,

$$\chi = \prod_{p=1}^{M} \left[\chi_p \oplus \right] \tag{1}$$

The Gaussian functions which comprise the basis subset χ_p are centred on the point labelled p.

$$\chi_p = \left\{ \chi_p^{(k)}; k = 1, 2, ..., N \right\} \tag{2}$$

where, in this work, $\chi_p^{(k)}$ will be taken to be an s-type Gaussian function

$$\chi_p^{(k)}(\mathbf{r}) = \left(\frac{2\zeta_k}{\pi} \right)^{\frac{3}{4}} \exp \left(-\zeta_k |\mathbf{r} - \mathbf{r}_p|^2 \right) \tag{3}$$

where ζ_k is an exponent.

Off-atom functions effectively include higher harmonics on the atom. Partial wave expansions of an off-centre $1s$-type Gaussian function have been discussed, for example, by Christoffersen et al[40] and by Kaufmann and Baumeister[41].

Consider the expansion about the origin of the coordinate system of a simple Gaussian function. We introduce a modified form of the Rayleigh expansion[42]

$$\exp \left(\mathbf{r}_1 \cdot \mathbf{r}_2 \right) = \sum_{\ell=0}^{\infty} (2\ell + 1) \; i_\ell (r_1 r_2) \; P_\ell(\cos \gamma) \tag{4}$$

in which $i_\ell(x)$ is a modified Bessel function and $P_\ell(\cos \gamma)$ is a Legendre polynomial of order ℓ. γ is the angle between the directions $\mathbf{r}_1$ and $\mathbf{r}_2$. Using the expansion (4) in an s-type Gaussian function, (3), with $\mathbf{r}_1$ assigned to $\mathbf{r}$ and $\mathbf{r}_2$ assigned to $\mathbf{r}_p$ and ignoring normalization gives

$$\exp \left(-\zeta |\mathbf{r} - \mathbf{r}_p|^2 \right) =$$
$$\exp \left[-\zeta (r^2 + r_p^2) \right] \sum_{\ell=0}^{\infty} (2\ell + 1) \; i_\ell (2\zeta \; r \; r_p) \; P_\ell(\cos \gamma) \tag{5}$$

where the normalization factor has been omitted. The addition theorem for surface spherical harmonics allows equation (5) to be written

$$\exp \left(-\zeta |\mathbf{r} - \mathbf{r}_p|^2 \right) = 4\pi \exp \left[-\zeta (r^2 + r_p^2) \right]$$

$$\sum_{\ell=0}^{\infty} \sum_{m=-\ell}^{+\ell} i_\ell(2\zeta\, r\, r_p)\, Y_{\ell m}\left(\Omega_r\right)\, Y_{\ell m}^*(\Omega_{r_\lambda}) \qquad (6)$$

which is the expansion of an off-centre Gaussian function about the origin.

2.2   Distribution of basis subsets

The Hartree-Fock limit for the ground state of the hydrogen molecule can be achieved in principle by using a basis set of s-type Gaussian functions distributed along the internuclear axis. Such a basis set will be termed an axis basis set.

The atom-centred basis functions, designated (ac), are located on the points

$$\left(0, 0, \pm\frac{1}{2}R\right) \qquad (7)$$

where R is the internuclear distance. In the majority of contemporary molecular electronic structure studies these are the only centres employed in the basis set development. (ac) basis sets capable of describing atomic systems are supplemented by polarization functions in the molecular environment.

The bond-centred basis functions, designated (bc), are located at the point

$$(0, 0, 0) \qquad (8)$$

There has been continued interest in the effectiveness of such functions for more than forty years. Such functions are known to be very effective in matrix Hartree-Fock calculations describing the build up of charge in the bond region. They are not so effective in electron correlation studies.

Two further types of centre on the axis passing through the nuclei are introduced:- the bond-axis functions, designated (ba), lie midway between the (ac) and (bc) centres having the coordinates

$$\left(0, 0, \pm\frac{1}{4}R\right) \qquad (9)$$

and the off-centre functions, designated (oc), lie beyond the internuclear axis having the coordinates

$$\left(0, 0, \pm\left\{\frac{1}{2}R + \frac{1}{m}R\right\}\right) \qquad (10)$$

where m is an integer which is to be determined. The bond axis basis subsets supplement the bond centre subset in describing the build up of charge in the internuclear region. The off-centre basis subsets provide the flexibility required to account for the depletion of charge in the regions beyond the nuclei.

A basis set containing only s type Gaussian functions distributed along the line passing through the nuclei is formally capable of describing the Hartree-Fock ground state of the hydrogen molecule exactly since the occupied orbital is of σ

symmetry. However, the exact description of the second order correlation energy requires the addition of functions centred on points off the straight line passing through the nuclei. Furthermore, if a basis set containing functions centred only on the line through the nuclei but not supporting the Hartree-Fock limit for the ground state energy is supplemented by functions centred on off axis points then not only will an increased fraction of the correlation energy be recovered but the matrix Hartree-Fock energy will be improved. The primary off axis basis functions in the planes perpendicular to the internuclear axis and passing through the atom-centres, designated (oa/ac), are located at the points

$$\left(\pm\frac{R}{n_1}, 0, \pm\frac{1}{2}R\right), \ \left(0, \pm\frac{R}{n_1}, \pm\frac{1}{2}R\right) \tag{11}$$

where n_1 is an integer which is to be determined. The primary off axis basis functions in the planes perpendicular to the internuclear axis and passing through the bond-centre, designated (oa/bc), are located at the points

$$\left(\pm\frac{R}{n_1'}, 0, 0\right), \ \left(0, \pm\frac{R}{n_1'}, 0\right) \tag{12}$$

where n_1' is another integer to be determined. The primary off axis basis functions in the planes perpendicular to the internuclear axis and passing through the bond-axis, designated (oa/ba), are located at the points

$$\left(\pm\frac{R}{n_1''}, 0, \pm\frac{1}{4}R\right), \ \left(0, \pm\frac{R}{n_1''}, \pm\frac{1}{4}R\right) \tag{13}$$

where the integer n_1'' is to be determined. The secondary off axis basis functions in the planes perpendicular to the internuclear axis and passing through the atom-centres, designated (oa'/ac), are located at the points

$$\left(\pm\frac{R}{n_2\sqrt{2}}, \pm\frac{R}{n_2\sqrt{2}}, \pm\frac{1}{2}R\right) \tag{14}$$

where n_2 is an integer to be determined. The secondary off axis basis functions in the planes perpendicular to the internuclear axis and passing through the bond-centre, designated (oa'/bc), are located at the points

$$\left(\pm\frac{R}{n_2'\sqrt{2}}, \pm\frac{R}{n_2'\sqrt{2}}, 0\right) \tag{15}$$

where n_2' is again an integer to be determined.

2.3   Exponents for basis subsets

Now it has been observed that exponents which have been carefully optimized for atoms often form a good approximation to a geometric progression

$$\zeta_k = \alpha\beta^k, \ \beta > 1, \ k = 1, 2, ..., N \tag{16}$$

Conversely, if it is assumed that the exponents do form a geometric progression and the parameters α and β are optimized for atoms then there is found to be little lost in accuracy. Basis sets developed in this way are termed even-tempered basis sets (for a discussion see [2]) and open up the possibility of constructing the large and flexible basis sets that are inevitably required for calculations of high precision.

As the number of basis functions, N, is increased we require that our basis set approach a complete set. The generalized Müntz-Szász theorem[43] [44] [45] can be used to show that this is not the case if α and β are held fixed as N is increased. One possible choice which does lead to a complete set as $N \to \infty$ is

$$\begin{aligned} \alpha &\to 0 \\ \beta &\to 1 \\ \beta^N &\to \infty \end{aligned} \tag{17}$$

and these limits can be guaranteed by generating successive basis sets according to the following empirical recursions [2]

$$\alpha_N = \left[\frac{\beta_N - 1}{\beta_{N-1} - 1} \right]^a \alpha_{N-1}, \ a > 0 \tag{18}$$

$$\ln \beta_N = \left[\frac{N}{N-1} \right]^b \ln \beta_{N-1}, \ -1 < b < 0 \tag{19}$$

However, it should be emphasized that when these recursions are applied to a set of s-type Gaussian functions centred on some point, they generate a complete set of functions of s-symmetry, which should be supplemented by complete sets of functions of higher symmetry centred on the same point and/or complete sets of functions centred on other points.

2.4   Control of computational linear dependence

Near computational linear dependence in the basis set was monitored in all calculations reported in this paper by diagonalizing the overlap matrix. A $30s$ basis subset was centred on each of the points defining a particular distributed basis set. Diffuse basis functions were deleted from off-atom basis sets until the smallest eigenvalue of the overlap matrix, ϵ, satisfied the condition $\epsilon < 10^{-7}$. So, for example, the basis set designated $30s \ ac; 28s \ oa(ac) \ [n_1 = 5]$ which arises in

Table 1 consists of a $30s$ subset centred on each of the atoms supplemented by $28s$ subsets, obtained by deleting the two most diffuse functions from the $30s$ set, centred on the eight off axis atom centre, $oa(ac)$, positions defined by (8) with $n_1 = 5$.

3   Results and Discussion

The results of a series of calculations in which off axis basis subsets were added to an axis basis set consisting of only atom-centred basis function are summarized in Table 1. In this Table E_{mHF} denotes the matrix Hartree-Fock energy obtained with the specified basis set. The difference between the energy obtained with a given basis set and the exact Hartree-Fock energy is given in parenthesis. E_2 denotes the second-order many-body perturbation theory electron correlation energy component obtained with a given basis set and the difference between the given value and the estimate of the exact value is given in μHartree in parenthesis.

For the basis set designated $30s$, which can be regarded as a "nearly-saturated", atom-centred basis set, the matrix Hartree-Fock energy is in error by ~ 5 mHartree whilst the error in the second order correlation energy component is more than three times larger at 15 mHartree. The results obtained with this atom centred basis set are taken as a reference with respect to which other results in Table 1 are analyzed. The addition of four sets of off axis basis subsets in the planes perpendicular to the internuclear axis and passing through each of the atomic centres reduces the error in the matrix Hartree-Fock energy by 2264.0 μHartree, when $n_1 = 3$, to ~ 2.8 mHartree, which is 55.5% of the error associated with the reference calculation. The error in the second order correlation energy is reduced by 11500.6 μHartree, when $n_1 = 4$, to ~ 3.9 mHartree or 25.2% of the error in the reference calculation. The error in the second order correlation energy is less than ~ 1.4 times that in the matrix Hartree-Fock energy. Off axis basis subsets are more effective in recovering correlation effects than are the axis basis subsets. This is a reflection of the relative importance of angular correlation effects.

Table 1

The addition of off axis basis functions in the planes perpendicular to the internuclear axis and passing through the atomic centres to an axis basis set containing only atom-centred basis functions. The differences between the calculated and exact energy values are given in parentheses.

Basis set specification	E_{mHF}	E_2
$30s\ ac$	-1.128 542 133 (5087.4)	-0.018 507 185 (15370.546)
$30s\ ac;\ 30s\ oa(ac)\ [n_1 = 1]$	-1.130 015 240 (3614.3)	-0.025 151 756 (8725.975)
$30s\ ac,\ 30s\ oa(ac)\ [n_1 = 2]$	-1.130 765 717 (2863.9)	-0.029 434 182 (4443.549)
$30s\ ac;\ 30s\ oa(ac)\ [n_1 = 3]$	-1.130 806 204 (2823.4)	-0.029 924 482 (3953.249)
$30s\ ac;\ 29s\ oa(ac)\ [n_1 = 4]$	-1.130 803 723 (2825.8)	-0.030 007 764 (3869.967)
$30s\ ac;\ 28s\ oa(ac)\ [n_1 = 5]$	-1.130 753 573 (2876.0)	-0.030 005 973 (3871.758)

The addition of off axis basis functions in the plane perpendicular to the internuclear axis and passing through the bond centre to an axis basis set consisting of both atom-centred and bond-centred basis functions is explored in Table 2. Comparing the errors associated with the $30s\ ac; 30s\ bc$ basis set with those of the $30s\ ac$ set presented in Table 1, it can be seen that the error in the matrix Hartree-Fock energy is reduced by 5013.3 μHartree to only 1.5% of the error measured for the $30s\ ac$ set whereas for the electron correlation energy the error is reduced by only 1474.6 μHartree to 90.4% of the reference value in Table 1. This illustrates the effectiveness of bond centred basis subsets in reducing the errors matrix Hartree-Fock energies but the relative ineffectiveness of such subsets in significantly reducing the errors in calculated correlation energies. The energies presented in Table 2 should be compared with those obtained with the $30s\ ac; 30s\ bc$ basis set which is regarded as a reference in this table. The matrix Hartree-Fock energy is reduced by 65 μHartree on adding four off axis basis subsets in the plane perpendicular to the internuclear axis and passing through the bond centre to the $30s\ ac; 30s\ bc$ basis set. Thus, for $n_1' = 5$, the error in the matrix Hartree-Fock energy is $\sim$ 12.0% of that in the reference energy in Table 2 and 0.2% of the error in the reference energy in Table 1. For the second order correlation energy the error is reduced by 9799.3 μHartree with respect to the reference energy in Table 2 when $n_1' = 4$. The corresponds to 29.5% of the error in the reference in Table 2 and 26.6% of the error in the reference in Table 1. However, the $oa(ac)$ functions are more effective than the $oa(bc)$ in recovery of the correlation energy. The $oa(bc)$ functions are very effective in recovery of

the matrix Hartree-Fock energy, the error being reduced to less than 9 μHartree when $n'_1 = 5$.

Table 2
The addition of off axis basis functions in the plane perpendicular to the internuclear axis and passing through the bond centre to an axis basis set consisting of both atom-centred and bond-centred basis functions. The differences between the calculated and exact energy values are given in parentheses.

Basis set specification	E_{mHF}	E_2
$30s\ ac;\ 30s\ bc$	-1.133 555 451 (74.12)	-0.019 981 777 (13895.954)
$30s\ ac;\ 30s\ bc;\ 30s\ oa(bc)\ [n'_1 = 1]$	-1.133 558 116 (71.45)	-0.025 705 273 (8172.458)
$30s\ ac;\ 30s\ bc;\ 29s\ oa(bc)\ [n'_1 = 2]$	-1.133 579 210 (50.36)	-0.029 259 590 (4618.141)
$30s\ ac;\ 30s\ bc;\ 27s\ oa(bc)\ [n'_1 = 3]$	-1.133 607 768 (21.80)	-0.029 689 320 (4188.411)
$30s\ ac;\ 30s\ bc;\ 27s\ oa(bc)\ [n'_1 = 4]$	-1.133 617 370 (12.20)	-0.029 781 120 (4096.611)
$30s\ ac;\ 30s\ bc;\ 26s\ oa(bc)\ [n'_1 = 5]$	-1.133 620 710 (8.86)	-0.029 264 511 (4613.22)

The addition of off axis basis functions in the planes perpendicular to the internuclear axis and passing through the atomic centres and the bond centre to an axis basis set consisting of both atom-centred and bond-centred basis functions is considered in Table 3. The reference energies with respect to which the results presented in Table 3 should be assessed correspond to the $30s\ ac;\ 30s\ bc$ basis set which is also used as a reference in Table 2. The addition of eight sets of off axis functions in planes passing through the atomic centres is not as effective as the four sets of off axis functions in the plane passing through the bond centre in reducing the error in the matrix Hartree-Fock energy. However, for the second order correlation energy the off axis functions in planes passing through the atomic centres are more effective than the corresponding bond centre functions reducing the error by 11365.1 μHartree when $n'_1 = 4$ to 18.2% of the error in the reference second order correlation energy. Combining the use of off axis atom centre basis subsets with off axis bond centre subsets reduces the error in the matrix Hartree-Fock energy by 66.1 μHartree to $\sim$ 10.8% of the reference value whereas for the second order correlation energy there is a reduction of 12470.2 μHartree or $\sim$ 10.3% of the reference value; an error of $\sim$ 1.4 mHartree, approaching the target accuracy of the present study.

Table 3

The addition of off axis basis functions in the planes perpendicular to the internuclear axis and passing through the atomic centres and the bond centre to an axis basis set consisting of both atom-centred and bond-centred basis functions. The differences between the calculated and exact energy values are given in parentheses.

Basis set specification	E_{mHF}	E_2
$30s\ ac;\ 30s\ bc$	-1.133 555 451 (74.119)	-0.019 981 777 (13895.954)
$30s\ ac;\ 30s\ bc;\ 29s\ oa(ac)\ [n_1 = 3]$	-1.133 590 993 (38.577)	-0.031 265 198 (2612.533)
$30s\ ac;\ 30s\ bc;\ 27s\ oa(ac)\ [n_1 = 4]$	-1.133 592 605 (36.965)	-0.031 346 893 (2530.838)
$30s\ ac;\ 30s\ bc;\ 28s\ oa(ac)\ [n_1 = 4]$ $26s\ oa(bc)\ [n_1' = 4]$	-1.133 621 535 (8.035)	-0.032 451 958 (1425.773)

The effects of adding secondary off axis basis functions are summarized in Table 4. The results obtained with the largest basis set considered in Table 3, $30s\ ac;\ 30s\ bc;\ 28s\ oa(ac)\ [n_1 = 4]\ 26s\ oa(bc)\ [n_1' = 4]$, are used as a reference with respect to which the results presented in Table 4 are analyzed. The addition of secondary off axis basis functions reduces the error in the matrix Hartree-Fock energy to ~ 4 μHartree. For the second order correlation energy the addition of secondary off axis basis subsets reduces the error to ~ 723 μHartree, thereby achieving the target accuracy of the present study.

Table 4

The addition of secondary off axis basis functions in the planes perpendicular to the internuclear axis and passing through the atomic centres and the bond centre to an axis basis set consisting of both atom-centred and bond-centred basis functions. The differences between the calculated and exact energy values are given in parentheses.

Basis set specification	E_{mHF}	E_2
30s ac; 30s bc; 28s oa(ac) $[n_1 = 4]$ 26s oa(bc) $[n_1' = 4]$	-1.133 621 535 (8.035)	-0.032 451 958 (1425.773)
30s ac; 30s bc; 28s oa(ac) $[n_1 = 4]$; 26s oa(bc) $[n_1'' = 4]$; 23s oa'(ac) $[n_2 = 2]$; 23s oa'(bc) $[n_2' = 4]$	-1.133 625 594 (3.976)	-0.033 021 570 (856.161)
30s ac; 30s bc; 28s oa(ac) $[n_1 = 4]$; 26s oa(bc) $[n_1' = 4]$; 23s oa'(ac) $[n_2 = 3]$; 23s oa'(bc) $[n_2' = 4]$	-1.133 625 727 (3.843)	-0.033 154 302 (723.429)
30s ac; 30s bc; 28s oa(ac) $[n_1 = 4]$; 26s oa(bc) $[n_1' = 4]$; 23s oa'(ac) $[n_2 = 4]$; 23s oa'(bc) $[n_2' = 4]$	-1.133 625 373 (4.197)	-0.032 932 991 (944.740)
30s ac; 30s bc; 28s oa(ac) $[m = 4]$; 26s oa(bc) $[m = 4]$; 23s oa'(ac) $[m = 5]$; 23s oa'(bc) $[m = 4]$	-1.133 625 193 (4.377)	-0.032 916 770 (960.961)

In a previous study[27] of the matrix Hartree-Fock description of the hydrogen molecule ground state the addition of basis subsets at the off-centre and the bond axis positions has been found to be beneficial.. In Table 5, it is shown that supplementing the 30s ac; 30s bc; 28s oa(ac) $[n_1 = 4]$; 26s oa(bc) $[n_1' = 4]$; 23s oa'(ac) $[n_2 = 5]$; 23s oa'(bc) $[n_2' = 4]$ by two subsets in the off centre (oc) positions the accuracy of the matrix Hartree-Fock energy is increased to the sub-μHartree level. The corresponding second order correlation energy is improved by 282 μHartree to give an accuracy of better than 0.7 mHartree. Adding subsets at the two bond axis positions (ba) reduces the error in the matrix Hartree-Fock energy to less than one tenth of a μHartree but the addition of off axis bond axis functions yields no further improvement. The corresponding improvements for the second order correlation energy are 19.5 μHartree and 100.38 μHartree, respectively, so again, in the case of the bond axis subsets, the off axis subsets are more effective in recovering correlation effects than the on axis subsets.

Table 5

The addition of off centre, bond axis and off axis/bond axis basis functions. The differences between the calculated and exact energy values are given in parenthese

Basis set specification	E_{mHF}	E_2
$30s\ ac;\ 30s\ bc; 28s\ oa(ac)\ [n_1 = 4];$ $26s\ oa(bc)\ [n_1' = 4]; 23s\ oa'(ac)\ [n_2 = 5];$ $23s\ oa'(bc)\ [n_2' = 4]$	-1.133 625 193 (4.377)	-0.032 916 770 (960.961)
$30s\ ac;\ 30s\ bc; 28s\ oa(ac)\ [n_1 = 4];$ $26s\ oa(bc)\ [n_1' = 4]; 23s\ oa'(ac)\ [n_2 = 4];$ $24s\ oa'(bc)\ [n_2' = 3]; 21s\ oc\ [m = 121]$	-1.133 629 422 (0.148)	-0.033 198 818 (678.913)
$30s\ ac;\ 30s\ bc; 28s\ oa(ac)\ [n_1 = 4];$ $26s\ oa(bc)\ [n_1'' = 4]; 23s\ oa'(ac)\ [n_2 = 4];$ $24s\ oa'(bc)\ [n_2' = 3]; 21s\ oc\ [m = 121];$ $21s\ ba$	-1.133 629 476 (0.094)	-0.033 218 347 (659.384)
$30s\ ac;\ 30s\ bc; 28s\ oa(ac)\ [n_1 = 4];$ $26s\ oa(bc)\ [n_1' = 4]; 23s\ oa'(ac)\ [n_2 = 4];$ $24s\ oa'(bc)\ [n_2' = 4]; 21s\ oc\ [m = 121];$ $21s\ ba; 21s\ oa(ba)\ [n_1'' = 4]^\dagger$	-1.133 629 476 (0.094)	-0.033 318 725 (559.006)

$\dagger$ Not optimized.

It is instructive to compare the results of the present study with those reported in our previous work[11] on the hydrogen molecule ground state in which the "traditional" approach to basis set construction was followed and higher harmonics centred on the nuclei were employed. A $20s$ basis set centred on each nucleus yields a matrix Hartree-Fock energy of -1.1284986 Hartree and a second order correlation energy of -18.496 mHartree. Thus the errors in the matrix Hartree-Fock energy and the second order energy are comparable with that recorded in Table 1 for the $30s$ ac basis set. A $20s10p$ basis set lowers the matrix Hartree-Fock energy by 5.026 mHartree to -1.1335251 Hartree and the second order correlation energy by 13.252 mHartree to -31.748 mHartree. The errors in the matrix Hartree-Fock energy and the second order energy are 104.4 μHartree and 2129 μHartree. A further lowering of 0.094 mHartree in the matrix Hartree-Fock energy is observed on using a $20s10p10d$ atom centred basis set giving a total matrix Hartree-Fock energy of -1.1336197 Hartree, which is therefore in error by 9.9 μHartree. The corresponding reduction in the second order correlation energy is 1.361 mHartree giving a total second order correlation energy of -33.109 mHartree, corresponding to an error of 768 μHartree. Finally, adding a set of atom centred functions of f-symmetry giving a $20s10p10d10f$ set on each atom gives a lowering of 0.006 mHartree to -1.1336260 Hartree for the matrix Hartree-Fock energy and a lowering of 0.617 mHartree to -33.726 mHartree for the second order component of the correlation energy. For the $20s10p10d10f$ ac basis set, the errors in the matrix Hartree-Fock and second order correlation

energies are thus 3 μHartree and 151 μHartree, respectively.

4   Conclusions

It has been shown that the second order electron correlation energy for the ground state of the hydrogen molecule at its equilibrium nuclear geometry can be described to an accuracy below the sub-*milli*Hartree level using a distributed basis set of Gaussian basis subsets containing only s-type functions only. Each of the basis subsets are taken to be even-tempered sets. The distribution of the subsets is empirical but nevertheless physically motivated.

References

[1] S. Wilson, 1983, *Methods in Computational Molecular Physics*, edited by G.H.F. Diercksen and S. Wilson (Dordrecht: Reidel)

[2] S. Wilson, 1987, *Adv. Chem. Phys.* **69**, 439

[3] S. Huzinaga, 1985, Comput. Phys. Rep. **2**, 279

[4] E.R. Davidson, and D. Feller, 1990, *Reviews in Computational Chemistry* **1**, 1

[5] R.K. Nesbet , 1960, *Rev. Mod. Phys.* **32**, 272

[6] C.M. Reeves, 1963, *J. Chem. Phys.* **39**, 1

[7] C.M. Reeves, and M.C. Harrison, 1963, *J. Chem. Phys.* **39**, 11

[8] R. Fletcher, and C.M. Reeves, 1963, *Comput. J.* **6**, 287

[9] I. Shavitt, 1993, *Israel J. Chem.* **33**, 357

[10] J. Almlof, J., K. Faegri, and K. Korsell, K., 1982, *J. Comput. Chem.* **3**, 385

[11] D. Moncrieff, and S. Wilson, 1997, in *Quantum Systems in Chemistry and Physics*, Proceedings of a European Workshop held at San Miniato, Italy, April 1996, Kluwer.

[12] D. Moncrieff, and S. Wilson, 1993, *Chem. Phys. Lett.* **209**, 423

[13] D. Moncrieff, and S. Wilson, 1993, *J. Phys. B: At. Mol. Opt. Phys.* **26**, 1605

[14] J. Kobus, D. Moncrieff, and S. Wilson, 1994, *J. Phys. B: At. Mol. Opt. Phys.* **27**, 5139

[15] J. Kobus, D. Moncrieff, and S. Wilson, 1994, *J. Phys. B: At. Mol. Opt. Phys.* **27**,

[16] D. Moncrieff, and S. Wilson, 1994, *J. Phys. B: At. Mol. Opt. Phys.* **27**, 1

[17] D. Moncrieff, J. Kobus, and S. Wilson, 1994, *J. Phys. B: At. Mol. Opt. Phys.* **28**, 4555

[18] L. Laaksonen, L., P. Pyykkö and D. Sundholm, 1986, *Comput. Phys. Reports* **4**, 313

[19] P. Pyykkö, 1989, in *Numerical Determination of the Electronic Structure of Atoms, Diatomic and Polyatomic Molecules*, edited by M. Defranceschi and J. Delhalle, NATO ASI Series C271, *p.* 161

[20] J. Kobus, 1994, *Comput. Phys. Commun.* **78**, 247

[21] J. Kobus, L. Laaksonen, and D. Sundholm, 1996, *Comput. Phys. Commun.* **98**, 346

[22] D. Heinemann, B. Fricke and D. Kolb, 1988 *Phys. Rev. A* **38** 4994

[23] D. Heinemann, A. Rosen, and B. Fricke, 1990 *Physica Scripta* **42** 692

[24] S. Hackels, D. Heinemann, D., D. Kolb, and B. Fricke, 1993 *Chem. Phys. Lett.* **206** 91

[25] L. Yang, L., D. Heinemann, D. and D. Kolb, 1993 *Phys. Rev. A* **48** 2700

[26] S. Wilson, and D. Moncrieff, 1993, *Molec. Phys.* **80**, 461

[27] D. Moncrieff, and S. Wilson, 1994, *Molec. Phys.* **82**, 523

[28] D. Moncrieff, and S. Wilson, 1995, *Molec. Phys.* **85**, 103

[29] D. Moncrieff, and S. Wilson, 1997, *Adv. Quantum Chem.* **28**, 47

[30] B.J. Ralston, and S. Wilson, 1995, *J. Molec. Struct. (Theochem)* **341**, 115

[31] S. Wilson, 1995, *J. Molec. Struct. (Theochem)* **357**, 37

[32] S. Wilson, 1996, *Intern. J. Quantum Chem.* **60**, 47

[33] L.M. Haines, J.N. Murrell, B.J. Ralston and D.J. Woodnutt, 1974, *J. Chem. Soc. Faraday Trans. II* **70**, 1794

[34] S. Wilson, 1995, *J. Phys. B: At. Mol. Opt. Phys.* **28**, L495

[35] S. Wilson, 1996, in *New Methods in Quantum Theory*, NATO ASI Series 3 - High Technology - Vol. 8, edited by C.A. Tsipis, V.S. Popov, D.R. Herschbach, and J.S. Avery, Kluwer Academic Publishers, Dordrecht.

[36] L. Laaksonen, P. Pyykko, and D. Sundholm, 1983, *Intern. J. Quantum Chem.*

[37] W. Kolos, and L. Wolniewicz, 1968, *J. Chem. Phys.* **49**, 404

[38] S. Wilson, 1984, *Electron correlation in molecules*, Clarendon Press, Oxford.

[39] S. Wilson, 1997, in *Problem Solving in Computational Molecular Science. Molecules in Different Environments*, Proceedings of NATO ASI held at Bad Windsheim, German, August 1996, edited by S. Wilson and G.H.F. Diercksen, Kluwer Academic, Dordrecht.

[40] R.E. Christoffersen, D. Spanglet, G.G. Hall and G.M. Maggiora, 1973, *J. Amer. Chem. Soc.* **95**, 8526

[41] K. Kaufmann and W. Baumeister, 1989, *J. Phys. B: At. Mol. Opt. Phys.* **22**, 1

[42] M. Abramowitz, and I. Stegun, 1970, *Handbook of Mathematical Functions*, Dover, New York

[43] H. Müntz, 1914, *Festschrift*, edited by H.A. Schwartz, p.303, Springer-Verlag, Berlin

[44] O. Szász, 1926, Math. Ann. **77**

[45] B. Klahn, 1985, *J. Chem. Phys.* **83**, 5748

[46] M.W. Schmidt and K. Ruedenberg, 1979, *J. Chem. Phys.* **71**, 3951

Explicitly Correlated Functions in Molecular Quantum Chemistry*

Jacek Rychlewski

Quantum Chemistry Group, Department of Chemistry, A.Mickiewicz University
ul.Grunwaldzka 6, 60-780 Poznań, Poland
and Institute of Bioorganic Chemistry, Polish Academy of Sciences
ul.Noskowskiego 12-14, Poznań, Poland

ABSTRACT

Variational methods based on the use of explicitly correlated wavefunctions are reviewed. Different types of such functions are considered. Application of explicitly correlated functions as basis functions in variational calculations on two-, three- and four-electrons molecules is presented. The state of art calculations and future perspectives are briefly discussed.

I. INTRODUCTION

The basic equation for molecular quantum chemistry, the Schrödinger equation, was introduced in 1926 (Schrödinger, 1926) and already in the next year the new theory was applied to the smallest molecular systems, *i.e.* the hydrogen molecular ion (Burrau, 1927) and the hydrogen molecule (Condon, 1927; Heitler and London, 1927). In that year another important paper dealing with nuclear motion in molecules was published (Born and Oppenheimer, 1927). The early numerical results for molecules obtained using the methods of quantum mechanics were of qualitative, or at the most semiquantitative character. Very soon it has been realised that inclusion of interelectronic distance into the wave function is a powerful way of improving the accuracy of calculated results. This has been first demonstrated by Hylleraas (Hylleraas,1929) for helium atom and by James and Coolidge (James and Coolidge,1933) for the hydrogen molecule. Today, methods based on explicitly correlated wave functions are capable of yielding the "spectroscopic" accuracy in molecular energy calculations (errors less than the orders of one μhar-

---

* dedicated to the memory of Włodzimierz Kołos

tree). Such accuracy is already possible to achieve via some experimental techniques, but is not easily accessible in most theoretical methods. For example, the Configuration Interaction (CI) method is in principle a method approaching the exact solution of the nonrelativistic Schrödinger equation as closely as desired. However, in practice, the convergence to the exact solution is frustratingly slow and, therefore, this method is unable to yield results of the spectroscopic accuracy. Explicit inclusion of an r_{ij} dependent term in the wave function leads to much faster convergence of the CI expansion. Several methods using different expressions of r_{ij} dependence have been proposed and developed. They can be divided into two groups depending on the form of the correlation factor used. In the first group the correlation factor has a form of r_{ij}^{ν} whereas in the second one the correlation factor

has the exponential form of $\exp(-ar_{ij}^2)$. All these methods give very accurate wave functions and energies, however, the area of their application is rather limited to small molecules.

This paper presents a brief review of the use of explicitly correlated wave functions in molecular quantum chemistry computations. This review is restricted mainly to the direct variational approaches. Special attention will be given to two-electron molecular systems. The possible direction of extending the use of the correlated wave function for three- and four-electron molecular systems as well as the accuracy of the results will be discussed.

II. THEORY

The direct variational solution of the Schrödinger equation after separation of the center of mass motion is in general possible and can be performed very accurately for three- and four- body systems such as H_2^+ (Kołos, 1969) and H_2 (Kołos and Wolniewicz, 1963; Bishop and Cheung, 1978). For larger systems it is unlikely to perform such calculations in the near future. Therefore the usual way in quantum chemistry is to introduce the adiabatic approximation. The nonrelativistic hamiltonian for a diatomic N-electron molecule in the center of mass system has the following form (in atomic units).

$$H = H_0 + H', \tag{1}$$

where

$$H_0 = -(1/2)\sum_{i=1}^{N} \Delta_{r_i} + V \tag{2}$$

$$H' = -(1/2\mu)\Delta_R - (1/8\mu)(\sum_{i=1}^{N} \nabla_{r_i})^2 - (1/2\mu_a)\nabla_R \sum_{i=1}^{N} \nabla_{r_i} \tag{3}$$

V represents coulombic interaction between all particles, r_i and R denote the position vector of the ith electron and the relative position vector of the nuclei respectively. μ is the reduced mass of the nuclei and $\mu_a^{-1} = M_a^{-1} - M_b^{-1}$ where M_a and M_b are the nuclear masses.

In the adiabatic approximation the N-electron wave function is assumed in the form of a single product:

$$\Psi_k^{ad}(1,2,...,N) = \Psi_k(r_1,r_2,...,r_N;R)\chi_k^{ad}(R) \tag{4}$$

with $\Psi_k(r_1,r_2,...,r_N;R)$ being the kth solution of the electronic Schrödinger equation :

$$H_0\Psi_k(r_1,r_2...,r_N;R) = E_k(R)\Psi_k(r_1,r_2...,r_N;R) \tag{5}$$

for a fixed value of the internuclear distance R. Under this assumption the Schrödinger equation for nuclear motion is

$$[-(1/2\mu)\Delta_\mathbf{R} + E_k(R) + H_{kk}'(R) - E_k^{ad}]\chi_k^{ad}(\mathbf{R}) = 0 \tag{6}$$

where H_{kk}' is so-called adiabatic correction term being the expectation value of the H' operator calculated with the $\Psi_k(r_1,r_2,...r_N;R)$ function (Kołos, 1970)

$$H_{kk}'(R) = \int \Psi_k(r_1,r_2,...r_N;R)H'\Psi_k(r_1,r_2,...r_N;R)dr_1dr_2dr_N \tag{7}$$

and can be decomposed into three parts :

$$H' = H_1' + H_2' + H_3' \tag{8}$$

where:

$$H_1' = -(1/2\mu)\Delta_\mathbf{R} \tag{9}$$

$$H_2' = -(1/8\mu)\sum_i \Delta_i \tag{10}$$

$$H_3' = -(1/4\mu)\sum_{i \neq j} \nabla_i\nabla_j \tag{11}$$

H_1' is the operator of the relative kinetic energy of the nuclei, H_2' is a correction to the kinetic energy of the electrons, H_3' is a mass polarisation correction and μ denotes the reduced mass of the nuclei. The explicit expression for $H_1'(R)$ in terms of elliptic coordinates is given in Ref.(Kołos and Wolniewicz, 1964). In the BO approximation the H_{kk}' term is neglected.

The method of calculating adiabatic corrections described above involves extremely cumbersome expressions and therefore this method has been applied for two-electron systems only.

Another approach has been proposed and employed to a number of molecules by Handy et al. (Handy et al., 1986; Ioannou et al., 1996; Handy and Lee, 1996). In this method the adiabatic correction is computed without separation of center of mass motion and :

$$H_{kk}'(R_i) = \int \Psi_k(r_1, r_2, \ldots, r_N; R) \; T^{nucl}(R_1, R_2) \Psi_k(r_1, r_2, \ldots, r_N; R) dr_1 dr_2 \ldots dr_N \quad (12)$$

with

$$T^{nucl}(R_1, R_2) = -\sum_{i=1}^{2} \frac{1}{2M_i} \Delta_{R_i} \quad (13)$$

where R_i is the coordinate of ith nucleus in laboratory fixed system. This approach has been justified recently by Kutzelnigg (Kutzelnigg 1997) and applied, using the explicitly correlated gaussian wave functions with the correlation term of exponential type, to H_2 and H_3^+ (Cencek and Kutzelnigg, 1997; Cencek et al., 1997).

Apart from the fully nonadiabatic variational approach mentioned above, the first typical step in molecular calculations is to solve the electronic Schrödinger equation Eq.(5). Most of such *ab initio* calculations are performed for a fixed position of the nuclei, usually for the equilibrium geometry. Only some of them are done with the changes in the internuclear distances. In such a case a potential energy curve (or a surface in the case of polyatomic molecules) in the BO approximation can be obtained. Then for each internuclear distance the adiabatic correction can be calculated resulting in the adiabatic potential energy curve for a given electronic state. The nonadiabatic effects, being the result of the interaction between electronic adiabatic states via perturbed operator of the form of H' Eq.(3), can be obtained as the correction to the adiabatic energy of a given rovibrational level using both the variational method and the perturbation theory.

Two additional corrections should be mentioned here. First one is the relativistic correction which is of order of α^2 where α is the fine structure constant and the other is the radiative correction which can be derived from quantum electrodynamics. (Bethe and Salpeter, 1957; Kołos, 1993)

III. TWO-ELECTRON MOLECULES
Kołos-Wolniewicz wave function

The simplest molecular system exhibiting effects of electron correlation is the hydrogen molecule. For this molecule the explicitly correlated wave function has been applied in the early days of quantum mechanics (James and Coolidge, 1933). It was later generalised by Kołos and Wolniewicz (Kołos and Wolniewicz, 1965) and successfully used to solve variety of problems in the ground and excited states of the hydrogen molecule. This wave function, called there the Kołos-Wolniewicz function (Kołos and Wolniewicz, 1965) is assumed in the form of an expansion :

$$\Psi(1,2) = \sum c_i \left[\Phi_i(1,2)(x_1 + iy_1)^{\Lambda} \pm \Phi_i(2,1)(x_2 + iy_2)^{\Lambda} \right] \tag{14}$$

The function $\Psi(1,2)$ is in fact the space part of the total wave function, since a non-relativistic two-electron wave function can always be represented by a product of the spin and space parts, both having opposite symmetries with respect to the electrons permutations. Thus, one may skip the spin function and use only the space part of the wave function. The only trace that spin leaves is the definite permutational symmetry and „$\pm$" sign in Eq.(14) refers to singlet as "+" and to triplet as "-". x_i and y_i denote cartesian coordinates of the ith electron. Λ is commonly known angular projection quantum number and Λ is equal to 0, 1, and 2 for Σ, Π and Δ symmetry of the electronic state respectively. The linear variational coefficients c_i are found by solving the secular equations. The basis functions $\Phi_i(1,2)$ which possess Σ symmetry are expressed in elliptic coordinates as:

$$\Phi_i(1,2) = \exp(-\alpha\,\xi_1 - \overline{\alpha}\xi_2)\xi_1^{n_i}\eta_1^{k_i}\xi_2^{m_i}\eta_2^{l_i}(2r_{12}/R)^{\mu_i}$$
$$\times \left[\exp(\beta\eta_1 + \overline{\beta}\eta_2) + (-1)^{k_i + l_i + s}\exp(-\beta\eta_1 - \overline{\beta}\eta_2) \right] \tag{15}$$

where $\alpha, \beta, \overline{\alpha}, \overline{\beta}$ are variational parameters; $n_i, k_i, m_i, l_i, \mu_i$ are integers and r_{12} and R denote the interelectronic and internuclear distances, respectively. s determines the u or g symmetry of the given state.
The wave function of Eqs. (14) and (15) was widely used to obtain BO potential energy curves and adiabatic corrections for the ground state (Kołos et al., 1986; Kołos and Rychlewski 1993, Wolniewicz 1993, 1995a) and electronically excited states of the hydrogen molecule: EF, GK, $H\overline{H}_1\Sigma_g^+$ (Wolniewicz and Dressler, 1985), B, B', $B''\overline{B}^1\Sigma_u^+$ (Kołos, 1976, 1981; Wolniewicz and Dressler, 1988; Kołos and Rychlewski, 1981;), $C,D^1\Pi_u$ (Kołos and Rychlewski, 1976; Wolniewicz

and Dresssler, 1988), $I^1\Pi_g$ (Kołos and Rychlewski, 1977; Dressler and Wolniewicz, 1984), $J, S^1\Delta_g$ (Kołos and Rychlewski, 1982, Rychlewski, 1991, Wolniewicz, 1995b), $a, h, g, (4s)^3\Sigma_g^+$, (Kołos and Wolniewicz, 1968; Kołos and Rychlewski, 1987,1990, 1991, 1995; Rychlewski, 1989a,b, 1992a), $b, e, f^3\Sigma_u^+$, (Kołos and Wolniewicz, 1965; Kołos and Rychlewski, 1990b, 1994; Rychlewski, 1988), $c^3\Pi_u, i^3\Pi_g$ (Kołos and Rychlewski, 1978; Rychlewski, 1992b), and j, $s^3\Delta_g$. (Rychlewski, 1984, 1991; Wolniewicz, 1995) Adding all remaining corrections, *i.e.* relativistic, radiative and nonadiabatic, results in the most accurate theoretical dissociation energy D_0 and ionisation potential for the ground state of H_2, HD and D_2 ever obtained in quantum chemistry.

The theoretical energy of the hydrogen molecule is obtained by piecing together a number of contributions resulting from separate calculations. They include the Born-Oppenheimer (BO) potential energy curve, and the (i) adiabatic, (ii) nonadiabatic, (iii) relativistic and (iv) estimated radiative corrections. The values of these contributions to the total energy and to the dissociation energy are given in table 1.

TABLE 1

Contributions to the total and dissociation energy for the ground state of H_2

	E	**D**
Electronic energy R=1.4011	-1.174475930742 [a)] a.u.	38293.041 cm^{-1}
Corrections	**[cm[-1]]**	**[cm[-1]]**
1. Adiabatic R=1.4	114.592 [b)]	4.938
2. Relativistic R=1.4	-2.405 [c)]	-0.517
3. Radiative R=1.4	0.747 [c)]	0.205
4. Nonadiabatic v=0, J=0		0.500 [a)]

[a)] Wolniewicz, 1995 ;
[b)] Kołos and Rychlewski, 1993 ;
[c)] Wolniewicz, 1993

In table 2 the present state of agreement between theoretical and experimental dissociation energies of the three most common isotopic species of the hy-

drogen molecule is shown. It is evident from this table that the agreement between these two sets of results is excellent. The differences for H_2 and D_2 are well within experimental error limits. There is also an agreement with the experimental dissociation energy of HD, although in this case the experimental accuracy is by one order of magnitude worse than for H_2 and D_2.

It is worth mentioning that the new experimental result for D_2 (Balakrishman and Stoicheff, 1992), which has changed significantly the value of the experimental dissociation energy, removed the disturbing, long standing discrepancy between the

TABLE 2
Dissociation energy for the ground state of the hydrogen molecule and its isotopes (in cm^{-1})

	H_2	HD	D_2
theory			
Kołos and Rychlewski, 1993	36118.049	36405.763	36748.345
Wolniewicz, 1995	36118.069	36405.787	36748.364
experiment			
Balakrishnan et al., 1992	36118.11 ± 0.08		
Stwaley, 1970		36406.2 ± 0.4	
Balakrishnan and Stoicheff, 1992			36748.38 ± 0.07
discrepancy [a]	0.006 ± 0.08	0.4 ± 0.4	0.03 ± 0.07
discrepancy [b]	0.04 ± 0.08	0.4 ± 0.4	0.02 ± 0.07

[a] with respect to the Kołos and Rychlewski results; [b] with respect to the Wolniewicz results

theory and experiment. Futhermore, current increase in accuracy of both theoretical and experimental techniques opens the possibility to investigate effects as small as radiative and relativistic corrections which are now larger than the experimental error. The ionisation potential, $IP(H_2)$, and the dissociation energy, $D_0(H_2)$, of the hydrogen molecule are linked by the dissociation energy of the one-electron ion, $D_0(H_2^+)$, and the ionisation potential of atomic hydrogen $IP(H)$ according to the relation :

$$IP(H_2) = IP(H) + D_0(H_2) - D_0(H_2^+) \qquad (16)$$

By combining these quantities the ionisation potential for the hydrogen molecule can be derived (Kołos and Rychlewski 1993; Wolniewicz, 1995).

Table 3 presents the comparison between theoretical value and the experimental data (Gilligan and Eyler, 1992, Jungen et. al., 1992). The agreement is fairly good, although not ideal. This is not surprising. The theoretical values are obviously not final. The relativistic and radiative corrections for the neutral molecule were calculated with considerably less accurate wave functions than the nonrela-

tivistic part of the energy. A computation of more accurate values of these corrections may slightly change the theoretical ionisation potential. It seems, however, that also the experimental approach still needs to be improved. Let us point out that the discrepancies for H_2 and HD are positive, whereas for D_2 the discrepancy has a negative value. Thus, if more accurate values of the relativistic and radiative corrections will change the theoretical value of the ionisation potential they will change it by approximately the same amount for all isotopic species. Therefore, if the change improves the agreement for H_2, it will worsen the agreement for D_2 and *vice versa*.

TABLE 3
Ionisation potential of hydrogen molecule (in cm^{-1}).

	H₂	**HD**	**D₂**
theory Kołos and Rychlewski, 1993	124417.471	124568.465	124745.377
experiment Jungen et al., 1992 discrepancy	124417.488±0.017 0.017±0.017		124745.362±0.024 -0.015±0.024
experiment Gilligan and Eyler, 1992 discrepancy	124417.507±0.012 0.036±0.012	124568.481±0.012 0.016±0.012	
theory Wolniewicz, 1995 discrepancy discrepancy	124417.491 -0.003±0.017 0.016±0.012	124568.489 -0.008±0.012	124745.395 -0.033±0.024

The excellent agreement between theory and experiment for the dissociation energy of H_2 is a result of more than six decades of research on both sides - theoretical and experimental. In table 4 a review is given of selected experimental and theoretical results of the dissociation energy for the ground state of the hydrogen molecule.

This is obviously only a small portion of the results that have been obtained, especially theoretically. These results have been extracted in such a way that, in the author's opinion, reflect significant stages of progress in the description of the ground state of the hydrogen molecule. In the earlier theoretical works only the binding energy, D_e, was published. This is not a measurable quantity being the depth of the potential energy curve. To make the figures listed in table IV comparable, wherever the binding energy was given, it has been scaled by subtracting from it the accurate value of zero point energy. This table is an example of mutual influences and competition between theory and experiment. It is shown that since

the sixties inclusion of adiabatic correction and then the remaining corrections has become essential to make the comparison satisfactory.

As it was mentioned before, the wave functions have been widely used to study the excited states of H_2.

TABLE 4

Dissociation energy for the ground state of the hydrogen molecule (in cm^{-1})

Year	Author	Experiment	Theory
1926	Witmer	3500	
1927	Heitler and London		23110
1933	James and Coolidge		36104
1935	Beutler	36116 ± 6	
1960	Kołos and Roothaan		36113.5
1960	Herzberg and Monfils	36113.6 ± 0.6	
1964	Kołos and Wolniewicz		36117.3
1968	Kołos and Wolniewicz		36117.4
1970	Herzberg (upper limit)	36116.3	
1970	Stwalley	36116.3 ± 0.5	
1975	Kołos and Wolniewicz		36118.0
1978	Kołos and Rychlewski		36118.12
1978	Bishop and Cheung		36117.92
1983	Wolniewicz		36118.01
1986	Kołos et al.		36118.023
1991	McCormack and Eyler	36118.26 ± 0.20	
1992	Balakrishnan et al.	36118.11 ± 0.08	
1993	Kołos and Rychlewski		36118.049
1995	Wolniewicz		36118.069

For excited states of the hydrogen molecule the quality of theoretical results are slightly worse since:

1. in the BO approximation the convergence of the energy is slower for higher excited states; for the lowest state of the given symmetry the quality of the results are expected to be better than 1 cm^{-1}

2. no nonadiabatic, relativistic and radiative corrections were applied to most of the states

3. excited states are not so well separated therefore the nonadiabatic effects are expected to be much larger than those calculated for the ground state.

In this paper only two examples of such studies, yielding the discovery of new, unexpected effects, are given.

The first example is concerned with the study on the h and g states of $^3\Sigma_g^+$ where the double minimum in the potential curves is created exclusively by the adiabatic effect. The existence of a double-minimum in the BO potential energy curves for some electronically excited states in diatomic molecules is well established. A double-minimum potential energy curve results from an avoided crossing of two adiabatic potential energy curves of the same symmetry or, in other words, from a drastic change in the character of the wavefunction for the given excited state. The formation of the double minimum may occur if the two potential energy curves have minima at significantly different values of the internuclear distance. The well-know examples are the EF, GK and H $\overline{H}$ $^1\Sigma_g^+$ states of the hydrogen molecule (Kołos and Wolniewicz, 1969; Wolniewicz and Dressler, 1985) where the double-minimum results from an avoided crossing of potential energy curves for a Rydberg-type configuration and a doubly excited $(2p\sigma_u)^2$ configuration. The minima for these two curves are separated by 2.5 bohr. If, however, the two minima appear at almost the same value of internuclear distance, the resulting potential energy curve has a single minimum even if there is a strong interaction between these two states. The h and g states of H_2 are the prime examples of it. These two states are nearly degenerate in the vicinity of the equilibrium (Wakefield and Davidson, 1965; Rychlewski, 1989a). For small R the h and g states are characterised by the $1s\sigma_g 3s\sigma_g$ and $1s\sigma_g 3d\sigma_g$ configurations respectively. For $R > R_e$, due to avoided crossing, the assignment of configurations becomes reversed. In Fig.1 the vertical ionisation energy of these two configurations as a function of R is plotted (Wakefield and Davidson, 1965) illustrating the crossing of these two curves. The crossing appears almost exactly at equilibrium of the h and g states. In Fig.2 the BO potential energy curves for the h and g are shown and it is seen that, in this approximation, the potential energy curves for these two states retain a single minimum. The smallest BO energy difference for these two states is 131.75 cm^{-1} for R=1.95 bohr (Rychlewski, 1989a; Kołos and Rychlewski, 1990a).

The adiabatic corrections for a double-minimum state are characterised by their large values in the region where drastic change in the character of the wavefunction occurs *i.e.* in the vicinity of the potential barrier. This is the case for the EF, GK and H$\overline{H}$ states. The largest values of the adiabatic corrections for the EF, GK and H$\overline{H}$ states are 499, 681 and 859 cm^{-1}, respectively (Wolniewicz and Dressler, 1986). A new effect, however, has been observed for the h and g$^3\Sigma_g^+$ states (Rychlewski, 1989b; Kołos and Rychlewski, 1990). The adiabatic corrections for
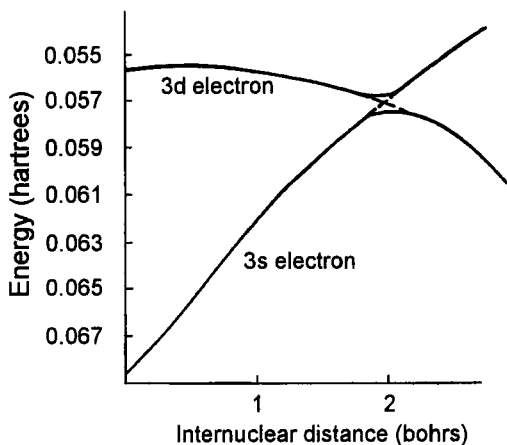
Fig. 1 Vertical ionization energy for the 3s and 3d $^3\Sigma_g^+$ states illustrating the near intersection.
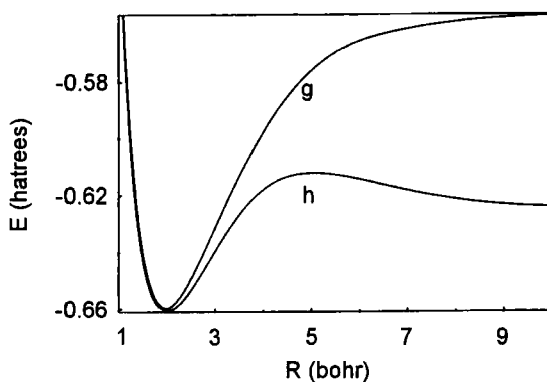
Fig. 2 The BO potential energy curves for the h and g states of H_2.

these states have an unusually large values (about 4000 cm^{-1}) in the vicinity of the equilibrium and, in consequence, the adiabatic potential energy curves for this pair of states are characterised by a double minimum with the potential barrier located near the equilibrium. Fig.3 shows the components of the adiabatic correction (Eq.8) for the g state and it is evident that the adiabatic correction is dominated by the $\langle H'_1 \rangle$ term. Similar picture can be plotted for the h state. The large value of $\langle H'_1 \rangle$ near the equilibrium for the h and g states is due to the drastic changes in the character of the wavefunction, which in turn leads to the large values of derivatives of the electronic wavefunction with respect to the internuclear distance. In

Fig.4 the adiabatic double-minimum energy curve and adiabatic vibrational levels for the
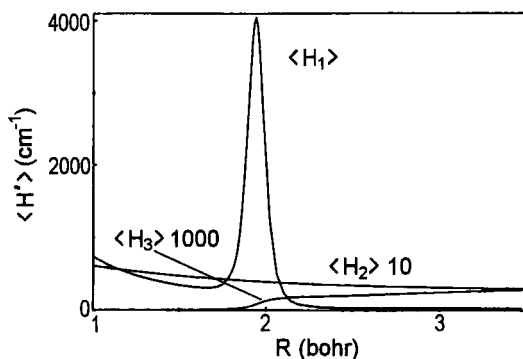
Fig. 3 Components of the adiabatic correction for the g state of H_2.
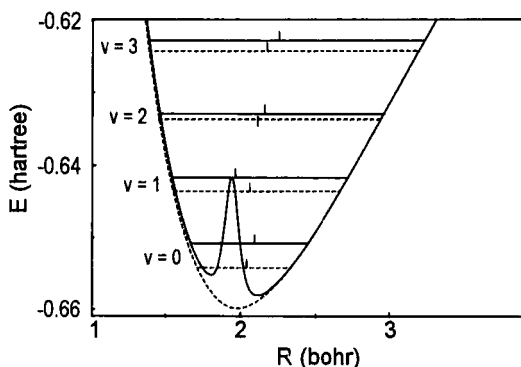
Fig. 4 The BO (dashed line) and adiabatic (solid line) potential energy curves for the g $^3\Sigma_g^+$ state of H_2. The vertical bar above each of the vibrational energy lines marks the value of $R_v = \left\langle R^{-2} \right\rangle^{-1/2}$

g state are shown and compared with the BO results. Similar picture can be plotted for the h state. It is worth to note that the smallest adiabatic energy difference for the *h* and *g* states amounts to 28 cm^{-1} and occurs at R=2.02 bohr. (Kołos and Rychlewski, 1990a).

The existence of a double minimum potential energy curve for the h and g states has important consequences. The lowest two vibrational levels of both states lie below the barrier top while the all higher levels, $v \geq 2$, lie above it (see Fig.4). The amplitude of the adiabatic wavefunction for the $v=0$ level is shifted to the right as compared with the BO result, so the maximum of the probability density is located in the outer minimum whereas the amplitude for the $v=1$ level is shifted to the left. As a result, a significant difference in rotational constant B_v for the two levels is observed and $B_0 < B_1$. For largest v the irregularities still remain although they become smaller with increasing v, showing that, in fact, vibrational level form two sets of levels, one belonging to the inner minimum and second to the outer minimum. This is also seen on Fig.4 from the behaviour of $R_v = <R^{-2}>_v^{-1/2}$.

The next two states of the same symmetry, the $4s$ and the $4d$ $^3\Sigma_g^+$ states, form a pair of states analogous to the h and g states. (Rychlewski, 1992a; Kołos and Rychlewski, 1995) These pairs of states, are examples of an avoided crossing systems where the region of avoided crossing coincides with the minima on the potential energy curves. Therefore, in the BO approximation, the potential energy curves for the $4s$ and $4d$ states retain a single minimum. However, if the adiabatic effects are taken into account the resulting adiabatic energy curves are characterised by double minima. This seems to be a general rule: whenever two states are nearly degenerate in the vicinity of the equilibrium these two states possess single minimum potential energy curves in the BO approximation and may have double minimum energy curves in the adiabatic approximation. The h, g, $4s$ and $4d$ $^3\Sigma_g^+$ states of the hydrogen molecule are the prime example of the above rule.

Second example concerns the study of magnetic effect in the B and B' states of $^1\Sigma_u^+$ symmetry. (Rychlewski and Raynes, 1981, 1983; Rychlewski, 1985, 1988) When a molecule is placed in an external magnetic field it can be described in terms of molecular parameters such as permanent magnetic moments, magnetizability (magnetic susceptibility), rotation g-factor, nuclear shielding etc. For a molecule like H_2 possessing no permanent magnetic moment the leading term describing the interaction with the field is magnetizability tensor. The three non-vanishing components of this tensor with the vector potential at the bond midpoint are:

$$\chi_{\parallel}^d = -\frac{1}{2}\sum_j < \Psi_k^0 | x_j^2 + y_j^2 | \Psi_k^0 > \tag{17}$$

$$\chi_{\perp}^d = -\frac{1}{2}\sum_j < \Psi_k^0 | x_j^2 + z_j^2 | \Psi_k^0 > \tag{18}$$

$$\chi_{\perp}^p = -\frac{1}{2}\sum_{n \neq k} \frac{|< \Psi_k^0 | \sum_j l_{jx} | \Psi_n^0 >|^2}{E_n^0 - E_k^0} \tag{19}$$

where superscripts p and d denote paramagnetic and diamagnetic components, $\parallel$ and $\perp$ denote the direction of the field to the bond, *i.e.* parallel and perpendicular respectively. The expectation values: x^2, y^2 and z^2 are taken over the electronic wave function of a given electronic state k. The summation in Eq.(19) is over all electronic states except a given one k, E_n^0 is the unperturbed energy of the nth electronic state, l_{jx} is the x component of the orbital angular momentum operator of jth electron around the origin.

The B state of the hydrogen molecule exhibits unique properties. It has very broad potential energy curve with relatively large value of the equilibrium distance R_e (Kołos and Wolniewicz, 1968b) and considerable ionic contribution in the range of 3.0<R<7.0 bohr (Kołos and Wolniewicz, 1966). This state is also unique from the point of view of its magnetic properties. It has been shown, using Kołos-Wolniewicz wave function and variation-perturbation technique, that the hydrogen molecule in the B state is paramagnetic (Rychlewski and Raynes, 1981, 1983). The only diatomic molecule in a singlet sigma state known to be paramagnetic, except the B and B' states of H_2,(Rychlewski et al., 1990) is the BH molecule in its ground state (Stevens and Lipscomb, 1965; Hegstrom and Lipscomb, 1966; Jaszuński, 1978; Corcoran and Hirschfelder, 1980; Schindler and Kutzelnigg, 1982). In Fig. 5 the components of the magnetizability tensor for the B state of H_2 as functions of R are plotted. It is seen that the $\chi_\perp^p$ component possesses maximum near R=1.6 bohr. As a result of it the total magnetizability χ, which is initially negative, becomes positive at about 1.3 bohr, reaches a peak at about 1.9 bohr and becomes negative again near 3.8 bohr. This means that the hydrogen molecule in the B state is paramagnetic in the region of R, 1.4<R<3.5 bohr. For a comparison in Fig. 6 the components of the magnetizability as functions of R are plotted for the ground state of H_2, which can be considered as a typical plot for diamagnetic diatomic molecule (Rychlewski and Raynes, 1980).

It was believed for many years that the total magnetizability of a closed shell, linear molecule in a $^1\Sigma$ state was necessarily negative. However, it was shown (Rebane, 1960; Hegstrom and Lipscomb, 1968,) that this is true only for electronic ground state of two-electron molecules. The proof of orbital diamagnetism is based on finding a transformation which causes $\chi_\perp^p$ to vanish thus demonstrating that the total magnetizability is negative *i.e.* the molecule is diamagnetic. This proof is limited to the case when the unperturbed wave function Ψ^0 does not have nodal surface. Thus it is not imposible for a molecule with more than two electrons in its
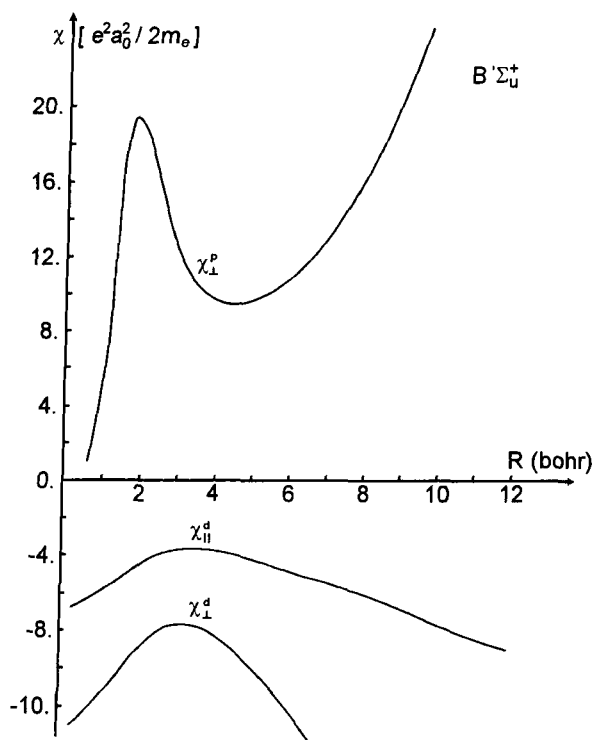
Fig. 5 Components of the magnetizability tensor plotted as function of R for the B
  state of H_2

ground state or for a molecule in an excited state to be paramagnetic. The hydro-
gen molecule in the B state is an example of such temperature independent par-
amagnetism. The paramagnetism is restricted to the region of R, $1.4<R<3.5$ bohr.
As a consequence, the molecule is paramagnetic for $v<10$, for higher vibrational
levels the paramagnetism disappears and the molecule has a negative magnetizabil-
ity. The abnormal behaviour of the paramagnetic component for the B state can be
explained by a strong interaction of the B state with low-lying $C^1\Pi_u$ state in the
presence of external magnetic field. This property influences also rotational mag-
netism of the molecule which is almost entirely produced by electrons. The par-
amagnetism of the hydrogen molecule in the B state has been recently obtained
from less accurate calculations using full-CI technique (Helgaker et al., 1997).
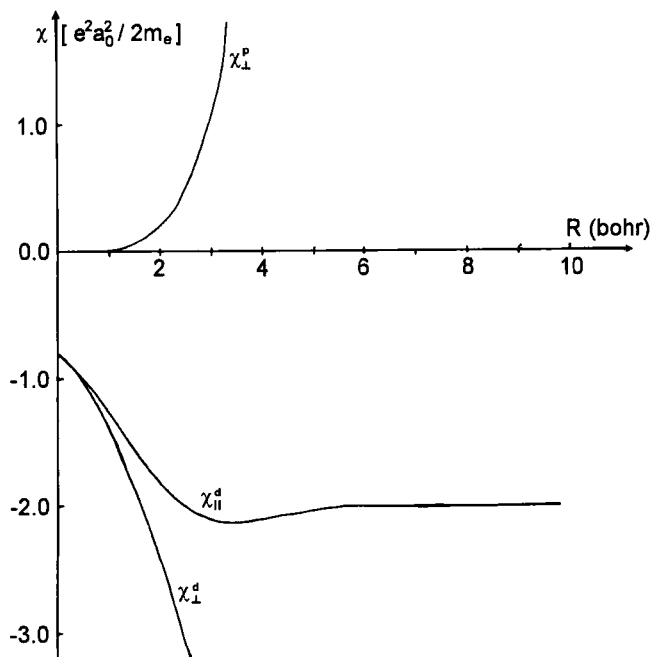
Fig. 6 Components of the magnetizability tensor plotted as function of R for the ground state of H_2

Other types of explicitly correlated functions

The power series expansion of the generalised James-Coolidge function, given in elliptic coordinates, has been, therefore, developed specially for two-electron systems and, moreover, cannot be used for nonlinear molecules.

There have been, therefore, several attempts to construct wave functions that for two-electron diatomic molecules can give results of similar accuracy as those obtained using KW wave function and that can be at the same time applied to more complicated systems. Three types of such functions should be mentioned here.

Hylleraas-CI function (Hy-CI)

This type of function is constructed as a product of the terms of standard CI expansion into Gaussian functions and the linear correlation factor r_{ij}^{v}. This approach

is a special case of the Hylleraas-CI (Hy-CI) method (Sims and Hagstrom, 1971). This function was introduced by Preiskorn and Woźnicki (Preiskorn and Woźnicki, 1982,1984). The Hy-CI wave function for two-electron molecule is given in the following form (Frye et. al., 1989):

$$\Psi(\vec{r}_1,\vec{r}_2) = \sum_{k=1}^{M} c_k \Psi_k(\vec{r}_1,\vec{r}_2) + r_{12}\sum_{k=1}^{M} c_k' \Psi_k(\vec{r}_1,\vec{r}_2) \tag{20}$$

where $\vec{r}_i$ is the position vector of electron ith, $\Psi_k(\vec{r}_1,\vec{r}_2)$ the kth configuration state function (CSF) and M is the total number of CSFs. Thus the total two-electron wave function is decomposed into two parts; the first summation in Eq.(20) corresponds to the conventional CI method and the second summation forms the explicitly correlated part. The configuration expansion coefficients c_k s and c_k s are solution of the eigenvalue problem in which the matrix elements depend in general on the power of r_{12}.

The Hy-CI wave function has been applied successfully by Clementi's group (Frye et. al. 1989; Preiskorn et. al., 1990, 1991) for two-electron molecules: H_2, HeH^+ and H_3^+. Two-electron integrals appearing in these calculations are relatively simple and require at most the one-dimensional numerical integration (Largo-Cabrerizo and Clementi, 1987) . However, this is not the case when one tries to extend this approach to many-electron molecules, because a large number of cumbersome three- and four-electron integrals involving two-dimensional integration have to be computed (Largo-Cabrerizo et.al, 1987). This leads to discouraging results, as was demonstrated by Clementi (Frye et al.,1991) for three-electron H_3 molecule.

Hylleraas-CIVB function (Hy-CIVB)

The Hy-CI function used for molecular systems is based on the MO theory, in which molecular orbitals are many-center linear combinations of one-center Cartesian Gaussians. These combinations are the solutions of Hartree-Fock equations. An alternative way is to employ directly in CI and Hylleraas-CI expansions simple one-center basis functions instead of producing first the molecular orbitals. This is a subject of the valence bond theory (VB). This type of approach, called Hy-CIVB, has been proposed by Cencek et al. (Cencek et.al. 1991). In the full-CI or full-Hy-CI limit (all possible CSF-s generated from the given one-center basis set), MO and VB wave functions become identical: each term in a MO-expansion is simply a linear combination of all terms from a VB-expansion. Due to the non-orthogonality of one-center functions the mathematical formalism of the VB theory for many-electron systems is rather cumbersome. However, for two-electron systems this drawback is not important and, moreover, the VB function seems in this case more natural.

The spatial part of the two-electron $\Psi_{Hy-CIVB}(1,2)$ is constructed as a linear combination of the form (apart from the normalization constant):

$$\Psi_{Hy-CIVB}(1,2) = \sum_i \sum_{j \geq i} c_{ij} F_{ij} r_{12}^{v_{ij}} \tag{21}$$

(which, in the particular case of $v_{ij} = 0$ for all values of i,j, represents the CIVB function), where

$$F_{ij} = [1 \pm (1,2)] \hat{P} [g_i(1) g_j(2)] \tag{22}$$

and g_p are primitive Cartesian Gaussian functions:

$$g_p(k; \vec{A}, \alpha, l, m, n) = (x_k - A_x)^l (y_k - A_y)^m (z_k - A_z)^n \exp(-\alpha |\vec{r}_k - \vec{A}|^2), \tag{23}$$

$\hat{P}$ is a symmetry operator ensuring the proper spatial symmetry of the function, (1,2) stands for the permutation (exchange) of both electrons' coordinates and the sign in Eq. (22) determines the multiplicity: for (+) F_{ij} represents the singlet state and for (-) the triplet state.

Exponentially correlated gaussian type wave function

Almost forty years ago Boys (Boys, 1960) and Singer (Singer, 1960) suggested that Gaussian functions with the exponential correlation factor, $\exp(-\beta r_{ij}^2)$, could be applied to molecular calculations. This type of basis function although employed by different authors for two-electron systems with quite encouraging results (Lester Jr. and Krauss 1964, Longstaff and Singer, 1960, 1964, 1965, Handy, 1973, Salmon and Poshusta, 1973), was long underestimated and claimed to be much slower convergent than that containing the powers of r_{ij}. It was later shown, however, that the careful optimization of non-linear parameters allows to obtain very short expansions of high quality for the H_2 molecule (Jeziorski and Szalewicz, 1979; Kołos et.al., 1982a, 1982b). The explicitly correlated Gaussian wave function for two-electron diatomic molecule may be assumed in the following form:

$$\Psi(\vec{r}_1, \vec{r}_2) = (1 + P_{12})(1 + I) \sum_{k=1}^M c_k \Psi_k(\vec{r}_1, \vec{r}_2) \tag{24}$$

where

$$\Psi(\vec{r}_1, \vec{r}_2) = \exp\left(-\alpha_k r_{a1}^2 - \beta_k r_{b1}^2 - \alpha'_k r_{a2}^2 - \beta'_k r_{b2}^2 - \gamma_k r_{12}^2\right), \tag{25}$$

where the operator P_{12} interchanges the electronic coordinates, the operator I inverts the wave function through the midpoint of the internuclear axis, and r_{a1}, r_{b1}, r_{a2}, r_{b2} and r_{12} are the distances between the electrons (1,2) and the nuclei (a,b) specified by the respective subscripts.

BO energies for two-electron molecular systems

The hydrogen molecule is the simplest molecular system for which a comparison of accuracy of the methods taking into account electron correlation effects can be provided. In Table V the BO energies of the ground state of H_2 for a single internuclear distance obtained using the wave functions disccussed above are collected. These are the best energies obtained so far using : ECG functions containing 1200 (Cencek and Kutzelnigg, 1997) and 760 (Komasa et.al., 1996) terms, KW wave function with 883 terms (Wolniewicz 1995), random-tempered ECG function containing 900 terms (Alexander et.al., 1990), Hy-CI function (Frye et.al., 1989) with Gaussian basis set of the size 15s7p2d1f, Hy-CIVB function with Gaussian functions s-f containing 372 terms without and selected 128 terms with linear r_{12} factor; the non linear variational parameters were optimized only once (Cencek et.al., 1991). For comparison the best energies obtained using wave function not depending explicitly on interelectronic distance are also listed in Table V. They are : full-CI function with 5s3p2d2f Slater functions (Liu and Hagström, 1993), CIVB function with Gaussians s-f; the function containing 372 terms (Cencek et al., 1991) and full CI function with Gaussian basis set 15s7p2d1f (Frye et al., 1989)

TABLE 5
BO energies of the ground state of H_2, R=1.4011 bohr (see text)

Function	Energy [hartree]	Error [cm⁻¹]
ECG function, 1200 terms	-1.174475931211	
ECG function, 760 terms	-1.1744759310	
KW function, 883 terms	-1.1744759307	
random-tempered ECG function, 900 terms	-1.17447485	0.24
Hy-CI (MO) function, full CI with 15s7p2d1f Gaussians + r_{12} terms	-1.17447467	0.28
Hy-CIVB function with Gaussians s-f, 372 + 128 r_{12} terms	-1.17446270	2.8
full CI (MO) with 5s3p2d2f Slater functions	-1.1743043	38
CIVB function with Gaussians s-f, 372 terms	-1.17405900	91
full-CI (MO) function with 15s7p2d1f Gaussians	-1.173987	107

As it is seen from this table the energy of the ground state of H_2 calculated with ECG function represents the same level of accuracy as that obtained with KW function. It is worth to note, however, that the energy calculated with ECG was obtained after very time-consuming optimization process in which 5 nonlinear parameters per basis function (this means 6000 parameters for 1200 term function) were optimized, whereas the optimization process for the KW function is based on the selection of the terms of the form of Eq.(15), i.e. the powers n_i, k_i, m_i, l_i, and μ_i

and afterwards the optimization of only 4 parameters $\alpha, \beta, \overline{\alpha}$ and $\overline{\beta}$. The other types of correlated functions *i.e.* Hy-CI and Hy-CIVB are somewhat less accurate. It must be noted, however, that in the case of Hy-CIVB function the exponential parameters were optimized only once. This demonstrates that the optimization of nonlinear parameters is a very important part of the method and is crucial for obtaining accurate results. Table 5 also demonstrates that the error of the best energy calculated using explicitly correlated wave functions is at least four orders of magnitude lower than that calculated with full CI wave functions.

The same conclusion can be drawn from the results obtained for excited states of H_2. As an example, in Table VI the energies for the unbounded lowest triplet b state obtained using ECG, KW, Hy-CI and conventional CI are compared. For higher excited (Rydberg) states the difference between energies calculated using explicitly correlated functions and CI function becomes smaller since the importance of the effect of electron correlation is decreasing.

TABLE 6

The BO energies for the b $^3\Sigma_u^+$ state of H_2 computed variationally using differnt types of wave functions (R=2.0 bohr)

Function	Energy (hartree)	Δ (cm^{-1})
ECG, 600 terms.(Cencek et.al. 1995)	-0.897076330	
KW, 110 terms (Kolos and Rychlewski 1990)	-0.897076017	0.070
Hy-CI 1578 CSF 14s7p1d basis set (Frye et.al. 1989)	-0.89707050	1.28
CI 6s 4p2d basisi set (Borondo et.al. 1987)	-0.8902	1509

For other two-electron diatomic sysytems like HeH$^+$ the ECG wave function gives the energies of comparable level of accuracy as KW wave function (Cencek et al., 1995). For polyatomic two-electron molecular ion H_3^+, for which the KW function can not be applied, the energy calculated using ECG wave function is more accurate than any previously reported. (Cencek et al., 1995)

Three- and four-electron molecules

Explicitly correlated wave functions described above have been specifically designed for two-electron molecular systems. As it was demonstrated in the previous section these functions give the energies which appear to be superior to the variational energies reported. Therefore several attempts have been made to extend this approach to many-electron molecules. The James-Coolidge (JC) type of function has been extended to three- and four-electron diatomic molecules by Clary and

Handy (Clary and Handy, 1977). The wave function proposed by them is expanded as a linear combination of configuration Φ_k

$$\Psi = \sum_k c_k \Phi_k \tag{26}$$

$$\Phi = \hat{O}_{as} \left[\chi \, r_{ij}^{\nu} \prod_{m=1}^{N} \Theta_m(r_m) \right] \tag{27}$$

The operator $\hat{O}_{as}$ makes the wave function antisymmetric to the exchange of any two electrons, χ is the appropriate spin function and ν takes value 0 or 1. N denotes the number of electrons in the molecule (3 or 4). $\Theta_m(r_m)$ are non-orthogonal orbitals given in the elliptic coordinates as:

$$\Theta_m(r_m) = \exp(-\alpha \xi_m + \beta \eta_m) \xi_m^p \eta_m^q \tag{28}$$

and p., q = 0, 1, 2, 3.

In practical application to three- and four-electron diatomic molecules Clary and Handy optimised first the exponents α, β from a small CI calculation then an exte-

TABLE 7

BO energies for three- and four- electron molecules

Function	Energy (hartree)	Δ (cm⁻¹)
H₃ (R1=R2=1.757 bohr)		
ECG 600 terms (Komasa et al.,1996)	-1.65914905	
Hy-CI 3s1p basis set (Frye et al.,1991)	-1.636637	4941
CI (R1=R2=1.7572bohr) (Peterson et al., 1994)	-1.6589596	42
He₂⁺(R=2.042 bohr)		
ECG 600 terms (Komasa et al., 1996)	-4.99464087	
JC function 29 terms (Clary, 1977)	-4.98706	1664
CI (R=2.043 bohr) (Carrington et al., 1995)	-4.994284	78
LiH (R=3.015 bohr)		
ECG 600 terms (Komasa et al., 1996)	-8.070449	
JC function, 119 terms (R=3.0) (Clary and Handy, 1977)	-8.0630	1634
CI (Handy et al.,1984)	-8.06904	309
He₂ (R=5.6 bohr)		
ECG 1600 terms (Komasa and Rychlewski, 1996)	-5.807483462	
CI (van Mourik and van Lenthe, 1995)	-5.806110	301

nsive CI calculation is performed using the optimised exponents and selected values of p and q as defined in Eq.28. Finally a few configurations multiplied by interelectronic distance were added to the wave function. Also the Hy-CI approach has been extended to many-electron molecular systems and applied to H_3 molecule (Frye et al.,1991).

Extension of ECG function to many-electron molecules has been proposed recently by Cencek and the present author (Cencek and Rychlewski, 1995). The N-electron wave function is assumed in a form of the following expansion:

$$\Phi = \sum_i c_i \phi_i \qquad (29)$$

where:

$$\phi_i = \hat{O}_{as}\left\{ \hat{P}_R\left[\prod_{k=1}^{N} g_{ik}(\mathbf{r}_k)\exp\left(-\sum_{p=1}^{N-1}\sum_{q=p+1}^{N}\beta_{ipq}r_{pq}^2\right)\right]\Xi^{N,S,M_s}(\sigma_1,\ldots,\sigma_N)\right\} \qquad (30)$$

In the above equation, $\hat{O}_{as}$ is the antisymmetrizer working on both the space-~and spin coordinates, $g(\mathbf{r}_k)$ are primitive Cartesian Gaussian functions Eq. (23) and Ξ^{N,S,M_s} is the N-electron spin eigenfunction such that:

$$\hat{S}^2\Xi^{N,S,M_s} = S(S+1)\Xi^{N,S,M_s}, \qquad (31)$$

$$\hat{S}_z\Xi^{N,S,M_s} = M_s\Xi^{N,S,M_s}. \qquad (32)$$

$\hat{P}_R$ is a projection operator ensuring the proper spatial symmetry of the function. The above method is general and can be applied to any molecule. In practical application this method requires an optimisation of a huge number of nonlinear parameters. For two-electron molecule, for example, there are 5 parameters per basis function which means as many as 5000 nonlinear parameters to be optimised for 1000 term wave function. In the case of three and four-electron molecules each basis function contains 9 and 14 nonlinear parameters respectively (all possible correlation pairs considered). The process of optimisation of nonlinear parameters is very time consuming and it is a bottle neck of the method.

For three- and four-electron molecular systems the computations using explicitly correlated wave functions have been performed for H_3, He_2^+, He_2, and LiH. In Table VII the energies calculated for the ground states of these molecules with ECG, Hy-CI, JC functions are listed and compared with the best CI energies obtained so far. It is easily seen from this table that ECG function gives significantly lower BO energies than all previously published variational results. It is also seen that the computations employing the Hy-CI function for H_3 molecule have given

quite discouraging result. It is mainly due to very limited bases set (3s1p) used. A really good computation for H_3 would require the same type of basis set as used for H_2. However, for three-electron molecule the complexity of the integral computations goes up considerably and limits the size of basis set dramatically. The energies obtained for He_2^+ and LiH with JC function are more than 1600 cm^{-1} above the ECG results (Clary, 1977; Clary and Handy, 1977), however, it is due to very limited length of the expansion where only three terms for He_2^+ and two terms for LiH containing the linear correlation term were used.

IV. CONCLUSIONS

In this paper we have considered the ability of the explicitly correlated wave functions to achieve the spectroscopic accuracy of variational energy of systems with a few electrons. Such accuracy has been obtained for two-electron diatomic molecules since the sixties using the KW functions. This includes not only BO energies but also adiabatic, relativistic, radiative and nonadiabatic corrections. For two electron molecules all explicitly correlated functions are capable of achieving the level of accuracy of BO energies calculated using KW function. Moreover, it has been shown that adiabatic and relativistic corrections can be calculated quite easily using the ECG functions (Cencek and Kutzelnigg, 1996, 1997). When more than two-electron molecules are concerned, applications of JC and Hy-CI functions are quite discouraging, due to the problems with evaluation of some integrals. Only the ECG functions are capable of achieving spectroscopic accuracy for three- and four-electron molecules. This method is in principle general and could be applied to more complicated molecules. It must be stressed, however, that really accurate energy calculations using the ECG function require large basis set and therefore the optimisation of exponential parameters is a crucial procedure of the method. This procedure is very time consuming which is now limiting the area of application of the method. However, assuming a significant improvement in either, and probably all, theoretical methods, numerical implementation and computer's performance, it is likely to expect in the near future the progress in the application of correlated wave functions to larger molecular systems.

ACKNOWLEDGEMENTS

REFERENCES
Alexander, S.A., Monkhorst, H.J, Roeland, R. and Szalewicz, K. (1990). *J.Chem.Phys.*, **93**,4230

Balakhrishnan, A., Smith, V. and Stoicheff, B.P. (1992). *Phys.Rev.Lettrrs*, **68**, 2149

Balakhrishnan, A. and Stoicheff, B.P. (1992). *J.Mol.Spectroscopy*, **156**, 517

Bethe, H.A. and Salpeter, E.E. (1957) „Quantum Mechanics for One- and Two-Electron Systems", Academic Press, New York

Beutler, H. (1935). *Z.Physik. Chem.* **B29** 315

Bishop, D.M. and Cheung, L.M. (1978). *Phys.Rev.* **A18**, 1846

Born, M. and Oppenheimer, R. (1927). *Ann. Physik*, 84, 457

Borondo, F., Martin, F, and Yanez, M. (1987). *J.Chem.Phys.* **86**, 4982

Boys,S.F. (1960). *Proc. Roy. Soc.,* **A258**, 402

Burrau, O.K. (1927). *Danske.Vidensk. Selsk.,* 7,1

Carrington,A., Pyne, C.H., and Knowles, P.J. (1995). *J.Chem.Phys.,* **102**, 5979

Cencek,W., Komasa,J. and Rychlewski, J., (1991). *J. Chem.Phys.,* **95**, 2572

Cencek W. Komasa, J. and Rychlewski J, (1995). *Chem.Phys.Letters*, **246**, 117

Cencek W. and Kutzelnigg, W., (1996). *J.Chem.Phys.,* **105**, 5878

Cencek, W. and Kutzelnigg, W. (1997). *Chem. Phys. Letters*, **266**, 383

Cencek, W., Rychlewski, J., Jaquat, R. and Kutzelnigg, W. (1997) . in preparation

Clary, D.C.(1977). *Mol.Phys.,* **34**, 793

Clary, D.C and Handy N,C.,(1977). *Chem.Phys.Letters*, **51**, 483

Comdon, E. U. (1927). *Proc.Natl.Acad.Sci.USA*, **13**,466

Corcoran, O.T. and Hirschfelder, J.O. (1980). *J. Chem. Phys.,* **72**, 1524

Dressler, K. and Wolniewicz, L. (1984). *Can. J. Phys.,* **62**, 1706

Dressler, K. and Wolniewicz, L. (1986). *J.Mol.Spectroscopy*,85,2821

Frye,D., Lie,G.C., Chakravorty, S.J., Preiskorn, A. and Clementi,E. (1989). in: *Modern Techniques in Computational Chemistry*, edited by E.Clementi (ESCOM), Leiden,

Frye,D., Lie G.C., and Clementi, E. (1989). *J.Chem. Phys.,* **91**, 2366, 2369

Frye,D., Preiskorn,A., and Clementi, E. (1991). *J.Comput.Chem.,* **12**, 560

Gilligan and Eyler (1992) *Phys. Rev.,* **A46**, 3676

Handy,N.C. (1973). *Mol. Phys,.* **26**, 169

Handy, N.C., Yamaguchi, Y. and Schaeffer III, H.F. (1986). *J. Chem. Phys.,* **84**, 4481

Handy, N.C. and Lee, A.M. (1996). *Chem. Phys. Letters*, **252**, 425

Hegstrom, R.A. and Lipscomb, W.N. (1966). *J. Chem. Phys.,* **45**, 2378

Hegstrom, R.A. and Lipscomb, W.N. (1968). *Rev. Mod. Phys.,* **40**, 354

Heitler, W. and London. F. (1927). *Z.Physik*, **44**,455

Helgaker, T., Jaszuński, M. and Rund, K. (1997) *Polish J. Chem.,* in press

Herzberg, G. and Monfils, A. (1960). *J.Mol.Spectroscopy*,5, 482

Herzberg, G. (1970). *J.Mol.Spectroscopy*, **33**, 147

Hylleraas, E.A. (1929). *Z. Phys.,* **54**, 347

James, H.M. and Coolidge,A.S. (1933). *J.Chem.Phys.* 1, 825

Jaszuński, M. (1978). *Theoret. Chim. Acta*, **48**, 323

Jeziorski, B. and Szalewicz, K. (1979). *Phys. Rev.*, **A19**, 2360

Joannou, A.G., Amos, R.D. and Handy, N.C. (1996). *Chem. Phys. Letters*, **251**, 52

Jungen, Ch., Dąbrowski, I., Herzberg, G.and Vervloet, M. (1992*). J. Mol. Spectroscopy*, **153**, 11

Kołos, W. (1969). *Acta Phys. Acad. Sci. Hung.*, **27**, 241

Kołos,W. (1970). *Adv. Quantum Chem.*, **5**, 99

Kołos, W. (1976) *J. Mol. Spectroscopy*, **62**, 429

Kołos, W. (1981). *J. Mol. Spectroscopy*, **86**, 42

Kołos, W. (1993). *Polish J. Chem.*, **67**, 553

Koł os, W., Monkhorst, H.J. and Szalewicz, K. (1982a). *J.Chem. Phys.*, 77, 1323

Kołos, W., Monkhorst, H.J. and Szalewicz, K. (1982b). *J.Chem. Phys,.* 77, 1335

Kołos, W. and Roothaan, C.C.J. (1960). *Rev.Mod.Phys.*, **32**, 219

Kołos, W. and Rychlewski, J. (1976). *J. Mol. Spectroscopy*, **62**, 109

Kołos, W. and Rychlewski, J. (1977). *J. Mol. Spectroscopy*, **66**, 428

Kołos, W. and Rychlewski, J. (1978). *Acta Phys. Polonica*, **A53**, 281

Kołos, W. and Rychlewski, J. (1981). *J. Mol. Spectroscopy*, **88**, 1

Kołos, W. and Rychlewski, J. (1982). *J. Mol. Spectroscopy*, **91**, 128

Kołos, W. and Rychlewski, J. (1987). *J. Mol. Spectroscopy*, **125**, 159

Kołos,W. and Rychlewski, J. (1990a). *J.Mol.Spectroscopy*, **143**, 212

Kołos, W. and Rychlewski, J. (1990b). *J. Mol. Spectroscopy*, **143**, 237

Kołos, W. and Rychlewski, J. (1993). *J.Chem.Phys.*, **98**,3960

Kołos, W. and Rychlewski, J. (1994). *J. Mol. Spectroscopy*, **166**, 12

Kołos, W. and Rychlewski, J. (1995). *J. Mol. Spectroscopy*, **169**, 341

Kołos,W. and Rychlewski, J. (1996). *J.Mol.Spectroscopy*, **177**,146

Kołos,W., Szalewicz, K. and Monkhorst, H.J. (1986). *J.Chem.Phys.*, **84**,3278

Kołos,W. and Wolniewicz,L.(1963). *Rev.Mod.Phys.*, **35**, 473

Kołos,W. and Wolniewicz, L. (1964). *J.Chem.Phys.*, **41**, 3663

Kołos,W. and Wolniewicz, L. (1965). *J.Chem.Phys.*, **43**, 2429

Kołos,W. and Wolniewicz, L. (1966). *J. Chem. Phys.*, **45**, 509

Kołos,W. and Wolniewicz,L.(1968a). *Phys.Rev.Lettrrs*, **20**, 243

Kołos, W. and Wolniewicz, L. (1968b). *J. Chem. Phys.*, **48**, 3672

Kołos,W. and Wolniewicz, L. (1969). *J.Chem.Phys.*, **50**,3228

Kołos,W. and Wolniewicz, L. (1975). *J.Mol.Spectroscopy*, **54**,303

Komasa, J., Cencek, W. and Rychlewski, J. (1996). *Comput. Methods in Technol.*, **2**, 87

Komasa, J. and Rychlewski, J. (1996). *Chem.Phys.Letters*, **249**, 253

Kutzelnigg, W. (1997). *Mol. Phys.*, **90**, 909

Largo-Cabrerizo, A., and Clementi, E., (1987). *J.Comput. Chem,.* **8**,1191

Largo-Cabrerizo, A., Urdaneta, C., Lie, G.C. and Clementi, E. (1987). *Int. J. Quant. Chem.,* **S21**, 677

Lester Jr.,W.A., and Krauss, M. (1964). *J.Chem. Phys,.* **41**, 1407 and (1965) **42**, 2990(E)

Liu,B. and Hegström, S. (1993). *Phys. Rev. A,* **48**, 166

Longstaff, J.V.L., and Singer, K., (1960). *Proc. Roy. Soc,.* **A258**, 421

Longstaff, J.V.L., and Singer, K., (1964). *Theor. Chim. Acta,* **2**, 265

Longstaff, J.V.L., and Singer, K., (1965). *J.Chem. Phys.,* **42**, 801

McCormack, E.F. and Eyler, E.E. (1991). *Phys.Rev.Letters,* **66**, 1042

van Mourik, T. and van Lenthe, J.H. (1995). *J.Chem.Phys.,* **102**, 7479

Peterson, K.P., Woon,D.E. and Dunning Jr., T.H. (1994). *J.Chem.Phys.,* **100**, 7410

Preiskorn A. and Woźnicki, W. (1982). *Chem.Phys.Letters,* **86**,369

Preiskorn A. and Woźnicki,W. (1984). *Mol.Phys,.* **52**, 1291

Preiskorn,A., Lie,G.C., Frye,D. and Clementi, E. (1990). *J.Chem. Phys,.***92**, 4941, 4948

Preiskorn,A., Frye,D. and Clementi, E. (1991). *J.Chem. Phys.,* **94**, 7204

Rebane, T.K. (1960). *Zh. Exp. Teoret. Fiz.,* **38**, 963 (English translation: *Soviet Phys. JFTP,* **11**, 694, (1960)

Rychlewski, J. (1984). *J.Mol.Spectroscopy,* **104**, 253

Rychlewski, J. (1985). *Phys. Rev.,* **A31**, 2091

Rychlewski, J. (1988). In „Molecules in Physics, Chemistry and Biology", J. Maruani Ed. Kluwer Academic Publishers, Vol. II, p.207-255

Rychlewski, J. (1988). *J. Mol. Spectroscopy,* **151**, 553

Rychlewski, J. (1989a). *J.Mol.Spectroscopy,* **136**,333

Rychlewski, J. (1989b). *Phys.Rev.Letters,* **63**, 1223

Rychlewki, J. (1991). *J.Mol.Spectroscopy,* **149**, 125

Rychlewski, J. (1992a). *Phys. Rev.,* **A45**, 5270

Rychlewski, J. (1992b). *Theoret. Chim. Acta,* **83**, 249

Rychlewski, J. Komasa, J. and Cencek, W. (1990). *Phys. Rev. A,* **41**, 5825

Rychlewski, J. and Raynes, W.T. (1980). *Mol. Phys.,* **41**, 843

Rychlewski, J. and Raynes, W.T. (1981). *Chem. Phys. Letters,* **79**, 310

Rychlewski, J. and Raynes, W.T. (1983). *Mol. Phys.,* **50**, 1335

Salmon, L. and Poshusta, R.D. (1973). *J.Chem. Phys.,* **59**, 3497

Schindler, M. and Kutzelnigg, W. (1982). *J. Chem. Phys.,* **76**, 1919

Schrödinger, E. (1926). *Ann. Physik,* **79**, 361

Sims J.S. and Hagstrom, S.A. (1971). *Phys. Rev,.* **A4**, 908 .

Singer,K. (1960). *Proc. Roy. Soc.,* **A258**, 412

Stevens, R.M. and Lipscomb, W.N. (1965). *J. Chem. Phys.,* **42**, 3666

Stwalley, W.C. (1970). *Chem.Phys.Letters,* **6**, 241

Wakefield, C.B. and Davidson E.R. (1965). *J.Chem.Phys.,* **43**,834

Witmer, E.F. (1926). *Phys.Rev.*, **28**, 1223

Wolniewicz, L. (1983). *J.Chem.Phys.*, **78**, 6173

Wolniewicz, L and Dressler K. (1985a). *J.Chem.Phys.*, **82**,3292

Wolniewicz, L and Dressler K. (1988). *J.Chem.Phys.*, **88**,3861

Wolniewicz, L. (1993). *J. Chem. Phys.*, **99**, 1851

Wolniewicz, L. (1995a). *J.Chem.Phys.*, **103**, 1792

Wolniewicz, L. (1995b). *J. Mol. Spectroscopy*, **169**, 329

MANY-ELECTRON STURMIANS AS AN ALTERNATIVE TO THE SCF-CI METHOD

John Avery

Department of Chemistry, University of Copenhagen

Universitetsparken 5, DK-2100 Denmark

Abstract

Methods are introduced for generating many-electron Sturmian basis sets using the actual external potential experienced by an N-electron system, i.e. the attractive potential of the nuclei. When such basis sets are employed, very few basis functions are needed for an accurate representation of the system; the kinetic energy term disappears from the secular equation; solution of the secular equation provides automatically an optimal basis set; and a solution to the many-electron problem is found directly, including electron correlation, and without the self-consistent field approximation. In the case of molecules, the momentum-space hyperspherical harmonic methods of Fock, Shibuya and Wulfman are shown to be very well suited to the construction of many-electron Sturmian basis functions.

Contents

1 Introduction

Schull and Löwdin [1] originally introduced single-electron hydrogenlike Sturmian basis functions into quantum chemistry because these functions are complete without the inclusion of the continuum. Sturmian basis functions (broadly defined) are solutions for the Schrödinger equation for some easily-solved potential, $V_0(\mathbf{x})$, where the potential is weighted by a factor, β_ν, especially chosen in such a way as to make all of the basis functions in the set correspond to the same energy, regardless of their quantum numbers. The name "Sturmian" was introduced by Rotenberg [2] in order to emphasize the connection with Sturm-Liouville theory. Weniger [3] has studied the orthonormality and completeness properties of Sturmian basis sets and shown that such a set forms the basis of a Sobolev space. The present paper will discuss the many-particle generalization of Sturmian basis sets, and will show that the use of such basis sets offers us a means of solving the Schrödinger equation of an N-electron system directly, thus avoiding the self-consistent field approximation. We shall also see that when many-electron Sturmian basis sets are used, the kinetic energy term disappears from the secular equation. As an additional benefit, there is an automatic optimization of the orbital exponents. Many-electron Sturmian basis functions were discussed several years ago by Avery and Herschbach [4,5]; but the potential, $V_0(\mathbf{x})$, used in these two references was the d-dimensional hydrogenlike potential, where $d = 3N$; and many basis functions of this type were needed for accurate representation of cusps [6]. Recently Aquilanti and Avery [7,8] introduced a method for constructing many-electron Sturmians based on the actual external potential experienced by an N-electron system; and the convergence with this new type of basis set has proved to be very rapid. It seems, therefore, that the new many-electron Sturmian method offers a promising alternative to SCF-CI methods in atomic and molecular electron structure calculations.

2 Orthonormality relations for many-electron Sturmians

If atomic units are used, the position-space Schrödinger equation can be written in the form:

$$\left[-\Delta + p_0^2 + 2V(\mathbf{x}) \right] \psi(\mathbf{x}) = 0 \tag{1}$$

where

$$p_0^2 \equiv -2E \tag{2}$$

and where Δ is the generalized Laplacian operator:

$$\Delta \equiv \sum_{j=1}^{d} \frac{\partial^2}{\partial x_j^2} \tag{3}$$

where $x_1, ..., x_d$ are the $d = 3N$ mass-weighted Cartesian coordinates of the particles in an N-particle system. Suppose that we have two solutions of the Schrödinger equation for some potential, $V_0(\mathbf{x})$, so that

$$\begin{aligned}
\left[\Delta - p_0^2\right] \phi_\nu(\mathbf{x}) &= 2\beta_\nu V_0(\mathbf{x})\phi_\nu(\mathbf{x}) \\
\left[\Delta - p_0^2\right] \phi_{\nu'}^*(\mathbf{x}) &= 2\beta_{\nu'}^* V_0(\mathbf{x})\phi_{\nu'}^*(\mathbf{x})
\end{aligned} \tag{4}$$

where ν stands for a set of quantum numbers labeling the solutions to (4). Here β_ν is a weighting factor, chosen is such a way that both solutions correspond to the same value of p_0 and hence the same energy, although their quantum numbers may be different. If we multiply the two equations respectively by $\phi_{\nu'}^*(\mathbf{x})$ and $\phi_\nu(\mathbf{x})$, integrate over the coordinates, take the difference between the two equations, and make use of the Hermiticity of the operator $\Delta - p_0^2$, we obtain [9]:

$$0 = (\beta_{\nu'}^* - \beta_\nu) \int dx \ \phi_{\nu'}^*(\mathbf{x})V_0(\mathbf{x})\phi_\nu(\mathbf{x}) \tag{5}$$

Thus β_ν must be real, and whenever $\beta_{\nu'} \neq \beta_\nu$, the two Sturmian functions are orthogonal with respect to potential-weighted integration over the coordinates. It is convenient to normalize our Sturmian basis sets in such a way that

$$\int dx \ \phi_{\nu'}^*(\mathbf{x})V_0(\mathbf{x})\phi_\nu(\mathbf{x}) = -\frac{p_0^2}{\beta_\nu}\delta_{\nu',\nu} \tag{6}$$

This special normalization is convenient because it leads to momentum-space orthonormality relations of the form:

$$\int dp \left(\frac{p_0^2 + p^2}{2p_0^2} \right) \phi_{\nu'}^{*t}(\mathbf{p}_j)\phi_\nu^t(\mathbf{p}_j) = \delta_{\nu',\nu} \tag{7}$$

regardless of the dimension of the space. To show that (7) follows from (6), we first introduce the Fourier transform relationships

$$\begin{aligned}
\phi_\nu(\mathbf{x}) &= \frac{1}{(2\pi)^{d/2}} \int dp \ e^{i\mathbf{p}\cdot\mathbf{x}}\phi_\nu^t(\mathbf{p}_j) \\
\phi_\nu^t(\mathbf{p}_j) &= \frac{1}{(2\pi)^{d/2}} \int dx \ e^{-i\mathbf{p}\cdot\mathbf{x}}\phi_\nu(\mathbf{x})
\end{aligned} \tag{8}$$

where $e^{i\mathbf{p}\cdot\mathbf{x}}$ is a d-dimensional plane wave defined by:

$$e^{i\mathbf{p}\cdot\mathbf{x}} \equiv e^{i(p_1 x_1 + \cdots + p_d x_d)} \tag{9}$$

If we introduce the Fourier transform expression for $\phi_\nu(\mathbf{x})$ into the left-hand side of the first of equations (4), we obtain:

$$\frac{1}{(2\pi)^{d/2}} \int dp\ e^{i\mathbf{p}\cdot\mathbf{x}} \left[p^2 + p_0^2\right] \phi_\nu^t(\mathbf{p}) = -2\beta_\nu V_0(\mathbf{x})\phi_\nu(\mathbf{x}) \qquad (10)$$

Next, we multiply both sides of (10) by $e^{-i\mathbf{p}'\cdot\mathbf{x}}/(2\pi)^{d/2}$ and integrate over $dx \equiv dx_1 dx_2...dx_d$ This gives us:

$$(p'^2 + p_0^2)\phi_\nu^t(\mathbf{p}) = -\frac{2\beta_\nu}{(2\pi)^{d/2}} \int dx\ e^{-i\mathbf{p}'\cdot\mathbf{x}} V_0(\mathbf{x})\phi_\nu(\mathbf{x}) \qquad (11)$$

where we have made use of the fact that

$$\frac{1}{(2\pi)^d} \int dx\ e^{-i(\mathbf{p}-\mathbf{p}')\cdot\mathbf{x}} = \delta(\mathbf{p} - \mathbf{p}') \qquad (12)$$

Since the scalar product of two functions in position space is equal to the scalar product of their Fourier transforms in momentum space, we can write

$$\int dx\ \phi_{\nu'}^*(\mathbf{x}) V_0(\mathbf{x})\phi_\nu(\mathbf{x}) = \int dp\ \phi_{\nu'}^{*t}(\mathbf{p}) \left[V_0(\mathbf{x})\phi_\nu\right]^t(\mathbf{p}) = -\frac{p_0^2}{\beta_\nu}\delta_{\nu',\nu} \qquad (13)$$

From (11), we have

$$(p^2 + p_0^2)\phi^t(\mathbf{p}) = -2\beta_\nu \left[V_0(\mathbf{x})\phi_\nu\right]^t(\mathbf{p}) \qquad (14)$$

and by combining (13) and (14) we obtain the momentum-space orthonormality relation, (7). Since we are dealing with a many-dimensional space, ν represents a set of quantum numbers rather than a single quantum number. Orthogonality with respect to the quantum number (or numbers) on which β_ν depends follows automatically from (6) and (7), i.e. Sturmian basis functions corresponding to different values of β_ν are necessarily orthogonal; but orthogonality with respect to the minor quantum numbers must be constructed or proved in some other way, for example by symmetry arguments.

3   Elimination of the kinetic energy

If we begin with the position-space Schrödinger equation, (1), and expand the wave function in terms of a set of many-particle Sturmian basis functions, so that

$$\psi(\mathbf{x}) = \sum_\nu \phi_\nu(\mathbf{x})B_\nu \qquad (15)$$

we obtain:

$$\sum_{\nu} \left[-\Delta + p_0^2 + 2V(\mathbf{x})\right] \phi_{\nu}(\mathbf{x})B_{\nu} = 0 \tag{16}$$

Since the Sturmian basis functions, $\phi_{\nu}(\mathbf{x})$, are solutions of (4), equation (15) can be rewritten in the form:

$$\sum_{\nu} \left[-\beta_{\nu}V_0(\mathbf{x}) + V(\mathbf{x})\right] \phi_{\nu}(\mathbf{x})B_{\nu} = 0 \tag{17}$$

we now multiply (17) on the left by $\phi_{\nu'}^*(\mathbf{x})$ and integrate over the coordinates, making use of the orthonormality relation shown in equation (6):

$$\sum_{\nu} \left[p_0^2 \delta_{\nu',\nu} + \int dx\ \phi_{\nu'}^*(\mathbf{x})V(\mathbf{x})\phi_{\nu}(\mathbf{x})\right] B_{\nu} = 0 \tag{18}$$

If we let

$$T_{\nu',\nu} \equiv -\frac{1}{p_0} \int dx\ \phi_{\nu'}^*(\mathbf{x})V(\mathbf{x})\phi_{\nu}(\mathbf{x}) \tag{19}$$

(where the minus sign is motivated by the fact that the potential is assumed to be attractive), then we obtain the Sturmian secular equation:

$$\sum_{\nu} \left[T_{\nu',\nu} - p_0 \delta_{\nu',\nu}\right] B_{\nu} = 0 \tag{20}$$

For systems interacting through Coulomb forces, $T_{\nu',\nu}$, as defined by equation (19), is independent of p_0. Notice that the eigenvalues of the Sturmian secular equation (20) are not values of the energy but values of the parameter p_0, which is related to the binding energy of bound states by equation (2).

4   Construction of many-electron Sturmians

If we let $\mathbf{x}_j$ represent the Cartesian coordinates of the jth electron in an N-electron system, and if $V_0(\mathbf{x})$ is an external potential, then

$$V_0(\mathbf{x}) = \sum_{j=1}^{N} v(\mathbf{x}_j) \tag{21}$$

where $v(\mathbf{x}_j)$ is the potential experienced by a single electron. Suppose that we know a set of functions, $\chi_{\mu}(\mathbf{x})$ which satisfy one-electron equations of the form

$$[\Delta_j - k_{\mu}^2]\chi_{\mu}(\mathbf{x}_j) = 2b_{\mu}k_{\mu}v(\mathbf{x}_j)\chi_{\mu}(\mathbf{x}_j) \tag{22}$$

where

$$\Delta_j \equiv \frac{\partial^2}{\partial x_j^2} + \frac{\partial^2}{\partial y_j^2} + \frac{\partial^2}{\partial z_j^2} \tag{23}$$

so that

$$\sum_{j=1}^{N} \Delta_j = \Delta \tag{24}$$

and let us suppose that the parameters k_μ and b_μ are chosen in such a way that

$$k_\mu^2 + k_{\mu'}^2 + k_{\mu''}^2 + \dots = p_0^2 \tag{25}$$

and

$$k_\mu b_\mu = \beta_\nu \tag{26}$$

Then

$$\phi_\nu(\mathbf{x}) = \chi_\mu(\mathbf{x}_1)\chi_{\mu'}(\mathbf{x}_2)\dots\chi_{\mu''}(\mathbf{x}_N) \tag{27}$$

will satisfy

$$\left[\Delta - p_0^2\right]\phi_\nu(\mathbf{x}) = 2\beta_\nu V_0(\mathbf{x})\phi_\nu(\mathbf{x}) \tag{28}$$

with

$$p_0^2 = \beta_\nu^2 \left(\frac{1}{b_\mu^2} + \frac{1}{b_{\mu'}^2} + \frac{1}{b_{\mu''}^2} + \dots\right) \tag{29}$$

This gives us a prescription for constructing many-electron Sturmians provided we are able to solve the single-electron Schrödinger equation, (22), and provided that the parameters k_μ and b_μ satisfy the subsidiary relations, (25) and (26). Antisymmetrized products of functions of the form shown in equation (27) will, of course, also satisfy (28).

5   N-electron atoms

As an illustrative example, we can consider the ground states and excited states of N-electron atoms in the approximation where the nucleus is assumed to be infinitely heavy. In this example,

$$v(\mathbf{x}_j) = -\frac{Z}{r_j} \tag{30}$$

where Z is the nuclear charge, and where r_j is the distance of the jth electron from the nucleus. We next let

$$\begin{aligned}
\chi_{nlm,+1/2}(\mathbf{x}_j) &= R_{nl}(r_j)Y_{lm}(\theta_j, \phi_j)\alpha(j) \\
\chi_{nlm,-1/2}(\mathbf{x}_j) &= R_{nl}(r_j)Y_{lm}(\theta_j, \phi_j)\beta(j)
\end{aligned} \tag{31}$$

where

$$\begin{aligned}
R_{nl}(r_j) &= \mathcal{N}_{nl}(2k_n r_j)^l e^{-k_n r_j} F(l+1-n|2l+2|2k_n r_j) \\
\mathcal{N}_{nl} &= \frac{2k_n^{3/2}}{(2l+1)!}\sqrt{\frac{(l+n)!}{n(n-l-1)!}}
\end{aligned} \tag{32}$$

and where $F(a|b|c)$ is a confluent hypergeometric function. The hydrogenlike functions $\chi_{nlms}(\mathbf{x}_j)$ can be shown to obey the following equations:

$$[\Delta_j - k_n^2]\chi_{nlms}(\mathbf{x}_j) = 2\left(\frac{nk_n}{Z}\right)\left(-\frac{Z}{r_j}\right)\chi_{nlms}(\mathbf{x}_j) \tag{33}$$

$$\int d\tau_j |\chi_{nlms}(\mathbf{x}_j)|^2 \left(-\frac{Z}{r_j}\right) = -\frac{k_n^2}{(nk_n/Z)} \tag{34}$$

and

$$\int d\tau_j |\chi_{nlms}(\mathbf{x}_j)|^2 = 1 \tag{35}$$

where $\int d\tau_j$ stands for integration over the space coordinates and summation over the spin coordinates of the jth electron. Within the set of one-electron hydrogenlike functions corresponding to a particular value of β_ν, an additional orthonormality relation holds:

$$\int d\tau_j\, \chi_{nlms}^*(\mathbf{x}_j)\chi_{n'l'm's'}(\mathbf{x}_j) = \delta_{n'n}\delta_{l'l}\delta_{m'm}\delta_{s's} \tag{36}$$

Then

$$\phi_\nu(\mathbf{x}) \equiv \chi_{nlms}(\mathbf{x}_1)\chi_{n'l'm's'}(\mathbf{x}_2)...\chi_{n''l''m''s''}(\mathbf{x}_N) \tag{37}$$

will satisfy equation (28), provided that

$$\beta_\nu = \frac{nk_n}{Z} = \frac{n'k_{n'}}{Z} = ... \tag{38}$$

In other words, we must make the identification

$$b_n = \frac{n}{Z} \tag{39}$$

From the subsidiary relations

$$p_0^2 = k_n^2 + k_{n'}^2 + ... \tag{40}$$

we can now find values for the one-electron orbital exponents k_n in terms of p_0:

$$k_n = \frac{Z\beta_\nu}{n} = \frac{p_0}{n\sqrt{\frac{1}{n^2} + \frac{1}{n'^2} + ...}} \tag{41}$$

The value of p_0 for a particular state of an atom appears as a root of the secular equation, and is therefore determined by diagonalization of the matrix $T_{\nu',\nu}$, equation (19), a matrix which is independent of p_0. Thus the values of the orbital exponents k_n are completely determined by solution of the secular equation. In the lowest approximation, we can represent the ground-state of

an atom or ion by a single determinential Sturmian function. For example, the ^1S ground states of the two-electron isoelectronic series can be represented in the lowest approximation by the single determinential Sturmian basis function:

$$\phi_0(\mathbf{x}) = |\chi_{1s}\chi_{\bar{1}s}| \equiv \frac{1}{\sqrt{2}}[\chi_{1s}(1)\chi_{\bar{1}s}(2) - \chi_{1s}(2)\chi_{\bar{1}s}(1)] \tag{42}$$

Similarly, the ^2S ground states of the three-electron isoelectronic series can be approximates by

$$\phi_0(\mathbf{x}) = |\chi_{1s}\chi_{\bar{1}s}\chi_{2s}| \tag{43}$$

and the ^1S ground states of the four-electron isoelectronic series by

$$\phi_0(\mathbf{x}) = |\chi_{1s}\chi_{\bar{1}s}\chi_{2s}\chi_{\bar{2}s}| \tag{44}$$

The determinential wave functions shown in equations (42)-(44) have the correct normalization for many-electron Sturmians (i.e. the normalization required by equation (6)). To see this, we can make use of the Slater-Condon rules, which hold for the diagonal matrix elements of

$$V_0(\mathbf{x}) = -\sum_{j=1}^{N}\frac{Z}{r_j} \tag{45}$$

because of equation (36). From the Slater-Condon rules, and from the subsidiary relations (38)-(41), it follows that

$$\begin{aligned}
-\frac{1}{p_0}\int dx|\phi_0(\mathbf{x})|^2 V_0(\mathbf{x}) &= -\frac{1}{p_0}\sum_{\mu}\int d\tau_1|\chi_\mu(1)|^2\left(-\frac{Z}{r_1}\right) \\
&= \frac{1}{p_0}\sum_n\frac{k_n^2}{(nk_n/Z)} = \frac{p_0}{\beta_0} \\
&= Z\left(\frac{1}{n^2} + \frac{1}{n'^2} + ...\right)^{1/2}
\end{aligned} \tag{46}$$

so that the determinential functions in equations (42)-(44) have the normalization required by (6).

In our example,

$$V(\mathbf{x}) = V_0(\mathbf{x}) + V'(\mathbf{x}) \tag{47}$$

where $V'(\mathbf{x})$ is the interelectron repulsion term:

$$V'(\mathbf{x}) = \sum_{i>j}^{N}\sum_{j=1}^{N}\frac{1}{r_{ij}} \tag{48}$$

Again making use of the Slater-Condon rules, we find that

$$-\frac{1}{p_0} \int dx |\phi_0(\mathbf{x})|^2 V'(\mathbf{x}) = -\frac{1}{p_0} \sum_{\mu'>\mu} \sum_{\mu} \int d\tau_1 \int d\tau_2 \left[|\chi_\mu(1)|^2 |\chi_{\mu'}(2)|^2 \right.$$
$$\left. - \chi_\mu^*(1)\chi_{\mu'}(1)\chi_\mu(2)\chi_{\mu'}^*(2) \right] \frac{1}{r_{12}} \equiv T'_{0,0} \qquad (49)$$

The Coulomb and exchange integrals can be evaluated exactly [8] yielding the values:

$$\frac{1}{(4\pi)^2} \int d^3 x_1 \int d^3 x_2 \frac{1}{r_{12}} |R_{10}(r_1)|^2 |R_{10}(r_2)|^2 = \frac{5}{8} k_1 \qquad (50)$$

and similarly,

$$\frac{1}{(4\pi)^2} \int d^3 x_1 \int d^3 x_2 \frac{1}{r_{12}} |R_{20}(r_1)|^2 |R_{20}(r_2)|^2 = \frac{77}{256} k_2 \qquad (51)$$

$$\frac{1}{(4\pi)^2} \int d^3 x_1 \int d^3 x_2 \frac{1}{r_{12}} |R_{10}(r_1)|^2 |R_{20}(r_2)|^2 = \frac{34}{81} k_2 \qquad (52)$$

$$\frac{1}{(4\pi)^2} \int d^3 x_1 \int d^3 x_2 \frac{1}{r_{12}} R_{10}(r_1)R_{20}(r_1)R_{10}(r_2)R_{20}(r_2) = \frac{32}{729} k_2 \qquad (53)$$

where we have made use of the fact that, from equation (41), $k_1 = 2k_2$. The integrals shown in equations (50)-(53) are the ones which we need to solve the Sturmian secular equations for the 2-electron,3-electron and 4-electron isoelectronic series of atoms and ions in the crudest approximation. Substituting the integrals into equation (20) (where the summation disappears because only a single basis function is used), we obtain respectively for the 2-electron series:

$$p_0 = \sqrt{2} \left[Z - \left(\frac{1}{2}\right)\left(\frac{5}{8}\right) \right] \qquad (54)$$

for the 3-electron series:

$$p_0 = \frac{3}{2} Z - \left(\frac{2}{3}\right)\left(\frac{5}{8}\right) - \left(\frac{2}{3}\right)\left(\frac{34}{81}\right) + \left(\frac{1}{3}\right)\left(\frac{32}{729}\right) \qquad (55)$$

and for the 4-electron series:

$$p_0 = \sqrt{\frac{5}{2}} \left[Z - \left(\frac{2}{5}\right)\left(\frac{5}{8}\right) - \left(\frac{1}{5}\right)\left(\frac{77}{256}\right) - \left(\frac{4}{5}\right)\left(\frac{34}{81}\right) + \left(\frac{2}{5}\right)\left(\frac{32}{729}\right) \right] \qquad (56)$$

Table 1 shows analogous equations for p_0 for the ground states of higher isoelectronic series, derived in the crude approximation where only one many-electron Sturmian basis function is used. Figure 1 shows the Clementi's values [10] for the Hartree-Fock ground state energies of the 6-electron isoelectronic series
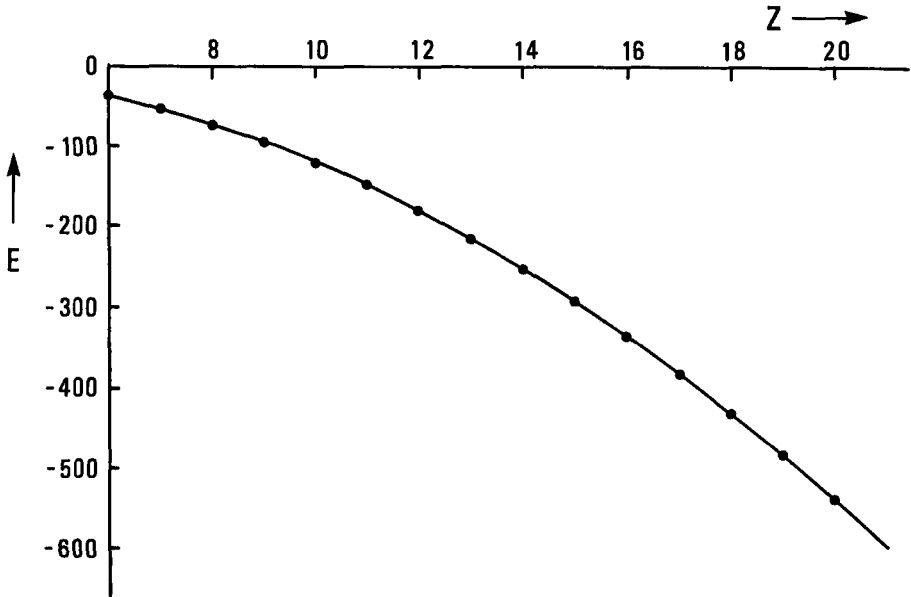
Figure 1: This figure shows the ground-state energies of the 6-electron iso-electronic series of atoms and ions, C, N^+, O^{2+}, F^{3+} etc., as a function of the atomic number, Z. The energies in Hartrees, calculated in the crudest approximation, with only one 6-electron Sturmian basis function (as in Table 1), are represented by the smooth curve, while Clementi's Hartree-Fock values [10] are indicated by dots.

(points) compared with a smooth curve showing the energies derived from Table 1 through the relationship $E = -p_0^2/2$. Equations (54)-(56) and Table 1 can also be compared with Linderberg's perturbation treatment of atoms [11, 12], which, like Clementi's calculation, results in an expansion of the energies in powers of Z. The differences between Table 1 and the results of Clementi and Linderberg follow from the fact that in Table 1, only one basis function of fixed form is used, and thus the present calculation has less freedom for adjustment of the wave functions.

Tables 2, 3 and 4 show the first few excitation energies for the ions Be^{2+}, B^{3+} and C^{4+}, again calculated in the crudes approximation: Only one many-electron Sturmian basis function is used for the ground state, and only one for the excited state. As can be seen from the tables, where the experimental values [13] are also listed, even this very crude approximation gives reasonable results.

If we wish to achieve high accuracy in atomic calculations it is necessary to use basis sets consisting of many Sturmian basis functions $\phi_\nu(\mathbf{x})$, and with these will be associated various values of the parameters β_ν. Inserting the basis functions into equation (19), we construct the matrix $T_{\nu',\nu}$, making use of equations (7) and (46) for evaluating matrix elements of the nuclear attraction part of the potential. In evaluating matrix elements of the interelectron repulsion part of the potential, we must remember that the orthonormality relation shown in equation (36) holds only within the set of one-electron hydrogenlike functions corresponding to a particular value of β_ν. For $\beta_\nu \neq \beta_{\nu'}$, the subsidiary relation shown in equation (41) will result in different values of k_n in the determinential Sturmian basis functions which enter the matrix element of the interelectron repulsion part of the potential. The usual Slater-Condon rules must then be replaced by the generalized Slater-Condon relations, which have been developed by Löwdin [14], Amos and Hall [15], and King et al. [16].

6   Molecular Sturmians

Momentum-space methods, pioneered by McWeeny, Fock, Shibuya, Wulfman, Judd, Koga, Aquilanti and others [4,17-26] provide us with an easy and accurate method for constructing solutions to the Schrödinger equation of a single electron moving in a many-center Coulomb potential

$$v(\mathbf{x}_j) = \sum_a \frac{Z_a}{|\mathbf{x}_j - \mathbf{X}_a|} \tag{57}$$

Thus, we are able to solve the one-electron equation:

$$[\Delta_j - k_\mu^2]\varphi_\mu(\mathbf{x}_j) = 2b_\mu k_\mu v(\mathbf{x}_j)\varphi_\mu(\mathbf{x}_j) \tag{58}$$

where $v(\mathbf{x}_j)$ is the actual external potential for an electron moving in the attractive Coulomb potential of the nuclei in a molecule. Having found solutions to (58), we can then apply the formalism outline in equations (21)-(29) to construct a many-electron molecular Sturmian basis set based on the nuclear attraction potential experienced by the electrons in a molecule. Let us begin by reviewing the momentum-space methods for solving the many-center one-particle problem, since these methods are unfamiliar to most quantum chemists: Let

$$\varphi_\mu^t(\mathbf{p}_j) \equiv \frac{1}{(2\pi)^{3/2}} \int d^3x_j e^{-i\mathbf{p}_j \cdot \mathbf{x}_j} \varphi_\mu(\mathbf{x}_j) \tag{59}$$

and

$$\chi_{nlm}^t(\mathbf{p}_j) \equiv \frac{1}{(2\pi)^{3/2}} \int d^3x_j e^{-i\mathbf{p}_j \cdot \mathbf{x}_j} \chi_{nlm}(\mathbf{x}) \tag{60}$$

where $\chi_{nlm}(\mathbf{x}) = R_{nl}(r_j)Y_{lm}(\hat{\mathbf{x}}_j)$ and where the functions $R_{nl}(r_j)$ are defined by (32) with $k_n = k_\mu$ for all the functions of the set. If we next let

$$\xi_\tau(\mathbf{p}_j) \equiv \sqrt{\frac{Z_a}{n}} e^{i\mathbf{p}_j \cdot \mathbf{X}_a} \chi_{nlm}^t(\mathbf{p}_j) \tag{61}$$

and

$$\varphi_\mu^t(\mathbf{p}_j) = \sum_\tau \xi_\tau(\mathbf{p}_j) C_{\tau,\mu} \tag{62}$$

then the functions $\varphi_\mu(\mathbf{x}_j)$ will satisfy (58) provided that [4,17-26]

$$\sum_\tau \left[K_{\tau',\tau} - b_\mu^{-1} \delta_{\tau',\tau} \right] C_{\tau,\mu} = 0 \tag{63}$$

where

$$K_{\tau',\tau} \equiv \int d^3p_j \left(\frac{p_j^2 + k_\mu^2}{2k_\mu^2} \right) \xi_{\tau'}^*(\mathbf{p}_j) \xi_\tau(\mathbf{p}_j) \tag{64}$$

Substitution of the definition (61) into (64) yields

$$K_{\tau',\tau} = \sqrt{\frac{Z_{a'} Z_a}{n'n}} \int d^3p_j \left(\frac{p_j^2 + k_\mu^2}{2k_\mu^2} \right) e^{i\mathbf{p}_j \cdot (\mathbf{X}_a - \mathbf{X}_{a'})} \chi_{nlm}^{t*}(\mathbf{p}_j) \chi_{nlm}^t(\mathbf{p}_j) \tag{65}$$

Thus the many-center one-electron problem is easily solved, provided that the integrals shown in equation (65) can be evaluated. The reciprocals of the parameters b_μ can then be identified with the roots of the secular equation (63).

7 Evaluation of the Shibuya-Wulfman integrals

The Fourier transforms of the hydrogenlike orbitals were shown by Fock [18] to be expressible in terms of 4-dimensional hyperspherical harmonics when momentum space is mapped onto the surface of a 4-dimensional unit hypersphere by the transformation:

$$
\begin{aligned}
u_j &= \frac{k_\mu p_j}{p_j^2 + k_\mu^2} \qquad j = 1, 2, 3 \\
u_4 &= \frac{p_j^2 - k_\mu^2}{p_j^2 + k_\mu^2}
\end{aligned}
\tag{66}
$$

With this transformation, as Fock was able to show, the Fourier-transformed hydrogenlike orbitals become:

$$
\chi_{nlm}^t(\mathbf{p}_j) = \frac{4k_\mu^{5/2}}{(k_\mu^2 + p_j^2)^2} Y_{n-1,l,m}(\mathbf{u})
\tag{67}
$$

The first few 4-dimensional hyperspherical harmonics $Y_{n-1,l,m}(\mathbf{u})$ are shown in Table 5. Shibuya and Wulfman [19] extended Fock's momentum-space method to the many-center one-particle Schrödinger equation, and from their work it follows that the solutions can be found by solving the secular equation (63). If Fock's relationship, equation (67), is substituted into (65), we obtain:

$$
K_{\tau', \tau} = \sqrt{\frac{Z_{a'} Z_a}{n'n}} S_{n'l'm'}^{nlm}
\tag{68}
$$

where

$$
S_{n'l'm'}^{nlm} = \int d^3 p_j \left(\frac{2k_\mu}{p_j^2 + k_\mu^2} \right)^3 e^{i \mathbf{p}_j \cdot \mathbf{R}} Y_{n'-1,l',m'}^*(\mathbf{u}) Y_{n-1,l,m}(\mathbf{u})
\tag{69}
$$

and where $\mathbf{R} \equiv \mathbf{X}_a - \mathbf{X}_{a'}$. When 3-dimensional momentum space is mapped onto a 4-dimensional unit sphere by Fock's transformation, the resulting 4-dimensional solid angle $d\Omega$ is related to the volume element in momentum space by

$$
d\Omega = d^3 p_j \left(\frac{2k_\mu}{p_j^2 + k_\mu^2} \right)^3
\tag{70}
$$

Thus we can rewrite (69) in the form:

$$
S_{n'l'm'}^{nlm} = \int d\Omega e^{i \mathbf{p}_j \cdot \mathbf{R}} Y_{n'-1,l',m'}^*(\mathbf{u}) Y_{n-1,l,m}(\mathbf{u})
\tag{71}
$$

Shibuya and Wulfman evaluated this integral for $m = m' = 0$ for the first few values of the other quantum numbers using a method involving the coupling

coefficients for 4-dimensional hyperspherical harmonics; and this allowed them to treat the problem of an electron moving in the field of two nuclei. Koga and his co-workers [22] developed the method further, and achieved remarkable (10-figure) accuracy in treating one-electron diatomic molecules. An alternative and easier method for evaluating the Shibuya-Wulfman integrals, (71), was developed and successfully used at our laboratory in Copenhagen [25-27]. Like the Shibuya-Wulfman method, this alternative procedure makes use of the relationship:

$$\chi_{nlm}(\mathbf{R}) \equiv \frac{1}{(2\pi)^{3/2}} \int d^3 p_j e^{i\mathbf{p}_j \cdot \mathbf{R}} \chi_{nlm}^t(\mathbf{p}_j) \tag{72}$$

which is just the inverse of the Fourier transform shown in equation (60), with x_j replaced by $\mathbf{R}$. Making use of (72), (32) and the definition of the 4-dimensional hyperspherical harmonics [4], we obtain [25-27]:

$$\frac{1}{2\pi^2} \int d\Omega \ e^{i\mathbf{k}\cdot\mathbf{R}} \ u_4^k h_l(u_j) = \mathcal{F}_{k,l}(s) h_l(s_j) \tag{73}$$

where $s \equiv k_\mu R$,

$$s_j \equiv k_\mu R_j \qquad j = 1, 2, 3 \tag{74}$$

and where $\mathcal{F}_{k,l}(s)$ is the easily-programmed function

$$\mathcal{F}_{k,l}(s) \equiv \frac{i^l k! e^{-s}}{2^k (2l+1)!} \left[\sum_{q=0}^{[k/2]} \frac{2(k+2l+1-2q)! F(2q-k|2l+2|2s)}{q!(k+l+1-q)!(k-2q)!} \right.$$

$$\left. -(k+1) \sum_{q=0}^{[(k+1)/2]} \frac{(k+2l+2-2q)! F(2q-k-1|2l+2|2s)}{q!(k+l+2-q)!(k+1-2q)!} \right] \tag{75}$$

In (73), $h_l(u_j)$ is an harmonic polynomial of order l in u_1, u_2 and u_3, while $h_l(s_j)$ is the same harmonic poynomial with u_j replaced by s_j [25-27]. The Shibuya-Wulfman integrals can then be calculated by resolving the product of hyperspherical harmonics in (71) into terms of the form $u_4^k h_l(u_j)$ For example, when $u_4^k h_l = 1$, (73) becomes:

$$\frac{1}{2\pi^2} \int d\Omega e^{i\mathbf{p}\cdot\mathbf{R}} = \mathcal{F}_{0,0}(s) = e^{-s}(1+s) \tag{76}$$

Since $Y_{000}(\mathbf{u}) = 1/\sqrt{2\pi^2}$, we have

$$S_{100}^{100} = \int d\Omega e^{i\mathbf{p}_j \cdot \mathbf{R}} Y_{000}^*(\mathbf{u}) Y_{000}(\mathbf{u}) = e^{-s}(1+s) \tag{77}$$

The functions $F_{k,l}(s)$ are illustrated in Table 6, while Shibuya-Wulfman integrals derived from equation (73)-(75) are shown in Table 7 for the first few

atomic orbitals. The Shibuya-Wulfman integrals can be evaluated once and
for all using a program such as Mathematica; and they can afterwards be
incorporated as functions into Fortran programs.

As a simple example to illustrate reciprocal-space solutions to the many-
center one-particle problem, we can think of an electron moving in the Coulomb
potential of two nuclei, with nuclear charges Z_1 and Z_2, located respectively at
positions $\mathbf{X}_1$ and $\mathbf{X}_2$. In the crude approximation where we use only a single
$1s$ orbital on each nucleus, we can represent the electronic wave function of
this system by:

$$\varphi_\mu(\mathbf{p}_j) \approx \xi_1(\mathbf{p}_j)C_{1,\mu} + \xi_2(\mathbf{p}_j)C_{2,\mu} \tag{78}$$

where

$$\xi_1(\mathbf{p}_j) \equiv \sqrt{Z_1}\ e^{i\mathbf{p}_j \cdot \mathbf{X}_1} Y_{000}(\mathbf{u}) = \frac{1}{\pi}\sqrt{\frac{Z_1}{2}}\ e^{i\mathbf{p}_j \cdot \mathbf{X}_1}$$

$$\xi_2(\mathbf{p}_j) \equiv \sqrt{Z_2}\ e^{i\mathbf{p}_j \cdot \mathbf{X}_2} Y_{000}(\mathbf{u}) = \frac{1}{\pi}\sqrt{\frac{Z_2}{2}}\ e^{i\mathbf{p}_j \cdot \mathbf{X}_2} \tag{79}$$

Then (using (76) and the orthonormality of the 4-dimensional hyperspherical
harmonics) we obtain:

$$K_{\tau',\tau} = \begin{pmatrix} Z_1 & \sqrt{Z_1 Z_2}\ e^{-s}(1+s) \\ \sqrt{Z_1 Z_2}\ e^{-s}(1+s) & Z_2 \end{pmatrix} \tag{80}$$

where

$$s \equiv k_\mu R = k_\mu |\mathbf{X}_1 - \mathbf{X}_2| \tag{81}$$

The secular equations, (63), then require that

$$\begin{vmatrix} Z_1 - b_\mu^{-1} & \sqrt{Z_1 Z_2}\ e^{-s}(1+s) \\ \sqrt{Z_1 Z_2}\ e^{-s}(1+s) & Z_2 - b_\mu^{-1} \end{vmatrix} = 0 \tag{82}$$

or

$$2b_\mu^{-1} = Z_1 + Z_2 \pm \sqrt{(Z_1 + Z_2)^2 + 4Z_1 Z_2 \left[(1+s)^2 e^{-2s} - 1\right]} \tag{83}$$

We can use equation (83) to generate a curve representing the ground-state
one-electron energy of the system, $\epsilon_\mu = -1/(2b_\mu^2)$ as a function of the inter-
nuclear distance, R. We do this by picking a value of s, substituting it into
(83) to find the corresponding value of b_μ^{-1}, and then finding the internuclear
separation by means of the relationships, $R = s/k_\mu$ and $k_\mu b_\mu = \beta_\nu$. In the
united-atom limit, $R = 0$, the $+$-root of the quadratic equation, (83), yields
the exact one-electron ground-state energy of the system.

$$b_{\mu+}^{-1} = Z_1 + Z_2 \qquad \epsilon_+ = -\frac{(Z_1 + Z_2)^2}{2} \tag{84}$$
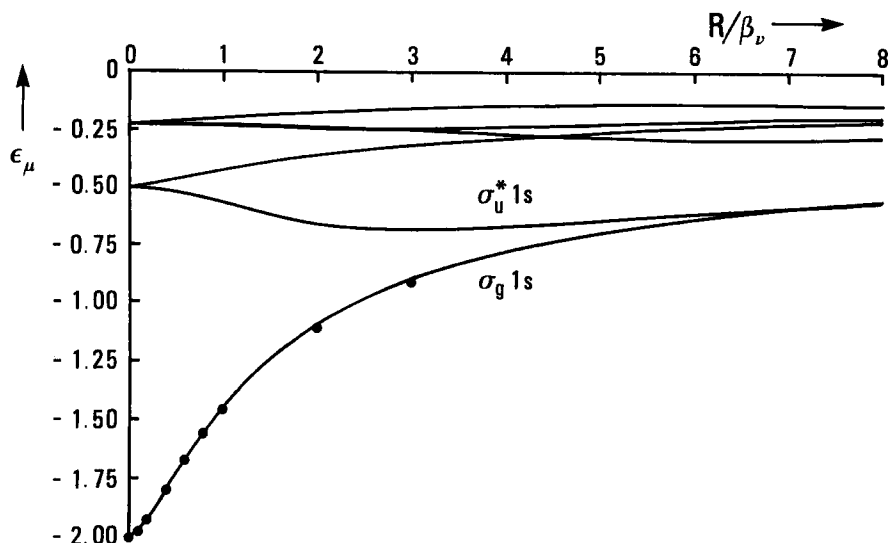
Figure 2: The one-electron energies $\epsilon_\mu = -1/(2b_\mu^2)$ for an electron moving in the field of two protons are shown here as functions of the internuclear distance R. The energies represented by the smooth curves were calculated using 10 atomic basis functions on each center. For the lowest curve, the best available calculated values [22] are indicated by dots. All energies are in Hartrees.

In the separated-atom limit, $R = \infty$, equation (83) also yields exact energies:

$$b_{\mu+}^{-1} = Z_1 \qquad \epsilon_+ = -\frac{Z_1^2}{2}$$

$$b_{\mu-}^{-1} = Z_2 \qquad \epsilon_- = -\frac{Z_2^2}{2} \qquad (85)$$

For intermediate values of R, the ground-state energies predicted by (83) are appreciably above the best available values found from direct space calculations; but when more basis functions are added, the Sturmian expansion converges rapidly towards the best available wave functions and energies, as illustrated in Figure 2. By using many basis functions in a calculation of the type sketched above, Koga and Matsuhashi [22] obtained electronic energies with 10-figure accuracy for the H_2^+ ion. Their energies at various internuclear

separations agreed with the best available values from direct-space calculations; but the Koga-Matsuhashi momentum-space values were of higher precision.

8   Normalization of molecular Sturmians

If we wish to make accurate molecular calculations with many-electron Sturmians, we must pay careful attention to the question of normalization: Suppose that we wish to find the normalization constant $\mathcal{N}$ for the basis function:

$$\phi_\nu(\mathbf{x}) = \mathcal{N}\varphi_\mu(\mathbf{x}_1)\varphi_{\mu'}(\mathbf{x}_2)...\varphi_{\mu''}(\mathbf{x}_N) \tag{86}$$

and its Fourier transform

$$\phi_\nu^t(\mathbf{p}) = \mathcal{N}\varphi_\mu^t(\mathbf{p}_1)\varphi_{\mu'}^t(\mathbf{p}_2)...\varphi_{\mu''}^t(\mathbf{p}_N) \tag{87}$$

according to the requirements of equations (6) and (7). We know that

$$\varphi_\mu^t(\mathbf{p}_1) = \sum_\tau \xi_\tau(\mathbf{p}_1)C_{\tau,\mu} \tag{88}$$

is a solution to the secular equation (63); and we can normalize $\varphi_\mu^t(\mathbf{p}_1)$ in such a way that $C_{\tau,\mu}$ is a unitary matrix. Then

$$\sum_\tau C_{\tau,\mu'}^* C_{\tau,\mu} = \delta_{\mu',\mu} \tag{89}$$

and

$$C_{\tau,\mu}^* = C_{\mu,\tau}^{-1} \tag{90}$$

From (7) we have the requirement:

$$
\begin{aligned}
1 &= \int dp \left(\frac{p^2 + p_0^2}{2p_0^2}\right) |\phi_\nu^t(\mathbf{p})|^2 \\
&= \frac{\mathcal{N}^2}{p_0^2}\left[k_\mu^2 \int d^3p_1 \left(\frac{p_1^2 + k_\mu^2}{2k_\mu^2}\right) |\varphi_\mu^t(\mathbf{p}_1)|^2 \int d^3p_2 |\varphi_{\mu'}^t(\mathbf{p}_2)|^2 ..... \right. \\
&\qquad \left. + k_{\mu'}^2 \int d^3p_1 |\varphi_\mu^t(\mathbf{p}_1)|^2 \int d^3p_2 \left(\frac{p_2^2 + k_{\mu'}^2}{2k_{\mu'}^2}\right) |\varphi_{\mu'}^t(\mathbf{p}_2)|^2 ..... + ... \right]
\end{aligned}
\tag{91}
$$

where we have used the relationships:

$$p_1^2 + p_2^2 + ... + p_M^2 = p^2 \tag{92}$$

and

$$k_\mu^2 + k_{\mu'}^2 + \ldots + k_{\mu''}^2 = p_0^2 \tag{93}$$

Thus, to calculate the normalization constant $\mathcal{N}$, we need to evaluate two kinds of integrals. The first type is easy: Using equations (26), (62)-(64) and (92) we obtain:

$$k_\mu^2 \int d^3 p_1 \left(\frac{p_1^2 + k_\mu^2}{2 k_\mu^2} \right) |\varphi_\mu^t(\mathbf{p}_1)|^2$$

$$= \frac{\beta_\nu^2}{b_\mu^2} \sum_{\tau', \tau} C_{\tau' \mu}^* \left[\int d^3 p_1 \left(\frac{p_1^2 + k_\mu^2}{2 k_\mu^2} \right) \xi_{\tau'}^*(\mathbf{p}_1) \xi_\tau(\mathbf{p}_1) \right] C_{\tau \mu}$$

$$= \frac{\beta_\nu^2}{b_\mu^2} \sum_{\tau', \tau} C_{\mu \tau'}^{-1} K_{\tau' \tau} C_{\tau \mu} = \frac{\beta_\nu^2}{b_\mu^3} \tag{94}$$

The second type of integral has the form:

$$\int d^3 p_1 |\varphi_\mu^t(\mathbf{p}_1)|^2 = \sum_{\tau', \tau} C_{\tau' \mu}^* \left[\int d^3 p_1 \xi_{\tau'}^*(\mathbf{p}_1) \xi_\tau(\mathbf{p}_1) \right] C_{\tau \mu}$$

$$= \sum_{\tau', \tau} C_{\mu \tau'}^{-1} W_{\tau' \tau} C_{\tau \mu} \tag{95}$$

where

$$W_{\tau' \tau} \equiv \int d^3 p_1 \xi_{\tau'}^*(\mathbf{p}_1) \xi_\tau(\mathbf{p}_1)$$

$$= \sqrt{\frac{Z_{a'} Z_a}{n' n}} \int d^3 p_1 e^{i \mathbf{p}_1 \cdot (\mathbf{X}_a - \mathbf{X}_{a'})} \chi_{n' l' m'}^{t*}(\mathbf{p}_1) \chi_{n l m}^t(\mathbf{p}_1)$$

$$= \sqrt{\frac{Z_{a'} Z_a}{n' n}} \int d^3 x_1 \chi_{n' l' m'}^*(\mathbf{x}_1 - \mathbf{X}_{a'}) \chi_{n l m}(\mathbf{x}_1 - \mathbf{X}_a) \tag{96}$$

is proportional to the overlap integral between one-electron hydrogenlike Sturmian basis functions localized on the nuclei a and a'. Luckily these integrals too are easy to evaluate, since they can be generated in much the same way as the Shibuya-Wulfman integrals: Remembering that

$$\chi_{n l m}^t(\mathbf{p}_j) = \frac{4 k_\mu^{5/2}}{(p_j^2 + k_\mu^2)^2} Y_{n-1, l, m}(\mathbf{u}) \tag{97}$$

we can write:

$$\int d^3 p_j e^{i \mathbf{p}_j \cdot (\mathbf{X}_a - \mathbf{X}_{a'})} \chi_{n' l' m'}^{t*}(\mathbf{p}_j) \chi_{n l m}^t(\mathbf{p}_j)$$

$$\int d^3 p_j \left(\frac{2 k_\mu}{p_j^2 + k_\mu^2} \right)^3 e^{i \mathbf{p}_j \cdot \mathbf{R}} \left(\frac{2 k_\mu^2}{p_j^2 + k_\mu^2} \right) Y_{n'-1, l, 'm'}^*(\mathbf{u}) \chi_{n l m}(\mathbf{u})$$

$$\int d\Omega e^{i \mathbf{p}_j \cdot \mathbf{R}} (1 - u_4) Y_{n'-1, l, 'm'}^*(\mathbf{u}) Y_{n-1, l, m}(\mathbf{u}) \tag{98}$$

where $\mathbf{R} = \mathbf{X}_a - \mathbf{X}_{a'}$ and

$$u_4 = \frac{p_j^2 - k_\mu^2}{p_j^2 + k_\mu^2} \tag{99}$$

Just as in the case of the Shibuya-Wulfman integrals, we can make use of equation (73), from which we obtain:

$$\frac{1}{2\pi^2} \int d\Omega e^{i\mathbf{p}_j \cdot \mathbf{R}} (1 - u_4) u_4^k h_l(u_j) = \mathcal{G}_{k,l}(s) h_l(s_j) \tag{100}$$

where $\mathbf{s} = k_\mu \mathbf{R}$ and

$$\mathcal{G}_{k,l}(s) \equiv \mathcal{F}_{k,l}(s) - \mathcal{F}_{k+1,l}(s) \tag{101}$$

For example,

$$\begin{aligned}
\int d^3 x_1 \chi_{1s}^*(\mathbf{x}_1 - \mathbf{X}_{a'}) \chi_{1s}(\mathbf{x}_1 - \mathbf{X}_a) &= \frac{1}{2\pi^2} \int d\Omega e^{i\mathbf{p}_j \cdot \mathbf{R}} (1 - u_4) \\
&= \mathcal{F}_{0,0}(s) - \mathcal{F}_{1,0}(s) \\
&= (1 + s + \frac{s^2}{3}) e^{-s}
\end{aligned} \tag{102}$$

where we have made use of Tables 5 and 6. This is, in fact, just the result which one would have obtained by performing the integration in an elliptic coordinate system. If we assume that the many-electron molecular Sturmian basis functions are properly normalized, matrix elements of the nuclear attraction part of the potential may be evaluated using equation (6), together with the subsidiary conditions (25) and (26):

$$-\frac{1}{p_0} \int dx \; \phi_{\nu'}^*(\mathbf{x}) V_0(\mathbf{x}) \phi_\nu(\mathbf{x}) = \frac{p_0}{\beta_\nu} \delta_{\nu',\nu} = \delta_{\nu',\nu} \left(\frac{1}{b_\mu^2} + \frac{1}{b_{\mu'}^2} + \frac{1}{b_{\mu''}^2} + \ldots \right)^{1/2} \tag{103}$$

where the quantities b_μ^{-1} are roots of equation (63).

9   Interelectron repulsion integrals

The problem of evaluating matrix elements of the interelectron repulsion part of the potential between many-electron molecular Sturmian basis functions has the degree of difficulty which is familiar in quantum chemistry. It is not more difficult than usual, but neither is it less difficult. Both in the present method and in the usual SCF-CI approach, the calculations refer to exponential-type orbitals, but for the purpose of calculating many-center Coulomb and exchange integrals, it is convenient to expand the ETO's in terms of a Cartesian Gaussian basis set. Work to implement this procedure is in progress in our laboratory,

but the program has not yet been completed. However, although accurate evaluation of the matrix elements of the interelectron repulsion part of the potential is not yet possible, it is interesting to see, from a very rough approximation of these matrix elements, that the many-electron molecular Sturmian method gives reasonable results. For example, the H_2 molecule was treated in this way in reference [8], using only two many-electron molecular Sturmians. The resulting equilibrium bond distance was $R = 1.46$ atomic units, which can be compared with the experimental value, $R = 1.40$ atomic units.

10 Discussion

Although the derivations in sections 1-4 are not confined to systems interacting through Coulomb forces, the matrix $T_{\nu',\nu}$ defined in equation (19) is independent of p_0 only in the case of such systems. For Coulomb systems, this independence can be demonstrated with the help of hyperspherical coordinates and hyperspherical Sturmian basis functions, as shown in reference [4], Appendix E and in reference [5]. The examples given in the present paper illustrate this independence for other types of Sturmian basis sets. Furthermore, for the bound states of Coulomb systems, it is always possible to find a set of parameters β_ν which make the solutions to equation (4) all correspond to the same value of the energy, $E = -p_0^2/2$, regardless of the quantum numbers; but if $V_0(\mathbf{x})$ is produced by interactions of another type, this is not always possible. Thus, in two important respects, the method described above is restricted to systems interacting through Coulomb forces.

The simple examples given above show that the many-electron Sturmian approach to atomic and molecular electronic structure calculations yields reasonably accurate results even with very few basis functions, and in the atomic case, with only a single basis function. Calculations using large numbers of many-electron Sturmian basis functions have not yet been made, although a preliminary calculation on the 2-electron isoelectronic series of atoms and ions using 4 basis functions [7] has yielded results considerably closer to experimental values than the Hartree-Fock limit. In the molecular case, accurate evaluation of matrix elements of the interelectron repulsion part of the potential is not yet possible. It seems likely that when many basis functions are used and when interelectron repulsion integrals are accurately evaluated, high calculational precision will be possible using the new method. The advantages of the many-electron Sturmian method are as follows: vanishing of the kinetic energy term in the secular equation; the diagonal form of matrix elements of the nuclear attraction potential; automatic optimization of the orbital exponents; and direct solution of the many-electron Schrödinger equation without

the use of the self-consistent-field approximation. Because of these advantages, the method of many-electron Sturmians and hyperspherical harmonics seems to offer an interesting and useful alternative to the SCF-CI method.

References

1. H. Schull and P.O. Löwdin, J. Chem. Phys. **30**, 617 (1959).

2. M. Rotenberg, Adv. At. Mol. Phys. **6**, 233 (1970).

3. E.J. Weniger, J. Math. Phys. **26**, 276 (1985).

4. J. Avery, *Hyperspherical Harmonics; Applications in Quantum Theory*, Kluwer Academic Publishers, Dordrecht, Netherlands, (1989).

5. J. Avery and D.R. Herschbach, Int. J. Quantum Chem. **41**, 673 (1992).

6. J. Avery and F. Antonsen, J. Math. Chem. **19** 289 (1996).

7. V. Aquilanti and J. Avery, Chem. Phys. Letters, **267**, 1 (1997).

8. J. Avery, J. Math. Chem. (1997) (in press)

9. O. Goscinski, *Preliminary Research Report No. 217*, Quantum Chemistry Group, Uppsala University, (1968).

10. E. Clementi, J. Chem. Phys. **38**, 996 (1963).

11. J. Linderberg, Phys. Rev. **121**, 818 (1961).

12. J. Linderberg, J. Mol. Spec. **9**, 95 (1962).

13. C.E. Moore, *Atomic Energy Levels, Circular of the National Bureau of Standards 467*, Superintendent of Documents, U.S. Government Printing Office, Washington 25 D.C., (1949).

14. P.O. Löwdin, J. Appl. Phys. Suppl. **33**, 251 (1962).

15. A.T. Amos and G.G. Hall, Proc. Roy. Soc. (London) **A263**, 483 (1961).

16. H.F. King, R.E. Stanton, H. Kim, R.E. Wyatt, and R.G. Parr, J. Chem. Phys. **47**, 1936 (1967).

17. R. McWeeny, Proc. Phys. Soc. (London) **A62**, 509 (1949).

18. V.A. Fock, Z. Phys. **98**, 145 (1935); Bull. Acad. Sci. USSR, (1935).

19. T. Shibuya and C.E. Wulfman, Proc. Roy. Soc. **A286**, 376 (1965).

20. B.R. Judd, *Angular Momentum Theory for Diatomic Molecules*, Academic Press, New York, (1975).

21. H. Monkhorst, and B. Jeziorski, J. Chem. Phys. **71**, 5268 (1979).

22. T. Koga and T. Matsuhashi, J. Chem. Phys. **89**, 983 (1988).

23. V. Aquilanti, S. Cavalli, C. Coletti, D. De Fazio and G. Grossi, in *New Methods in Quantum Theory*, C.A. Tsipis, V.S. Popov, D.R. Herschbach and J.S. Avery editors, Kluwer, (1996).

24. V. Aquilanti, S. Cavalli and D. De Fazio, J. Phys. Chem., **99**, 15694 (1995); V. Aquilanti, S. Cavalli, C. Coletti and G. Grossi, Chem. Phys., **209**, 405 (1996).

25. J. Avery, in *Conceptual Trends in Quantum Chemistry*, E.S. Kryachko and J.L. Calais (eds.), Kluwer Academic Publishers, Dordrecht, Netherlands, (1994), pp. 135-169.

26. J. Avery and T.B. Hansen, Int. J. Quantum Chem. **60**, 201 (1996).

27. J. Avery in *New Methods in Quantum Theory*, C.A. Tsipis, V.S. Popov, D.R. Herschbach and J.S. Avery editors, Kluwer, (1996).

Table 1 p_0 **for the first few isoelectronic series of atoms and ions, calculated in the crudest approximation.** $E = -p_0^2/2$.

N	p_0
2	$Z\sqrt{\frac{2}{1}} - .441942$
3	$Z\sqrt{\frac{2}{1} + \frac{1}{4}} - 0.681870$
4	$Z\sqrt{\frac{2}{1} + \frac{2}{4}} - 0.993588$
5	$Z\sqrt{\frac{2}{1} + \frac{3}{4}} - 1.40773$
6	$Z\sqrt{\frac{2}{1} + \frac{4}{4}} - 1.88329$
7	$Z\sqrt{\frac{2}{1} + \frac{5}{4}} - 2.41491$

Table 2 The first few excitation energies for the Be^{2+} ion in $cm.^{-1}$, calculated in the crudest approximation.

name	calc.	expt.	% error
$2s\ ^3S$	951476	956496	0.5
$2s\ ^1S$	969978	—	—
$2p\ ^3P^o$	983287	983348	0.006
$2p\ ^1P^o$	997571	997466	0.01
$3s\ ^3S$	1114864	—	—
$3s\ ^1S$	1119818	—	—
$3p\ ^1P^0$	1127824	1132323	0.4

Table 3 The first few excitation energies for the B^{3+} ion in $cm.^{-1}$, calculated in the crudest approximation.

name	calc.	expt.	% error
$2s \ ^3S$	1596277	1601505	0.3
$2s \ ^1S$	1619597	–	–
$2p \ ^3P^o$	1636385	1636898	0.03
$2p \ ^1P^o$	1654416	1658020	0.2
$3s \ ^3S$	1876161	–	–
$3s \ ^1S$	1882380	–	–
$3p \ ^1P^0$	1892436	1898180	0.3

Table 4 The first few excitation energies for the C^{4+} ion in $cm.^{-1}$, calculated in the crudest approximation.

name	calc.	expt.	% error
$2s\ ^3S$	2405683	2411266	0.2
$2s\ ^1S$	2433821	–	–
$2p\ ^3P^o$	2454088	2455165	0.04
$2p\ ^1P^o$	2483240	2475866	0.3
$3s\ ^3S$	2832546	–	–
$3s\ ^1S$	2840031	–	–
$3p\ ^1P^0$	2852136	2859350	0.3

Table 5:
4-dimensional hyperspherical harmonics

λ	l	m	$\sqrt{2}\pi\ Y_{\lambda,l,m}(\mathbf{u})$
0	0	0	1
1	1	1	$i\sqrt{2}(u_1 + iu_2)$
1	1	0	$-i2u_3$
1	1	-1	$-i\sqrt{2}(u_1 - iu_2)$
1	0	0	$2u_4$

λ	l	m	$\sqrt{2}\pi\ Y_{\lambda,l,m}(\mathbf{u})$
2	2	2	$-\sqrt{3}(u_1 + iu_2)^2$
2	2	1	$2\sqrt{3}u_3(u_1 + iu_2)$
2	2	0	$-\sqrt{2}(2u_3^2 - u_1^2 - u_2^2)$
2	2	-1	$-2\sqrt{3}u_3(u_1 - iu_2)$
2	2	-2	$-\sqrt{3}(u_1 - iu_2)^2$
2	1	1	$2i\sqrt{3}\ u_4(u_1 + iu_2)$
2	1	0	$-2i\sqrt{6}\ u_4u_3$
2	1	-1	$-2i\sqrt{3}\ u_4(u_1 - iu_2)$
2	0	0	$4u_4^2 - 1$

Table 6 $\mathcal{F}_{k,l}(s)$ (equation (75))

k	l	$\mathcal{F}_{k,l}(s)$ $\qquad s \equiv k_\mu R$
0	0	$(1+s)e^{-s}$
0	1	$(i/3)(1+s)e^{-s}$
0	2	$(-1/12)(1+s)e^{-s}$
1	0	$(-1/3)s^2 e^{-s}$
1	1	$(i/12)(1+s-s^2)e^{-s}$
1	2	$(1/60)(-2-2s+s^2)e^{-s}$
2	0	$(1/12)(3+3s-2s^2+s^3)e^{-s}$
2	1	$(i/60)(5+5s-4s^2+s^3)e^{-s}$
2	2	$(1/360)(-9-9s+6s^2-s^3)e^{-s}$

Table 7: Shibuya-Wulfman integrals

	$1s$	$2s$
$1s$	$(1+s)e^{-s}$	$-2s^2 e^{-s}/3$
$2s$	$-2s^2 e^{-s}/3$	$(3+3s-2s^2+s^3)e^{-s}/3$
$2p_j$	$2s_j(1+s)e^{-s}/3$	$s_j(1+s-s^2)e^{-s}/3$

	$2p_1$
$2p_1$	$(3+3s+s^2-s_1^2-ss_1^2)e^{-s}/3$
$2p_2$	$s_1 s_2(1+s)e^{-s}/3$
$2p_3$	$s_1 s_3(1+s)e^{-s}/3$

A study of weakly interacting systems in localized representation, including the many-body effect

Cornelia Kozmutza
Department of Theoretical Physics,
Physics Institute,
Technical University of Budapest,
Hungary

Ernő Tfirst
Central Research Institute for Chemistry
of the Hungarian Academy of Sciences,
Hungary

Abstract

The method of the separated molecular orbitals (SMOs), as a version of the localized representation is discussed as a useful tool for studying weakly interacting systems. As to the Hartree-Fock level, the contributions of the atomic basis sets in some dimers and their counter-poise (CP) corrected systems are compared. The results suggest, that using SMOs the validity of the CP recipe can be demonstrated. The localized many-body perturbation theory (LMBPT) incorporating the method of SMOs makes it possible to study the van der Waals type systems at several levels of correlation. This allows using the SMO-LMBPT scheme for discussing not only the two-body but the many-body interaction energy quantities as well. As an example, the results obtained for the three-body interaction energies in some He-clusters are given. These results show that the three-body effects are negligible in comparison to the two-body ones, the relative significance of the charge-transfer components, on the other hand, are important.

List of contents

1. Introduction

In the present work we summarize and continue a systematic study on van der Waals (vdW) interacting molecules using separated molecular orbitals (SMOs). Since the avoidance of basis set superposition error (BSSE) ([1] and reference therein) turned out to be one of the main problems in the study of vdW systems, we pay special attention to this question. It is known that the counter-poise (CP) method [2] is often used in order to correct the BSSE.

One of our paper [3] dealt with the interaction of homonuclear systems. Another one [4] discussed the water and hydrogen fluoride dimers. The basis sets taken in these cases were not too large. The conclusions we are looking for are especially important when studying the effects in the presence of small basis sets. As it has been described in some of our earlier papers [3-6] the procedure for obtaining SMOs starts from the occupied and virtual canonical molecular orbitals (CMOs) of the supersystem: it uses a bridge in order to transform the CMOs towards a prescribed set of orbitals. The criterion prescribes, that the overlap between the constructed orbitals ψ_i of a supermolecule (SM) should be maximal with the initial, canonical orbitals φ_i of the non-interacting molecules, the bridge thus implies an overlap criterion:

$$\sum_{i=1}^{N} \left| \langle \varphi_i | \psi_i \rangle \right|^2 = \max .$$

It is important to emphasize, that the CMOs of the corresponding CP-corrected subsystems can be separated in a similar manner. The SMOs can thus unambigously be attributed to one ore another of the interacting monomers. Furthermore, the different energy quantities in a supersystem can be simply obtained by suming over the corresponding quantities calculated from the contributing subsystems [7-10].

2. The Hartree-Fock level in a localized representation

At the Hartree-Fock SCF level the total energy has the following form:

$$E_{HF} = E_0 + 2\sum_{i}\left(T_i + V_i\right) + \sum_{i,j}\left(2J_{ij} - K_{ij}\right),$$

where

$$E_0 = \sum_{\substack{a,b \\ a>b}} Z_a Z_b R_{ab}^{-1},$$

$$T_i = -\frac{1}{2}\int \psi_i{}^*(\mathbf{r})(\Delta\psi)(\mathbf{r})d^3\mathbf{r},$$

$$V_i = -\sum_a Z_a \int \psi_i{}^*(\mathbf{r})|\mathbf{r} - \mathbf{R}_a|^{-1}\psi_i(\mathbf{r})d^3\mathbf{r},$$

$$J_{ij} = \iint \psi_i{}^*(\mathbf{r}_1)\psi_j{}^*(\mathbf{r}_2)|\mathbf{r}_1 - \mathbf{r}_2|^{-1}\psi_i(\mathbf{r}_1)\psi_j(\mathbf{r}_2)d^3\mathbf{r}_1 d^3\mathbf{r}_2,$$

$$K_{ij} = \iint \psi_i{}^*(\mathbf{r}_1)\psi_j{}^*(\mathbf{r}_2)|\mathbf{r}_1 - \mathbf{r}_2|^{-1}\psi_j(\mathbf{r}_1)\psi_i(\mathbf{r}_2)d^3\mathbf{r}_1 d^3\mathbf{r}_2.$$

Using SMOs, this expression can be separated into one- and two-body terms by

$$E_{HF} = \sum_A E_{HF}^A + \sum_{\substack{A,B \\ A>B}} E_{HF}^{AB},$$

where

$$E_{HF}^A = E_0^A + 2\sum_{i\in O_A}\left(T_i + V_i^A\right) + \sum_{i,j\in O_A}\left(2J_{ij} - K_{ij}\right),$$

$$E_{HF}^{AB} = E_0^{AB} + 2\left(\sum_{i\in O_A}V_i^B + \sum_{i\in O_B}V_i^A\right) + 2\sum_{\substack{i\in O_A \\ j\in O_B}}\left(2J_{ij} - K_{ij}\right).$$

In these expressions A and B denote the monomers, O_A (O_B) denotes the set of indices of the occupied orbitals for monomer A (B), and

$$E_0^A = \sum_{\substack{a,b\in N_A \\ a>b}} Z_a Z_b R_{ab}^{-1},$$

$$E_0^{AB} = \sum_{\substack{a\in N_A \\ b\in N_B}} Z_a Z_b R_{ab}^{-1},$$

$$V_i^A = -\sum_{a\in N_A} Z_a \int \psi_i{}^*(\mathbf{r})|\mathbf{r} - \mathbf{R}_a|^{-1}\psi_i(\mathbf{r})d^3\mathbf{r},$$

where N_A (N_B) denotes the indices of the nuclei for monomer A (B).

Hence, at the Hartree-Fock SCF level for a dimer (AB) we have the following terms:

$E_0^{A\text{ or }B}$ is the nuclear-nuclear interaction on monomer A/B (N/N),

E_0^{AB} is the nuclear-nuclear interaction between A and B (N/N),

$2\displaystyle\sum_{i\in O_A \text{ or } O_B} T_i$ is the kinetic energy on monomer A/B (EKIN),

$2\displaystyle\sum_{i\in O_A \text{ or } O_B} V_i^{A \text{ or } B}$ is the electron-nuclear attraction on monomer A/B (E/N),

$2\displaystyle\sum_{i\in O_A} V_i^B$ is the electron (on A)-nuclear (on B) attraction (E/N),

$2\displaystyle\sum_{i\in O_B} V_i^A$ is the electron (on B)-nuclear (on A) attraction (E/N),

$\displaystyle\sum_{i,j\in O_A \text{ or } O_B} \left(2J_{ij} - K_{ij}\right)$ is the Coulomb + exchange interaction on monomer A/B

(E/E),

and

$2\displaystyle\sum_{\substack{i\in O_A \\ j\in O_B}} \left(2J_{ij} - K_{ij}\right)$ is the Coulomb + exchange interaction between A and B

(E/E).

From the above definitions it is evident that these components are invariant when the SMOs are subjected to unitary transformations U^A, U^B, ... by

$$\psi_i' = \sum_{j\in O_A} U_{ji}^A \psi_j, \quad \text{if} \quad i \in O_A,$$

$$\psi_i' = \sum_{j\in O_B} U_{ji}^B \psi_j, \quad \text{if} \quad i \in O_B,$$

etc.

Let us briefly summarize the results obtained (using several basis sets) for some energy quantities at the HF level in a previous study [3]. Interesting conclusions were found concerning the electron/electron repulsion (E/E), electron/nuclear (E/N) attraction and the kinetic energy partioned in the supermolecules and their CP-corrected systems. The difference in the E/E terms manifests itself in the total energy changes. As to the saturation of the basis set phenomenon, we can predict when will the size of a given basis set be large enough at the HF-SCF level, without any CP calculations. The quantities obtained and collected in the group denoted as 'Within the dimer between the monomers' (see Table I. of ref.3) are convenient for the above purpose: each of the values shows convergence as the basis set becomes saturated. These quantities are the following: E/N, E/E and also the Coulomb or exchange parts of the electron-electron repulsion.

Similar quantities were calculated and reported for the $(H_2O)_2$ and the $(HF)_2$ molecules (both SM- and CP-systems) in ref.4. The change in the kinetic energy

terms does not follow the change in the E/N terms for these molecules. The E/E quantities are not alone responsible for the total energy changes between the SM and CP systems. The results for the water dimer show differences for the two monomers, as expected. Some systematic trends can be found in the values for the electron/donor monomer1 for the SM and CP systems. The same does not hold for the electron/acceptor monomer2: a small difference between the kinetic energy terms in the SM and CP systems was found in comparison to the large deviation in the E/N terms. Similar conclusions hold for the $(HF)_2$ system [4].

3. Results obtained at the Hartree-Fock level

It was clearly stated recently [11] that the CP method introduced by Boys and Bernardi [1] for correcting the BSSE is a correct approach to the evaluation of the interaction energies, e.g., in vdW systems. Certain scepticism [12,13] is also reported against the use of the CP recipe especially at the correlated level. In order to gain insight into this field, we discuss in detail the contributions of the atomic (basis) orbitals to each of the SMOs, determined in the SM- and/or CP-systems, respectively. A comparison of the corresponding contributions (at the HF-SCF level), in the SM- and CP-systems is expected to help a better understanding of the effects arising in the different systems. The He_2 dimer and the dimer of H_2O was chosen for our study. For the water dimer the orientation of the monomers was taken from our earlier studies [3,4]. A basis set of (sp) quality was used in the study of the He_2 dimer [14]. As to the dimer of H_2O, the commonly used 6-311G/d basis [15] was applied in the actual calculations.

The results obtained for the monomer, the dimer and the CP-corrected system of the He_2 dimer are given in Table I. Under heading "Dimer", e.g., the contributions of the given functions from the atomic basis set of (any of) the He-atoms are tabulated, as they participate in the occupied SMO of the dimer (SM-) system. The contributions for the CP-system is tabulated in a similar way.

These results can be summarized as follows. From the comparison of the contributions for the s orbitals of the monomers to the dimer (SM) and to the CP-system, respectively, it is clear that the contributions in the latter systems are much closer to each other, than to those of monomers. This affirms (by numerical values) our earlier suggested conclusion [3,4], that the use of SMO's implies the advantages of using the CP-recipe, namely its "benefit effect". The similar effects of the SMO- and CP recipes are thus pointed out "numerically" for s orbitals in homonuclear systems at the Hartree-Fock level. The same does not hold, however, for basis functions of p (in our cases p_z) type.

These contributions are not existing for the He atom, but as to the values for the SM and CP systems, they are systematically different (the contributions from the CP system are larger than those from the SM system). A quite different conclusion holds for the ghost contributions: these values, calculated in the dimer system are much higher (for some functions with one or two magnitudes!) than in the CP system. This is contrary to common belief: the lower total energy of a CP

system, namely, is not due to the larger contributions of ghost orbitals. It might rather be the result of the more "effective" use of the own orbitals (that is p_z ones, in our case, see Table I).

The significant values calculated for the occupied SMOs in the water dimer are given in Table II. and Table III. (only for orbitals which have relevant contributions due to the symmetry).

It is worthwhile to mention that a similar conclusion holds for the s functions (for both monomers) as it was found for the He$_2$ dimer. The value for monomer1 is presented in Table II. The contributions of p functions (due to the orientation of molecules, the p_x type contributions are relevant), however, behave themselves similar to that found in the He$_2$ system, only for the electron-donor monomer (monomer1 in our case, see the values in Table II). The contributions of the p_x functions for the electron-donor monomer are usually higher in the CP system than in the dimer, while usually an opposite trend can be noticed when comparing the corresponding values in the electron-acceptor monomer2 (numerical results are given in Table III). This discrepancy might cause later a difference between the correlation energy components in the SM- and CP- systems, respectively. This result may explain, e.g., the deviations found in the charge transfer components (see ref.4) calculated for the electron-acceptor monomer, in the SM- and CP- systems, respectively.

As to the contributions of the ghost functions, those of s type are of the same behaviour than in the He$_2$ dimer (see Table II, values are given for monomer1). The contributions of p functions, as expected, show a systematic trend: it is to be emphasized that the contributions from monomer2 in the SMOs for monomer1 are usually higher than those from monomer1 to monomer2. However, not so large difference can be noticed for the contributions in the corresponding CP-systems. These results also suggest that one cannot expect a similar correspondence for the correlation energy contributions in the SM- and CP-systems for the electron-donor and electron-acceptor monomers, respectively.

4. The correlated level in the LMBPT

At the correlated level the many-body perturbation theory is employed, the localized version of which (LMBPT) has already proven to be useful in the study of molecular electronic structure [7-10]. The LMBPT is a double perturbation theory, and the perturbational corrections are calculated as:

$$E_{loc}^{corr} = \sum_N \sum_M E_{loc}^{(N,M)} \, ,$$

where N is the order of the two-particle perturbation and M is the order of the single-particle perturbation (see equations in ref. 7). Summing to infinite order over the index M, the canonical correlation energy corrections are obtained:

$$\sum_{M=1}^{\infty} E_{\text{loc}}^{(N,M)} = E_{\text{can}}^{(N)}.$$

The rate of convergence depends, as expected, on the localization method applied. As we obtain the values for the diagonal Fock-matrix elements (Lagrangian multipliers [7]) of the resulting SMOs very close to the canonical ones, the convergence is fast, so it is enough to calculate the first two or three terms. Using the SMO-LMBPT scheme, an excellent convergence was found in each case of the interacting systems studied.

For the two-particle perturbations we can easily separate the energy-components of the interacting system into different terms. The general expression of the N-th order MBPT correlation energy has the form

$$E^{(N)} = \sum_{I=2}^{2N-2} E_I^{(N)} = \sum_{I=2}^{2N-2} \sum_{m_1 m_2 \dots m_I n_1 n_2 \dots n_{2N-I}} \sum e\big(m_1 m_2 \dots m_I n_1 n_2 \dots n_{2N-I}\big),$$

where the indices $m_1, m_2, \dots, m_I, n_1, n_2, \dots, n_{2N-I}$ run over the set of monomers. Terms $e\big(m_1 m_2 \dots m_I n_1 n_2 \dots n_{2N-I}\big)$ can be expressed by the following way:

$$e\big(m_1 m_2 \dots m_I n_1 n_2 \dots n_{2N-I}\big) = \sum_{h_1 \in m_1^h} \dots \sum_{h_I \in m_I^h} \sum_{p_1 \in n_1^p} \dots \sum_{p_{2N-I} \in n_{2N-I}^p} e\big(h_1 h_2 \dots h_I p_1 p_2 \dots p_{2N-I}\big).$$

Here $h_1, h_2, \dots, h_I$ ($p_1, p_2, \dots, p_{2N-I}$) denote the occupied (virtual) orbitals (holes and particles), m_i^h (n_i^p) is the set of the occupied (virtual) orbitals belonging to monomer m_i (n_i).

In order to make these general expressions clear, we give some examples according to the equations of ref. 16. Let us denote the two-electron integrals by the following way:

$$\langle ab|cd \rangle = \iint \psi_a{}^*(\mathbf{r}_1) \psi_b{}^*(\mathbf{r}_2) |\mathbf{r}_1 - \mathbf{r}_2|^{-1} \psi_c(\mathbf{r}_1) \psi_d(\mathbf{r}_2) \mathrm{d}^3\mathbf{r}_1 \mathrm{d}^3\mathbf{r}_2$$

For the second order correlation energy the value of index I can only be 2, and

$$e\big(h_1 h_2 p_1 p_2\big) = \langle p_1 p_2 | h_1 h_2 \rangle c\big(h_1 h_2 p_1 p_2\big).$$

For the third order correlation energy I can set the values 2, 3, and 4, and

$$e\big(h_1 h_2 p_1 p_2 p_3 p_4\big) = c\big(h_1 h_2 p_1 p_2\big) \frac{\langle p_1 p_2 | p_3 p_4 \rangle \langle p_3 p_4 | h_1 h_2 \rangle}{\varepsilon_{h_1} + \varepsilon_{h_2} - \varepsilon_{p_3} - \varepsilon_{p_4}},$$

$$e\left(h_{1}h_{2}h_{3}p_{1}p_{2}p_{3}\right) = c\left(h_{1}h_{2}p_{1}p_{2}\right)\left\{-2\frac{\left\langle h_{3}p_{3}\left|h_{1}p_{3}\right.\right\rangle\left\langle p_{1}p_{3}\left|h_{1}h_{2}\right.\right\rangle}{\varepsilon_{h_{3}}+\varepsilon_{h_{1}}-\varepsilon_{p_{2}}-\varepsilon_{p_{3}}}-\right.$$

$$-2\frac{\left\langle h_{3}p_{1}\left|p_{3}h_{1}\right.\right\rangle\left\langle p_{2}p_{3}\left|h_{1}h_{2}\right.\right\rangle}{\varepsilon_{h_{2}}+\varepsilon_{h_{3}}-\varepsilon_{p_{2}}-\varepsilon_{p_{3}}}+2\frac{\left(2\left\langle h_{3}p_{1}\left|p_{3}h_{1}\right.\right\rangle-\left\langle h_{3}p_{1}\left|h_{1}p_{3}\right.\right\rangle\right)\left\langle p_{1}p_{3}\left|h_{1}h_{2}\right.\right\rangle}{\varepsilon_{h_{3}}+\varepsilon_{h_{1}}-\varepsilon_{p_{2}}-\varepsilon_{p_{3}}}\right\},$$

$$e\left(h_{1}h_{2}h_{3}h_{4}p_{1}p_{2}\right) = c\left(h_{1}h_{2}p_{1}p_{2}\right)\frac{\left\langle h_{3}h_{4}\left|h_{1}h_{2}\right.\right\rangle\left\langle p_{1}p_{2}\left|h_{3}h_{4}\right.\right\rangle}{\varepsilon_{h_{3}}+\varepsilon_{h_{4}}-\varepsilon_{p_{1}}-\varepsilon_{p_{2}}}.$$

where

$$c\left(h_{1}h_{2}p_{1}p_{2}\right) = \frac{2\left\langle h_{1}h_{2}\left|p_{1}p_{2}\right.\right\rangle-\left\langle h_{1}h_{2}\left|p_{2}p_{1}\right.\right\rangle}{\varepsilon_{h_{1}}+\varepsilon_{h_{2}}-\varepsilon_{p_{1}}-\varepsilon_{p_{2}}}.$$

Let $\mathcal{L} = \left\{l_{1}, l_{2}, ..., l_{L}\right\}$ is a subset of the set of monomers ($l_{i} \neq l_{j}$ if $i \neq j$). The total L-body energy for these monomers at the N-th order level is defined by

$$E^{(N)}\left(\mathcal{L}, \text{total}\right) = \sum_{I=2}^{2N-2}\sum_{\substack{m_{1}m_{2}...m_{I}n_{1}n_{2}...n_{2N-I}\\ \mathcal{M}=\mathcal{L}}}\sum e\left(m_{1}m_{2}...m_{I}n_{1}n_{2}...n_{2N-I}\right),$$

while the dispersion (or net L-body) energy has the following form:

$$E^{(N)}\left(\mathcal{L}, \text{disp}\right) = \sum_{I=2}^{2N-2}\sum_{\substack{m_{1}m_{2}...m_{I}n_{1}n_{2}...n_{2N-I}\\ \mathcal{M}=\mathcal{L}\\ \mathcal{N}=\mathcal{L}}}\sum e\left(m_{1}m_{2}...m_{I}n_{1}n_{2}...n_{2N-I}\right).$$

In these expressions $\mathcal{M} = \left\{m_{1}\right\}\cup\left\{m_{2}\right\}\cup...\cup\left\{m_{I}\right\}$, $\mathcal{N} = \left\{n_{1}\right\}\cup\left\{n_{2}\right\}\cup...\cup\left\{n_{2N-I}\right\}$ (the sets of the indices). If I (or $2N - I$) is less than L, then the corresponding energy component is zero. Finally, we introduce the charge-transfer components as well, by

$$E^{(N)}\left(\mathcal{L}, \text{CT}\right) = E^{(N)}\left(\mathcal{L}, \text{total}\right) - E^{(N)}\left(\mathcal{L}, \text{disp}\right).$$

We note, that from the above equation it is evident that the total N-th order correlation energy can be separated into one-, two-, ... $2N - 2$ -body terms by the following way:

$$E^{(N)} = \sum_{m_1} E^{(N)}\left(\{m_1\}, \text{total}\right) + \sum_{\substack{m_1, m_2 \\ m_1 > m_2}} E^{(N)}\left(\{m_1, m_2\}, \text{total}\right) +$$

$$+ \ldots + \sum_{\substack{m_1, m_2, \ldots, m_{2N-2} \\ m_1 > m_2 > \ldots > m_{2N-2}}} E^{(N)}\left(\{m_1, m_2, \ldots, m_{2N-2}\}, \text{total}\right).$$

The SMO-LMBPT method conveniently uses the transferability of the intracorrelated (one-body) parts of the monomers. This holds, according to our previous results [3-10], at the second (MP2), third (MP3) and fourth (MP4) level of correlation, respectively. The two-body terms (both dispersion and charge-transfer components) have also been already discussed for several systems [3-5]. A transferable property of the two-body interaction energy is valid in the studied He- and Ne-clusters, too [6]. In this work we focus also on the three-body effects which can be calculated in a rather straightforward way using the SMO-LMBPT formalism.

The interaction energy of two (weakly) interacting monomers can be calculated as the difference between the total energy of the supersystem and that of the contributing monomers, as follows:

$$\Delta E_{\text{int}} = \Delta E_{\text{SCF}} + \Delta E_{\text{C}} = \Delta E_{\text{SCF}} + \Delta E_{\text{N}} + E_{\text{D}} + E_{\text{CT}},$$

where the following notations are used:

C = correlated part
N = intra-components (changes in the total one-body terms)
D = dispersion terms (excluding the one-body dispersion components)
CT = charge-transfer terms (excluding the one-body charge-transfer components)

(see above).

The ΔE_{SCF} term is calculated using the standard CP-method. At the correlated MP2 level, we have shown for several systems [7-10], that the ΔE_{N} terms are usually and systematically smaller than the dominant ($E_{\text{D}} + E_{\text{CT}}$) terms. The sum of these two terms provides a good approximation to the total interaction energy at the correlated level. It is important to emphasize that the ΔE_{N} values were obtained by making the difference with the values of the CP-corrected subsystems i.e. taking into consideration the "benefit effect" of the superposition of the basis set [3, 6]. As the charge-transfer components are of importance in the two-body interaction, (see a discussion in ref. 10), we will also investigate them separately for the three-body terms in the studied systems.

Let us now turn to the discussion of the three-body terms at the correlated level. The calculation were performed at the MP3 and MP4 levels, using the SMO-LMBPT formalism. Certain problems arise as to the definition. Namely, there is no general agreement in the literature how to define the three-body

energy. As it is defined in [23], the deviation from the transferability of the intra-energy terms is also included. The SMO-LMBPT formalism, on the other hand, is able to separate the two-, three-, and four-body interaction terms as well as the corresponding components of the intra-terms. The additivity of these last terms has already been discussed in ref. 6. The many-body terms, therefore, can be calculated without the above-mentioned possible deviation from the additivity of the intra-components. As for the higher order terms (three- and four-body), there are not many references in the literature. This may certainly be due to the fact that in canonical representation these terms can not easily be calculated. It is generally believed that the higher order interaction energies are usually small but not negligible. There are some excellent, partly review, articles in the literature dealing with the many-body effects both from theoretical and experimental points of view [17-24].

A well-known prototype of three-body interaction is the helium trimer [25-28]. The three-body interaction energy is discussed in detail in the above-mentioned works. It is interesting that the results, certainly due to the different approaches used, are not uniform. As demonstrated this by one example, the three-body term is found to be negative at the correlated level for a linear He-trimer (in ref.28.) while other authors (ref.27.) obtained a positive value for the same term.

In order to have an insight into the three-body effect,we continue the study of the He-clusters. Fortunately, there are published examples for several He-clusters, as cited above. All of these studies, however, were performed in the canonical representation. The use of the localized representation allows us to separate the dispersion and the charge transfer components of the interaction energy for the three-body effects as it was similarly done for the two-body effects. The calculation of the interaction energy in the SMO-LMBPT framework has been discussed in detail in several papers [8-10] The formulae given at the correlated level, however, were restricted to the two-body interaction.

5. Results obtained at the correlated level

As it was pointed out in one of our recent paper [6], the interaction energy in He-clusters can be calculated to a rather good approximation using an extended (sp) basis set. We applied, therefore, an (8s3p) set reported by Huzinaga (for details see ref.6) in our calculations. We performed the calculations for several He-clusters, following partly the geometries considered by Parish and Dykstra [27], and Fink and Staemmler [28]. The calculations were carried out for He-clusters containing three, four, five and six atoms, respectively. The geometries considered are given in Figure I. The pair-interaction energies at the SCF level are well-know from the literature (at the experimental potential minimum of the He_2 system it is about 29 µH). As to the three-body effects in the trimer systems considered (linear, equilateral/60° and triangle/120°) for the first and last trimers

the values are zero. Using our basis set, we obtained -0.35 μH for the triangle/60° He$_3$ cluster.

The correlation energy contribution to the interaction energy in the dimer at the MP2 correlated level (about -34 μH) is also reported in several papers (refs 26, 27 and some references in ref. 6.). As the charge-transfer components at the correlated level are of great importance, it is worthwhile first to discuss these values obtained for the one-body and two-body interaction energy terms. A simple linear four-member He-cluster was chosen for the study. The results demonstrate, that the charge-transfer contributions do not give a significant contribution to the one-body and two-body interaction energies. The values are summarized in Table IV, at different levels of correlation: MP2, MP3 and MP4, respectively. The results clearly show, that the charge-transfer components are about with two order of magnitude smaller than the corresponding total interaction energy terms for the one-body (He(1), He(2), etc.) components. Its is remarkable, on the other hand, that the weight of the charge-transfer components (CTC) is always significantly larger in the two-body than in the one-body term: the percentage of the CTC in some cases even reaches term 30% (especially at the MP4 level, see Table IV). It is thus expected, that the significance of the charge-transfer terms within the three-body effects will further increase.

Let us now discuss the three-body effects at the correlated level for the studied clusters. As pointed out in ref.6. for some He, Ne and Ar- clusters, these can be investigated to a rather good approximation without the explicit use of the CP procedure, while the "benefit effect" of the basis set superposition, is inherently included into the so-called intra-terms at each level of correlation when using the SMO-LMBPT scheme. We can, therefore, discuss the three-body interaction energy terms free of BSSE as well as free of any possible error due to the non-additivity of the pair interaction contributions. The following geometries were considered for the He-trimer in the calculations: an equilateral triangle, a 120°-triangle as well as a linear trimer (see Figure I.), where all of the He-He distances are of 5.6 bohr. These trimer configurations are then extended to four, five and six-member clusters, respectively. The results obtained for the three-body interaction energy at the correlated level are summarized in Tables V and VI, respectively. The main conclusions are the following:

1. Accordingly to most of the results found in earlier works, the three-body interaction energy terms at the correlated level are small.

2. As to the sign of the values obtained for the different geometrical arrangement, they are in agreement with those reported by Fink and Staemmler and in disagreement with those given by Parish and Dykstra. The sign of the three-body interaction energy term (both at the MP3 and MP4 levels) for the linear trimer is negative (but much smaller than reported in ref. 28), while the sign for the other two trimers are positive (and roughly of the same magnitude, again alike in ref. 28). We also suggest that the neglect of the CP-corrections may deteriorate the

values obtained in ref. 27. This raises the issue that the BSSE, as calculated in ref.28 is also only approximate. Our results given in Table V, on the other hand, suggest, that the SMO-LMBPT scheme takes into account correctly the different effects in the He-clusters of different geometries.

3. When looking at the charge-transfer components of the three-body term (these are collected in Table VI), it is obvious that they represent a significant (sometimes dominant) part of the interaction energy. It is interesting to note that while the total three-body interaction energy at the MP3 correlated level for the studied systems (see part 1. of Table V) has not the same sign, the charge transfer components lowers the energy in each case (see Table VI). It is also remarkable, that for the triangle/60° and triangle/120° systems the charge-transfer contributions are significantly larger at the MP4 than at the MP3 correlated level.

It is worthwhile to emphasize an advantage of the SMO-LMBT procedure: this is its simplicity. Without any tiresome work the decomposition into contributions (for the individual atom-pairs, - tryads etc.) makes it possible to study the transferability properties in the clusters. This allows us to extend our method in order to investigate the van der Waals interactions in one- and two-dimensional infinite systems. This would make it possible to compare the results on the binding energies in systems of such type as given in ref. 28. This is one of our projects in the future.

The calculation of the many-body interaction energy by the SMO-LMBPT method using (relatively) small basis sets opens the way for studying large and/or extended systems. There are several types of aggregates, zeolites, building materials, etc., which could be discussed theoretically using our method in a straightforward manner. This project is also planned in the next future.

Acknowledgment

References

[1]   J. H. van Lenthe, J. G. C. M. van Duijneveldt-van de Rijdt and F. B. van Duijneweldt: *Advances in Chemical Physics*, **69**, 521 (1987)
[2]   S. F. Boys and F. Bernardi: *Mol. Phys.* **19**, 553 (1970)
[3]   C. Kozmutza, E. Tfirst and E. Kapuy: *Mol. Phys.* **87**, 569 (1996)
[4]   E. Kapuy, C. Kozmutza and L. Óvári: *J. Mol. Struct. (Theochem)* (in press)
[5]   E Kapuy and C. Kozmutza: *Chem. Phys. Letters* **226**, 484 (1994)
[6]   C. Kozmutza, E. Tfirst and E. Kapuy: *Mol. Phys.* **82**, 343 (1994)
[7]   E. Kapuy, Z Csépes and C. Kozmutza: *Int. J. Quant. Chem.* **23**, 981 (1983)
[8]   C. Kozmutza and E. Kapuy: *Int. J. Quant. Chem.* **38**, 665 (1990)

[9]   E. Kapuy and C. Kozmutza: *J. Chem. Phys.* **94**, 5565 (1991)

[10] C. Kozmutza, E. Kapuy, E. M. Evleth, J. Pipek, L. Trézl: *Int. J. Quant. Chem.* **57**, 775 (1996)

[11] F. B. van Duijneveldt, J. G. C. M. van Duijneveldt-van de Rijdt and J. H. van Lenthe: *Chem. Rev.* **94**, 1873 (1994)

[12] S. Saebø, W. Tong, P. Pulay: *J. Chem. Phys.* **98**, 2170 (1993)

[13] F. F. Muguet and G. W. Robinson: *J. Chem Phys.* **102**, 3648 (1995)

[14] S. Huzinaga: *J. Chem. Phys.* **42**, 1293 (1965)

[15] Krishnan, J. S. Binkley, R. Seeger and J A. Pople: *J. Chem. Phys.* **72**, 650 (1980)

[16] V. Kvasnicka, V. Laurinc and S. Bishupic: *Mol. Phys.* **39**, 143 (1980)

[17] M. J. Elrod and R. J. Saykally: *Chem. Rev.* **94**, 1975 (1994)

[18] G. Chalasinski, M. M. Szczesniak and S. M. Cybulski: *J. Chem. Phys.* **92**, 2481 (1990)

[19] M. M. Szczesniak and G. Chalasinski: *J. Mol. Structure (Theochem)* **261**, 37 (1992)

[20] L. W. Bruch, E. Blaisten-Barojas and O. Novaro: *J. Chem. Phys.* **67**, 4701 (1977)

[21] S. S. Xantheas and B.T.Sutcliffe: *J. Chem. Phys.* **103**, 8022 (1995)

[22] R. Moszynski, P. E. S. Wormer, B. Jeyiorski and Ad van der Avoird: *J. Chem. Phys.* **103**, 8058 (1995)

[23] C. Muguruma, N. Koga, K. Kitaura and K. Morokuma: *Chem. Phys. Letters* **224**, 139 (1994)

[24] C. Muguruma, N. Koga, K. Kitaura and K. Morokuma: *J. Chem. Phys.* **103**, 9274 (1995)

[25] A. Bhattacharya and J. B. Anderson: *J. Chem. Phys.* **100**, 8999 (1994)

[26] Fu-Ming Tao: *Chem. Phys. Letters.* **227**, 401 (1994)

[27] C. A. Parish and C. E. Dykstra: *J. Chem. Phys.* **98**, 437 (1993)

[28] K. Fink and V. Staemmler: *J. Chem. Phys.* **103**, 2603 (1995)

Table I. The contributions to the occupied SMO in the He monomer and He dimer systems

Orbitals	Monomer	Dimer	CP-system
s_1	0.07998558	0.07998498	0.07998359
s_2	0.02133655	0.02133713	0.02133691
s_3	0.00414911	0.00414913	0.00414906
s_4	0.00053307	0.00053308	0.00053308
s_5	0.21021360	0.21022251	0.21022189
s_6	0.36990119	0.36988270	0.36987300
s_7	0.36948358	0.36955199	0.36955108
s_8	0.11781757	0.11776359	0.11774697
p_{z1}	-	0.00000566	0.00000898
p_{z2}	-	0.00002358	0.00003343
p_{z3}	-	0.00004006	0.00005265

Ghost contributions:

Orbitals	Dimer	CP-system
s_1	0.00021533	0.00000506
s_2	0.00005872	0.00000093
s_3	0.00001114	0.00000013
s_4	0.00000145	0.00000001
s_5	0.00060774	0.00002321
s_6	0.00099663	0.00009911
s_7	0.00147264	0.00025220
s_8	0.00044370	0.00032220
p_{z1}	0.00008888	0.00001430
p_{z2}	0.00003161	0.00008002
p_{z3}	0.00012195	0.00003516

Table II. *The contributions to the occupied SMOs in the water dimer for monomer1*
(SM = supermolecule, CP = CP-corrected system)

Orbital		O_1s_1	O_1s_2	O_1s_3
1	SM	0.55148459	0.47142772	0.00612933
	CP	0.55149117	0.47144103	0.00607426
2	SM	0.11357290	0.18807682	0.53555057
	CP	0.11355771	0.18794625	0.53590727
3	SM	0.03824003	0.06687784	0.20456175
	CP	0.03895279	0.06803484	0.20990185
4	SM	0.00049232	0.00064257	0.00577575
	CP	0.00010207	0.00014682	0.00054241

Orbital		O_1p_{x1}	O_1p_{x2}	O_1p_{x3}
1	SM	0.00090526	0.00033138	0.00020044
	CP	0.00100909	0.00036695	0.00023018
2	SM	0.02007120	0.04587701	0.02530907
	CP	0.01926743	0.04537795	0.02635210
3	SM	0.13619372	0.21228605	0.20180494
	CP	0.13686776	0.21289807	0.19704887
4	SM	0.24291904	0.36565825	0.40470495
	CP	0.24419681	0.36700225	0.40462019

Orbital		O_2s_1	O_2s_2	O_2s_3
1	SM	0.00001525	0.00002063	0.00009700
	CP	0.00000126	0.00000461	0.00001714
2	SM	0.00025760	0.00026991	0.00186652
	CP	0.00002302	0.00009454	0.00113045
3	SM	0.00144302	0.00260681	0.00500044
	CP	0.00002915	0.00012042	0.00102101
4	SM	0.00200788	0.00320595	0.01049126
	CP	0.00002316	0.00013818	0.00243626

Table II. (Continued)

Orbital		O_2p_{x1}	O_2p_{x2}	O_2p_{x3}
1	SM	0.00026375	0.00041834	0.00042694
	CP	0.00000151	0.00000836	0.00009050
2	SM	0.00467268	0.00870086	0.00318530
	CP	0.00005996	0.00047200	0.00553824
3	SM	0.01026623	0.01694856	0.02653080
	CP	0.00011941	0.00083745	0.00135955
4	SM	0.01180117	0.02080369	0.01511831
	CP	0.00004696	0.00023609	0.01862553

Table III. The contributions to the occupied SMOs in the water dimer for monomer2
(SM = supermolecule, CP = CP-corrected system)

Orbital		O_2p_{x1}	O_2p_{x2}	O_2p_{x3}
1	SM	0.00092891	0.00027533	0.00014924
	CP	0.00102332	0.00034552	0.00015624
2	SM	0.02093521	0.04628869	0.03512635
	CP	0.01954310	0.04392212	0.03219674
3	SM	0.18871443	0.31447191	0.21796668
	CP	0.18554925	0.30539676	0.20473979
4	SM	0.14193458	0.21605691	0.22508535
	CP	0.13876871	0.21135875	0.21233637

Orbital		O_1p_{x1}	O_1p_{x2}	O_1p_{x3}
1	SM	0.00003427	0.00004645	0.00006256
	CP	0.00000131	0.00000341	0.00000547
2	SM	0.00366671	0.00662064	0.00277526
	CP	0.00014723	0.00340917	0.00002396
3	SM	0.00684004	0.00761331	0.01891211
	CP	0.00012644	0.00083639	0.00037305
4	SM	0.00369119	0.00567232	0.00416548
	CP	0.00008559	0.00069149	0.00649096

Table IV. Correlation energy decomposition for the one- and two-body terms in a linear tetramer He-cluster (values are given in mHartree, the numbering of atoms are given from left to right, see Figure I.)

MP2 correlated level

	E(total)	E(charge-transfer)
He(1) and He(4)	-29.458	-0.137
He(2) and He(3)	-29.456	-0.272
He(12) and He(34)	-0.0351	-0.005
He(31) and He(42)	-0.0005	0.000
He(32)	-0.0352	-0.005
He(41)	-0.0001	0.000

MP2 total correlation energy: -0.117935

MP3 correlated level

	E(total)	E(charge-transfer)
He(1) and He(4)	-5.2692	-0.0193
He(2) and He(3)	-5.1763	-0.0387
He(12) and He(34)	-0.0057	-0.0006
He(31) and He(42)	-0.0001	0.0000
He(32)	-0.0055	-0.0006
He(41)	0.0000	0.0000

MP3 total correlation energy: -0.020907

MP4 correlated level

	E(total)	E(charge-transfer)
He(1) and He(4)	-0.9635	-0.0049
He(2) and He(3)	-0.9354	-0.0095
He(12) and He(34)	-0.0004	-0.0001
He(31) and He(42)	0.0000	0.0000
He(32)	-0.0003	-0.0001
He(41)	0.0000	0.0000

MP4 total correlation energy: -0.003799

Table V. Three-body interaction energy terms at the correlated level in the studied He-clusters (in µH, see Figure I. for notations, numbering of atoms are given from left to right))

Values calculated for He-atoms 3-2-1

		MP3	MP4
trimer	linear	-0.025	-0.011
	triangle/60°	+0.034	-0.010
	triangle/120°	+0.042	-0.012
tetramer	linear	-0.026	-0.013
	triangle/60°	+0.037	-0.011
	triangle/120°	+0.042	-0.014
pentamer	linear	-0.026	-0.014
	triangle/60°	+0.038	-0.013
	triangle/120°	+0.043	-0.015
hexamer	linear	-0.026	-0.014
	triangle/60°	+0.038	-0.014
	triangle/120°	+0.043	-0.015

Values calculated for He-atoms 4-2-1

		MP3	MP4
trimer	linear	-0.0010	-0.0004
	triangle/60°	-0.0023	-0.0009
	triangle/120°	-0.0020	-0.0008
tetramer	linear	-0.0010	-0.0005
	triangle/60°	-0.0023	-0.0010
	triangle/120°	-0.0021	-0.0010
pentamer	linear	-0.0011	-0.0005
	triangle/60°	-0.0024	-0.0011
	triangle/120°	-0.0022	-0.0011
hexamer	linear	-0.0011	-0.0005
	triangle/60°	-0.0024	-0.0011
	triangle/120°	-0.0022	-0.0011

Table VI. Charge transfer contributions to the three-body interaction energy at the MP3 and MP4 correlated levels for the studied He-clusters (in μH, see Figure I. for notations, numbering of atoms are given from left to right))

Values calculated for He-atoms 3-2-1

		MP3	MP4
trimer	linear	-0.0046	-0.0020
	triangle/60°	-0.0002	-0.0023
	triangle/120°	-0.0001	-0.0025
tetramer	linear	-0.0048	-0.0022
	triangle/60°	-0.0002	-0.0024
	triangle/120°	-0.0001	-0.0025
pentamer	linear	-0.0048	-0.0022
	triangle/60°	-0.0002	-0.0025
	triangle/120°	-0.0001	-0.0025
hexamer	linear	-0.0049	-0.0023
	triangle/60°	-0.0002	-0.0025
	triangle/120°	-0.0001	-0.0026

Values calculated for He-atoms 4-2-1

		MP3	MP4
trimer	linear	-0.0002	-0.0001
	triangle/60°	-0.0004	-0.0006
	triangle/120°	-0.0003	-0.0005
tetramer	linear	-0.0003	-0.0001
	triangle/60°	-0.0004	-0.0007
	triangle/120°	-0.0004	-0.0006
pentamer	linear	-0.0003	-0.0001
	triangle/60°	-0.0005	-0.0007
	triangle/120°	-0.0004	-0.0007
hexamer	linear	-0.0003	-0.0001
	triangle/60°	-0.0005	-0.0007
	triangle/120°	-0.0004	-0.0007

Figure I. Structures of the studied He-clusters

	linear	triangle/60°	triangle/120°
trimer			
tetramer			
pentamer			
hexamer			
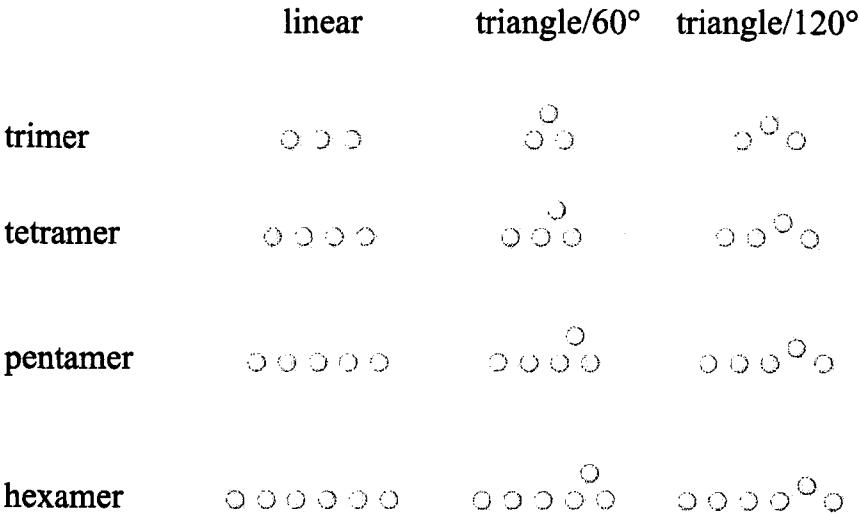
Extension of the SCF-MI Method to the Case of K Fragments one of which is an Open-Shell System.

E. GIANINETTI, I. VANDONI, A. FAMULARI, and M. RAIMONDI.

Dipartimento di Chimica Fisica ed Elettrochimica and Centro CNR CSRSRC, Università di Milano, via Golgi 19, 20133 Milano, Italy.

Abstract

Roothaan equations have been modified in a previous work with the aim of avoiding BSSE at the Hartree-Fock level of theory. The resulting scheme, called SCF-MI (Self Consistent Field for Molecular Interactions), underlines its special usefulness for the computation of intermolecular interactions.

In the present work we present the generalisation of the theory to the case of K interacting fragments one of which may be described by an open shell configuration. This extension implies a drastic modification of the procedure which is here reported in full detail.

The method provides a complete *a priori* elimination of the BSSE while taking into account the *natural* non orthogonality of the MO's of the interacting fragments.

251

I. Introduction

Due to their essential role played in the determination of the structural properties of matter, intermolecular forces have always received great attention in the field of physical chemistry.

It is well known that for a valuable starting point for the treatment of condensed matter properties it is fundamental to possess an accurate knowledge of the interaction potential between the individual molecules.

Among the causes of inaccuracy, BSSE (van Duijneveldt *et al.*, 1994) represents a well-known serious inconvenience for any variational computational approach to the problem. This error has a strong effect on the intermolecular potential interaction when weakly interacting systems are investigated. In hydrogen bonded systems, it is common that the BSSE is of the same order of magnitude of the interaction energy involved.

There have been many attempts to formulate a procedure to avoid it and both *a posteriori* and *a priori* schemes are available. The counterpoise approach (CP) (Boys and Bernardi, 1970) and related methods are the most common *a posteriori* procedures. Although this technique represents the most frequently employed *a posteriori* procedure to estimate this error, several authors have emphasised that the method introduced by Boys and Bernardi does not allow a clear and precise determination of the BSSE. The addition of the partner's functions introduces the "secondary superposition error" a spurious electrostatic contribution due to the modification of the multipole moments and polarizabilities of the monomers. This is particularly important in the case of anisotropic potentials where these errors can contribute to alter the shape of the PES and the resulting physical picture (Xantheas, 1996 and Simon *et al.* ,1996).

The proposed SCF-MI ab initio variational method (Gianinetti, Raimondi and Tornaghi, 1996) avoids the BSSE in an *a priori* fashion. The method is based on a modification of Roothan equations for closed shell systems.
While the CP procedure is exact only in the case of Full CI wavefunctions, the *a priori* SCFMI method is always correct and geometry relaxation effects are naturally taken into account.

Here we extend the theory to the case of K interacting fragments one of which may be described by an open shell configuration. In this version the orthonormalization criterion for the orbitals (separately for each fragment) is left free. For the treatment of the open fragment we have modified Guest and Saunders (1974) equations.

In this paper we give a detailed presentation of the theory and its related formalism.

As a test, we present here results on a few examples including an open shell dimer: the He - Cu, a closed shell trimer: $(H_2O)_3$ and open shell trimers: Li $(He)_2$ and Cu $(He)_2$. All these systems have in common the fact that their potentials can

be strongly affected by BSSE so that it is crucial to possess a strategy to avoid it without increasing computational costs in comparison with usual SCF MO methods.

II. Notations and Statement of the Problem.

Let us study a system constituted of K fragments $a_1 \ldots a_K$. We assume that the first (K-1) fragments are closed-shell systems described by doubly occupied orbitals. The last fragment a_K has an open-shell configuration, consisting of singly occupied molecular orbitals of parallel spin. Obviously, the theory here developed can easily be restricted to the case of K closed-shell fragments.

We adopt the following notations referring to the orbitals:

- $\chi_k = \left(\chi_{k,1} \ldots \chi_{k,M_k} \right)$ are the M_k basis orbitals centered on the fragment a_k (k=1...K)

- $\varphi_k = \left(\varphi_{k,1} \ldots \varphi_{k,N_k} \right)$ are the N_k doubly occupied molecular orbitals of the fragment a_k (k=1...K)

- We assume:

$$\varphi_k = \chi_k \, T_k \qquad (k=1...K) \tag{1}$$

where T_k is an $M_k \times N_k$ matrix.

- $\varphi^o = (\varphi_1^o \ldots \varphi_{N^o}^o)$ are the N^o singly occupied molecular orbitals of the last fragment a_K.

- We assume:

$$\varphi^o = \chi_K \, V_K \tag{2}$$

where V_K is an $M_K \times N^o$ matrix.

When referring to the supersystem it will be convenient to adopt a compact notation as follows:

- $\chi = (\chi_1 \mid \chi_2 \mid \ldots \chi_K)$ is the total basis set for the supersystem. It is obtained collecting the $M=M_1+\ldots\ldots+M_K$ atomic orbitals of each fragment.

- $\varphi = (\varphi_1 \mid \varphi_2 \mid \ldots \ldots \varphi_K)$ is the set of all the $N=N_1+N_2+\ldots N_K$ doubly occupied molecular orbitals.

- For the supersystem Eq.(1) can be written:

$$\varphi = \chi \, T \tag{3}$$

where T is a $M \times N$ matrix. T is partitioned in $K \times K$ blocks. The diagonal blocks are the $T_1 \ldots T_K$ matrices of Eq.(1) while the other blocks are null matrices.

- Analogously we define the $M \times N^o$ matrix V such that :

$$\varphi^o = \chi \, V \tag{4}$$

The last M_K rows of **V** are coincident with V_K, the other elements of **V** are zero. Fig. 1 exemplifies a case of $K=3$ fragments.
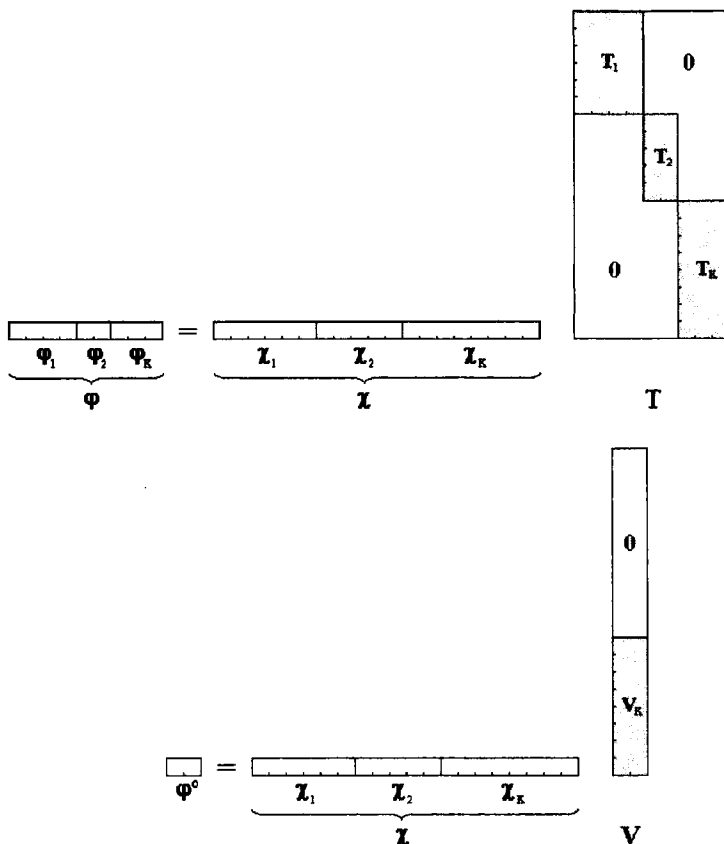
Fig.1. *Atomic and molecular orbitals in a case of K=3 fragments.*

The supersystem is described by the one determinant wave function

$$\Psi(1.....2N + N^\circ) =$$
$$= \mathscr{A}\left[\varphi_{1,1}(1)\overline{\varphi}_{1,1}(2)...\varphi_{K,N_K}(2N-1)\overline{\varphi}_{K,N_K}(2N)\varphi_1^\circ(2N+1)...\varphi_{N^\circ}^\circ(2N+N^\circ)\right] \quad (5)$$

where $\mathscr{A}$ is the antisymmetrizer.
We notice that, owing to the overlap between the basis sets of different fragments, it is impossible to impose the global orthonormalization to the total   set of

molecular orbitals (φ, φ^o). On the other hand, in order to compute the energy corresponding to the wave function (5), it is useful to express it in terms of orthonormal molecular orbitals φ' and $\varphi^{o'}$.

The transformation $(\varphi, \varphi^o) => (\varphi', \varphi^{o'})$ which leaves Ψ invariant is obtained in two steps:

a) build φ' orthonormalizing φ : $\varphi' = \chi T'$ with $T' = T (T^\dagger S T)^{-1/2}$

It is then possible to write the density matrix R which refer to the space spanned by the doubly occupied orbitals :

$$R = T' T'^\dagger = T (T^\dagger S T)^{-1} T^\dagger \qquad (6)$$

b) build $\varphi^{o'}$ orthogonalizing φ^o with respect to φ (i.e. φ') and then orthonormalizing the orbitals so obtained within themselves: $\varphi^{o'} = \chi V'$ with

$$V' = (1^M - R S) V [V^\dagger (S - S R S) V]^{-1/2}$$

We write now R^o, the density matrix relative to the space spanned by the singly occupied orbitals:

$$R^o = V' V'^\dagger = (1^M - RS)V[V^\dagger(S-SRS)V]^{-1} V^\dagger (1^M-SR) \qquad (7)$$

In the Born-Oppenheimer approximation the formula for the energy corresponding to the wave function Ψ is (McWeeny, 1964):

$$E = 2\{TrRH + TrRG(R)\} + \{TrR^oH + \tfrac{1}{2}TrR^oG'(R^o)\} + 2TrRG(R^o) \qquad (8)$$

To specify the symbology we remember the familiar notation for the integrals over the basis set orbitals:

$$S_{pq} = \langle \chi_p | \chi_q \rangle = \int \chi_p^*(r)\chi_q(r)dr \qquad (p,q = 1 \dots M)$$

$$H_{pq} = \langle \chi_p | \hat{h} | \chi_q \rangle = \int \chi_p^*(r)\hat{h}\chi_q(r)dr \qquad (p,q = 1 \dots M)$$

$$\langle pq | rs \rangle = \int \chi_p^*(r_1)\chi_q^*(r_2)\frac{1}{r_{12}} \chi_r(r_1)\chi_s(r_2)dr_1 dr_2 \qquad (p,q,r,s=1 \dots M)$$

$G(X)$ and $G'(X)$ are two M×M matrices, functions of the M×M variable matrix X:

$$G_{pq}(X) = \sum_{r,s=1}^{M} X_{sr}(\langle pr|qs \rangle - \tfrac{1}{2}\langle pr|sq \rangle) \qquad (p,q=1 \dots M) \qquad (9)$$

$$G'_{pq}(X) = \sum_{r,s=1}^{M} X_{sr}(\langle pr|qs \rangle - \langle pr|sq \rangle) \qquad (p,q=1 \dots M) \qquad (10)$$

It is easy to show that the two matrices G and G' have the following properties, being X and Y two generic matrices:

a) Tr **Y** G(**X**) = Tr **X** G(**Y**)   Tr **Y** G'(**X**) = Tr **X** G'(**Y**)

b) If **X** is a hermitian matrix G(**X**) and G'(**X**) are also hermitian matrices.

We are interested in the minimisation of the energy with respect to the matrices $T_1 .... T_K$ and V_K . To this aim it is useful to know δE as function of the variations of these matrices. Being **R** and **R°** functions of **T** and **V** we begin expressing δE as function of δ**R** and δ**R°**. It is

$$\delta E = 2 \text{ Tr } \delta\mathbf{R} \, [\mathbf{H} + 2 \, G(\mathbf{R}) + G(\mathbf{R°})] + \text{Tr } \delta\mathbf{R°} [\mathbf{H} + G'(\mathbf{R°}) + 2G(\mathbf{R})] \quad (11)$$

We must now evaluate the expressions of δ**R** and δ**R°** as functions of the variations of the matrices **T** and **V**.

From Eq.(6), remembering the relation $\delta\mathbf{W}^{-1} = -\mathbf{W}^{-1} \delta\mathbf{W} \, \mathbf{W}^{-1}$ we have

$$\delta\mathbf{R} = \mathbf{T} \, (\mathbf{T}^\dagger\mathbf{S} \, \mathbf{T})^{-1} \, \delta\mathbf{T}^\dagger \, [\mathbf{1}^M - \mathbf{ST}(\mathbf{T}^\dagger\mathbf{S} \, \mathbf{T})^{-1} \, \mathbf{T}^\dagger] + \underline{\text{hermitian conjugate}} =$$
$$= \mathbf{T} \, (\mathbf{T}^\dagger\mathbf{S} \, \mathbf{T})^{-1} \, \delta\mathbf{T}^\dagger \, [\mathbf{1}^M - \mathbf{S} \, \mathbf{R}] + \text{h.c.} \quad (12)$$

From Eq.(7) one can see that **R°** depends on **V** and, through the matrix **R,** on **T.** We may then write:

$$\delta\mathbf{R°} = \delta\mathbf{R°}_T + \delta\mathbf{R°}_V \quad (13)$$

$$\delta\mathbf{R°}_T = (\mathbf{1}^M - \mathbf{RS})\mathbf{V}[\mathbf{V}^\dagger(\mathbf{S} - \mathbf{SRS})\mathbf{V}]^{-1}[\mathbf{V}^\dagger\mathbf{S} \, \delta\mathbf{R} \, \mathbf{SV}] \, [\mathbf{V}^\dagger(\mathbf{S} - \mathbf{SRS})\mathbf{V}]^{-1} \mathbf{V}^\dagger(\mathbf{1}^M - \mathbf{SR}) -$$
$$- \left\{ (\mathbf{1}^M - \mathbf{RS})\mathbf{V}[\mathbf{V}^\dagger(\mathbf{S} - \mathbf{SRS})\mathbf{V}]^{-1} \mathbf{V}^\dagger \mathbf{S} \, \delta\mathbf{R} \, + \text{h.c} \right\}$$

Defining

$$\mathbf{P} = (\mathbf{1}^M - \mathbf{RS})\mathbf{V}[\mathbf{V}^\dagger (\mathbf{S} - \mathbf{SRS})\mathbf{V}]^{-1}\mathbf{V}^\dagger\mathbf{S} \quad (14)$$

we obtain:

$$\delta\mathbf{R°}_T = \mathbf{P} \, \delta\mathbf{R} \, \mathbf{P}^\dagger - \mathbf{P} \, \delta\mathbf{R} - \delta\mathbf{R} \, \mathbf{P}^\dagger$$

$$\delta\mathbf{R°}_V = (\mathbf{1}^M - \mathbf{RS})\mathbf{V}[\mathbf{V}^\dagger(\mathbf{S} - \mathbf{SRS})\mathbf{V}]^{-1} \delta\mathbf{V}^\dagger (\mathbf{1}^M - \mathbf{SR}) -$$

$$-(\mathbf{1}^M - \mathbf{RS})\mathbf{V}[\mathbf{V}^\dagger(\mathbf{S} - \mathbf{SRS})\mathbf{V}]^{-1} \delta\mathbf{V}^\dagger(\mathbf{S} - \mathbf{SRS})\mathbf{V} \, [\mathbf{V}^\dagger(\mathbf{S} - \mathbf{SRS})\mathbf{V}]^{-1} \mathbf{V}^\dagger(\mathbf{1}^M - \mathbf{SR}) + \text{h.c.} =$$

$$= (\mathbf{1}^M - \mathbf{RS}) \, \mathbf{V} \, [\mathbf{V}^\dagger(\mathbf{S} - \mathbf{SRS})\mathbf{V}]^{-1} \, \delta\mathbf{V}^\dagger \, (\mathbf{1}^M - \mathbf{SR} - \mathbf{SR°}) + \text{h. c.}$$

Substituting δ**R** and δ**R°** in Eq (11) one may write δE as a sum of the two terms δE_T and δE_V where:

$$\delta E_T = \text{Tr } \delta\mathbf{T}^\dagger \, (\mathbf{1}^M - \mathbf{S} \, \mathbf{R}) \, \mathbf{F} \, \mathbf{T} \, (\mathbf{T}^\dagger\mathbf{S} \, \mathbf{T})^{-1} + \underline{\text{complex conjugate}} \quad (15)$$

$$\delta E_V = \text{Tr } \delta\mathbf{V}^\dagger \, (\mathbf{1}^M - \mathbf{SR} - \mathbf{SR°}) \, \mathbf{L}(\mathbf{1}^M - \mathbf{RS})\mathbf{V} \, [\mathbf{V}^\dagger(\mathbf{S} - \mathbf{SRS})\mathbf{V}]^{-1} + \text{c.c.} \quad (16)$$

The hermitian M×M matrices **L** and **F** are so defined:

$$\mathbf{L} = \mathbf{H} + \mathbf{G'}(\mathbf{R}^{\circ}) + 2\mathbf{G}(\mathbf{R}) \tag{17}$$

$$\mathbf{F} = 2(\mathbf{H} + 2\ \mathbf{G}(\mathbf{R}) + \mathbf{G}(\mathbf{R}^{\circ})] + \mathbf{P}^{\dagger}\mathbf{LP} - \mathbf{LP} - \mathbf{P}^{\dagger}\mathbf{L} \tag{18}$$

We stress that these formulae for E and δE have been obtained and are valid independently of any condition on **T**, **V**, δ**T** and δ**V**.

Our task consists now in the minimisation of E when the matrices **T** and **V** (and then δ**T** and δ**V**) have the block structure described after Equations (3) and (4) and depicted in Fig.1.

As a first step we rewrite Equations(15) and (16) in the following form:

$$\delta E_{\mathbf{T}} = \sum_{k=1}^{K} \ \mathrm{Tr}\ \delta\mathbf{T}_k^{\dagger}\ \left[(\mathbf{1}^{M} - \mathbf{SR})\mathbf{FT}(\mathbf{T}^{\dagger}\mathbf{S}\ \mathbf{T})^{-1}\right]_{kk} + \text{c.c} \tag{19}$$

$$\delta E_{\mathbf{V}} = \mathrm{Tr}\,\delta\mathbf{V}_K^{\dagger}\{(\mathbf{1}^{M} - \mathbf{SR} - \mathbf{SR}^{\circ})\mathbf{L}(\mathbf{1}^{M} - \mathbf{RS})\mathbf{V}\ [\mathbf{V}^{\dagger}(\mathbf{S} - \mathbf{SRS})\mathbf{V}]^{-1}\}_K + \text{c.c.} \tag{20}$$

In Eq.(19) and (20) we have adopted a notation which expresses the partitioning of the matrices in blocks referring to the different fragments. We notice that:

- Given an M×M matrix **X** whose rows and whose columns refer to the basis orbitals we shall denote $\mathbf{X}_{hk}$ the $M_h \times M_k$ block whose rows refer to the atomic orbitals χ_h of the fragment a_h and whose columns refer to the atomic orbitals χ_k of the fragment a_k.

- Given an M×N matrix **X** whose rows refer to the basis orbitals and whose columns refer to the molecular orbitals, we shall denote $\mathbf{X}_{hk}$ the $M_h \times N_k$ block whose rows refer to the atomic orbitals χ_h of the fragment a_h and whose columns refer to the molecular orbitals φ_k of the fragment a_k.

- Analogously for the N×M or N×N matrices.

- We define "diagonal block matrix" a matrix **X** whose off-diagonal blocks ($\mathbf{X}_{hk}$ with $h \neq k$) are null. In this case we prefer, for simplicity, to denote the diagonal blocks by $\mathbf{X}_k$ instead of $\mathbf{X}_{kk}$. Obviously if **X** is a rectangular matrix, the $\mathbf{X}_k$ blocks are also rectangular. It is the case of the **T** matrix.

- Given an M×N° matrix **X** we shall denote by $\mathbf{X}_K$ the $M_K \times N^{\circ}$ block of the last M_K rows. It is the case of the **V** matrix.

- Given two blocks it is obviously possible to perform the product provided that the columns of the first block correspond to the rows of the second one. When the product $\mathbf{X}_{hk}\mathbf{Y}_k$ is feasible ($\mathbf{Y}_k$ is then a "diagonal block" or the Kth block of an M×N° matrix) it holds: $\mathbf{X}_{hk}\mathbf{Y}_k = (\mathbf{XY})_{hk}$. Analogously it is $\mathbf{X}_h\mathbf{Y}_{hk} = (\mathbf{XY})_{hk}$.

In order to minimise E with respect to the matrices $\mathbf{T}_1 \ldots \ldots \mathbf{T}_K$ and $\mathbf{V}_K$ one could use directly Equations (19) and (20) which are valid independently of any condition on $\mathbf{T}_1 \ldots \ldots \mathbf{T}_K$ $\mathbf{V}_K$ and on their variations. But it is more efficient to introduce new conditions which, without diminishing the generality of the model here proposed, simplify the formulae and transform the problem into a set of pseudo- secular equations.

III. The Minimisation Procedure

Let us define the M×M matrix $\mathbf{Q}$ whose generic block $\mathbf{Q}_{hk}$ is

$$\mathbf{Q}_{hk} = \left[\mathbf{T}(\mathbf{T}^\dagger \mathbf{S}\mathbf{T})^{-1}\right]_{hk}\left[(\mathbf{T}^\dagger \mathbf{S}\mathbf{T})^{-1}\mathbf{T}^\dagger \mathbf{S}\right]_{kk} \qquad (h,k=1\ldots K) \qquad (21)$$

and the M×M "diagonal block" matrix $\mathbf{S}'$ whose k^{th} block is:

$$\mathbf{S}'_k = [\mathbf{S} - \mathbf{S}\mathbf{R}\mathbf{S} + \mathbf{S}\mathbf{Q}]_{kk} \qquad\qquad (k=1\ldots K) \qquad\qquad (22)$$

It can be shown that
$$\mathbf{Q} = \mathbf{Q}\ \mathbf{T}\ \mathbf{T}^\dagger \mathbf{S}'$$
and that $\mathbf{S}'_k$ (and then $\mathbf{S}'$) are hermitian and non singular matrices.

From the definition (22) of the "block matrix" $\mathbf{S}'$ it is easy to see that the matrix $\mathbf{T}$ and its blocks $\mathbf{T}_1 \ldots \ldots \mathbf{T}_K$ satisfy the relations

$$\mathbf{T}_k^\dagger \mathbf{S}'_k \mathbf{T}_k = \mathbf{1}^{N_k} \qquad (k=1\ldots K) \qquad \text{i.e.} \qquad \mathbf{T}^\dagger \mathbf{S}'\mathbf{T} = \mathbf{1}^N \qquad (23)$$

We stress that the previous relations are not "conditions" imposed on $\mathbf{T}$, but are just properties of $\mathbf{S}'$.

Matrices $\mathbf{Q}$ and $\mathbf{S}'$ allow us to write
$$\mathbf{T}\,(\mathbf{T}^\dagger \mathbf{S}\,\mathbf{T})^{-1} = (\mathbf{1}^M - \mathbf{R}\mathbf{S} + \mathbf{Q}\,)\,\mathbf{T}$$
and $\qquad (\mathbf{1}^M - \mathbf{S}\mathbf{R}) = (\mathbf{1}^M - \mathbf{S}'\mathbf{T}\mathbf{T}^\dagger)\,(\mathbf{1}^M - \mathbf{R}\mathbf{S} + \mathbf{Q})^\dagger$

Equation (19) now reads
$$\delta E_T = \sum_{k=1}^{K} \text{Tr }\delta \mathbf{T}_k^\dagger \left[(\mathbf{1}^M - \mathbf{S}'\mathbf{T}\mathbf{T}^\dagger)(\mathbf{1}^M - \mathbf{R}\mathbf{S} + \mathbf{Q})^\dagger \mathbf{F}(\mathbf{1}^M - \mathbf{R}\mathbf{S} + \mathbf{Q})\mathbf{T}\right]_{kk} + \text{c.c.}$$

i.e.

$$\delta E_T = \sum_{k=1}^{K} \text{Tr }\delta \mathbf{T}_k^\dagger\ (\mathbf{1}^{M_k} - \mathbf{S}'_k \mathbf{T}_k \mathbf{T}_k^\dagger)\left[(\mathbf{1}^M - \mathbf{R}\mathbf{S} + \mathbf{Q})^\dagger \mathbf{F}(\mathbf{1}^M - \mathbf{R}\mathbf{S} + \mathbf{Q})\right]_{kk} \mathbf{T}_k + \text{c.c.}$$

Defining for each $k=1\ldots K$ the $M_k \times M_k$ matrix
$$\mathbf{F}'_k = \left[(\mathbf{1}^M - \mathbf{R}\mathbf{S} + \mathbf{Q})^\dagger\ \mathbf{F}\ (\mathbf{1}^M - \mathbf{R}\mathbf{S} + \mathbf{Q}\,)\right]_{kk} \qquad (24)$$
one gets

$$\delta E_{\mathrm{T}} = \sum_{k=1}^{K} \mathrm{Tr} \delta \mathbf{T}_{k}^{\dagger} \left(\mathbf{1}^{M_{k}} - \mathbf{S}_{k}^{'} \mathbf{T}_{k} \mathbf{T}_{k}^{\dagger} \right) \mathbf{F}_{k}^{'} \mathbf{T}_{k} + \mathrm{c.c.} \tag{25}$$

It is now convenient to impose to the block $\mathbf{V}_K$ the following conditions which can be fulfilled leaving Ψ invariant (see step (6) of the iterative procedure)

$$\begin{cases} \mathbf{T}_{K}^{\dagger} \, \mathbf{S}_{K}^{'} \mathbf{V}_{K} \; = \; \mathbf{0}^{N_K \times N^o} \\ \mathbf{V}_{K}^{\dagger} \, \mathbf{S}_{K}^{'} \mathbf{V}_{K} \; = \; \mathbf{1}^{N^o} \end{cases} \tag{26}$$

These conditions are equivalent to

$$\begin{cases} \mathbf{T}^{\dagger} \, \mathbf{S}^{'} \, \mathbf{V} \; = \; \mathbf{0}^{N \times N^o} \\ \mathbf{V}^{\dagger} \, \mathbf{S}^{'} \, \mathbf{V} \; = \; \mathbf{1}^{N^o} \end{cases}$$

From these conditions many useful identities descend. In particular

$$\mathbf{Q} \, \mathbf{V} = \mathbf{Q} \mathbf{T} \, \mathbf{T}^{\dagger} \mathbf{S}' \mathbf{V} = \mathbf{0}^{M \times N^o}$$

$$\mathbf{V}^{\dagger} \, (\, \mathbf{S} \, - \mathbf{S} \mathbf{R} \mathbf{S} \,) \, \mathbf{V} \; = \mathbf{V}^{\dagger} \, (\mathbf{S} - \mathbf{S} \, \mathbf{R} \mathbf{S} + \mathbf{S} \, \mathbf{Q}) \, \mathbf{V} = \mathbf{V}^{\dagger} \, \mathbf{S}' \, \mathbf{V} = \mathbf{1}^{N^o}$$

$$\mathbf{R}^{\circ} = (\mathbf{1}^{M} - \mathbf{R} \mathbf{S}) \, \mathbf{V} \, \mathbf{V}^{\dagger} (\mathbf{1}^{M} - \mathbf{S} \mathbf{R} \,) \tag{27}$$

$$\mathbf{P} = (\mathbf{1}^{M} - \mathbf{R} \mathbf{S}) \, \mathbf{V} \, \mathbf{V}^{\dagger} \, \mathbf{S} \tag{28}$$

$$\mathbf{S} \mathbf{R}^{\circ} = (\mathbf{S} - \mathbf{S} \mathbf{R} \mathbf{S} + \mathbf{S} \mathbf{Q}) \, \mathbf{V} \mathbf{V}^{\dagger} (\mathbf{1}^{M} - \mathbf{S} \mathbf{R} + \mathbf{Q}^{\dagger})$$

$$(\mathbf{1}^{M} - \mathbf{S} \mathbf{R} - \mathbf{S} \mathbf{R}^{\circ}) = (\mathbf{1}^{M} - \mathbf{S}' \mathbf{T} \mathbf{T}^{\dagger})(\mathbf{1}^{M} - \mathbf{R} \mathbf{S} + \mathbf{Q})^{\dagger} - (\mathbf{S} - \mathbf{S} \mathbf{R} \mathbf{S} + \mathbf{S} \mathbf{Q}) \mathbf{V} \mathbf{V}^{\dagger} (\mathbf{1}^{M} - \mathbf{R} \mathbf{S} + \mathbf{Q})^{\dagger} =$$

$$= \left[(\mathbf{1}^{M} - \mathbf{S}' \mathbf{T} \mathbf{T}^{\dagger}) - (\mathbf{S} - \mathbf{S} \mathbf{R} \mathbf{S} + \mathbf{S} \mathbf{Q}) \, \mathbf{V} \mathbf{V}^{\dagger} \right] (\mathbf{1}^{M} - \mathbf{R} \mathbf{S} + \mathbf{Q})^{\dagger}$$

Eq.(20) now reads

$$\delta E_{V} = \mathrm{Tr} \delta \mathbf{V}_{K}^{\dagger} \left\{ \left[(\mathbf{1}^{M} - \mathbf{S}' \mathbf{T} \mathbf{T}^{\dagger}) - (\mathbf{S} - \mathbf{S} \mathbf{R} \mathbf{S} + \mathbf{S} \mathbf{Q}) \mathbf{V} \mathbf{V}^{\dagger} \right] (\mathbf{1}^{M} - \mathbf{R} \mathbf{S} + \mathbf{Q})^{\dagger} \mathbf{L} (\mathbf{1}^{M} - \mathbf{R} \mathbf{S} + \mathbf{Q}) \mathbf{V} \right\}_{K} + \mathrm{c.c.}$$

With the definition

$$\mathbf{L}_{K}^{'} = \left[(\mathbf{1}^{M} - \mathbf{R} \mathbf{S} + \mathbf{Q})^{\dagger} \mathbf{L} (\mathbf{1}^{M} - \mathbf{R} \mathbf{S} + \mathbf{Q}) \right]_{KK} \tag{29}$$

one gets

$$\delta E_{V} = \mathrm{Tr} \delta \mathbf{V}_{K}^{\dagger} \left(\mathbf{1}^{M_K} - \mathbf{S}_{K}^{'} \mathbf{T}_{K} \mathbf{T}_{K}^{\dagger} - \mathbf{S}_{K}^{'} \mathbf{V}_{K} \mathbf{V}_{K}^{\dagger} \right) \mathbf{L}_{K}^{'} \mathbf{V}_{K} + \mathrm{c.c.} \tag{30}$$

The variation $\delta E = \delta E_{\mathrm{T}} + \delta E_{V}$ with δE_{T} and δE_{V} expressed by (25) and (30) now clearly highlights the contributions of the different fragments and suggests how to decompose the iterative step into K rotations each one in the orbital space of one fragment.

Closed shell fragments.

For $k=1....(K-1)$ the contribution of each a_k to δE is

$$\delta E_{k} = \mathrm{Tr} \delta \mathbf{T}_{k}^{\dagger} \left(\mathbf{1}^{M_k} - \mathbf{S}_{k}^{'} \mathbf{T}_{k} \mathbf{T}_{k}^{\dagger} \right) \mathbf{F}_{k}^{'} \mathbf{T}_{k} + \mathrm{c.c.} \tag{31}$$

Remembering (23), Eq.(31) suggests to perform the iterative step $\mathbf{T}_k => \mathbf{T}'_k$ through the solution of the secular problem

$$\begin{cases} \mathbf{F}_k' \mathbf{T}_k' = \mathbf{S}_k' \mathbf{T}_k' \mathbf{D}_k \\ \mathbf{T}_k'^\dagger \mathbf{S}_k' \mathbf{T}_k' = \mathbf{1}^{N_k} \end{cases} \qquad (32)$$

where $\mathbf{D}_k$ is an $N_k \times N_k$ diagonal matrix.

In effect, near the minimum of E, the $\delta \mathbf{T}_k$ obtained through a perturbative analysis of (32) when substituted in (31) gives $\delta E_k < 0$.

If necessary, the convergence of the process may be improved by means of the "level shifting" technique (Saunders and Hillier, 1973). In our case this means substituting $\mathbf{F}_k'$ in Eq (32) with the matrix $[\mathbf{F}_k' + \alpha_k(\mathbf{S}_k' - \mathbf{S}_k' \mathbf{T}_k \mathbf{T}_k'^\dagger \mathbf{S}_k')]$ with α_k empirical parameter.

The open shell fragment.

The contribution of the fragment a_K to δE is

$$\delta E_K = \mathrm{Tr} \delta \mathbf{T}_K^\dagger \left(\mathbf{1}^{M_K} - \mathbf{S}_K' \mathbf{T}_K \mathbf{T}_K^\dagger\right) \mathbf{F}_K' \mathbf{T}_K +$$
$$+ \mathrm{Tr} \delta \mathbf{V}_K^\dagger \left(\mathbf{1}^{M_K} - \mathbf{S}_K' \mathbf{T}_K \mathbf{T}_K^\dagger - \mathbf{S}_K' \mathbf{V}_K \mathbf{V}_K^\dagger\right) \mathbf{L}_K' \mathbf{V}_K + \mathrm{c.c.} \qquad (33)$$

To the aim of obtaining a minimisation algorithm, it may be advantageous the application of the strategy of Guest and Saunders (1974) to Eq.(33).

Let us introduce the $N^w = M_K - N_K - N^o$ non occupied orbitals φ^w of the fragment a_K. $\varphi^w = \chi_K \mathbf{W}_K$ where $\mathbf{W}_K$ is an $M_K \times N^w$ matrix. Remembering (23) and (26), it is convenient to impose to $\mathbf{W}_K$ orthogonality conditions in such a way that the $M_K \times M_K$ matrix $\mathbf{Z}_K = (\mathbf{T}_K \mid \mathbf{V}_K \mid \mathbf{W}_K)$ fulfils the global condition

$$\mathbf{Z}_K^\dagger \mathbf{S}_K' \mathbf{Z}_K = \mathbf{1}^{M_K} \qquad (34)$$

In each step the new orbital matrix $\mathbf{Z}_K'$ is evaluated through the unitary transformation $\mathbf{Z}_K' = \mathbf{Z}_K \mathbf{U}$. The $M_K \times M_K$ unitary matrix $\mathbf{U}$ is obtained solving the problem

$$\begin{cases} \mathbf{B} \mathbf{U} = \mathbf{U} \mathbf{D}_K \\ \mathbf{U}^\dagger \mathbf{U} = \mathbf{1}^{N_K} \end{cases} \qquad (35)$$

where $\mathbf{D}_K$ is an $N_K \times N_K$ diagonal matrix and the $M_K \times M_K$ matrix $\mathbf{B}$ is so defined

$$
\mathbf{B} = \begin{bmatrix}
\mathbf{T}_K^\dagger \mathbf{B}^c \mathbf{T}_K & \mathbf{T}_K^\dagger \mathbf{F}' \mathbf{V}_K & \mathbf{T}_K^\dagger \mathbf{F}' \mathbf{W}_K \\[2ex]
\mathbf{V}_K^\dagger \mathbf{F}' \mathbf{T}_K & \mathbf{V}_K^\dagger \mathbf{B}^o \mathbf{V}_K + \alpha \mathbf{1}^{N^o} & \mathbf{V}_K^\dagger \mathbf{L}' \mathbf{W}_K \\[2ex]
\mathbf{W}_K^\dagger \mathbf{F}' \mathbf{T}_K & \mathbf{W}_K^\dagger \mathbf{L}' \mathbf{V}_K & \mathbf{W}_K^\dagger \mathbf{B}^w \mathbf{W}_K + \beta \mathbf{1}^{N^w}
\end{bmatrix} \qquad (36)
$$

In (36) the matrix elements connecting orbitals of different categories (off-diagonal blocks) will be vanishing when the conditions for a stationary energy are satisfied. The $(M_K \times M_K)$ matrices $\mathbf{B}^c$, $\mathbf{B}^o$ and $\mathbf{B}^w$ appearing in the diagonal blocks have the effect of fixing "canonicalization conditions" (Guest and Saunders 1974) for $\mathbf{T}_K, \mathbf{V}_K$ and $\mathbf{W}_K$ respectively. Remembering that the unitary transformations that mix orbitals of each group among themselves do not alter the wave function nor the density matrices $\mathbf{R}$ and $\mathbf{R}^o$ and therefore the energy, $\mathbf{B}^c$, $\mathbf{B}^o$ and $\mathbf{B}^w$ may, in principle be arbitrary hermitian matrices. In practice an appropriate choice may affect the convergence. In our calculations we have chosen $\mathbf{B}^c = \mathbf{F}'_K$, $\mathbf{B}^o = \mathbf{L}'_K$ and $\mathbf{B}^w = \mathbf{L}'_K$. At convergence the orbitals $\mathbf{T}_K, \mathbf{V}_K$ and $\mathbf{W}_K$ will be canonical over these matrices. α and β are scalars used to denote the first and second "level shifters".

A perturbative analysis of the problem enclosed in Eq.(35) may be accomplished when the elements belonging to the off-diagonal blocks of $\mathbf{B}$ may be considered "small" with respect to the matrix consisting only of the diagonal blocks of $\mathbf{B}$. An appropriate choice of the "level shifters" α and β has the effect of making this hypothesis valid. We notice that the zero-order perturbation (depending on the diagonal blocks of $\mathbf{B}$) may imply a consistent transformation of the matrices $\mathbf{T}_K, \mathbf{V}_K$ and $\mathbf{W}_K$ in the sense of a linear combination of the columns of each of these matrices separately. But Eq.(33) shows that the only energetically significant variations are those that mix orbitals of different categories. It can be shown that this "mixing" is of the same order of the off-diagonal blocks. It is then possible to use Eq.(33) which yields a negative δE_K.

The procedure presented above has been implemented along the following scheme:

Iterative minimisation procedure:
1. Guess trial matrices $\mathbf{T}_1 \dots \mathbf{T}_K$, $\mathbf{V}_K$, $\mathbf{W}_K$.
2. Orthonormalize $\mathbf{T}_1 \dots \mathbf{T}_K$ (Separately for each fragment). The metric is free.
3. Evaluate $\mathbf{R}$ using Eq.(6).
4. Build $\mathbf{Q}$ defined by Eq. (21).
5. Compute $\mathbf{S}'_k$ (k=1...K) given by (22).
6. Orthonormalize $\mathbf{V}_K$, as required by (26), through the following procedure

$$V_K \Leftarrow \left(1^{M_K} - T_K T_K^\dagger S_K'\right) V_K$$

$$V_K \Leftarrow V_K \left(V_K^\dagger S_K' V_K\right)^{-\frac{1}{2}}$$

7. Build R^o using (27).
8. Compute $G(R)$, $G(R^o)$, $G'(R^o)$ as defined by Eqs. (9) and (10).
9. Compute the electronic energy E through Eq. (8).
10. Check the variations in the density matrices R and R^o : if less then tolerance, exit
11. Build P through Eq. (28)
12. Evaluate L, F,L_K', F_k' (for k=1...K) defined by Eqs. (17) (18) (29) (24).
13. For k=1...K-1 obtain the new T_k' solving the secular problem:

$$\begin{cases} \left[F_k' + \alpha_k \left(S_k' - S_k' T_k T_k^\dagger S_k'\right)\right] T_k' = S_k' T_k' E_k \\ T_k'^\dagger S_k' T_k' = 1^{N_k} \end{cases}$$

14. Orthonormalize W_K through the following procedure:

$$W_K \Leftarrow \left(1^{M_K} - T_K T_K^\dagger S_K' - V_K V_K^\dagger S_K'\right) W_K$$

$$W_K \Leftarrow W_K \left(W_K^\dagger S_K' W_K\right)^{-\frac{1}{2}}$$

15. Evaluate the matrix B given in Eq.(36) where $B^c = F_K'$, $B^o = L_K'$ and $B^w = L_K'$
16. Solve the problem (35) and evaluate $Z_K' = Z_K U$.
17. $T_k \Leftarrow T_k'$ (k=1...K-1)
    $Z_K \Leftarrow Z_K'$ i.e $(T_K|V_K|W_K) \Leftarrow (T_K'|V_K'|W_K')$
18. Go back to step 2.

IV. Calculations and Results

Cu-He , Cu (He)₂ , Li (He)₂
    We have performed a few full electron calculations using basis already employed for other studies: for Cu, see Poirier *et al.*, (1985) , for He see van Lenthe *et al.*, (1984) and for Li see Poirier *et al.*, (1985). The results are shown in Figures 2 - 5.
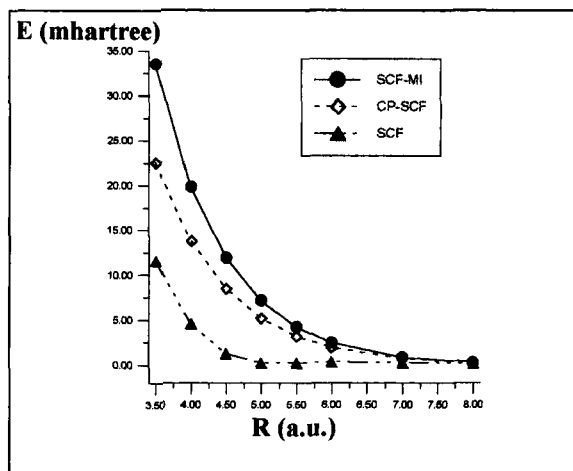
Fig. 2. *Cu-He; SCF-MI, CP-SCF and SCF Interaction Energy.*

As it can be seen in Figure 2, the energy curves for He-Cu turn out fully repulsive, with the SCF-MI values above the SCF ones. The SCF-CP values are almost everywhere intermediate between the SCF and the SCF-MI results, showing that the CP method does not correct entirely the BSSE. The fact that for this system the SCF-MI potential decreases faster then the SCF and the CP ones at larger distances are consistent with the study of Eichenauer *et al.* (1987)
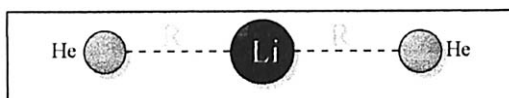
Fig. 3. *He₂-Li system.*

$R = 3.5$ *a..u.*; $\Delta E_{SCF-MI} = 47.155$ *mHartree*; $\Delta E_{SCF} = 37.199$ *mHartree*
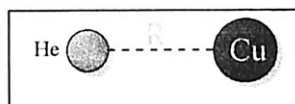
Fig. 4. *He-Cu system.*

$R = 3.5$ *a..u.*; $\Delta E_{SCF-MI} = 33.530$ *mHartree*
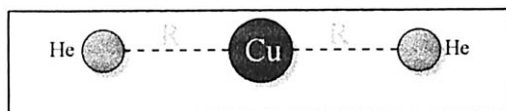
Fig. 5. *He₂-Cu system.*

$R = 3.5$ *a..u.*; $\Delta E_{SCF-MI} = 71.122$ *mHartree*

(H₂O)₃

In Table I we report the results on water trimer and in Fig.(6) the geometry adopted (Clementi *at al.* ,1980). A more complete work on this system will be presented later. The method has been applied to compute non additive effects, $\Delta E_{n.add.}$, for a variety of conformations of the trimer. The results have been used to generate a new *ab-initio* potential where many body effects were incorporated (Raimondi *et al.*,1997).
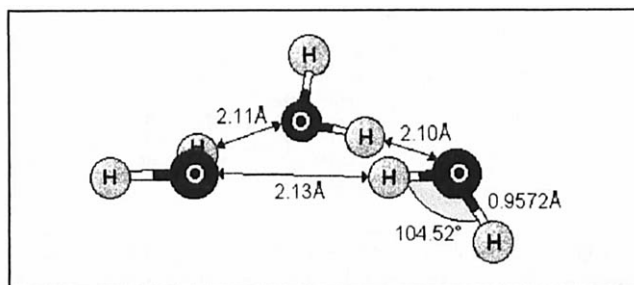
Fig. 6. *Geometry of the water trimer.*
TABLE I
WATER TRIMER: SCF AND SCF-MI RESULTS.

basis set	number of functions	ΔE_{ABC} SCF Kcal/mol	ΔE_{ABC} SCF-MI Kcal/mol	$\Delta E_{n.add.}$ SCF Kcal/mol	$\Delta E_{n.add.}$ SCF-MI Kcal/mol
6-31G	39	-18.79	-14.36	-4.11	-3.72
6-31G**	75	-15.35	-10.95	-2.22	-1.87
TZVP++	153	-10.30	-8.41	-2.32	-2.20
6s4p3d/4s3p[a]	186	-9.97	-8.08	-2.44	-2.29

[a] Basis set taken from Millot and Stone (1992)

V. Conclusions

We have presented the extension of the SCF-MI algorithm (Gianinetti, Raimondi and Tornaghi, 1996) to the more general case of the intermolecular interactions between closed- and open-shell systems. As in our previous work, the BSSE is excluded *a priori,* by allowing the expansion of molecular orbitals of each fragment only in the basis functions centred on the fragment itself.

The simplicity of the standard SCF procedure has been preserved. The closed shell Roothaan equations and the Guest and Saunders open shell equations have been modified at the cost of a negligible complication with respect to the usual algorithm.

For all the systems considered we did not observe any convergence difficulty, while the computer time turned out comparable with that of the standard SCF procedure.

The method appears stable and efficient and the choice of the most convenient values of the α and β level shifter parameters did not require any particular care. The program has been tested by means of a code based on an iterative first-order Brillouin scheme where the nonorthogonality of the orbitals of the two fragments is directly taken into account by a general VB program, finding perfect agreement.

We are aware that a possible criticism of the SCF-MI procedure might be that the method does not allow charge transfer effects to occur. As already discussed previously (Gianinetti, Raimondi and Tornaghi, 1996), we remind that the constraints on the SCF-MI orbitals - $\varphi_k = \chi_k \, T_k$ - do not prevent a certain amount of charge transfer to take place. The reason why this can occur is that the SCF-MI orbitals of different subgroups are not constrained to be orthogonal but are allowed to *overlap*. In this way the orbitals of a fragment can have tails on other fragments and viceversa; it is worth noting that these tails do not originate from unphysical nodes imposed by orthonormalisation processes. This peculiarity will be beneficial also to *all* the other terms which are sensitive to the detailed description of the overlap region as it provides to the SCF-MI orbitals the necessary flexibility and freedom to adapt under the effects of the physical interactions. For this to be true, it is sufficient to employ functions which are not too tightly localised. This last condition is obviously requested when studying van der Waals complexes or hydrogen bonded systems.

The SCF-MI BSSE free method does not take into account dispersion forces, connected to electronic intermolecular correlation effects. By using the SCF-MI wave function as a starting point, however, a *non orthogonal* BSSE free CI procedure can be developed. This approach was applied to compute intermolecular interactions in water dimer and trimer: the resulting *ab initio* values were used to generate a new NCC-like potential (Niesar *et al.*, 1990). Molecular dynamics simulation of liquid water were performed and satisfactory results obtained (Raimondi *et al.*, 1997).

References

Boys, S.F., and Bernardi, F. (1970). *Mol Phys.* **19**, 553.

Clementi, E., Kolos, W., Lie, G.C., and Ranghino, G. (1980). *Int. J. Quantum. Chem.* **17**, 377.

Eichenauer, D., Harten, U., Toennies, J.P., Celli, V. (1987). *J. Chem Phy.* **86**, 3693.

Gianinetti, E., Raimondi, M., and Tornaghi, E. (1996). *Int. J. Quantum Chem.* **60**, 157.

Guest, M.F., Saunders, V.R. (1974). *Mol. Phys.* **28**, 819.

Hillier, I.H., and Saunders, V.R. (1970). *Int. J. Quantum Chem.* **4**, 503.

McWeeny, R. (1964). *"Molecular Orbitals in Chemistry, Physics and Biology."* edited by P.-O.Lowdin and A. Pullmann (Academic Press), p.305.

Millot, C., and Stone, A. J. (1992). *Mol. Phys.* **77**, 439.

Niesar, U., Corongiu, G., Clementi, E., Kneller, G. R., and Bhattacharya, D. K. (1990). *J. Phys. Chem.* **94**, 7949.

Poirier, R., Kari, R., Csizmadia, I.G. (1985). *Handbook of gaussian basis sets.* Elsevier - Amsterdam.

Raimondi, M., Famulari, A., Gianinetti, E., Sironi, M., Specchio, R., and Vandoni, I.,(1997). *Adv. Quantum Chem.* this volume

Simon, S., Duran, M.,Dannenberg, J. J. (1996). *J. Chem. Phys.* **105**, 11024.

van Duijneveldt, J.G.C., vanDuijneveldt-van de Rijdt, M., and van Lenthe, J.H. (1994). *Chem. Rev.* **94**, 1973.

van Lenthe, J.H., van Duijneveldt, F.B. (1984). *J. Chem. Phys.* **81**, 7.

Xantheas, S. S. (1996). *J. Chem. Phys.* **104**, 8821 .

Parallelization of the CI Program PEDICI

Thorstein Thorsteinsson and Sten Rettrup

Department of Chemistry, Copenhagen University,
Universitetsparken 5, DK-2100 Copenhagen Ø, Denmark

Abstract

The general CI code PEDICI has been parallelized by decomposing the occurring summation over two-electron integrals. The parallelization was formulated in terms of a "master/slave" model, and realized through use of the "PVM" message passing facility. We have aimed at achieving a reasonably simple implementation for use on machines with intermediate numbers of processors. Exploratory test runs on an IBM SP supercomputer (consisting of RS/6000 model P2SC (120 MHz) nodes) show a very satisfactory performance increase with the number of processors used, as well as encouraging balancing of the workload. Our largest 32-processor test case gives a speed-up factor of 30.27.

Contents

1. Introduction

Parallel computations are now an integral part of quantum chemistry. During the past 10 years parallelization of most mainstream methodologies have been considered, and the number of publications in this area is growing rapidly (for reviews see, for example, Refs. 1–3). This is not surprising since purely theoretical development is unlikely to yield performance gains comparable to what may be obtained by proper utilization of modern parallel computers. On the other hand, parallel programming is a complex task, and it seems that the devoted attention of experts is required to attain maximum possible efficiency. In this work, however, we have adopted a more pragmatic attitude, with a main aim being to demonstrate that very satisfactory results may be obtained with a reasonable investment of human effort.

Configuration interaction (CI) constitutes one of the earliest concepts in quantum chemistry, and it remains one of the most accurate approaches for describing the electronic structure of small and medium-sized molecular systems. This is the case for the powerful combination of complete active space self-consistent field (CASSCF) calculations with multi-reference (MR) CI treatments, but also large scale full CI applications have been subject to increasing interest during the past years. They may, for example, provide useful benchmark results for methods at a lower level of theory. Significant efforts have therefore been directed towards parallelizing CI algorithms (for a comprehensive account see Ref. 1), and highly impressive results have thus been obtained. This is exemplified by a full CI calculation, reported by Harrison and Stahlberg [4], incorporating 95 million configuration state functions (CSFs). Also among the very most exciting results is the massively parallel implementation of the MRCISD program system COLUMBUS [5–7]. Reasonable efficiency was reported using up to 256 processors, and applications employing 38 million CSFs have been carried out [7].

The main objective of the present research project was to enable the utilization of modern parallel machines with moderate numbers of processors without substantially restructuring the existing CI code, PEDICI [8,9]. Keeping the implementation as simple as possible was a major concern, while retaining enough flexibility to allow possible future adaptation to massively parallel architectures. PEDICI is a general purpose multireference CI package not dedicated to any particular excitation scheme, using a strategy for matrix element evaluation based on the symmetric group approach.

A general outline of the parallelization of PEDICI is provided in Section 2, while Section 3 describes some of the practical aspects involved. Section 4 presents the results of test calculations on an IBM SP machine employing up to 32 processors. Finally in Section 5 we draw our main conclusions and give

some consideration to a possible massively parallel implementation.

2. Outline of implementation

The parallelization of PEDICI mainly concerned itself with the "direct CI" [10] part of the program, which generally is by far the most time consuming. In the iterative procedure first proposed by Davidson [11], or the many existing variants hereof, a central step consists of the efficient multiplication of the electronic Hamiltonian matrix onto a given trial vector:

$$\boldsymbol{\sigma} = \mathbf{H}\,\mathbf{c}. \tag{1}$$

Analogous considerations apply, for example, to the calculation of second-order properties, for which a very similar computational problem must be addressed. For typical applications this step constitutes 95–100% of the total computational effort, and a successful parallelization will therefore reflect directly on overall performance.

The strategy for matrix element evaluation used in PEDICI relies on the combination of graphical techniques for describing the configuration space with the symmetric group approach for the evaluation of CI coupling coefficients. Our graphical indexing procedure represents further development of the method first proposed by Shavitt [12,13], considered later also by Duch and Karwowski [14,15]. As is well known, there are few practical limitations on the form of CI spaces that may be represented by such graphs, but this generality also necessitates greater efficiency in the evaluation of indexing information than is likely to be the case for more restricted CI strategies. The CI coupling coefficients are obtained from representation matrices of S_N, the generation of which is described in detail in Ref. 16.

The integral-driven implementation of this strategy leads to a loop structure that may be written on the form:

1. Loop possible "integral shape" segments [8,9] for a batch of two-electron integrals.

2. Obtain line-up permutation, P, and position of corresponding block in the Hamiltonian.

3. Generate the corresponding spin representation matrix, $V(P)$, combine it with two-electron integrals, and apply the resulting components of the Hamiltonian to the CI vector.

For further details we refer to the previously published accounts [8,9]. In summarizing the time consuming part of the procedure it is convenient to

adopt the form:

$$\sigma_I = \sigma_I^{(1-el)} + \sum_{pqrs} \langle pq|rs \rangle \sum_J A_{pqrs}^{IJ} c_J, \qquad (2)$$

where the CI coupling coefficients, A_{pqrs}^{IJ}, are trivially related to the representation matrices, $V(P)$, for the line-up permutations. The efficient (sequential) implementation of Eq. (2) relies on an integral-driven algorithm in which contributing I-J pairs are exhausted for each integral $\langle pq|rs \rangle$. Also noteworthy is the inherent difficulty, within the symmetric group approach, associated with *vectorization* of this step, since the block-wise representation of CSFs leads to relatively short vector loops.

Within an integral-driven procedure it seems natural to perform the parallelizing decomposition according to the *pqrs* summation in Eq. (2). This must lead to a relatively coarse-grain parallelization, because the important computational effort associated with identification of I-J pairs and evaluation of the corresponding coupling coefficients, A_{pqrs}^{IJ}, then becomes distributed among all processors. Furthermore, the number of integrals, and thus overall parallel tasks, is sufficiently large that an even distribution of the work load can be expected.

As such, the total effect of the Hamiltonian matrix may be obtained by summing partial σ vectors, generated on P individual "slave processors":

$$\sigma = \sigma^{(1-el)} + \sigma_1 + \sigma_2 + \ldots + \sigma_P, \qquad (3)$$

with each slave process generating its σ vector from a subset of two-electron integrals. The following three steps summarizes our algorithm:

1. Distribute **c** vector of Eq. (1) from "master" to all "slaves":

$$\mathbf{c} \longrightarrow \left\{ \begin{array}{c} \mathbf{c} \\ \vdots \\ \mathbf{c} \end{array} \right.$$

2. Distribute blocks of integrals to "slaves" on request until end of integral file. Each slave carries out a part of the second summation given in Eq. (2):

$$\langle pq|rs \rangle \longrightarrow \left\{ \begin{array}{c} \sigma_1 \\ \vdots \\ \sigma_P \end{array} \right.$$

3. Collect partial σ vectors from all "slaves":

$$\sigma \longleftarrow \left\{ \begin{array}{c} \sigma_1 \\ \vdots \\ \sigma_P \end{array} \right.$$

A major determining factor for the parallelization overhead will thus be the data transfer associated with distributing and gathering the CI vectors, as well as the distribution of two-electron integrals.

3. Details of implementation

A more detailed account of the parallelization may be of interest to researchers seeking to parallelize electronic structure codes. We consider therefore in this section those aspects of the parallelization that are not directly related to the direct CI algorithm discussed in Section 2. We first state our overall implementational objectives, followed by some more practical details, including also a description of the PVM [17,18] message passing facility used.

Simplicity of implementation was, as discussed in previous sections, an important goal of this work. More specifically, our main objectives included: (1) a straightforward parallel control structure, (2) simple message passing between processors, (3) minimal restructuring of the existing algorithm, and (4) minimal change to the existing code. Point (3) may be the most difficult to comply with in practice, whereas the others will be under the programmers control to a greater extent. How much restructuring is required will depend strongly on the sequential program's suitability for parallelization, and in the worst case a successful parallelization may not be attainable without a complete recasting of the underlying algorithm. Alternatively, the form of the sequential program may dictate the use of a specific parallel algorithm, in order for a practical implementation to be possible. As such, the fact that the sequential algorithm in PEDICI was integral driven, quite naturally led to the parallelizing decomposition of the integral summation discussed in Section 2.

The simplest possible organizational scheme for parallel applications is likely to be in the form of a "master/slave" model. In such an approach, a given processor is assigned to controlling the parallel tasks, and often this process will also handle the primary I/O required. Devoting a processor to such tasks generally implies that the theoretical maximal efficiency will be somewhat reduced, simply because a processor less will be involved in actual computation. This is only likely to be serious for applications using very few processors, however, and for larger numbers it is likely to be of no practical concern. Of course, a master/slave implementation may, when suitable, also show *better* scalability compared to other parallelization models.

We decided that the least possible change to our code could only be achieved if it was kept in the form of one single program (what could be termed a "single program multiple data" (SPMD) implementation [2]). This is important when considering further development or maintenance of the program, but in many

ways it also turns out to simplify the parallelization significantly. There is no need to transmit large amounts of easily-generated indexing information, for example, as each slave simply processes the required input files, and executes all relevant parts of the code.

Two issues that deserve mentioning, but do not relate directly to the message passing process, are the handling of run-time errors and I/O. However, while the former is an important part of the reliability of a program, we feel that providing a detailed account is outside the scope of this paper. The special need for addressing this point when considering parallel computations stems from the fact that premature termination of one or more slave processes, if unchecked, not necessarily will be detected by the master process. The application is then likely to "hang", which can be wasteful in terms of computer resources. Special facilities for overcoming problems of this sort exist in most message passing libraries.

For considering the handling of I/O, it is useful to divide file types into three basic categories: (1) input files, (2) output files, and (3) scratch files. Input files constitute all prerequisites of the program, while output and scratch files are program-generated. We decided that the simplest differentiation between files would be achieved at the stage they are opened, a procedure which is easily automated by defining suitable subroutines. In our master/slave model, it is primarily input and output files belonging to the master process that are of interest. We assume that input files are only available on the master node, and such files will therefore be broadcasted as soon as they are first opened (of course, for large input files not required by slaves (e.g., the integral file), one may disable such broadcasting). Slave files are not generally of interest, and may as such be given scratch status. To take into account the possibility of a shared file system, file names may furthermore be given process-dependent extensions to avoid collisions.

It is appropriate to give a brief introduction to the use of message passing libraries, in particular PVM [17, 18] ("Parallel Virtual Machine") which was used in this work. For further details of these facilities we refer to the available literature. In PVM, message passing is carried out by daemon processes, which means, for example, that for parallel applications on workstation clusters PVM daemons must be running on each participating machine. Of course, implementations on multi-processor machines may differ from this. Once the PVM daemons are running and have established communication, the network of processors can be thought of as a single "virtual machine", and interaction between user processes then takes the form of simple calls to Fortran or C library subroutines. To facilitate the porting of our code to other message passing packages, such as MPI [19], we took care to use only the most basic of these message passing routines.

Start up:
Spawn: Starts child processes.
Mytid: Obtains own task ID (TID).
Parent: Obtains parent task ID.
Config: Obtains information about the virtual machine.
Exit:
Kill: Kills a specified PVM process.
Exit: Exits from the PVM daemon.
Data transfer:
Initsend: Prepares buffer for data transfer.
Pack: Packs data of specified type into PVM buffer.
Send/Mcast: Transmits data in current buffer.
Recv: Awaits receipt of data as specified by MSGTAG.
Bufinfo: Returns message buffer information (e.g., sender TID).
Unpack: Unpacks data of specified type.

Figure 1: Summary of PVM routines used in the parallelization of PEDICI.

Data transfer is in PVM done in three steps:

1. Initialize message buffer (routine initsend).

2. Pack data into message buffer.

3. Transmit data.

The reverse of this procedure is carried out by the receiving processor. Several different data types (e.g., integer*4 and real*8) may be packed into the same message buffer. A strength of PVM is that this packing also allows data to be transferred between workstations of different architecture. However, the effort associated with encoding and decoding data is likely to reduce communication speed. Specification of recipient, or sender, is achieved by using single-integer "task IDs", and so each process in the PVM virtual machine is assigned a unique such identifier. Also associated with each message is a "message tag".

A summary of all PVM routines used in PEDICI is given in Fig. 1. (We have given here the short version of the subroutine names—the complete names are of the form "PVMF*name*" for the Fortran library, and "pvm_*name*" in C.) Generally just one process is created at the beginning of a parallel job, such that this process must start slave processes by calls to the PVM spawn routine (this is true even for applications that do not use the master/slave model). When finishing the parallel application, the PVM daemon is notified by using

the PVM exit routine. Termination of other PVM processes, by calls to the
"kill" subroutine, is primarily suitable for handling of run-time errors.

4. Results of test calculations

Using the parallel version of our CI program, a series of test runs were carried
out on an IBM SP machine consisting of RS/6000 model P2SC (120 MHz)
nodes.

One set of test calculations was carried out on the low-lying electronic
singlet states of CO (see also Refs. [20,21]). Calculations were carried out at
the equilibrium bond length, 2.132 bohr [22], employing basis sets consisting
of [7,6,3] contracted functions for both carbon and oxygen [23]. This gives
a total of 86 basis functions. A CISD treatment based on the ground state
configuration $1\sigma^2 2\sigma^2 3\sigma^2 4\sigma^2 1\pi^4 5\sigma^2$ then leads to 22318 CSFs of $^1\Sigma^+$ symmetry.
For this job, the sequential version of PEDICI takes 511 CPU seconds pr.
Davidson iteration, compared to a total of 20 CPU seconds spent in other
parts of the program.
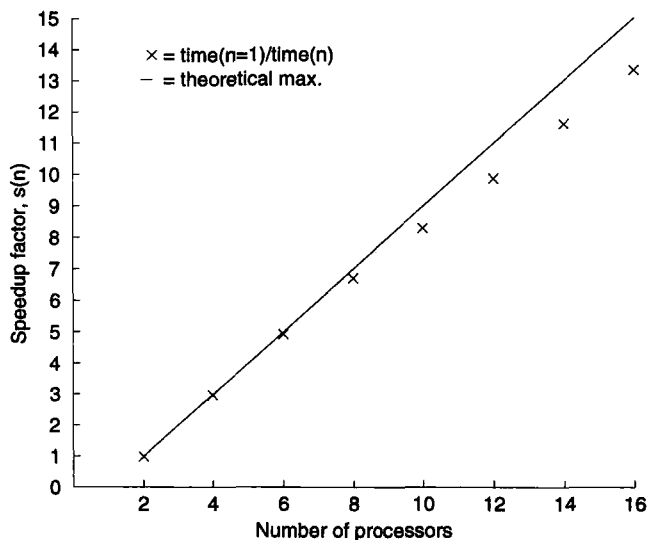
Figure 2: Speedup for CISD test calculations on CO using the public domain
PVM message passing interface.

We show in Figs. 2 and 3 the speed up for a Davidson iteration obtained with the PVM [17] ("Parallel Virtual Machine") and PVMe [18] ("PVM enhanced") message passing interfaces respectively. Speed-up factors are here relative to the sequential version of the program (n=1), and the theoretical maximum has been defined according to the expression $s(n) = n - 1$ appropriate to the used master/slave model.
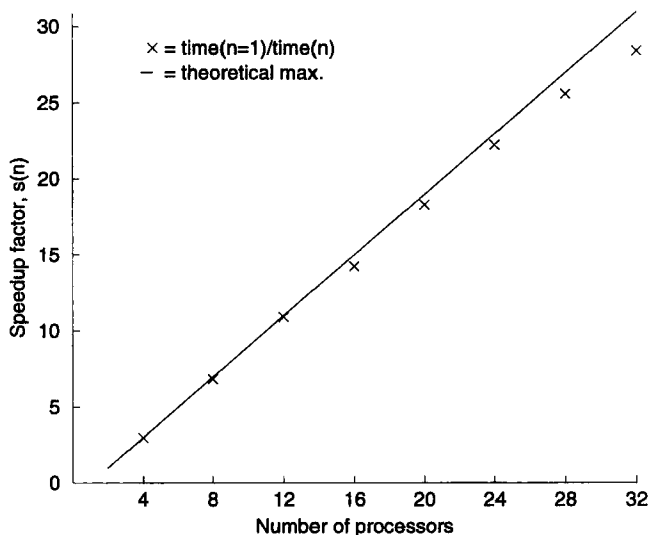
Figure 3: Speedup for CISD test calculations on CO using the IBM PVMe message passing interface.

The IBM product PVMe takes advantage of the IBM SP "high performance switch," and can as such be expected to perform somewhat better than the public domain version. Indeed, not until around 28 to 32 processors can a definite decrease in performance be detected. For the 32-processor calculation the speed-up factor was 28.44, which, given our initial aim, we find satisfactory.

As an illustration of the load balancing achieved in a typical 32 processor calculation, we present the CPU usage for each of the 31 slave processes in Fig. 4. The difference between maximum and minimum CPU times is here 0.41 sec., and the overall root mean square deviation is 0.45%. This is very satisfactory, and it would seem unlikely that load balancing will present serious problems in future applications unless a significantly larger number of processors is employed.
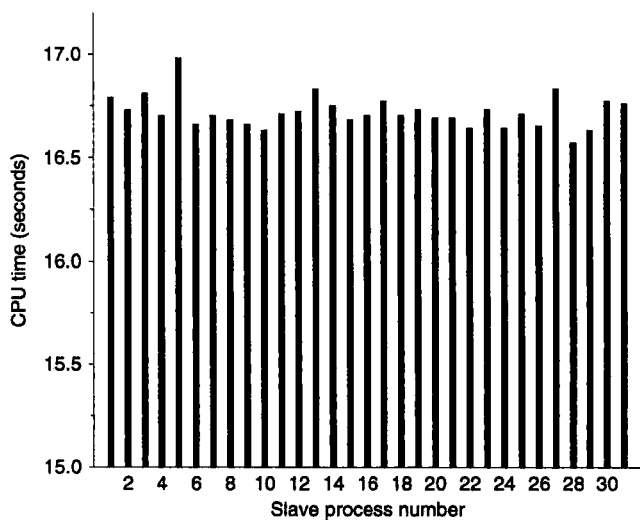
Figure 4: Load balancing between slave tasks for the 32-processor calculation on CO using PVMe.
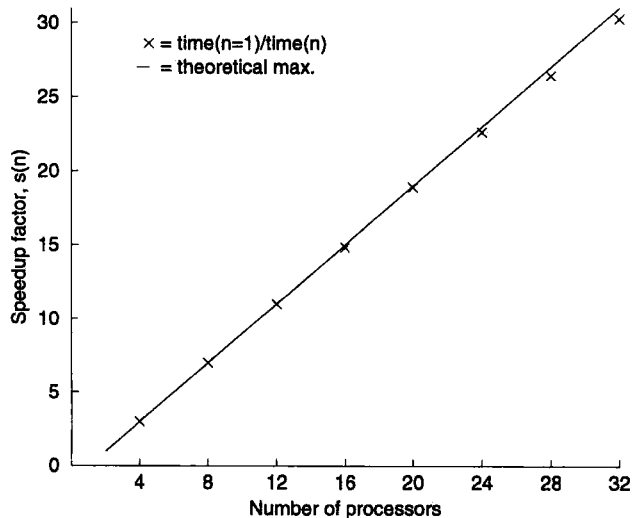
Figure 5: Speedup for CISD test calculations on MnO_4^- using the IBM PVMe message passing interface.

A second series of test calculations was performed on the permanganate ion (cf. Refs. 24, 25). A tetrahedral geometry was assumed with an Mn–O bond length of 1.629 Å [26], and we used basis sets consisting of [10,7,3] and [5,3] contracted functions for manganese and oxygen respectively [25,27]. The subsequent CI calculations were carried out in the largest Abelian subgroup, D_2, including all single and double excitations from the valence space. This leads to 185745 configuration state functions of ^1A symmetry. For the sequential version of the program, a single Davidson iteration took 6495 CPU seconds, compared to 224 CPU seconds spent in other stages of the job.

The resulting PVMe speed-up factors are shown in Fig. 5, with the load balancing for the 32-processor job given in Fig. 6. This application gives a near-perfect scalability for the range of processors considered, with a speed-up factor of 30.27 found for the 32-processor calculation. Compared with the theoretical maximum of 31 in our master/slave implementation, this represents a relative efficiency of 97.6%. For the load balancing, a maximum deviation of 2.6 secs. and RMS value of 0.16% is found. Both these values are largely determined by the deviations for processors 5 and 9. Indeed, the lower CPU times for processors 5 and 9 appear odd when taking into account the excellent
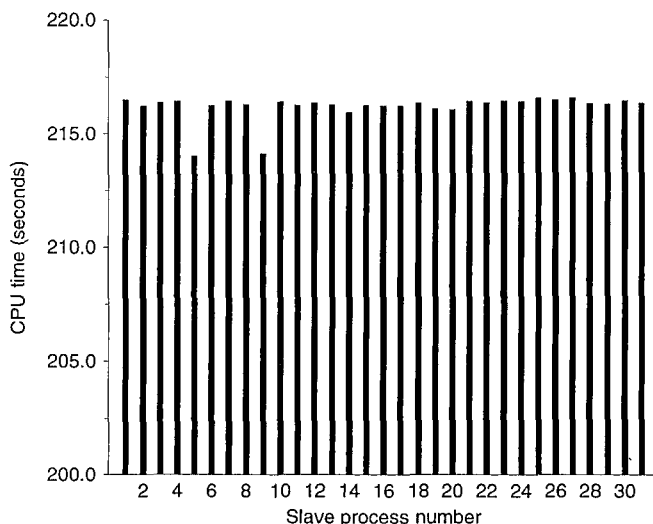
Figure 6: Load balancing between slave tasks for the 32-processor calculation on MnO_4^- using PVMe.

load balancing for all other processors, and the possibility of some anomalous occurrence, not directly associated with the present application, cannot be ruled out.

5. Discussion

We believe that our initial goal of keeping the parallelization relatively simple while still obtaining satisfactory performance has been achieved to a large extent. Of course, this motivation strongly influenced the details of our implementation, key features of which include the decomposition of work load according to the integral summation of Eq. (2); a "master/slave" model for parallelization; and the use of the PVM facility for data transfer. For the applications considered in Section 4 this leads to highly satisfactory speed-up factors for up to 32 processors. Since excellent load balancing is seen, the performance degradation for larger numbers of processors clearly occurs because of the overhead involved in data transfer. Further optimization of the code must therefore pay special attention to the distribution of integrals, as well as the broadcasting and gathering of CI vectors.

At present there exist several different systems for message passing in parallel applications, the two most widely used being MPI [19] ("message passing interface") and PVM. The lack of a universally accepted standard is unfortunate, and so, with the necessity of future porting in mind, we have restricted the use of PVM-specific features to a minimum. Since a base of message passing facilities must be common to all these systems, we envisage ŋo major portability problems for our code. Characteristics of PVM that influenced our choice were its fairly widespread use combined with the fact that it is freely available [17]. An additional advantage is PVM's suitability for use on workstation clusters—especially within scientific environments this option may be an economical alternative to the use of parallel supercomputers.

We have based our parallelization on decomposing the summation over integral labels given in Eq. (2), such that, in our master/slave model, integrals are distributed on request from slaves. The determining factors for the efficiency will therefore be the associated communication speed, and the possibility of achieving even load balancing. Several alternative strategies aiming to avoid extensive data transfer on one single node may be envisaged, such as for example:

- A "master/secondary master/slave" model.

- Distributing some or all integrals at the beginning of job.

- Allowing multiple simultaneous I/O operations on the integral file.

- An integral-direct procedure—integrals are evaluated as required.

The efficiency of these approaches will strongly depend on features relating to computer architecture, and so we shall forego a detailed discussion here. Of course, if all integrals are distributed at the beginning, this will involve an overhead, compared to alternative strategies, which will scale linearly with the number of processors used Also, in the context of a massively parallel implementation, an integral-direct strategy would certainly seem to have very great potential.

The size of integral batches we use typically range from 1000 to 5000 real*8 words (with some variation according to integral type), and, as seen in Section 4, this gives a satisfactory balancing of the workload. One could envisage some adjustment of the batch size according to particular applications, but the data transfer latency (i.e., start-up time) would rule out very small integral batches. Compared with possible alternative strategies, the flexibility in the choice of granularity counts in favour of a decomposition of the integral summation, as done here.

Straightforward summation of partial $\boldsymbol{\sigma}$ vectors involves $N_{\mathrm{proc}}-1$ summations, whereas simultaneous summations on the slave processors in principle can reduce this to $\log_2(N_{\mathrm{proc}})$. This would be the case with perfect load balancing, but for more realistic cases the optimal summation strategy is likely to involve a compromise between a simple summation on the master process and summation according to a binary tree structure. We foresee a need for addressing this problem when moving to a larger number of processors.

A main issue remaining is that of CI vector segmentation. This may be done in sequential calculations in order to handle larger dimensions of the CI space than may be kept in core memory, but a similar strategy may be invoked on distributed-memory parallel machines [7]. In this way problems may be considered that are a factor of $\sqrt{N_{\mathrm{proc}}}$ larger than what would otherwise be possible. The obvious overhead related to such an approach lies in the identification of the relevant two-electron integrals for given segment pairs, and this is a particularly serious problem for the very general types of CI expansion that may be considered within a graphical approach. However, it certainly seems worthwhile to pursue this idea further with a massively parallel implementation in mind.

Our previous conclusions will all have some dependence on the particular type of application considered, an aspect which may influence the total CPU work load, the amount of data transfer required, and the possibility of obtaining even load balancing. Our findings in this work would suggest that load balancing does not constitute a problem for CI applications of reasonable size, and the success or failure of the parallelization will therefore be determined

largely by the transfer of CI vectors and two-electron integrals. This dependence may be *direct*, if the total data transfer time becomes comparable to the single-processor CPU time, or *indirect*, if data transfer time leads to slave processors becoming idle while waiting for integral batches. In the present case, the MnO_4^- test job parallelized better than the CO job, and it is tempting to associate this with its greater size. If such a size-dependence is found to exist generally, scalability is likely to become even more favourable for larger examples than those considered here.

The parallel version of PEDICI developed here seems well suited for computations on distributed-memory machines such as the IBM SP, and the accurate dynamical load balancing would suggest that favourable results could also be obtained on heterogeneous workstation clusters. Further essential aspects for the success of our implementation were the optimal use of computer hardware (as exemplified by the importance of employing the SP "high performance switch"), and possibly an advantageous dependence on application size. While bearing these points in mind, we believe that the 95% overall efficiency we obtain for our largest 32-processor case demonstrates the viability of a practical approach to parallelization.

Acknowledgments

References

[1] R. J. Harrison and R. Shepard, *Ann. Rev. Phys. Chem.* **45**, 623 (1994).

[2] R. A. Kendall, R. J. Harrison, R. J. Littlefield and M. F. Guest, *Rev. Comp. Chem.* **VI**, 209 (1995).

[3] T. G. Mattson (ed.), *Parallel Computing in Quantum Chemistry* ACS Symposium Series 592, ACS, Washington, 1995.

[4] R. J. Harrison and E. A. Stahlberg, *Proceedings of the Mardi Gras '93 Conference: High Performance Computing and Its Applications in the Physical Sciences* (D. A. Browne, J. Callaway, J. P. Draayer, R. W. Haymaker, R. K. Kalia, J. E. Tohline and P. Vashishta eds.) World Scientific, New Jersey, 1994, 176.

[5] M. Schüler, T. Kovar, H. Lischka, R. Shepard and R. J. Harrison, *Theor. Chim. Acta* **84**, 489 (1993).

[6] H. Lischka, H. Dachsel, R. Shepard and R. J. Harrison, *Parallel Computing in Quantum Chemistry* (T. G. Mattson ed.) ACS Symposium Series 592, ACS, Washington, 1995, 75.

[7] H. Dachsel, H. Lischka, R. Shepard, J. Nieplocha and R. J. Harrison, *J. Comp. Chem.* **18**, 430 (1997).

[8] S. Rettrup, G. L. Bendazzoli, S. Evangelisti and P. Palmieri, *Understanding Molecular Properties* (J. S. Avery, J. P. Dahl and Aa. E. Hansen eds.) Reidel Publ. Co., Dordrecht, Holland, 1987, 533.

[9] A. Guldberg, S. Rettrup, G. L. Bendazzoli and P. Palmieri, *Int. J. Quant. Chem., Symp.* **21**, 513 (1987).

[10] B. O. Roos, *Chem. Phys. Lett.* **15**, 153 (1972).

[11] E. R. Davidson, *J. Comp. Phys.* **17**, 87 (1975).

[12] I. Shavitt, *Modern Theoretical Chemistry* III (H. F. Schaefer ed.) Plenum Press, New York, 1977, 189.

[13] I. Shavitt, *Int. J. Quant. Chem., Symp.* **11**, 131 (1977); *ibid.* **12**, 5 (1978).

[14] W. Duch and J. Karwowski, *Int. J. Quant. Chem.* **22**, 783 (1982).

[15] W. Duch and J. Karwowski, *Comp. Phys. Rep.* **2**, 93 (1985).

[16] S. Rettrup, *Int. J. Quant. Chem.* **29**, 119 (1986).

[17] A. Geist, A. Beguelin, J. Dongarra, W. Jiang, R. Manchek and V. Sunderam, "Parallel Virtual Machine," Oak Ridge National Laboratory, Oak Ridge, Tennessee 37831, available at http://www.netlib.org/pvm/ .

[18] "IBM AIX PVMe Release 3.1." A description of PVMe is available at http://ibm.tc.cornell.edu/ibm/pps/doc/pvme.html .

[19] Information and resources relating to the "Message Passing Interface" (MPI) project is available at http://www.netlib.org/mpi/ .

[20] B. J. Mogensen and S. Rettrup, *Int. J. Quant. Chem.* **44**, 1045 (1992).

[21] S. Rettrup and B. J. Mogensen, *Strongly Correlated Electron Systems in Chemistry* (S. Ramasesha and D. D. Sarma eds.) Narosa Publ. House, New Delhi, India, 1996, 55.

[22] K. P. Huber and G. Herzberg, *Constants of Diatomic Molecules*, Van Nostrand Reinhold, New York (1979).

[23] S. Rettrup, P. Pagsberg and C. Anastasi, *Chem. Phys.* **122**, 45 (1988).

[24] H. Johansen and S. Rettrup, *Chem. Phys.* **74**, 77 (1983).

[25] H. Johansen, *Chem. Phys. Lett.* **17**, 569 (1972).

[26] G. J. Palenik, *Inorg. Chem.* **6**, 503 (1967).

[27] E. Clementi, *IBM J. Res. Develop.* **9**, 2 (1965).

On the convergence of the many-body perturbation theory second-order energy component for negative ions using systematically constructed basis sets of primitive Gaussian-type functions

A.S. Shalabi[†] and S. Wilson[‡],
*[†]Department of Chemistry,
Benha University, Benha, Eygpt*
*[‡]Rutherford Appleton Laboratory, Chilton,
Oxfordshire OX11 0QX, England*

Abstract

Using the F^- ion as a prototype, the convergence of the many-body perturbation theory second-order energy component for negative ions is studied when a systematic procedure for the construction of even-tempered basis sets of primitive Gaussian type functions is employed. Calculations are reported for sequences of even-tempered basis sets originally developed for neutral atoms and for basis sets containing supplementary diffuse functions.

Contents
1. Introduction
2. Methods
    2.1 Systematic basis set generation
    2.2 Independent particle model and electron
        correlation expansion
    2.3 Computational details
3. Results and discussion

1 Introduction

The use of finite basis set expansions (the algebraic approximation) is ubiquitous in quantum chemistry[1]-[7]. Recent years have witnessed a growing interest in the systematic refinement of the algebraic approximation with the demand for increased precision in molecular electronic structure calculations facilitated by the availability of more powerful computing machines. The development of basis sets for studies of negative ions requires particular care and attention because of their extended charge distribution and the increased magnitude of electron correlation energies associated with such systems.

In a previous paper[8], we have examined the convergence of the matrix Hartree-Fock energy for negative ions, using the F^- anion as a prototype, when a systematic procedure for the construction of even-tempered basis sets of primitive Gaussian-type functions is employed. In the present paper, we consider the more challenging electron correlation problem in negative ions. In particular, we study the convergence of the many-body perturbation theory second order energy component for the F^- anion using systematically constructed even-tempered basis sets of primitive Gaussian-type functions. Now the description of the matrix Hartree-Fock ground state for the F^- anion requires on basis functions of s- and p- symmetry. Higher symmetry types are required for correlation studies. In this work, we restrict the basis sets employed to functions of s-, p- and d-symmetry and study the convergence of the second order many-body perturbation theory energy component with respect to the number of basis functions of each symmetry type. The convergence of the second order energy component with respect to the symmetry types included in the basis set expansion has been studied by Schwartz[9] [10] and subsequently by a number of other authors[11]-[14] and it is well established that for atomic systems this converges as $\left(\ell + \frac{1}{2}\right)^{-4}$.

In section 2, we provide a description of the methods employed in the present study: the generation of Gaussian-type basis sets, the independent particle model and the treatment of electron correlation effects, and, the computational details. Results are presented and discussed in section 3. Section 4 contains our conclusions.

2   Methods

2.1   Systematic basis set generation

An efficient scheme for generating the large and flexible Gaussian basis sets required for accurate atomic and molecular electronic structure calculations is provided by the even-tempered prescription in which the exponents are taken to form a geometric progression. Hence, the exponents, $\zeta_{kn\ell}$, are generated according to the following formula:-

$$\ln \zeta_{kn\ell} = \ln \alpha_{n\ell} + k \ln \beta_{n\ell}, \ \ k = 1, 2, ..., n \tag{1}$$

where the parameters $\alpha_{n\ell}$ and $\beta_{n\ell}$ depend on the number of basis functions, n, and their angular quantum number, ℓ. This approach, which was suggested by McWeeny[15] and explored by Reeves and Harrison[16] [17] in the early 1960s, was vigorously investigated by Ruedenberg and his coworkers[18]-[24] in the early 1970s. Klahn[25] has studied the completeness properties of sets of Gaussian-type functions and has generalized the theorem of Muntz and Szasz[26]-[28] to even-tempered Gaussian basis sets.

Even-tempered basis sets can be systematically increased (or decreased) in size by following the empirical prescription of Schmidt and Ruedenberg[29] in which the parameters $\alpha_{n\ell}$ and $\beta_{n\ell}$ depend on the number of functions, n, in the basis set. The following empirical formulae lead to a sequence of basis sets which become complete in the limit of large n

$$\ln \ln \beta_{n\ell} = b_\ell \ln n + b'_\ell \tag{2}$$

$$\ln \alpha_{n\ell} = a_\ell \ln(\beta_{n\ell} - 1) + a'_\ell \tag{3}$$

Schmidt and Ruedenberg[29] optimized the constants a_ℓ, a'_ℓ, b_ℓ and b'_ℓ, for individual atomic species. However, for the large and flexible even-tempered basis sets required for calculations of high precision it has been recognized that the precise values of these constants is not critical and, building on the concept of a universal basis set[30]-[36], a universal systematic sequence of even-tempered Gaussian basis sets has been investigated[37] [38].

The parameters employed in generating sequences of even-tempered basis sets for the neutral F and Ne atoms were taken from the work of Schmidt and Ruedenberg[29]:-

$$F: \quad \begin{array}{llll} a_s = 0.5487, & a'_s = -2.5436, & b_s = -0.5055, & b'_s = 1.2749 \\ a_p = 0.6678, & a'_p = -3.1389, & b_p = -0.4437, & b'_p = 0.9240 \end{array} \tag{4}$$

$$Ne: \quad \begin{array}{llll} a_s = 0.5587, & a'_s = -2.3315, & b_s = -0.5061, & b'_s = 1.2758 \\ a_p = 0.6964, & a'_p = -2.9669, & b_p = -0.4437, & b'_p = 0.9283 \end{array} \tag{5}$$

Diffuse functions were generated by admitting $k = 0, -1, ...$ in the generating formula (1). The F^- anion was describe by the basis set designed for F and by the basis set designed for Ne. The convergence is compared with that observed for the Ne atom described by the Ne basis set. Both the F and the Ne basis sets were supplemented by diffuse functions in the calculations for the anion F^- in order to improve the convergence properties of the algebraic approximation. Throughout this work the nomenclature $E(X;[Y])$ is used to denote the energy of the system X calculated with the basis set Y.

2.2   Independent particle model and electron correlation expansion

The many-body perturbation theory[39] [40] [41] was used to model the electronic structure of the atomic systems studied in this work. The theory developed with respect to a Hartree-Fock reference function constructed from canonical orbitals is employed. This formulation is numerically equivalent to the Møller-Plesset theory[42] [43].

The matrix Hartree-Fock energy, E_{mHF}, is given by the sum of the zero order and first order energies:-

$$E_{mHF} = E_{[1/0]} = E_0 + E_1 \qquad (6)$$

The correlation energy, $E_{correlation}$, is approximated by the second and higher order terms in the perturbation expansion:-

$$\begin{aligned} E_{correlation} &\approx E_{[p/0]} - E_{mHF} \\ &= E_2 + ... + E_p \end{aligned} \qquad (7)$$

where $E_{[p/q]}$ denotes the $[p/q]$ Padé approximant to the total energy. In this work, second-order energy component, E_2, is determined and the correlation energy is approximated as

$$E_{correlation} \approx E_2 + \mathcal{R}_{[2/0]} \qquad (8)$$

where $\mathcal{R}_{[2/0]}$ is the remainder term. E_2 is the dominant correlation energy component and for this simple and computationally tractable approach to be useful the remainder term, $\mathcal{R}_{[2/0]}$, must satisfy the condition

$$\mathcal{R}_{[2/0]} < \epsilon \qquad (9)$$

where ϵ is small.

2.3   Computational details

The calculations reported in this work were carried out with the *Gaussian-92W (Revision E-1)* molecular electronic structure programs of Frisch *et al*[44].

3   Results and discussion

3.1   Basis sets of *s*- and *p*-type functions

The Hartree-Fock ground state of the F^- anion is described by orbitals of s and of p symmetry. In the first part of this study, attention was restricted to the convergence of the second order many-body perturbation theory component of the correlation energy for systematically constructed even-tempered basis sets of primitive Gaussian-type functions of s and p symmetry.

3.1.1   Neutral atom basis sets

Total energies through second order, $E_{[2/0]}$, calculated for the ground state of the neon atom using systematic sequences of even-tempered basis sets of Gaussian functions designed for the Ne atom and designated $[2nsnp]$ for $n = 3, 4, ..., 13$ are presented in Table 1. The corresponding matrix Hartree-Fock energies have been given in Table 1 of our previous work[8] and agree with those given earlier by Schmidt and Ruedenberg[29].

The energy differences for the total energies calculated through second order, that is

$$\Delta E_{[p/0]}(X;[Y])_{[2nsnp]} = E_{[p/0]}(X;[Y])_{[2nsnp]} - E_{[p/0]}(X;[Y])_{[2(n-1)s(n-1)p]} \tag{10}$$

with $p = 2$, $X = Ne$ and $Y = Ne$, are collected in Table 1 for $n = 4, 5, ..., 13$.

The second order correlation energy component, $E_2(Ne;[Ne])$ calculated for the ground state of the neon atom using systematic sequences of even-tempered basis sets of Gaussian functions designed for the Ne atom and designated $[2nsnp]$ with $n = 3, 4, ..., 13$ are also collected in Table 1.

The correlation energy differences

$$\Delta E_p(X;[Y])_{[2nsnp]} = E_p(X;[Y])_{[2nsnp]} - E_p(X;[Y])_{[2(n-1)s(n-1)p]} \tag{11}$$

are also presented in Table 1 for $X = Ne$ and $Y = Ne$ and $n = 4, 5, ..., 13$.

The results presented in Table 1 should be compared with those given in Table 1 of our previous work on the F^- anion[8]. In that Table, $\Delta E(Ne;[Ne])$ for matrix Hartree-Fock energies was reduced to 10.7 $\mu Hartree$ for the largest

basis set studied ($n = 13$) whereas the corresponding $\Delta E_{[2/0]}(Ne; [Ne])$ in Table 1 of the present work is $3 - 4$ times larger because the value of $\Delta E_2(Ne; [Ne])$ is $2 - 3$ times larger. Nevertheless, the level of accuracy achieved in Table 1 for the Ne atom, described by a basis set of s- and p-functions, establishes the accuracy we seek to attain for the F^- anion.

Table 1
$E_{[2/0]}$, $\Delta E_{[2/0]}$, E_2 and ΔE_2 for the ground state of the neon atom using systematic sequences of even-tempered basis sets of Gaussian functions designed for the Ne atom and designated $[2nsnp]$.

n	$E_{[2/0]}(Ne; [Ne])$ (Hartree)	$\Delta E_{[2/0]}(Ne; [Ne])$ (μHartree)	$E_2(Ne; [Ne])$ (Hartree)	$\Delta E_2(Ne; [Ne])$ μHartree
3	-128.1962601	$-$	-0.1164873	$-$
4	-128.5734456	377185.5	-0.1342740	17786.7
5	-128.6612696	87824.0	-0.1419395	7665.5
6	-128.6839195	22649.9	-0.1445605	2621.0
7	-128.6902331	6313.6	-0.1454883	927.8
8	-128.6922150	1981.9	-0.1459132	424.9
9	-128.6929320	717.0	-0.1461155	202.3
10	-128.6932090	277.0	-0.1462207	105.2
11	-128.6933357	126.7	-0.1462832	62.5
12	-128.6934006	64.9	-0.1463223	39.1
13	-128.6934373	36.7	-0.1463483	26.0

In Table 2 the total energy through second-order and the second-order correlation energy component for the ground state of the fluoride anion determined with a sequence of basis sets designed for the neutral Ne atom are presented. Values of $\Delta E_{[p/0]}(F^-; [Ne])_{[2nsnp]}$ and $\Delta E_2(F^-; [Ne])_{[2nsnp]}$ are also collected in Table 2. The results presented in Table 2 should be compared with those given in Table 2 of our previous work on the F^- anion[8]. In that Table $\Delta E(F^-; [Ne])$ was reduced to 739.1 μHartree for the largest basis set studied ($n = 13$) whereas the corresponding $\Delta E_{[2/0]}(F^-; [Ne])$ in Table 2 of the present work is ~ 2 times larger because the $\Delta E_2(F^-; [Ne])$ value is comparable with $\Delta E(F^-; [Ne])$.

In Table 3 the total energy through second-order and the second-order correlation energy component for the ground state of the fluoride anion determined with a sequence of basis sets designed for the neutral F atom are presented. Values of $\Delta E_{[p/0]}(F^-; [F])_{[2nsnp]}$ and $\Delta E_2(F^-; [F])_{[2nsnp]}$ are collected in Table 3. The results presented in Table 3 should be compared with

those given in Table 2 of our previous work on the F^- anion[8]. In that Table $\Delta E(F^-; [F])$ was reduced to 316.6 $\mu Hartree$ for the largest basis set studied $(n = 13)$ whereas the corresponding $\Delta E_{[2/0]}(F^-; [F])$ in Table 3 of the present work is ~ 2 times larger because the $\Delta E_2(F^-; [F])$ value is comparable with $\Delta E(F^-; [F])$.

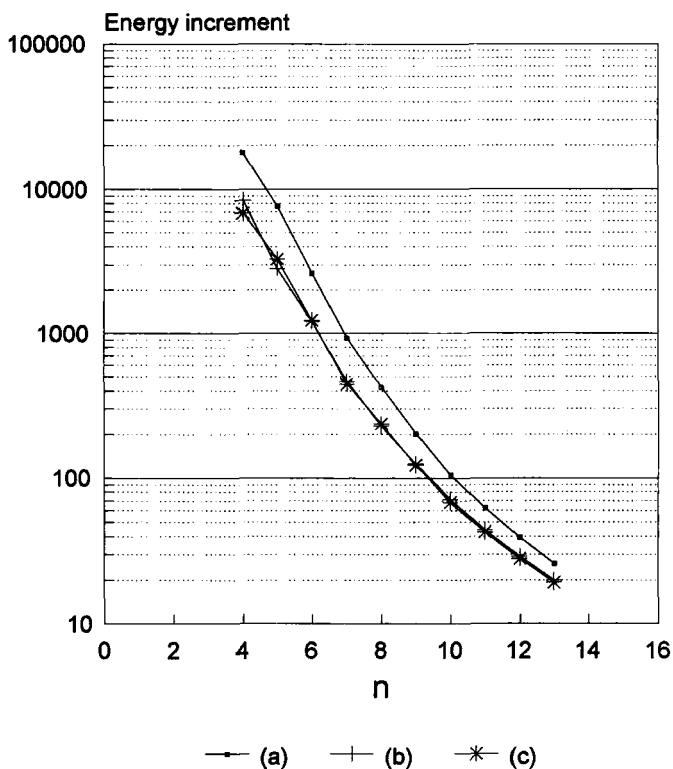The results presented in Tables 1, 2 and 3 are displayed graphically in Figure 1 where a comparison of the convergence behaviour of the second order correlation energy component for the F^- anion with sequences of even-tempered Gaussian basis sets containing s- and p-type functions designed for the neutral F and Ne atoms with the behaviour of this component for the Ne atom is made. ΔE_2 values are plotted on a logarithmic scale. It can be seen that the convergence of the energy increments for the Ne atom is much better than the convergence for the F^- anion. The observed convergence for the F^- anion is broadly similar for both the $[F]$ and the $[Ne]$ basis sets.

Table 2
$E_{[2/0]}$, $\Delta E_{[2/0]}$, E_2 and ΔE_2 for the ground state of the fluoride anion using systematic sequences of even-tempered basis sets of Gaussian functions designed for the Ne atom and designated $[2nsnp]$.

n	$E_{[2/0]}(F^-; [Ne])$ (Hartree)	$\Delta E_{[2/0]}(F^-; [Ne])$ ($\mu Hartree$)	$E_2(F^-; [Ne])$ Hartree	$\Delta E_2(F^-; [Ne])$ $\mu Hartree$
3	−98.8908265		−0.0878905	−
4	−99.3744224	483595.9	−0.1222665	34376.0
5	−99.5200051	145582.7	−0.1423719	20105.4
6	−99.5735399	53534.8	−0.1537715	11399.6
7	−99.5983259	24786.0	−0.1603994	6627.9
8	−99.6110758	12749.9	−0.1644968	4097.4
9	−99.6184147	7338.9	−0.1671850	2688.2
10	−99.6229570	4542.3	−0.1690227	1837.7
11	−99.6259425	2985.5	−0.1703261	1303.4
12	−99.6279852	2042.7	−0.1712742	948.1
13	−99.6294282	1443.0	−0.1719781	703.9

Table 3

$E_{[2/0]}$, $\Delta E_{[2/0]}$, E_2 and ΔE_2 for the ground state of the fluoride anion using systematic sequences of even-tempered basis sets of Gaussian functions designed for the F atom and designated $[2nsnp]$.

n	$E_{[2/0]}(F^-;[F])$ (Hartree)	$\Delta E_{[2/0]}(F^-;[F])$ (μHartree)	$E_2(F^-;[F])$ Hartree	$\Delta E_2(F^-;[F])$ μHartree
3	−99.0910873	−	−0.1077912	−
4	−99.4618356	370748.3	−0.1371702	29379.0
5	−99.5653030	103467.4	−0.1533787	16208.5
6	−99.6005807	35277.7	−0.1615677	8189.0
7	−99.6152640	14683.3	−0.1660254	4457.7
8	−99.6223158	7051.8	−0.1686844	2659.0
9	−99.6262428	3927.0	−0.1703758	1691.4
10	−99.6286054	2362.6	−0.1715000	1124.2
11	−99.6301355	1530.1	−0.1722795	779.5
12	−99.6311667	1031.2	−0.1728329	553.4
13	−99.6318846	717.9	−0.1732342	401.3

3.1.2   Basis sets with one set additional diffuse functions of each symmetry

Consider now the addition of one set of additional diffuse functions of each symmetry type to the basis sets of s- and p-functions used in the preceding section. The exponent for the additional function is generated by means of equation (1). These basis sets are designated $[Y']$ when obtained by adding one diffuse s-function and a set of three diffuse p-functions to the basis set designated $[Y]$.

In Table 4 the total energy through second-order and the second-order correlation energy component for the ground state of the fluoride anion determined with a sequence of basis sets designed for the neutral Ne atom, supplemented by one set of diffuse functions of each symmetry type included, are presented. Values of $\Delta E_{[2/0]}(F^-;[Ne'])$ and $\Delta E_2(F^-;[Ne'])$ are also collected in Table 4. Comparison of Table 4 with Table 2 reveals that the addition of a single diffuse function for each symmetry type to the $[Ne]$ basis set improves both the total energy through second order and the second order energy component considerably. For the total energy, the energy difference, $\Delta E_{[2/0]}(F^-;[Ne'])$, for the largest basis set considered ($n = 13$), assumes a
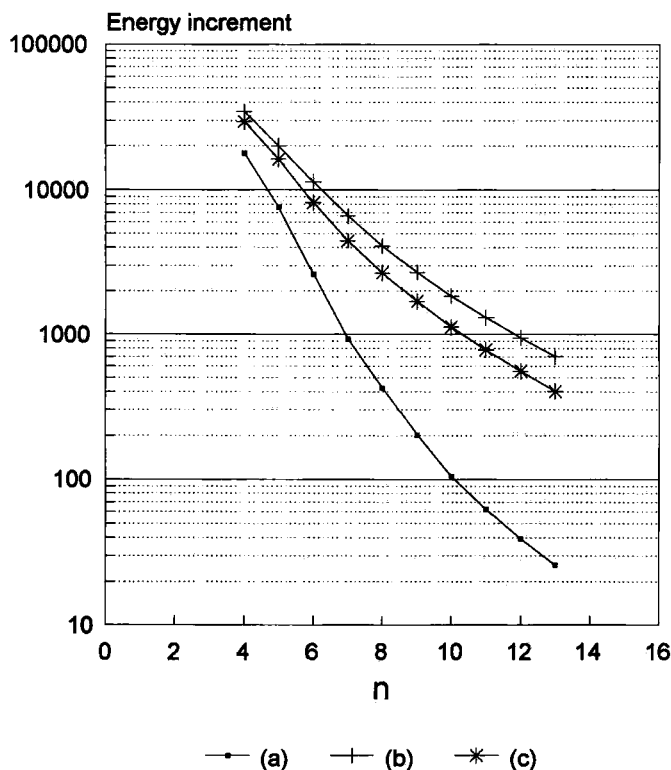
Figure 1: Comparison of the convergence behaviour of the second order correlation energy component for the F^- anion with sequences of even-tempered Gaussian basis sets containing s- and p-type functions designed for the neutral F and Ne atoms with the behaviour of this component for the Ne atom. The curves are labelled as follows:- (a) $\Delta E_2(Ne; [Ne])$; (b) $\Delta E_2(F^-; [Ne])$; (c) $\Delta E_2(F^-; [F])$.

value which is just 3.0% of the corresponding value measured for the $[Ne]$ basis set. For the second order electron correlation energy component, the energy difference, $\Delta E_2(F^-; [Ne'])$, is only 4.8% of the value for the $[Ne]$ basis set.

Table 4

$E_{[2/0]}$, $\Delta E_{[2/0]}$, E_2 and ΔE_2 for the ground state of the fluoride anion using systematic sequences of even-tempered basis sets of Gaussian functions designed for the Ne atom, supplemented by one set of diffuse functions of each symmetry type included and designated $[(2nsnp)']$.

n	$E_{[2/0]}(F^-; [Ne'])$ (Hartree)	$\Delta E_{[2/0]}(F^-; [Ne'])$ ($\mu Hartree$)	$E_2(F^-; [Ne'])$ Hartree	$\Delta E_2(F^-; [Ne'])$ $\mu Hartree$
3	-99.3825308	—	-0.1599082	—
4	-99.5700970	187566.2	-0.1686829	8774.7
5	-99.6175451	47448.1	-0.1718185	3135.6
6	-99.6286152	11070.1	-0.1731904	1371.9
7	-99.6319334	3318.2	-0.1737368	546.4
8	-99.6330258	1092.4	-0.1740256	288.8
9	-99.6334606	434.8	-0.1741947	169.1
10	-99.6336650	204.4	-0.1742996	104.9
11	-99.6337736	108.6	-0.1743680	68.4
12	-99.6338393	65.7	-0.1744153	47.3
13	-99.6338826	43.3	-0.1744490	33.7

Values of $E_{[2/0]}$, $\Delta E_{[2/0]}$, E_2 and ΔE_2 are given in Table 5 for the ground state of the fluoride anion using systematic sequences of even-tempered basis sets of Gaussian functions designed for the F atom, supplemented by one set of diffuse functions of each symmetry type included. Comparison of Table 5 with Table 3 reveals that the addition of a single diffuse function for each symmetry type to the $[F]$ basis set also improves both the total energy through second order and the second order energy component. For the total energy, the energy difference, $\Delta E_{[2/0]}(F^-; [F'])$, for the largest basis set considered ($n = 13$), takes a value of just 4.1% of the corresponding value measured for the $[F]$ basis set. For the second order electron correlation energy component, the energy difference, $\Delta E_2(F^-; [F'])$, is only 5.8% of the value for the $[F]$ basis set.

The values of ΔE_2 presented in Tables 4 and 5 are compared with the ΔE_2 for the Ne atom given in Table 1 in Figure 2. It can be seen that the addition of a single diffuse function of each symmetry type has improved the

Convergence of the Many-Body Perturbation Theory   293

convergence of the second order energy component considerably for the anion
with respect to the convergence patterns displayed in Figure 1.

Table 5

$E_{[2/0]}$, $\Delta E_{[2/0]}$, E_2 and ΔE_2 for the ground state of the fluoride anion
using systematic sequences of even-tempered basis sets of Gaussian
functions designed for the F atom, supplemented by one set of diffuse
functions of each symmetry type included and designated $[(2nsnp)']$.

n	$E_{[2/0]}(F^-;[F'])$ (Hartree)	$\Delta E_{[2/0]}(F^-;[F'])$ (μHartree)	$E_2(F^-;[F'])$ Hartree	$\Delta E_2(F^-;[F'])$ μHartree
3	−99.330 537 3	−	−0.1615582	−
4	−99.561 349 1	230811.8	−0.1687778	7219.6
5	−99.614 590 3	53241.2	−0.1721656	3387.8
6	−99.628 238 8	13648.5	−0.1734466	1281.0
7	−99.631 968 6	3729.8	−0.1739141	467.5
8	−99.633 150 5	1181.9	−0.1741689	254.8
9	−99.633 592 3	441.8	−0.1743052	136.3
10	−99.633 771 9	179.6	−0.1743841	78.9
11	−99.633 858 9	87.0	−0.1744341	50.0
12	−99.633 907 3	48.4	−0.1744675	33.4
13	−99.633 937 0	29.7	−0.1744908	23.3

3.1.3 Basis sets with two sets additional diffuse functions of each symmetry

Consider now the addition of a second diffuse function of each symmetry type
to the basis sets used in the preceding section. Such basis sets are designated
$[Y'']$.

In Table 6, values of $E_{[2/0]}$, $\Delta E_{[2/0]}$, E_2 and ΔE_2 are given for the ground
state of the fluoride anion using systematic sequences of even-tempered basis
sets of Gaussian functions designed for the Ne atom, supplemented by two
sets of diffuse functions of each symmetry type included. The value of the
energy difference $\Delta E_{[2/0]}(F^-;[Ne''])$ is 58.4% of that given in Table 4 for
the basis sets containing one set of supplementary diffuse functions whilst
$\Delta E_2(F^-;[Ne''])$ is 69.1% of the corresponding value in Table 4.

In Table 7 the total energy through second-order and the second-order
correlation energy component for the ground state of the fluoride anion de-
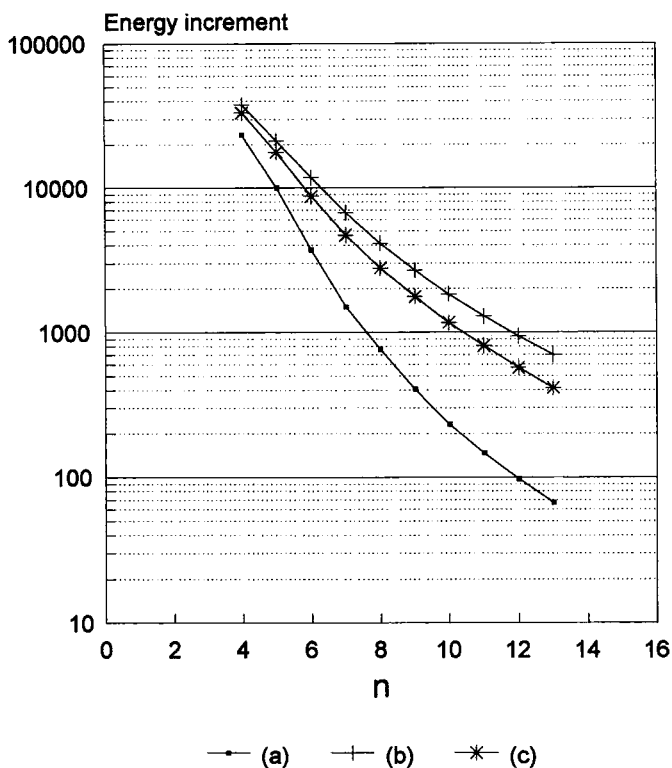termined with a sequence of basis sets designed for the neutral F atom,
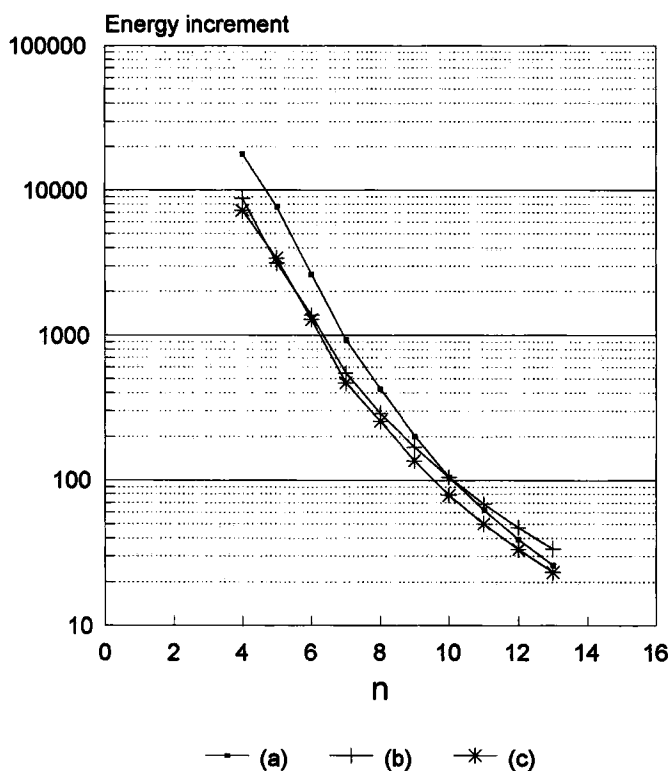
Figure 2: Comparison of the convergence behaviour of the second order correlation energy component for the F^- anion with sequences of even-tempered Gaussian basis sets containing s- and p-type functions for the neutral F and Ne atoms supplemented by one diffuse function of each symmetry type with the behaviour of this component for the Ne atom. The curves are labelled as follows:- (a) $\Delta E_2\,(Ne;\,[Ne])$, (b) $\Delta E_2\,(F^-;\,[Ne'])$, (c) $\Delta E_2\,(F^-;\,[F'])$

supplemented by two diffuse functions for each symmetry type included, are presented. Values of $\Delta E_{[2/0]}(F^-;[F''])$ and $\Delta E_2(F^-;[F''])$ are also collected in Table 7. The value of the energy difference $\Delta E_{[2/0]}(F^-;[F''])$ is 83.2% of that given in Table 5 for the basis sets containing one set of supplementary diffuse functions whilst $\Delta E_2(F^-;[F''])$ is 82.4% of the corresponding value in Table 5.

The values of ΔE_2 presented in Tables 6 and 7 are compared with the ΔE_2 for the Ne atom given in Table 1 in Figure 3. It can be seen that the addition of a second diffuse function of each symmetry type has resulted in a slight improvement the convergence of the second order energy component with respect to that displayed in Figure 2.

Table 6
$E_{[2/0]}$, $\Delta E_{[2/0]}$, E_2 and ΔE_2 for the ground state of the fluoride anion using systematic sequences of even-tempered basis sets of Gaussian functions designed for the Ne atom, supplemented by two sets of diffuse functions of each symmetry type included and designated $[(2nsnp)'']$.

n	$E_{[2/0]}(F^-;[Ne''])$ (Hartree)	$\Delta E_{[2/0]}(F^-;[Ne''])$ (μHartree)	$E_2(F^-;[Ne''])$ Hartree	$\Delta E_2(F^-;[Ne''])$ μHartree
3	−99.3842684	−	−0.1610744	−
4	−99.5711626	186894.2	−0.1694835	8409.1
5	−99.6181763	47013.7	−0.1723055	2822.0
6	−99.6290436	10867.3	−0.1735236	1218.1
7	−99.6322585	3214.9	−0.1739871	463.5
8	−99.6332721	1013.6	−0.1742149	227.8
9	−99.6336499	377.8	−0.1743399	125.0
10	−99.6338105	160.6	−0.1744115	71.6
11	−99.6338870	76.5	−0.1744556	44.1
12	−99.6339288	41.8	−0.1744846	29.0
13	−99.6339541	25.3	−0.1745046	20.0

Table 7

$E_{[2/0]}$, $\Delta E_{[2/0]}$, E_2 and ΔE_2 for the ground state of the fluoride anion using systematic sequences of even-tempered basis sets of Gaussian functions designed for the F atom, supplemented by two sets of diffuse functions of each symmetry type included and designated $[(2snp)'']$.

n	$E_{[2/0]}(F^-;[F''])$ (Hartree)	$\Delta E_{[2/0]}(F^-;[F''])$ ($\mu Hartree$)	$E_2(F^-;[F''])$ Hartree	$\Delta E_2(F^-;[F''])$ $\mu Hartree$
3	−99.3312236	−	−0.1621697	−
4	−99.5617022	230478.6	−0.1690343	6864.6
5	−99.6147585	53056.3	−0.1723119	3277.6
6	−99.6283566	13598.1	−0.1735447	1232.8
7	−99.6320607	3704.1	−0.1739904	445.7
8	−99.6332198	1159.1	−0.1742259	235.5
9	−99.6336451	425.3	−0.1743484	122.5
10	−99.6338117	166.6	−0.1744166	68.2
11	−99.6338897	78.0	−0.1744593	42.7
12	−99.6339315	41.8	−0.1744874	28.1
13	−99.6339562	24.7	−0.1745066	19.2

3.2   Basis sets of s-, p- and d-type functions

The accurate description of correlation effects requires the inclusion of functions of higher symmetry than those required for the matrix Hartree-Fock model. The most important of these functions for the F^- anion are functions of d-type. In this section, the convergence of the total energy through second order and the second order correlation energy component for a systematic sequence of even-tempered basis sets of Gaussian functions of s-, p- and d-type is investigated.

3.2.1   Neutral atom basis sets

In Table 8 the total energy through second-order and the second-order correlation energy component for the ground state of the Ne atom determined with a sequence of basis sets containing functions of s, p and d symmetry designed for the neutral Ne atom are presented. The exponents for the d functions were taken to be the same as those for the p functions. Values of

Figure 3: Comparison of the convergence behaviour of the second order correlation energy component for the F^- anion with sequences of even-tempered Gaussian basis sets containing s- and p-type functions for the neutral F and Ne atoms supplemented by two diffuse functions of each symmetry type with the behaviour of this component for the Ne atom. The curves are labelled as follows:- (a) $\Delta E_2\,(Ne; [Ne])$, (b) $\Delta E_2\,(F^-; [Ne''])$, (c) $\Delta E_2\,(F^-; [F''])$

$\Delta E_{[p/0]}(Ne;[Ne])_{[spd]}$ and $\Delta E_2(Ne;[Ne])_{[spd]}$ are also collected in Table 8. It is not the purpose of the present work to determine accurate correlation energies. However, it is known [45] [46] [47] that the exact second order energy for the neon atom ground state is -0.3879 *Hartree*. The largest basis set of s- and p- type functions considered in Table 1, therefore, recovers 37.7% of the exact second order correlation energy component whilst the largest basis set of functions with s-, p- and d-symmetries considered in Table 8 corresponds to 66.8% of the exact value.

In Figure 4, the convergence of the $\Delta E_2(Ne;[Ne])_{[spd]}$ values in Table 8 is compared with that of the $\Delta E_2(Ne;[Ne])_{[sp]}$ values given in Table 1. It can be seen that the calculations using basis sets containing d type functions do not converge as rapidly as those employing only s- and p- type functions. In both cases the convergence is monotonic. The value of $\Delta E_{[2/0]}(Ne;[Ne])_{[spd]}$ is more than twice that of $\Delta E_{[2/0]}(Ne;[Ne])_{[sp]}$ for the largest basis sets considered. The value of $\Delta E_2(Ne;[Ne])_{[spd]}$ is $2\frac{1}{2}$ times that of $\Delta E_2(Ne;[Ne])_{[sp]}$ for $n = 13$.

Table 8

$E_{[2/0]}$, $\Delta E_{[2/0]}$, E_2 and ΔE_2 for the ground state of the neon atom using systematic sequences of even-tempered basis sets of Gaussian functions designed for the Ne atom and designated $[2nsnpnd]$.

n	$E_{[2/0]}(Ne;[Ne])$ (Hartree)	$\Delta E_{[2/0]}(Ne;[Ne])$ (μHartree)	$E_2(Ne;[Ne])$ Hartree	$\Delta E_2(Ne;[Ne])$ μHartree
3	-128.2986758	—	-0.2189030	—
4	-128.6814007	382724.9	-0.2422291	23326.1
5	-128.7715646	90163.9	-0.2522345	10005.4
6	-128.7952908	23726.2	-0.2559318	4697.3
7	-128.8021745	6883.7	-0.2574297	1497.9
8	-128.8044928	2318.3	-0.2581910	761.3
9	-128.8054111	918.3	-0.2585946	403.6
10	-128.8058152	404.1	-0.2588269	232.3
11	-128.8060264	211.2	-0.2589739	147.0
12	-128.8061495	123.1	-0.2590712	97.3
13	-128.8062274	77.9	-0.2591382	67.0

In Table 9 the total energy through second-order and the second-order correlation energy component for the ground state of the F^- anion determined with a sequence of basis sets containing functions of s, p and d symmetry designed for the neutral Ne atom are presented. The exponents for

the d functions were taken to be the same as those for the p functions. Values of $\Delta E_{[2/0]}(F^-; [Ne])_{[spd]}$ and $\Delta E_2(F^-; [Ne])_{[spd]}$ are also collected in Table 9. The convergence pattern seen for both $\Delta E_{[2/0]}$ and ΔE_2 in Table 9 mirrors that observed in Table 2.

In Table 10 the total energy through second-order and the second-order correlation energy component for the ground state of the fluoride anion determined with a sequence of basis sets containing functions of s, p and d symmetry designed for the neutral F atom are presented. Values of $\Delta E_{[p/0]}(F^-; [F])_{[2nsnpnd]}$ and $\Delta E_2(F^-; [F])_{[2nsnpnd]}$ are collected in Table 10. Again, the convergence pattern for both $\Delta E_{[2/0]}$ and ΔE_2 in Table 10 mirrors that seen in Table 3.

The ΔE_2 values for the F^- anion given in Table 9 and 10 are compared with those for the Ne atom presented in Table 8 and Figure 5. Figure 5 should be compared with Figure 1. For the basis sets of s-, p- and d-type functions the convergence of the energy increments for the Ne atom is much better than the convergence for the F^- anion. The observed convergence pattern for the F^- anion is broadly similar for both the $[F]$ and $[Ne]$ basis sets.

Table 9
$E_{[2/0]}$, $\Delta E_{[2/0]}$, E_2 and ΔE_2 for the ground state of the fluoride anion using systematic sequences of even-tempered basis sets of Gaussian functions designed for the Ne atom and designated $[2nsnpnd]$.

n	$E_{[2/0]}(F^-; [Ne])$ (Hartree)	$\Delta E_{[2/0]}(F^-; [Ne])$ (μHartree)	$E_2(F^-; [Ne])$ Hartree	$\Delta E_2(F^-; [Ne])$ μHartree
3	-98.9924386	$-$	-0.1895026	$-$
4	-99.4792445	486805.9	-0.2270886	37586.0
5	-99.6260010	146756.5	-0.2483678	21279.2
6	-99.6799183	53917.3	-0.2601499	11782.1
7	-99.7047892	24870.9	-0.2668627	6712.8
8	-99.7175490	12759.8	-0.2709700	4107.3
9	-99.7248788	7329.8	-0.2736491	2679.1
10	-99.7294087	4529.9	-0.2754744	1825.3
11	-99.7323828	2974.1	-0.2767664	1292.0
12	-99.7344166	2033.8	-0.2777056	939.2
13	-99.7358529	1436.3	-0.2784028	697.2

Table 10
$E_{[2/0]}$, $\Delta E_{[2/0]}$, E_2 and ΔE_2 for the ground state of the fluoride anion using systematic sequences of even-tempered basis sets of Gaussian functions designed for the F atom and designated $[2nsnpnd]$.

n	$E_{[2/0]}(F^-;[F])$ (Hartree)	$\Delta E_{[2/0]}(F^-;[F])$ (μHartree)	$E_2(F^-;[F])$ Hartree	$\Delta E_2(F^-;[F])$ μHartree
3	−99.1910005	−	−0.2077044	−
4	−99.5656316	374631.1	−0.2409662	33261.8
5	−99.6705907	104959.1	−0.2586664	17700.2
6	−99.7064298	35839.1	−0.2674168	8750.4
7	−99.7213396	14909.8	−0.2721010	4684.2
8	−99.7285103	7170.7	−0.2748789	2777.9
9	−99.7325019	3991.6	−0.2766349	1756.0
10	−99.7349031	2401.2	−0.2777977	1162.8
11	−99.7364583	1555.2	−0.2786023	804.6
12	−99.7375068	1048.5	−0.2791730	570.7
13	−99.7382370	730.2	−0.2795866	413.6

3.2.2　Basis sets with one set of additional diffuse functions

Attention is now turned to basis sets containing functions of s-, p- and d-symmetry with one supplementary set of diffuse functions for each symmetry type. The exponent for the additional function is generated by means of equation (1).

In Table 11 the total energy through second-order and the second-order correlation energy component for the ground state of the fluoride anion determined with a sequence of basis sets designed for the neutral Ne atom, supplemented by one set of diffuse functions of each symmetry type included, are presented. Values of $\Delta E_{[p/0]}(F^-;[Ne'])_{[spd]}$ and $\Delta E_2(F^-;[Ne'])_{[spd]}$ are also collected in Table 11. Table 11 should be compared with Table 4, where the corresponding results for basis sets of s- and p-functions are given, and with Table 9, where the supplementary diffuse functions are not included.

Values of $E_{[2/0]}$, $\Delta E_{[2/0]}$, E_2 and ΔE_2 are given in Table 12 for the ground state of the fluoride anion using systematic sequences of even-tempered basis sets of Gaussian functions designed for the F atom, supplemented by one set of diffuse functions of each symmetry type included. Table 12 should be compared with Table 5, where the corresponding results for basis sets of
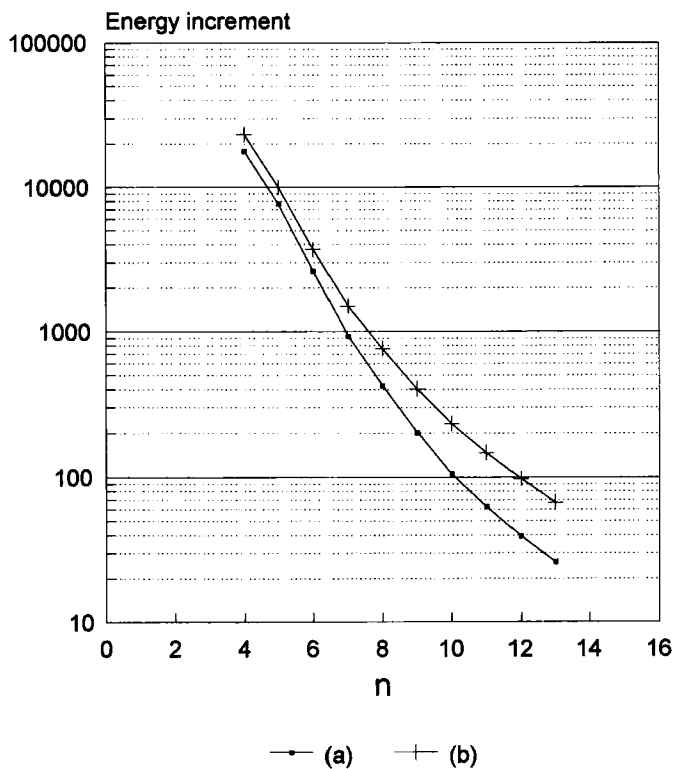
Figure 4: Comparison of the convergence behaviour of the second order correlation energy component for the Ne atom with sequences of even-tempered Gaussian basis sets containing s- and p-type functions designed for the neutral Ne atoms with the behaviour of this component for the Ne atom described by functions of s-, p- and d- symmetry. The curves are labelled as follows:- (a) sp; (b) spd.

Figure 5: Comparison of the convergence behaviour of the second order correlation energy component for the F^- anion with sequences of even-tempered Gaussian basis sets containing s-, p- and d-type functions designed for the neutral F and Ne atoms with the behaviour of this component for the Ne atom. The curves are labelled as follows:- (a) $\Delta E_2(Ne; [Ne])$; (b) $\Delta E_2(F^-; [Ne])$; (c) $\Delta E_2(F^-; [F])$.

s- and p-functions are given, and with Table 10, where the supplementary diffuse functions are not included.

The values of ΔE_2 presented in Tables 11 and 12 are compared with the ΔE_2 for the Ne atom given in Table 8 in Figure 6. It can be seen that the addition of a single diffuse function of each symmetry type has improved the convergence of the second order energy component considerably. Figure 6 should be compared with Figure 2.

Table 11

$E_{[2/0]}$, $\Delta E_{[2/0]}$, E_2 and ΔE_2 for the ground state of the fluoride anion using systematic sequences of even-tempered basis sets of Gaussian functions designed for the Ne atom, supplemented by one set of diffuse functions of each symmetry type included and designated $[(2nsnpnd)']$.

n	$E_{[2/0]}(F^-;[Ne'])$ (Hartree)	$\Delta E_{[2/0]}(F^-;[Ne'])$ (μHartree)	$E_2(F^-;[Ne'])$ Hartree	$\Delta E_2(F^-;[Ne'])$ μHartree
3	-99.4804020	$-$	-0.2577794	$-$
4	-99.6724466	192044.6	-0.2710325	13253.1
5	-99.7217115	49264.9	-0.2759849	4952.4
6	-99.7337071	11995.6	-0.2782823	2297.4
7	-99.7375095	3802.4	-0.2793129	1030.6
8	-99.7388771	1367.6	-0.2798769	564.0
9	-99.7394793	602.2	-0.2802134	336.5
10	-99.7397900	310.7	-0.2804246	211.2
11	-99.7399692	179.2	-0.2805636	139.0
12	-99.7400849	115.7	-0.2806609	97.3
13	-99.7401619	77.0	-0.2807283	67.4

Table 12

$E_{[2/0]}$, $\Delta E_{[2/0]}$, E_2 and ΔE_2 for the ground state of the fluoride anion using systematic sequences of even-tempered basis sets of Gaussian functions designed for the F atom, supplemented by one set of diffuse functions of each symmetry type included and designated $[(2nsnpnd)']$.

n	$E_{[2/0]}(F^-;[F'])$ (Hartree)	$\Delta E_{[2/0]}(F^-;[F'])$ (μHartree)	$E_2(F^-;[F'])$ Hartree	$\Delta E_2(F^-;[F'])$ μHartree
3	-99.4288653	$-$	-0.2598862	$-$
4	-99.6637370	234871.7	-0.2711657	11279.5
5	-99.7188166	55079.6	-0.2763919	5226.2
6	-99.7333617	14545.1	-0.2785695	2177.6
7	-99.7375590	4197.3	-0.2795045	935.0
8	-99.7390129	1453.9	-0.2800313	526.8
9	-99.7396187	605.8	-0.2803316	300.3
10	-99.7399021	283.4	-0.2805143	182.7
11	-99.7400582	156.1	-0.2806334	119.1
12	-99.7401546	96.4	-0.2807148	81.4
13	-99.7402185	63.9	-0.2807723	57.5

3.2.3   Basis sets with two sets of additional diffuse functions

In Table 13 the total energy through second-order and the second-order correlation energy component for the ground state of the fluoride anion determined with a sequence of basis sets designed for the neutral Ne atom, supplemented by two sets of diffuse functions of each symmetry type included, are presented. Values of $\Delta E_{[p/0]}(F^-;[Ne'])_{[spd]}$ and $\Delta E_2(F^-;[Ne'])_{[spd]}$ are also collected in Table 13.

Values of $E_{[2/0]}$, $\Delta E_{[2/0]}$, E_2 and ΔE_2 are given in Table 14 for the ground state of the fluoride anion using systematic sequences of even-tempered basis sets of Gaussian functions designed for the F atom, supplemented by two sets of diffuse functions of each symmetry type included.

The values of ΔE_2 presented in Tables 13 and 14 are compared with the ΔE_2 for the Ne atom given in Table 8 in Figure 7. It can be seen that the addition of a second diffuse function of each symmetry type leads to a smaller improvement in the convergence of the second order energy component than did the first set.
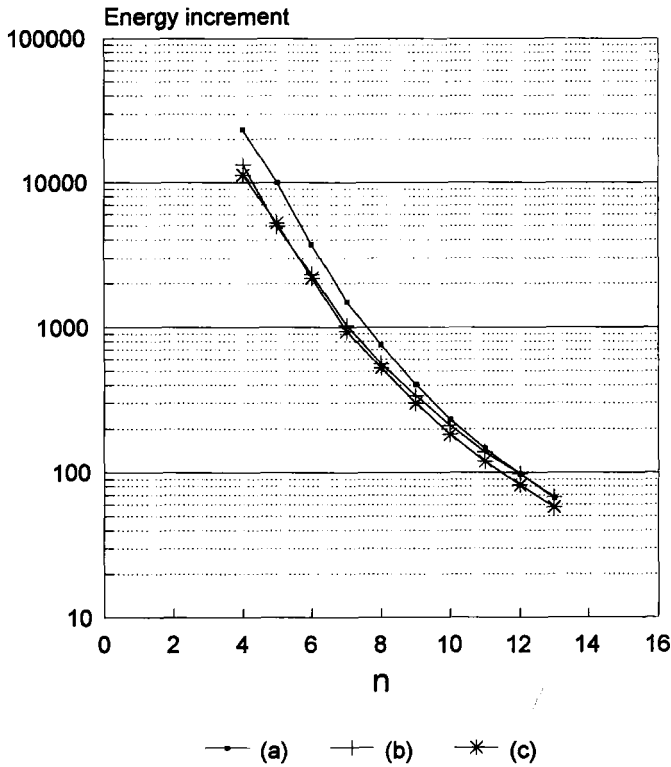
Figure 6: Comparison of the convergence behaviour of the second order correlation energy component for the F^- anion with sequences of even-tempered Gaussian basis sets containing s-, p- and d-type functions for the neutral F and Ne atoms supplemented by a single diffuse function for each symmetry type with the behaviour of this component for the Ne atom. The curves are labelled as follows:- (a) $\Delta E_2(Ne; [Ne])$; (b) $\Delta E_2(F^-; [Ne'])$; (c) $\Delta E_2(F^-; [F'])$.

Table 13

$E_{[2/0]}$, $\Delta E_{[2/0]}$, E_2 and ΔE_2 for the ground state of the fluoride anion using systematic sequences of even-tempered basis sets of Gaussian functions designed for the Ne atom, supplemented by two sets of diffuse functions of each symmetry type included and designated $[(2nsnpnd)'']$.

n	$E_{[2/0]}(F^-;[Ne''])$	$\Delta E_{[2/0]}(F^-;[Ne''])$	$E_2(F^-;[Ne''])$	$\Delta E_2(F^-;[Ne''])$
	$(Hartree)$	$(\mu Hartree)$	$Hartree$	$\mu Hartree$
3	-99.4822358	$-$	-0.2590418	$-$
4	-99.6735321	191296.3	-0.2718350	12793.2
5	-99.7223456	48813.5	-0.2764748	4639.8
6	-99.7341345	11788.9	-0.2786145	2139.7
7	-99.7378317	3697.2	-0.2795603	945.8
8	-99.7391200	1288.3	-0.2800628	502.5
9	-99.7396653	545.3	-0.2803553	292.5
10	-99.7399326	267.3	-0.2805336	178.3
11	-99.7400800	147.4	-0.2806486	115.0
12	-99.7401709	90.9	-0.2807267	78.1
13	-99.7402316	60.7	-0.2807821	55.4

Table 14

$E_{[2/0]}$, $\Delta E_{[2/0]}$, E_2 and ΔE_2 for the ground state of the fluoride anion using systematic sequences of even-tempered basis sets of Gaussian functions designed for the F atom, supplemented by two sets of diffuse functions of each symmetry type included and designated $[(2nsnpnd)'']$.

n	$E_{[2/0]}(F^-;[F''])$ (Hartree)	$\Delta E_{[2/0]}(F^-;[F''])$ ($\mu Hartree$)	$E_2(F^-;[F''])$ Hartree	$\Delta E_2(F^-;[F''])$ $\mu Hartree$
3	-99.4296384	$-$	-0.2605845	$-$
4	-99.6641261	234487.7	-0.2714582	10873.7
5	-99.7190007	54874.6	-0.2765541	5095.9
6	-99.7334878	14487.1	-0.2786755	2121.4
7	-99.7376553	4167.5	-0.2795850	909.5
8	-99.7390844	2017.3	-0.2800905	505.5
9	-99.7396726	588.2	-0.2803759	285.4
10	-99.7399425	269.9	-0.2805474	171.5
11	-99.7400893	146.8	-0.2806589	111.5
12	-99.7401789	89.6	-0.2807348	75.9
13	-99.7402378	58.9	-0.2807882	53.4

4   Conclusions

In this paper, we have demonstrated the use of systematic sequences of even-tempered basis sets of primitive Gaussian-type functions in calculations incorporating the effects of electron correlation for a prototypical negative ion, the F^- anion. It has been shown that improved convergence of the second order correlation energy component can be achieved by adding a single diffuse function for each symmetry type to a basis set designed for a neutral atom. A somewhat smaller improvement in the convergence characteristics of both the total energy through second order and the second order energy component is observed on adding a second set of more diffuse functions. Furthermore, it has been shown that a basis set suitable for the F^- anion can be obtained by supplementing either a basis set designed for the neutral Hartree-Fock F atom or one designed for the Hartree-Fock Ne atom with diffuse functions. Future work will extend this approach to molecular systems.
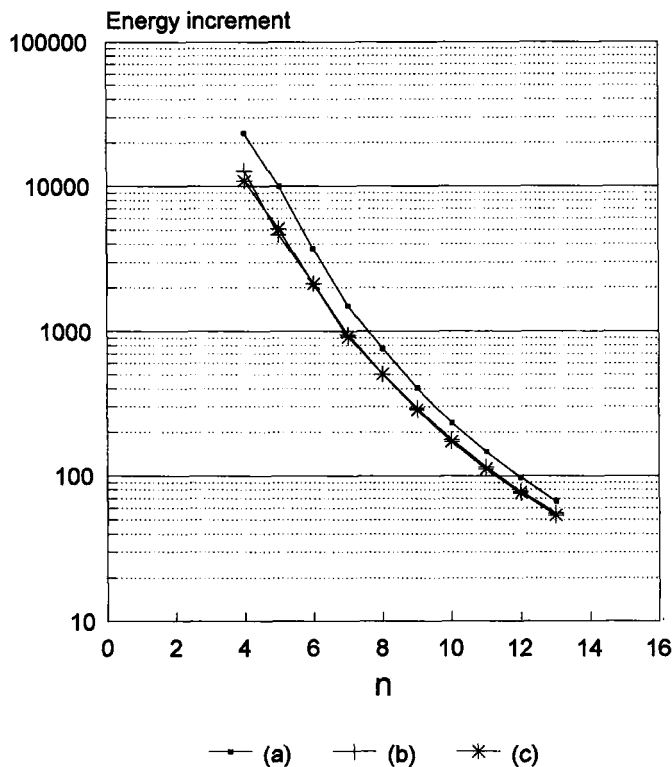
Figure 7: Comparison of the convergence behaviour of the second order correlation energy component for the F^- anion with sequences of even-tempered Gaussian basis sets containing s-, p- and d-type functions designed for the neutral F and Ne atoms supplemented by two diffuse functions of each symmetry type with the behaviour of this component for the Ne atom. The curves are labelled as follows:- (a) $\Delta E_2(Ne; [Ne])$; (b) $\Delta E_2(F^-; [Ne''])$; (c) $\Delta E_2(F^-; [F'''])$.

References

[1] T.H. Dunning, Jr., and P.J. Hay, 1977, *Methods in Electronic Structure Theory*, edited by H.F. Schaefer III, Plenum, New York

[2] R. Ahlrichs and P.R. Taylor, 1981, J. chim. Phys. **78**, 315

[3] S. Wilson, 1983, in *Methods in Computational Molecular Physics*, edited by G.H.F. Diercksen and S. Wilson, NATO ASI Series C, Vol. 113, Reidel, Dordrecht

[4] S. Huzinaga, 1985, Comput. Phys. Rept. **2**, 279

[5] E.R. Davidson and D. Feller, 1986, Chem. Rev. **86**, 681

[6] S. Wilson, 1987, Adv. Chem. Phys. **67**, 439

[7] S. Wilson, 1997, in *Problem Solving in Computational Molecular Science: Molecules in Different Environments*, edited by S. Wilson and G.H.F. Diercksen, NATO ASI, Bad Windsheim, August 1996, Kluwer, Dordrecht

[8] A.S. Shalabi and S. Wilson, 1995, J. Molec. Struct. (THEOCHEM) **341**, 165

[9] C.M. Schwartz, 1962, Phys. Rev. **126**, 1015

[10] C.M. Schwartz, 1963, Methods in Computational Physics **2**, 241

[11] D.P. Carroll, H.J. Silverstone, R.M. Metzger, 1979, J. Chem. Phys. **71**, 4142

[12] K. Jankowski and P. Malinowski, 1980, Phys. Rev. A **22**, 51

[13] K. Jankowski, 1987, in *Electron Correlation in Atoms and Molecules* (Methods in Computational Chemistry 1) edited by S. Wilson, Plenum Press, New York

[14] W. Kutzelnigg and J. Morgan III, 1992, J. Chem. Phys. **96**, 4484

[15] R. McWeeny, 1948, *Dissertation*, University of Oxford

[16] C. Reeves, 1963, J. Chem. Phys. **39**, 1

[17] C. Reeves and M. Harrison, 1963, J. Chem. Phys. **39**, 11

[18] K. Ruedenberg, R.C. Raffenetti and R. Bardo, 1973, in *Energy, Structure and Reactivity*, Proceedings of the 1972 Boulder Conference on Theoretical Chemistry, Wiley, New York

[19] R.C. Raffenetti and K. Ruedenberg, 1973, J. Chem. Phys. **59**, 5978

[20] R.C. Raffenetti, 1973, J. Chem. Phys. **58**, 4452

[21] R.C. Raffenetti, 1973, J. Chem. Phys. **59**, 5936

[22] R.D. Bardo and K. Ruedenberg, 1973, J. Chem. Phys. **59**, 5956

[23] R.D. Bardo and K. Ruedenberg, 1973, J. Chem. Phys. **59**, 5966

[24] R.D. Bardo and K. Ruedenberg, 1974, J. Chem. Phys. **60**, 918

[25] B. Klahn, 1985, J. Chem. Phys. **83**, 5748

[26] H. Muntz, 1914, Festscgrift H.A. Schwartz, 303

[27] O. Szasz, 1926, Math. Ann. 77

[28] J.R. Higgins, 1977, *Completeness and basis properties of sets of special functions*, Cambridge University Press

[29] M.W. Schmidt and K. Ruedenberg, 1979, J. Chem. Phys. **71**, 3951

[30] D.M. Silver, S. Wilson and W. Nieupoort, 1978, Intern. J. Quantum Chem.**14**, 635

[31] D.M. Silver and W. Nieupoort, 1978, Chem. Phys. Lett. **57**, 421

[32] D.M. Silver and S. Wilson, 1978, J. Chem. Phys. **69**, 3787

[33] S. Wilson and D.M. Silver, 1979, Chem. Phys. Lett. **63**, 367

[34] P. Mezey, 1979, Theoret. chim. Acta **53**, 187

[35] S. Wilson and D.M. Silver, 1980, J. Chem. Phys. **72**, 2159

[36] S. Wilson and D.M. Silver, 1982, J. Chem. Phys. **77**, 3674

[37] S. Wilson, 1980, Theoret. chim. Acta **58**, 31

[38] S. Wilson, 1981, Chem. Phys. Lett. **81**, 467

[39] N.H. March, W.H. Young and S. Sampanthar, 1967, *The many-body problem in quantum mechanics*, Cambridge University Press

[40] S. Wilson, 1984, *Electron correlation in molecules*, Clarendon Press, Oxford

[41] R. McWeeny, 1989, *Methods of Molecular Quantum Mechanics*, Academic Press, London

[42] Chr. Møller and M.S. Plesset, 1934, Phys. Rev. **46**, 618

[43] S. Wilson, 1992, J. Molec. Struct. (THEOCHEM) **261**, 287

[44] M.J. Frisch, G.W. Trucks, M. Head-Gordon, P.M.W. Gill et al, GAUSIAN92W, Gaussian Inc., Pittsburgh PA, 1992

[45] K. Jankowski and P. malinowski, 1980, Phys. Rev. **A21**, 45

[46] J.R. Flores, 1992, Phys. Rev. **A46**, 6063

[47] W. Klopper, 1995, J. Chem. Phys. **102**, 6168

High-Accuracy Calculations for
Heavy and Super-Heavy Elements

Uzi Kaldor and Ephraim Eliav

School of Chemistry, Tel Aviv University, 69978 Tel Aviv, Israel

Abstract

Energy levels of heavy and super-heavy (Z>100) elements are calculated by the relativistic coupled cluster method. The method starts from the four-component solutions of the Dirac-Fock or Dirac-Fock-Breit equations, and correlates them by the coupled-cluster approach. Simultaneous inclusion of relativistic terms in the Hamiltonian (to order α^2, where α is the fine-structure constant) and correlation effects (all products and powers of single and double virtual excitations) is achieved. The Fock-space coupled-cluster method yields directly transition energies (ionization potentials, excitation energies, electron affinities). Results are in good agreement (usually better than 0.1 eV) with known experimental values. Properties of superheavy atoms which are not known experimentally can be predicted. Examples include the nature of the ground states of elements 104 and 111. Molecular applications are also presented.

Table of Contents:

1   Introduction

The structure and chemistry of a light atom or molecule may be investigated by means of the pertinent Schrödinger equation. This equation may be solved to a good approximation by the methods of modern quantum chemistry. Relativistic effects are not very large for the first few rows of the periodic table. When knowledge of these is required, e.g., to understand the fine structure of atomic spectra, they may be calculated by perturbation theory [1]. This approach is not satisfactory for heavier atoms, where relativistic effects become too large for perturbative treatment, changing significantly even such fundamental properties of the atom as the order of orbitals. The Schrödinger equation must then be supplanted by an appropriate relativistic wave equation such as Dirac-Coulomb or Dirac-Coulomb-Breit. Approximate one-electron solutions to these equations may be obtained by the self-consistent-field procedure. The resulting Dirac-Fock or Dirac-Fock-Breit functions are conceptually similar to the familiar Hartree-Fock functions; the Hartree-Fock orbitals are replaced, however, by four-component vectors. Correlation is no less important in the relativistic regime than it is for the lighter elements, and may be included in a similar manner.

The present chapter describes methodology for high-accuracy calculations of systems with heavy and super-heavy elements. The no-virtual-pair Dirac-Coulomb-Breit Hamiltonian, which is correct to second order in the fine-structure constant α, provides the framework of the method. Correlation is treated by the coupled cluster (CC) approach. The method is described in section 2. Section 3 gives results for a few representative atomic systems; the main properties of interest are transition energies (ionization potentials, excitation energies, electron affinities). An interesting question for super-heavy elements is the nature of their ground state, which may differ from that of lighter atoms in the same group of the periodic table. Somewhat less accurate calculations for molecules, using one- or two-component wave functions, as well as a pilot four-component application, are described in section 4.

2   Methodology

2.1   The Relativistic Hamiltonian

The relativistic many-electron Hamiltonian cannot be written in closed form; it may be derived perturbatively from quantum electrodynamics [2]. The simplest form is the Dirac-Coulomb (DC) Hamiltonian, where the nonrelativistic one-electron terms in the Schrödinger equation are replaced by the one-electron

Dirac operator h_D,

$$H_{\text{DC}} = \sum_i h_D(i) + \sum_{i<j} 1/r_{ij} \,, \tag{1}$$

with

$$h_D = c\boldsymbol{\alpha} \cdot \boldsymbol{p} + \beta c^2 + V_{\text{nuc}}. \tag{2}$$

$\boldsymbol{\alpha}$ and β are the four-dimensional Dirac matrices, and V_{nuc} is the nuclear attraction operator, with the nucleus modeled as a point or finite-size charge. Only the one-electron terms in the DC Hamiltonian include relativistic effects, and the two-electron repulsion remains in the nonrelativistic form. The lowest-order correction to the two-electron repulsion is the Breit [3] operator

$$B_{12} = -\frac{1}{2}[\boldsymbol{\alpha}_1 \cdot \boldsymbol{\alpha}_2 + (\boldsymbol{\alpha}_1 \cdot \boldsymbol{r}_{12}) \cdot (\boldsymbol{\alpha}_2 \cdot \boldsymbol{r}_{12})/r_{12}^2]/r_{12} \,, \tag{3}$$

yielding the Dirac-Coulomb-Breit (DCB) Hamiltonian

$$H_{\text{DCB}} = \sum_i h_D(i) + \sum_{i<j}(1/r_{ij} + B_{ij}) \,. \tag{4}$$

All equations are in atomic units.

Neither the DC nor the DCB Hamiltonians are appropriate starting points for accurate many-body calculations. The reason is the admixture of the negative-energy eigenstates of the Dirac Hamiltonian by the two-body terms in an erroneous way [4, 5]. The no-virtual-pair approximation [6, 7] is invoked to correct this problem: the negative-energy states are eliminated by the projection operator Λ^+, leading to the projected Hamiltonians

$$H_{\text{DC}}^+ = \Lambda^+ H_{\text{DC}} \Lambda^+ \tag{5}$$

or

$$H_{\text{DCB}}^+ = \Lambda^+ H_{\text{DCB}} \Lambda^+ \,. \tag{6}$$

H_{DCB}^+ is correct to second order in the fine-structure constant α, and is expected to be highly accurate for all neutral and weakly-ionized atoms [8]. Higher quantum electrodynamic (QED) terms are required for strongly-ionized species; these are outside the scope of this chapter. A comprehensive discussion of higher QED effects and other aspects of relativistic atomic physics may be found in the proceedings of the 1988 Santa Barbara program [9].

2.2   The One-Electron Equation

The no-pair DCB Hamiltonian (6) is used as a starting point for variational or many-body relativistic calculations [10]. The procedure is similar to the nonrelativistic case, with the Hartree-Fock orbitals replaced by the four-component

Dirac-Fock-Breit (DFB) functions. The spherical symmetry of atoms leads to the separation of the one-electron equation into radial and spin-angular parts [11]. The radial four-vector has the so-called large component $P_{n\kappa}$ in the upper two places and the small component $Q_{n\kappa}$ in the lower two. The quantum number κ (with $|\kappa| = j + 1/2$) comes from the spin-angular equation, and n is the principal quantum number, which counts the solutions of the radial equation with the same κ. Defining

$$\phi_{n\kappa} = \begin{pmatrix} P_{n\kappa}(r) \\ Q_{n\kappa}(r) \end{pmatrix}, \tag{7}$$

the DFB equation has the form

$$F_\kappa \phi_{n\kappa} = \varepsilon_{n\kappa} \phi_{n\kappa}, \tag{8}$$

where the one-electron DFB operator F_κ is [12]–[16]

$$F_\kappa = \begin{pmatrix} V_{\text{nuc}} + U^{LL} & c\Pi_\kappa + U^{LS} \\ c\Pi_\kappa^+ + U^{SL} & V_{\text{nuc}} + U^{SS} - 2c^2 \end{pmatrix}, \tag{9}$$

with

$$\Pi_\kappa = -d/dr + \kappa/r \tag{10}$$

and

$$\Pi_\kappa^+ = d/dr + \kappa/r. \tag{11}$$

V_{nuc} is the nuclear attraction potential. In the uniform charge distribution model used here, the charge of a nucleus of atomic mass A is distributed uniformly over a sphere with radius $R = 2.2677 \times 10^{-5} A^{-1/3}$. The nuclear potential for a nucleus with charge Z is then

$$V_{\text{nuc}} = \begin{cases} -Z/r & \text{for } r > R \\ -(Z/2R)(3 - r^2/R^2) & \text{for } r \leq R. \end{cases} \tag{12}$$

The terms U^{LL} etc. represent the one-body mean-field potential, which approximates the two-electron interaction in the Hamiltonian, as is the practice in SCF schemes. In the DFB equations this interaction includes the Breit term (3) in addition to the electron repulsion $1/r_{ij}$.

The radial functions $P_{n\kappa}(r)$ and $Q_{n\kappa}(r)$ may be obtained by numerical integration [17, 18] or by expansion in a basis [19]. Since the Dirac Hamiltonian is not bound from below, failure to observe correct boundary conditions leads to "variational collapse" [20]–[27], where admixture of negative-energy solutions may yield energies much below experimental. To avoid this failure, the basis sets used for expanding the large and small components must maintain

"kinetic balance" [24, 25]. In the nonrelativistic limit ($c \to \infty$), the small component is related to the large component by [20]

$$Q_{n\kappa}(r) = (2c)^{-1}\Pi_\kappa^+ P_{n\kappa}(r)\,, \tag{13}$$

where Π_κ^+ is defined in (11). The simplest way to obtain kinetic balance is to derive the small-component basis functions from those used to span the large component by

$$\chi_{\kappa j}^S = \Pi_\kappa^+\chi_{\kappa j}^L\,. \tag{14}$$

Ishikawa and coworkers [16, 23] have shown that G-spinors, with functions spanned in Gaussian-type functions (GTF) chosen according to (14), satisfy kinetic balance for finite c values if the nucleus is modeled as a uniformly-charged sphere.

2.3   The Fock-Space Coupled-Cluster Method

The coupled-cluster method is well-known by now, and only a brief account of aspects relevant to our applications is given here.

The Dirac-Coulomb-Breit Hamiltonian H_{DCB}^+ may be rewritten in second-quantized form [6, 16] in terms of normal-ordered products of spinor creation and annihilation operators $\{r^+s\}$ and $\{r^+s^+ut\}$,

$$H = H_{\mathrm{DCB}}^+ - \langle 0|H_{\mathrm{DCB}}^+|0\rangle = \sum_{rs} f_{rs}\{r^+s\} + \frac{1}{4}\sum_{rstu}\langle rs||tu\rangle\{r^+s^+ut\}, \tag{15}$$

where

$$\langle rs||tu\rangle = \langle rs|tu\rangle - \langle rs|ut\rangle \tag{16}$$

and

$$\langle rs|tu\rangle = \int d\mathbf{x}_1 d\mathbf{x}_2 \Psi_r^*(\mathbf{x}_1)\Psi_s^*(\mathbf{x}_2)(r_{12}^{-1} + B_{12})\Psi_t(\mathbf{x}_1)\Psi_u(\mathbf{x}_2). \tag{17}$$

Here f_{rs} and $\langle rs||tu\rangle$ are, respectively, elements of one-electron Dirac-Fock and antisymmetrized two-electron Coulomb-Breit interaction matrices over Dirac four-component spinors. The effect of the projection operators Λ^+ is now taken over by the normal ordering, denoted by the curly braces in (15), which requires annihilation operators to be moved to the right of creation operators as if all anticommutation relations vanish. The Fermi level is set at the top of the highest occupied positive-energy state, and the negative-energy states are ignored.

By adopting the no-pair approximation, a natural and straightforward extension of the nonrelativistic open-shell CC theory emerges. The multireference valence-universal Fock-space coupled-cluster approach is employed [28], which defines and calculates an effective Hamiltonian in a low-dimensional

model (or P) space, with eigenvalues approximating some desirable eigenvalues of the physical Hamiltonian. The effective Hamiltonian has the form [29]

$$H_{\text{eff}} = PH\Omega P \qquad (18)$$

where Ω is the normal-ordered wave operator,

$$\Omega = \{\exp(S)\}. \qquad (19)$$

The Fock-space approach starts from a reference state (closed-shell in our applications, but other single-determinant functions may also be used), correlates it, then adds and/or removes electrons one at a time, recorrelating the whole system at each stage. The sector (m,n) of the Fock space includes all states obtained from the reference determinant by removing m electrons from designated occupied orbitals, called valence holes, and adding n electrons in designated virtual orbitals, called valence particles. The practical limit is $m + n \leq 2$, although higher sectors have also been tried [30]. The excitation operator is partitioned into sector operators

$$S = \sum_{m \geq 0} \sum_{n \geq 0} S^{(m,n)}. \qquad (20)$$

This partitioning allows for partial decoupling of the open-shell CC equations. The equations for the (m,n) sector involve only S elements from sectors (k,l) with $k \leq m$ and $l \leq n$, so that the very large system of coupled nonlinear equations is separated into smaller subsystems, which are solved consecutively: first, the equations for $S^{(0,0)}$ are iterated to convergence; the $S^{(1,0)}$ (or $S^{(0,1)}$) equations are then solved using the known $S^{(0,0)}$, and so on. This separation, which does not involve any approximation, reduces the computational effort significantly. The effective Hamiltonian (18) is also partitioned by sectors. An important advantage of the method is the simultaneous calculation of a large number of states.

Each sector excitation operator is, in the usual way, a sum of virtual excitations of one, two, ..., electrons,

$$S^{(m,n)} = \sum_{l} S_l^{(m,n)}, \qquad (21)$$

with l going, in principle, to the total number of electrons. In practice, l has to be truncated. The level of truncation reflects the quality of the approximation, i.e., the extent to which the complementary Q space is taken into account in the evaluation of the effective Hamiltonian. In the applications described below the series (21) is truncated at $l=2$. The resulting CCSD (coupled cluster with single and double excitations) scheme involves the fully self-consistent,

iterative calculation of all one- and two-body virtual excitation amplitudes and sums all diagrams with these excitations to infinite order. As negative-energy states are excluded from the Q space, the diagrammatic summations in the CC equations are carried out only within the subspace of the positive-energy branch of the DF spectrum.

The H_{eff} diagrams may be separated into core and valence parts,

$$H_{\text{eff}} = H_{\text{eff}}^{\text{core}} + H_{\text{eff}}^{\text{val}}, \tag{22}$$

where the first term on the right-hand side consists of diagrams without any external (valence) lines and describes core electron correlation. The eigenvalues of $H_{\text{eff}}^{\text{val}}$ will then give directly the transition energies from the reference state, with correlation effects included for both initial and final states. The physical significance of these energies depends on the nature of the model space. Thus, electron affinities may be calculated by constructing a model space with valence particles only [(0,n) sectors, $n > 0$], ionization potentials are given using valence holes [(n,0) sectors, $n > 0$], and both valence types are required to describe excitations out of the reference state [(m, n) sectors, $m, n > 0$].

3   Application to Atoms

Different ways of implementing the relativistic coupled cluster (RCC) method are known. A numerical procedure for solving the pair equation has been developed by Lindgren and coworkers [31] and applied to two-electron atomic systems [32]. Other approaches use discrete basis sets of local or global functions. This makes the application of the projection operators onto the positive-energy space much easier than in the numerical scheme; one simply ignores the negative-energy branch of the one-electron spectrum. A technique based on local splines was developed by Blundell et al. [33], while the Göteborg group introduced another type of local basis, obtained by discretizing the radial space [34]. The first relativistic coupled cluster calculation in a global basis [35] appeared in 1990, but was limited to s orbitals only, both in the occupied and virtual space. A more general and sustained implementation started two years later, with pilot calculations for light atoms in closed-shell [36] and open-shell [37] states. The method has since been applied to many heavy atoms, where relativistic effects are crucial to the correct description of atomic structure. Calculated properties include ionization potentials, excitation energies, electron affinities, fine-structure splittings, and for super-heavy elements — the nature of the ground state. The additivity of relativistic and correlation effects was also studied. Systems investigated include the gold atom [38], few-electron ions [39], the alkali-metal atoms Li–Fr [40], the Xe atom [41], the f^2 shells of

Pr^{3+} and U^{4+} [42], the ytterbium [43], lutetium [43], mercury [44], barium [45], radium [45], thallium [46], and bismuth [47] atoms, and the super-heavy elements lawrencium [43], rutherfordium [48], 111 [49], 112 [44], 113 [46], 115 [47], and 118 [50]. Representative applications are described below.

The spherical symmetry of atoms, which leads to angular decomposition of the wave function and coupled-cluster equations, is used at both the Dirac-Fock-Breit [16] and RCC [38, 40] stages of the calculation. The energy integrals and CC amplitudes which appear in the Goldstone-type diagrams defining the CC equations are decomposed in terms of vector-coupling coefficients, expressed by angular-momentum diagrams, and reduced Coulomb-Breit or S matrix elements, respectively. The reduced equations for single and double excitation amplitudes are derived using the Jucys-Levinson-Vanagas theorem [29] and solved iteratively. This technique makes possible the use of large basis sets with high l values, as a basis orbital gives rise to two functions at most, with $j = l \pm 1/2$, whereas in Cartesian coordinates the number of functions increases rapidly with l. Typically we go up to h ($l = 5$) or i ($l = 6$) orbitals. To account for core-polarization effects, which may be important for many systems, we correlate at least the two outer shells, usually 20–40 electrons. Finally, uncontracted Gaussians are used, since contraction leads to problems in satisfying kinetic balance and correctly representing the small components. On the other hand, it has been found that high-energy virtual orbitals have little effect on the transition energies we calculate, since these orbitals have nodes in the inner regions of the atom and correlate mostly the inner-shell electrons, which we do not correlate anyway. These virtual orbitals, with energies above 80 or 100 hartree, are therefore eliminated from the RCC calculation.

3.1   Gold

The gold atom exhibits very large relativistic effects on its chemical and physical properties, due to the contraction and stabilization of the $6s$ orbital. Non-relativistic calculations lead to large errors, including the reversal of the two lowest excited states [51, 52]. Gold was therefore selected as the first heavy atom to be treated by the RCC method [38]. Two closed-shell states can be used as starting points for the Fock-space treatment, defining the $(0,0)$ sector, namely Au^+ or Au^-. Electrons are then added or removed according to the schemes

$$Au^+(0,0) \rightarrow Au(0,1) \rightarrow Au^-(0,2), \qquad (23)$$

or

$$Au^-(0,0) \rightarrow Au(1,0) \rightarrow Au^+(2,0). \qquad (24)$$

The basis consisted of $21s17p11d7f$ Gaussian spinors [52], and the $4spdf5spd6s$ electrons were correlated. Table 1 shows the nonrelativistic, Dirac-Coulomb,

and Dirac-Coulomb-Breit total energies of the two ions. As expected, relativistic effects are very large, over 1100 hartree. A point to note is the nonadditivity of relativistic and correlation corrections to the energy. While the correlation energy of the electrons in the $4s$–$6s$ shells of Au$^-$ is -1.370 hartree in the nonrelativistic scheme, the corresponding relativistic values are -1.464 hartree without the Breit term and -1.467 hartree with it.

The various transition energies of the gold atom and its ions are shown and compared with experiment [53] in table 2. The nonrelativistic results have errors of several eV. The RCC values, on the other hand, are highly accurate, with an average error of 0.06 eV. The inclusion of the Breit effect does not change the result by much, except for a some improvement of the fine-structure splittings.

Table 1: Total energies of the closed-shell systems Au$^+$ and Au$^-$ (hartree), with the nonrelativistic, DF, and DFB Hamiltonians.

	Au$^+$		Au$^-$	
	Noncorrelated	Correlation	Noncorrelated	Correlation
NR	-17863.46301	-1.29756	-17863.68392	-1.37018
DC	-19029.01322	-1.36150	-19029.32077	-1.46436
DCB	-19007.42385	-1.36430	-19007.73063	-1.46690

Table 2: CCSD transition energies in Au (eV). IP is the ionization potential, EA denotes electron affinity, and EE — excitation energy relative to the ground state. FS denotes fine-structure splittings.

			NR	DC	DCB	Expt [53].
IP	$5d^{10}6s$	$^2S_{1/2}$	6.981	9.101	9.086	9.22
EE	$5d^96s^2$	$^2D_{3/2}$	5.301	2.661	2.669	2.658
	$5d^96s^2$	$^2D_{5/2}$	5.301	1.115	1.150	1.136
	$5d^{10}6p_{1/2}$	$^2P_{1/2}$	3.313	4.723	4.720	4.632
	$5d^{10}6p_{3/2}$	$^2P_{3/2}$	3.313	5.193	5.184	5.105
FS		^2D	0	1.546	1.519	1.522
		^2P	0	0.470	0.466	0.473
EA	$5d^{10}6s^2$	$^1S_0$	1.267	2.278	2.269	2.31

3.2   Ekagold (Element 111)

A major relativistic effect in the gold atom is the stabilization of the $6s$ orbital. This is manifested by the energy separation between the $5d^{10}6s$ ^2S ground state and the $5d^96s^2$ ^2D excited state. Looking at the group 11 (or coinage metal) atoms, the ^2D excitation energies of Cu are 1.389 ($J = 5/2$) and 1.642 ($J = 3/2$) eV, increasing to 3.749 and 4.304 eV for Ag [53]. Were it not for relativity, one would expect even higher energies for Au. Indeed, nonrelativistic CCSD (table 2) puts the ^2D energy at 5.301 eV above the ^2S ground state, in line with expectations. Relativistic effects reduce this value radically, giving 1.150 and 2.669 eV for the excited ^2D sublevels, within 0.015 eV of experiment [53]. An even larger stabilization may be expected for the next member of the group, element 111. The question arose whether this stabilization would be sufficient to push the ^2D level below the ^2S and make it the ground state of the atom.

Table 3: Orbital energies of the 111 anion (a.u., signs reversed).

Orbital	DFC	DFB	HF
$6s$	5.0071	4.9933	3.0831
$7s$	0.1367	0.1356	0.0181
$6p_{1/2}$	3.4887	3.4674	2.0249
$6p_{3/2}$	1.9396	1.9346	2.0249
$6d_{3/2}$	0.1863	0.1860	0.3550
$6d_{5/2}$	0.0789	0.0800	0.3550
$5f_{5/2}$	2.6778	2.6842	3.4884
$5f_{7/2}$	2.4530	2.4644	3.4884

The calculations were carried out as for gold above, starting with the 111^- anion as reference [49]. As expected, very large relativistic effects are observed. Energies of the highest occupied orbitals are shown in table 3, and atomic transition energies are collected in table 4. The $7s$ orbital energy of the anion goes down from -0.018 to -0.136 hartree, while the $6d$ goes up from -0.355 to -0.186 ($j = 3/2$) and -0.080 ($j = 5/2$) hartree. The s and p orbitals undergo very large contraction (see figure 1). Atomic energies also show dramatic changes. Of particular interest to us is the $6d^97s^2$ $^2D_{5/2}$ state, predicted by nonrelativistic CCSD to lie 5.43 eV above the $6d^{10}7s$ ^2S state, which is reduced relativistically to 3 eV *below* the ^2S, thus becoming the ground state. Ionization potentials of the atom show relativistic effects of 12–15 eV!
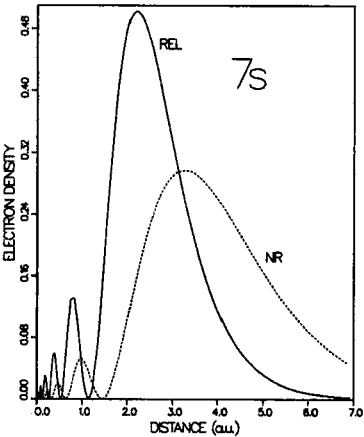
Figure 1: Relativistic and nonrelativistic densities of element 111 $7s$ orbital

3.3 Rutherfordium — Role of Dynamic Correlation

The nature of the rutherfordium ground state has been a subject of interest for a long time. Rutherfordium is the first atom after the actinide series, and in analogy with the lighter group 4 elements it should have the ground-state configuration $[\mathrm{Rn}]5f^{14}6d^27s^2$. Keller [54] suggested that the relativistic stabilization of the $7p_{1/2}$ orbital would yield a $7s^27p^2_{1/2}$ ground state. Recent multiconfiguration Dirac-Fock (MCDF) calculations [55, 56] found that the $7p^2$ state was rather high; they indicate a $6d7s^27p$ ground state, with the lowest state of the $6d^27s^2$ configuration higher by 0.5 [55] or 0.24 eV [56]. The

Table 4: CCSD excitation energies (EE), electron affinity (EA) and ionization potentials (IP) of element 111 (eV).

	Transition	DC	DCB	NR
EE	$6d^97s^2\ ^2D_{5/2} \to 6d^97s^2\ ^2D_{3/2}$	2.719	2.687	0
	$6d^97s^2\ ^2D_{5/2} \to 6d^{10}7s\ ^2S_{1/2}$	3.006	2.953	-5.430
EA	$6d^97s^2\ ^2D_{5/2} \to 6d^{10}7s^2\ ^1S_0$	1.542	1.565	6.484
IP	$6d^97s^2\ ^2D_{5/2} \to 6d^87s^2\ ^3D_4$	10.57	10.60	22.98
	$6d^97s^2\ ^2D_{5/2} \to 6d^97s\ ^3D_3$	12.36	12.33	0.92
	$6d^97s^2\ ^2D_{5/2} \to 6d^{10}\ ^1S_0$	15.30	15.23	-0.44

two calculations are similar, using numerical MCDF [57] in a space including all possible distributions of the four external electrons in the $6d$, $7s$ and $7p$ orbitals, and the difference may be due to the different programs used or to minor computational details. These MCDF calculations take into account nondynamic correlation only, which is due to near-degeneracy effects and can be included by using a small number of configurations. A similar approach by Desclaux and Fricke [58] gave errors of 0.4–0.5 eV for the energy differences between $(n-1)d$ and np configurations of Y, La and Lu, with the calculated np energy being too low. Desclaux and Fricke corrected the corresponding energy difference in Lr by a similar amount [58]. If a shift of similar magnitude is applied to the MCDF results for Rf, the order of the two lowest states may be reversed. It should also be noted that dynamic correlation, largely omitted from MCDF, has been shown to play a significant role in determining atomic excitation energies (see below), reducing the average error in calculating Pr^{3+} excitation energies by a factor of four relative to MCDF results. The RCC method has therefore been applied to Rf [48]. Starting from Rf^{2+} with the closed-shell configuration $[Rn]5f^{14}7s^{2}$, two electrons were added, one at a time, in the $6d$ and $7p$ orbitals, to form the low-lying states of Rf^{+} and Rf. A large basis set of $34s24p19d13f8g5h4i$ G spinors was used, and the external 36 electrons were correlated, leaving only the $[Xe]4f^{14}$ core uncorrelated. A series of calculations, with increasing l values in the virtual space, was performed to assess the convergence of the results. Some of the calculated transition energies are shown in table 5. Others may be found in the original publication [48].

The salient feature of the calculated transition energies is their monotonic behavior with the amount of correlation accounted for. The correlation of the $5f$ electrons and the gradual inclusion of higher l spaces all increase the four transition energies in table 5, as well as those not shown here. The MCDF results fall invariably between the d and f limits. This makes sense, since the MCDF function optimizes the orbitals and CI coefficients in a space including configuration state functions which correspond to all possible distributions of the four external electrons in the $6d$, $7s$ and $7p$ orbitals. Nondynamic correlation, resulting from interactions of configurations relatively close in energy, is thus described very well; the long-range dynamic correlation, which is more difficult to include, requiring many thousands of configurations, is not described as well, leading to an error in the identification of the Rf ground state. The latter is determined by the sign of the excitation energy in the last column of table 5. A negative energy means that the $7s^{2}7p6d$ configuration is lower than the $7s^{2}6d^{2}$, and is therefore the ground state. From the calculations reported, we estimate the CCSD converged value for this energy at 0.30–0.35 eV, making the $7s^{2}6d^{2}$ state the ground state of atomic Rf. Recent state-of-the-art experiments with Rf confirmed [59] that the chemistry of the atom is similar

Table 5: Transition energies in Rf$^+$ and Rf (eV)

	Rf$^+$		Rf	
	$7s^26d_{3/2}$	$7s^26d_{5/2}$	$7s^26d^2$	$7s^27p6d$
	$^2D_{3/2}$ IP	$^2D_{5/2}$ EE	$^3F_2$ IP	$^3D_2$ EE
MCDF [56]	13.47		5.30	-0.24
MCDF [55]				-0.50
RCCSD				
$l \leq 2^a$	13.37	0.79	5.15	-0.60
$l \leq 3^a$	13.95	0.82	5.65	-0.11
$l \leq 3$	14.05	0.87	5.76	0.03
$l \leq 4$	14.20	0.90	5.90	0.17
$l \leq 5$	14.34	0.92	5.99	0.25
$l \leq 6$	14.37	0.92	6.01	0.27
$l \leq 5^b$	14.34	0.87	5.99	0.27

$^a 5f$ electrons not correlated
^{b} With Breit interaction.

to that of Hf, which has a $6s^25d^2$ ground state.

   This example shows the intricate interplay of relativity and correlation. It is well known that relativity stabilizes s vs. d orbitals, and correlation has the opposite effect. When both effects are important and the result not obvious *a priori*, one must apply methods, such as RCC, which treat relativity and correlation simultaneously to high order.

3.4   Element 118 — a Rare Gas with Electron Affinity

One of the most dramatic effects of relativity is the contraction and concomitant stabilization of s orbitals (see Fig. 1) above. An intriguing question is whether the $8s$ orbital of element 118, the next rare gas, would be stabilized sufficiently to give the atom a positive electron affinity. Using the neutral atom Dirac-Fock orbitals as a starting point raises a problem, since the $8s$ orbital has positive energy and tends to "escape" to the most diffuse basis functions. This may be avoided by calculating the unoccupied orbitals in artificial fields, obtained by assigning partial charges to some of the occupied shells. The unphysical fields are compensated by including an appropriate correction in the perturbation operator. A series of calculations with a variety of fields gave electron affinities differing by a few wave numbers. The correlated relativistic electron affinity is 0.056 eV, with an estimated error of 0.01 eV. Inclusion of

both relativity and correlation is required to yield a positive EA. It should be noted that similar calculations did not give ^2S bound states for Rn^-. Further details may be found in the original publication [50].

3.5   The f^2 Levels of Pr^{3+}

The atomic systems in the previous examples have s, p, and/or d valence electrons. Here we discuss the energy levels of the Pr^{3+} ion, which has an f^2 configuration. The spectrum is well characterized experimentally [60] and provides a good test for high-accuracy methods incorporating relativity and correlation.

Starting from the Pr^{5+} closed shell as reference, two electrons were added in the $4f$ shell to obtain the levels of interest. Three basis sets were used, with l going up to 4, 5 and 6, and the $4spdf5sp$ electrons were correlated [42]. The excitation energies are compared with experiment [60] and with MCDF [61] in table 6.

Table 6: Excitation energies of Pr^{3+} $4f^2$ levels (cm^{-1})

Level	Expt. [60]	MCDF [61]	CCSD		
			$l \leq 4$	$l \leq 5$	$l \leq 6$
$^3H_5$	2152.09	2337	2273	2273	2270
$^3H_6$	4389.09	4733	4645	4641	4635
$^3F_2$	4996.61	4984	4749	4832	4843
$^3F_3$	6415.24	6517	6266	6345	6354
$^3F_4$	6854.75	6950	6808	6844	6843
$^1G_4$	9921.24	10207	10019	10014	10001
$^1D_2$	17334.39	18153	16803	16961	16998
$^3P_0$	21389.81	22776	20802	21109	21155
$^3P_1$	22007.46	23450	21443	21747	21791
$^1I_6$	22211.54	25854	22267	22061	22010
$^3P_2$	23160.61	24653	22719	23009	23051
$^1S_0$	50090.29	50517	48448	49072	49194
Avrg. error		853	394	245	222

The calculated excitation energies are in very good agreement with experiment, an agreement which improves with the size of the basis. All 13 levels appear in the correct order (in MCDF the $^3P_2$ level appears 1200 cm^{-1} below the $^1I_6$ instead of 950 cm^{-1} above it). Convergence with respect to the l value in the virtual space seems good, and the best basis gives an average error of

Table 7: Fine structure in Pr^{3+} (cm^{-1}).

	Expt. [60]	MCDF	DC $l \leq 4$	DC $l \leq 5$	DCB $l \leq 5$	DC $l \leq 6$
$^3H_5 - {}^3H_4$	2152	2337	2273	2273	2081	2270
$^3H_6 - {}^3H_5$	2237	2396	2369	2368	2169	2365
$^3F_3 - {}^3F_2$	1419	1533	1517	1513	1373	1511
$^3F_4 - {}^3F_3$	440	433	542	499	465	489
$^3P_1 - {}^3P_0$	618	674	631	638	585	636
$^3P_2 - {}^3P_1$	1153	1203	1276	1262	1090	1260
Avrg. error		95	98	89	51	86

222 cm^{-1} for the excitation energies. A full half of the total error is due to the high $^1S_0$ state; these states are notoriously difficult to calculate.

While including the Breit term has a rather small effect on the excitation energies of Pr^{3+}, it improves the fine-structure splittings (table 7). This is a general phenomenon, and may be traced to including the spin-other-spin interaction in the two-electron Breit term [62].

4   Application to Molecules

Molecules are always more difficult to treat accurately than atoms, because of the reduced symmetry. An additional complication arises in relativistic calculations: the Dirac-Fock(-Breit) orbitals will in general be complex. One way to circumvent this difficulty is by the Douglas-Kroll-Hess transformation [63], which yields a one-component function with computational effort essentially equal to that of a nonrelativistic calculation. Spin-orbit interaction may then be added as a perturbation. Implementation to AuH and Au_2 is described here. Progress has also been made in the four-component formulation [64], and the MOLFDIR package [65] has recently been extended to include the CC method. This is still a rather heavy calculation. SnH_4, calculated with the MOLFDIR DF package and our CC programs, is also presented below.

4.1   One-Component Applications: AuH, Au_2, E111H

Before implementing the Douglas-Kroll-Hess transformation to molecules, we tested its accuracy by applying it to the gold atom [66] and comparing with the full four-component results [38] and with experiment [53]. Since no spin-orbit interaction is present, only term energies (averaged over spin components) can be compared. All transition energies were within a few hundredth of an

Table 8: Molecular constants and vertical transition energies of AuH

	Nonrel	Rel	Expt
$R_e(\text{Å})$	1.749	1.525	1.524
$D_e(\text{eV})$	1.79	2.92	3.22
$\omega_e(\text{cm}^{-1})$	1565	2288	2305
IP to $X^2\Sigma^+(\text{eV})$	8.74	10.06	
IP to $A^2\Delta(\text{eV})$	13.11	11.63	
IP to $C^2\Sigma^+(\text{eV})$	13.72	14.41	
EA(eV)	0.56	0.54	
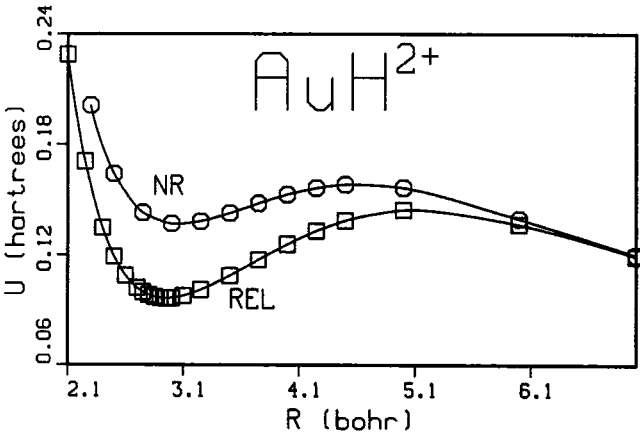
Figure 2: Relativistic and nonrelativistic potentials of AuH^{2+}
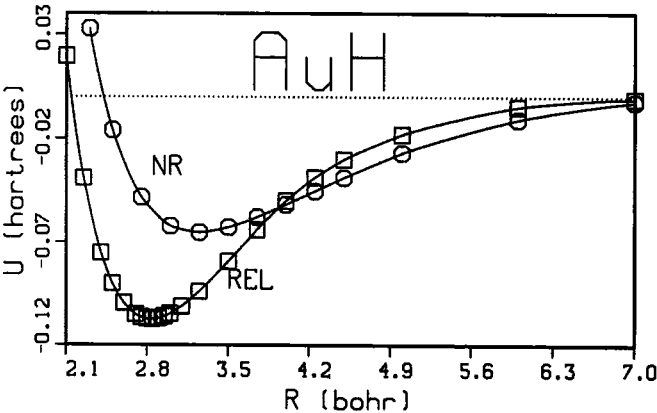
Figure 3: Relativistic and nonrelativistic potentials of AuH
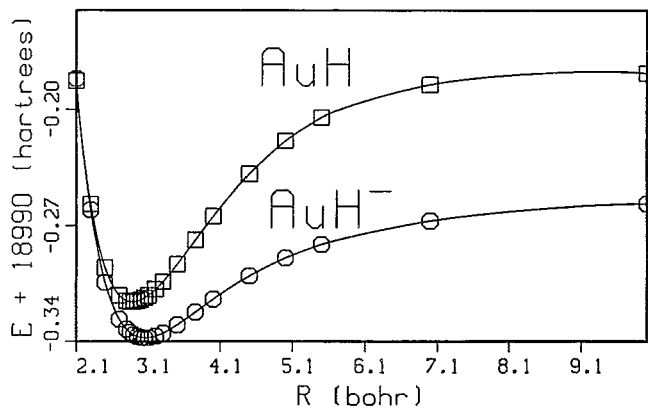
Figure 4: Relativistic potentials of AuH and AuH$^-$
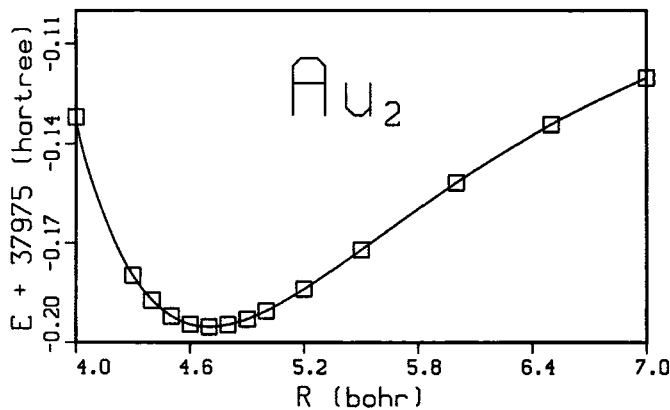
Figure 5: Relativistic potential of Au$_2$

eV of the corresponding four-component values. It seems therefore safe to apply the one-component method to states where spin-orbit effects are not significant. Calculations were carried out for AuH and some of its ions [66]. The first set of calculations started from the closed-shell AuH^{2+} ion, and added two electrons to obtain states of the monocation and neutral species. Figure 2 shows very large relativistic effects on the potential of the dication. The species is not bound, but it has a sizeable metastable well and barrier to dissociation. The shape of the potential comes from the crossing of two curves dissociating to $Au^{2+} + H$ and to $Au^+ + H^+$, respectively. The depth of the well is more than doubled by relativity. Similar effects occur in the AuH potential (see figure 3). Relativity shortens the bond length of the molecule by 15% and increases the bond energy by 60%. The relativistic potential of the anion is shown in figure 4, and the various spectroscopic constants and transition energies are collected and compared with experiment [67] in table 8.

Similar calculations were carried out for the hydride of element 111 [68]. As expected, realtivistic effects were even larger than for AuH. The equilibrium separation is reduced by relativity from 1.92 to 1.51Å, and the bond energy increases from 1.83 to 3.56 eV. Preliminary work on Au_2 has also been carried out [69]. The potential function shown in figure 5 gives molecular constants in good agreement with experiment: R_e is 2.487Å compared to the experimental 2.472Å, and the harmonic frequency is 2330 cm^{-1} compared to 2305 cm^{-1}.

4.2   Four-Component Application: SnH_4

Table 9: SCF, second-order perturbation theory, and coupled-cluster values of the equilibrium bond length R_e, energy E_e at R_e, and harmonic frequency ω_e of the breathing mode of SnH_4.

Method	R_e(Å)	E_e(a.u.)	ω_e(cm^{-1})
Nonrelativistic			
SCF	1.727	−6025.21370	2067
PT2	1.710	−6025.39218	2030
CCSD	1.717	−6025.41979	2025
Relativistic			
DF	1.711	−6172.71153	2073
PT2	1.694	−6172.89890	2034
CCSD	1.702	−6172.92553	2019
Expt. [71]	1.701		1955

The Dirac-Fock part of the MOLFDIR program has been interfaced with

our Fock-space coupled-cluster package. The first molecule investigated was SnH_4 [70]. The results, collected and compared with experiment [71] in table 9, show the relativistic and correlation effects on the energy and some spectroscopic constants of the molecule. The relativistic CC results show very good agreement with experiment.

5   Summary and Conclusion

The relativistic coupled-cluster method includes simultaneously relativistic terms through second order in the fine-structure constant α and correlation effects summed to all orders of the one- and two-electron excitations. In atomic systems, where spherical symmetry allows the use of large basis sets, the method makes possible calculation of large numbers of heavy-atom states with unprecedented accuracy, and gives reliable predictions for superheavy elements. The largest remaining source of error is probably the omission of triple virtual excitations. Molecules present a more difficult challenge, and few four-component RCC applications have been reported to date. The one-component Douglas-Kroll-Hess transformation provides a cheap, accurate alternative when spin-orbit interaction may be neglected.

Acknowledgments

References

[1] See, e.g., R. McWeeny and B.T. Sutcliffe, *Methods of Molecular Quantum Mechanics*, chap. 8 (Academic Press, London, 1969).

[2] See, e.g., J. Sucher, in *Relativistic, Quantum Electrodynamic, and Weak Interaction Effects in Atoms*, ed. W. Johnson, P. Mohr, and J. Sucher (American Institute of Physics, New York, 1989), p. 28.

[3] G. Breit, *Phys. Rev.* **B34**, 553 (1929); *ibid.* **36**, 383 (1930); *ibid.* **39**, 616 (1932).

[4] G.E. Brown and D.G. Ravenhall, *Proc. Roy. Soc.* A **208**, 552 (1951).

[5] H.A. Bethe and E.E. Salpeter, *Quantum Mechanics of One- and Two-Electron Atoms* (Springer-verlag, Berlin, 1957).

[6] J. Sucher, *Phys. Rev.* A **22**, 348 (1980); *Phys. Scr.* **36**, 271 (1987).

[7] W. Buchmüller and K. Dietz, *Z. Phys.* C **5**, 45 (1980).

[8] I. Lindgren, in *Many-Body Methods in Quantum Chemistry*, ed. U. Kaldor, Lecture Notes in Chemistry Vol. 52 (Springer-Verlag, Heidelberg, 1989) p. 293; *Nucl. Instrum. Methods* **B31**, 102 (1988).

[9] *Relativistic, Quantum Electrodynamic, and Weak Interaction Effects in Atoms*, ed. W. Johnson, P. Mohr, and J. Sucher (American Institute of Physics, New York, 1989).

[10] M. Mittleman, *Phys. Rev.* A **4**, 893 (1971); *ibid.* **5**, 2395 (1972); *ibid.* **24**, 1167 (1981).

[11] A.S. Davydov, *Quantum Mechanics* (NEO Press, Peaks Island, Maine, 1966) chap. VIII.

[12] Y.-K. Kim, *Phys. Rev.* **154**, 17 (1967).

[13] T. Kagawa, *Phys. Rev.* A **12**, 2245 (1975); *ibid.* **22**, 2340 (1980).

[14] W.R. Johnson and J. Sapirstein, *Phys. Rev. Lett.* **57**, 1126 (1986); W.R. Johnson, M. Idrees, and J. Sapirstein, *Phys. Rev.* A **35**, 3218 (1987); S.A. Blundell, W.R. Johnson, Z.W. Liu, and J. Sapirstein, *Phys. Rev.* A **39**, 3768 (1989); W.R. Johnson, S.A. Blundell, and J.W. Sapirstein, *Phys. Rev.* A **37**, 307 (1988); *ibid.* **37**, 2764 (1988); *ibid.* **41**, 1689 (1990).

[15] H.M. Quiney, I.P. Grant, and S. Wilson, *J. Phys.* B **20**, 1413 (1987); *Phys. Scr.* **36**, 460 (1987); in *Many-Body Methods in Quantum Chemistry*, ed. U. Kaldor, Lecture Notes in Chemistry Vol. 52 (Springer-Verlag, Heidelberg, 1989); *J. Phys.* B **23**, L271 (1990); I.P. Grant and H.M. Quiney, *Adv. Atom. Molec. Phys.* **23**, 37 (1988).

[16] Y. Ishikawa, R.C. Binning, and H. Sekino, *Chem. Phys. Lett.* **160**, 206 (1989); Y. Ishikawa, *Phys. Rev.* A **42**, 1142 (1990); *Chem. Phys. Lett.* **166**, 321 (1990); Y. Ishikawa and H.M. Quiney, *Phys. Rev.* A **47**, 1732 (1993); Y. Ishikawa and K. Koc, *Phys. Rev.* A **50**, 4733 (1994).

[17] J.-P. Desclaux, *Comput. Phys. Commun.* **9**, 31 (1975).

[18] I.P. Grant, B.J. McKenzie, P.H. Norrington, D.F. Mayers, and N.C. Pyper, *Comput. Phys. Commun.* **21**, 207 (1980).

[19] For a recent review see Y. Ishikawa and U. Kaldor, in *Computational Chemistry: Review of Current Trends*, ed. J. Leszczynski, (World Scientific, Singapore, 1996), vol. I, p. 1.

[20] Y.-S. Lee and A.D. McLean, *J. Chem. Phys.* **76**, 735 (1982).

[21] F. Mark and W.H.E. Schwartz, *Phys. Rev. Lett.* **48**, 673 (1982); W.H.E. Schwartz and H. Wallmeier, *Mol. Phys.* **46**, 1045 (1982).

[22] H. Wallmeier and W. Kutzelnigg, *Chem. Phys. Lett.* **78**, 341 (1981); *Phys. Rev. A* **28**, 3092 (1983).

[23] Y. Ishikawa, R.C. Binning, and K.M. Sando, *Chem. Phys. Lett.* **101**, 111 (1983); *ibid.* **105**, 189 (1984); *ibid.* **117**, 444 (1985); Y. Ishikawa, R. Baretty, and R.C. Binning, *Chem. Phys. Lett.* **121**, 130 (1985); Y. Ishikawa and H.M. Quiney, *Intern. J. Quantum Chem. Symp.* **21**, 523 (1987).

[24] R. E. Stanton and S. Havriliak, *J. Chem. Phys.* **81**, 1910 (1984).

[25] Y. Ishikawa, R. Baretty, and R.C. Binning, *Intern. J. Quantum Chem. Symp.* **19**, 285 (1985); Y. Ishikawa and H. Sekino, *Chem. Phys. Lett.* **165**, 243 (1990).

[26] K.G. Dyall, I.P. Grant, and S. Wilson, *J. Phys. B* **17**, 1201 (1984).

[27] P.J.C. Aerts and W.C. Nieuwpoort, *Chem. Phys. Lett.* **113**, 165 (1985); *ibid.* **125**, 83 (1986).

[28] For a discussion of Fock-space coupled cluster see U. Kaldor, *Theor. Chim. Acta* **80**, 427 (1991) and references therein.

[29] I. Lindgren and J. Morrison, *Atomic Many-Body Theory*, 2nd ed. (Springer Verlag, Berlin, 1986).

[30] S.R. Hughes and U. Kaldor, *Chem. Phys. Lett.* **194**, 99 (1992); *ibid.* **204**, 339 (1993); *Phys. Rev. A* **47**, 4705 (1993); *J. Chem. Phys.* **99**, 6773 (1993); *Intern. J. Quantum Chem.* **55**, 127 (1995).

[31] S. Salomonson, I. Lindgren, and A.-M. Mårtensson, *Phys. Scr.* **21**, 351 (1980).

[32] E. Lindroth, *Phys. Rev. A* **37**, 316 (1988).

[33] S.A. Blundell, W.R. Johnson, Z.W. Liu, and J. Sapirstein, *Phys. Rev.* A **39**, 3768 (1989); *ibid.* **40**, 2233 (1989); S.A. Blundell, W.R. Johnson, and J. Sapirstein, *Phys. Rev. Lett.* **65**, 1411 (1990); *Phys. Rev.* A **43**, 3407 (1991); Z.W. Liu and H.P. Kelly, *ibid.* **43**, 3305 (1991).

[34] S. Salomonson and P. Öster, *Phys. Rev.* A **40**, 5548 (1989); E. Lindroth and S. Salomonson, *ibid.* **41**, 4659 (1990); A.C. Hartly, E. Lindroth and A-M. Mårtensson-Pendrill, *J. Phys.* B **23**, 1990 (1990); A.C. Hartly and A-M. Mårtensson-Pendrill, *Z. Phys.* D **15**, 309 (1990); *J. Phys.* B **24**, 1193 (1991); A.-M. Mårtensson-Pendrill, S.A. Alexander, L. Adamowicz, N. Oliphant, J. Olsen, P. Öster, H.M. Quiney, S. Salomonson, and D. Sundholm, *Phys. Rev.* A **43**, 3355 (1991); E. Lindroth, H. Persson, S. Salomonson and A-M. Mårtensson-Pendrill, *Phys. Rev.* A **45**, 1493 (1992); E. Lindroth and J. Hvarfner, *ibid.* **45**, 2771 (1992).

[35] H. Sekino and R.J. Bartlett, *Intern. J. Quantum Chem. Symp.* **24**, 241 (1990).

[36] E. Ilyabaev and U. Kaldor, *Chem. Phys. Lett.* **194**, 95 (1992).

[37] E. Ilyabaev and U. Kaldor, *J. Chem. Phys.* **97**, 8455 (1994); *Phys. Rev.* A **47**, 137 (1993).

[38] E. Eliav, U. Kaldor, and Y. Ishikawa, *Phys. Rev.* A **49**, 1724 (1994).

[39] E. Eliav (Ilyabaev), U. Kaldor, and Y. Ishikawa, *Chem. Phys. Lett.* **222**, 82 (1994).

[40] E. Eliav, U. Kaldor, and Y. Ishikawa, *Phys. Rev.* A **50**, 1121 (1994).

[41] E. Eliav, U. Kaldor, and Y. Ishikawa, *Intern. J. Quantum Chem. Symp.* **28**, 205 (1994).

[42] E. Eliav, U. Kaldor, and Y. Ishikawa, *Phys. Rev.* A **51**, 225 (1995).

[43] E. Eliav, U. Kaldor, and Y. Ishikawa, *Phys. Rev.* A **52**, 291 (1995).

[44] E. Eliav, U. Kaldor, and Y. Ishikawa, *Phys. Rev.* A **52**, 2765 (1995).

[45] E. Eliav, U. Kaldor, and Y. Ishikawa, *Phys. Rev.* A **53**, 3050 (1996).

[46] E. Eliav, U. Kaldor, Y. Ishikawa, M. Seth, and P. Pyykkö, *Phys. Rev.* A **53**, 3926 (1996).

[47] E. Eliav, U. Kaldor, and Y. Ishikawa, Mol. Phys. in press.

[48] E. Eliav, U. Kaldor, and Y. Ishikawa, *Phys. Rev. Lett.* **74**, 1079 (1995).

[49] E. Eliav, U. Kaldor, P. Schwerdtfeger, B.A. Heß, and Y. Ishikawa, *Phys. Rev. Lett.* **73**, 3203 (1994).

[50] E. Eliav, U. Kaldor, Y. Ishikawa, and P. Pyykkö, *Phys. Rev. Lett.* **77**, 5350 (1996).

[51] P.J. Hay, W.R. Wadt, L.R. Kahn, and F.W. Bobrowicz, *J. Chem. Phys.* **69**, 984 (1978).

[52] A. Pizlo, G. Jansen, and B.A. Heß, *J. Chem. Phys.* **98**, 3945 (1993).

[53] C.E. Moore, *Atomic Energy Levels*, Natl. Bur. of Stand. (U.S.) Circ. No. 467 (U.S. GPO, Washington, DC, 1948).

[54] O.L. Keller, *Radiochim. Acta* **37**, 169 (1984). See also J. B. Mann, quoted by B. Fricke and J. T. Waber, Actinides Rev. **1**, 433 (1971).

[55] V.A. Glebov, L. Kasztura, V.S. Nefedov, and B.L. Zhuikov, *Radiochim. Acta* **46**, 117 (1989).

[56] E. Johnson, B. Fricke, O.L. Keller, C.W. Nestor Jr., and T. C. Tucker, *J. Chem. Phys.* **93**, 8041 (1990).

[57] For reviews of MCDF see I.P. Grant, *Adv. Phys.* **19**, 747 (1970); I.P. Grant and H.M. Quiney, *Adv. At. Mol. Phys.* **23**, 37 (1988).

[58] J.-P. Desclaux and B. Fricke, *J. Phys.* **41**, 943 (1980).

[59] M. Schädel, *Radiochim. Acta* **70/71**, 207 (1995).

[60] W.C. Martin, R. Zalubas, and L. Hagan, *Atomic Energy Levels — The Rare-Earth Elements*, Natl. Bur. Stand. Ref. Data Series, NBS Circ. No. 60 (U.S. GPO, Washington, DC, 1978).

[61] Z. Cai, V. Meiser Umar, and C. Froese Fischer, *Phys. Rev. Lett.* **68**, 297 (1992).

[62] B.A. Heß, C.M. Marian, and S.D. Peyerimhoff, in *Modern Electronic Structure Theory*, ed. D.R. Yarkony, (World Scientific, Singapore, 1995) p. 152.

[63] M. Douglas and N. M. Kroll, *Ann. Phys. (NY)* **82**, 89 (1974); B.A. Heß, *Phys. Rev. A* **32**, 756 (1982); *ibid.* **33**, 3742 (1986); G. Jansen and B.A. Heß, *Phys. Rev. A* **39**, 6016 (1989); R. Samzow, B.A. Heß, and G. Jansen,

   J. Chem. Phys. **96**, 1227 (1992); B.A. Heß, R. J. Buenker, and P. Chandra, *Intern. J. Quantum Chem.* **29**, 737 (1986); R. Samzow and B.A. Heß, *Chem. Phys. Lett.* **184**, 491 (1991).

[64] K.G. Dyall, *J. Chem. Phys.* **100**, 2118 (1994); L. Visscher, K.G. Dyall and T.J. Lee, *Intern. J. Quantum Chem. Symp.* **29**, 411 (1995).

[65] P.J.C. Aerts, O. Visser, L. Visscher, H. Merenga, W.A. de Jong, and W.C. Nieuwpoort, MOLFDIR, University of Groningen, The Netherlands; L. Visscher, T.J. Lee and K.G. Dyall, RELCCSD, NASA Ames Research Center, Moffett Field, California.

[66] U. Kaldor and B.A. Heß, *Chem. Phys. Lett.* **230**, 1 (1994).

[67] K.P. Huber and G. Herzberg, *Molecular Spectra and Molecular Structure Constants of Diatomic Molecules*, (Van Nostrand, New York, 1979).

[68] M. Seth, P. Schwerdtfeger, M. Dolg, K. Fægri, B.A. Heß, and U. Kaldor, *Chem. Phys. Lett.* **250**, 461 (1996).

[69] U. Kaldor and B.A. Heß, unpublished results.

[70] E. Eliav and U. Kaldor, *Chem. Phys. Lett.* **248**, 405 (1996).

[71] H. W. Kattenberg and A. Oskam, *J. Mol. Spectr.* **51**, 377 (1974); Y. Oshima, Y. Matsumoto, M. Takami, S. Yamamoto, and K. Kuchitsu, *J. Chem. Phys.* **87**, 5141 (1987); M. Halonen, H. Bürger, and S. Sommer, *J. Phys. Chem.* **94**, 5222 (1990).

Index

A

Ab initio calculations
  with Gaussian basis sets, 158
  many-body systems, 176
  SCF-MI, and BSSE, 252–253
  small metal clusters, 144–147
Argon
  BSSE, 114
  CBS limits, 113
  convergence behavior, 113
  counterpoise correction, 115–116
Atom basis sets, neutral
  s-, p-, and d-type functions, 296–299
  s- and p-type functions, 287–289
Atoms
  application of RCC method
    to ekagold, 322
    to element 118, 325–326
    to gold, 320–321
    methods, 319–320
    to Pr^{3+}, 326–327
    to Rutherfordium, 323–325
  application of response theory, 10
  N-electron, in many-electron Sturmians, 206–211
Averaging method
  self-consistent averaging
    first-order shell-effect terms, 62–67
    in HF scheme, 59–60
    by Strutinsky's method, 56–58
Axilrod–Teller term, in m-body energy approximation, 152

B

Basis sets
  complete BS limit
    argon, 113, 116
    extrapolation, 110

helium, 113, 116
  hydrogen chloride, 117–122
  hydrogen fluoride, 117–122
  molecular property, 111–112
  nitrogen, 117–122
correlation consistent BS
  as computational method, 111–113
  standard and augmented sets, 106
Gaussian
  in *ab initio* calculations, 158
  basis subset distribution, 161–162
  basis subset exponents, 163
  basis subsets, 160–161
  control of computational linear dependence, 163–164
  elements, 158–160
  HF energy from, 164–168
  s-, p- and d-type functions
    neutral atom basis sets, 296–299
    one set diffuse functions, 300–303
    two sets diffuse functions, 304–306
  s- and p-type functions
    neutral atom basis sets, 287–289
    one set symmetrical diffuse functions, 290–293
    two sets symmetrical diffuse functions, 293–295
  systematic generation, 285–286
Basis set superposition errors
  argon, 114–116
  ArHF, 123–125
  in calculations of matter properties, 252–253
  CP method, application, 235–236
  definition, 108–110
  effect on convergence behavior, 107–108
  HCO^-, 123–125
  helium, 114–116
  hydrogen chloride, 117–122
  hydrogen fluoride, 117–122
  nitrogen, 117–122

337